EnerNex

REPORT

IMPROVING ECONOMICS OF SOLAR POWER THROUGH ANALYSIS, FORECASTING, AND DYNAMIC SYSTEM MODELING

Submitted to

THE REGENTS OF THE UNIVERSITY OF CALIFORNIA; UNIVERSITY OF CALIFORNIA, SAN DIEGO

Principal Investigators

Jens Schoene, Director of Research Studies, EnerNex
Jan Kleissl, Associate Professor, UCSD

Project Team

EnerNex: Vadim Zheglov, Jiaxin Ning
UCSD: Andu Nguyen, Ben Kurtz

EnerNex Project Number: 1787

Contact Information

Jens Schoene | 865-218-4600 x 6172 | jens@enernex.com

October 2013

Executive Summary

Small scale renewable generation and non-renewable generation are being incentivized in California and nationwide. Currently 1% of San Diego Gas & Electric's (SDG&E's) customers have installed distributed solar PV systems. Pacific Gas & Electric (PG&E) leads the nation with the highest number of interconnected PV. Southern California Edison (SCE) reports PV penetration levels of up to 70% for some of their distribution feeder circuits. Small numbers of PV generation systems cause few or no problems on the grid, but as the percentage of PV generation grows, a number of issues begin to appear. The electrical impact that large penetrations of PV generators have on the system they are connected to with regards to power quality, power flow, protective relaying, intentional and unintentional islanding, etc. are concerns to utilities that should be assessed in engineering studies. Short-term irradiance fluctuations can cause voltage fluctuations that can trigger automated line equipment (e.g., tap changers) leading to larger maintenance costs for utilities and a reduction of the life-cycle of the stressed equipment. Some utilities report more frequent operation of voltage regulators on their high-PV penetration feeders leading to greater maintenance requirements. This study focuses on the integration and economic impacts of Distributed Renewable Generation on grid operation. Specifically, we investigated (1) how the distribution feeder loading changes with PV penetration level, (2) the impact of increased PV penetration on system losses, and (3) the effect of voltage fluctuation due to changing generation levels of PV on voltage regulator operation.

In typical distributed generation scenarios, large numbers of PV generators are connected to single phases at many locations within distribution systems that have thousands of buses. Often the analyst is taking "shortcuts" by aggregating multiple generators. Similarly, the complexity of load variability is often ignored in simulations by aggregating thousands of loads and/or by unrealistically (but conveniently) assuming that each load in the system follows the same electrical demand profile. A consequence of the generation and load aggregations is that the flow of power within the distribution feeder is not accurately represented in simulations, which leads to inaccurate predictions regarding tap changing operations of voltage regulators, line losses, etc. A unique aspect of our study is that we disaggregated the generation and the loads in the system as explained in the following paragraph.

The system impact study documented in this reports was conducted on a distribution feeder that is based on a real-world distribution feeder located in Southern California. We investigated the effect of aggregation by comparing simulation results from simulations with aggregated load/generation with results from highly detailed simulations. For the highly detailed simulations,

we explicitly represented the power generated at each PV installation by determining the irradiance at each PV location from experimentally determined shadow maps that have a temporal resolution of 30 seconds and spatial resolutions ranging from ten meters to 100 meters. This approach resulted in a realistic representation of the PV variability due to cloud movements. Similarly, the loads in our simulations were resolved down to the residential level assuming that each load varies based on a normal distribution. We investigated the issues related to different levels of PV penetration and highlight the importance of incorporating high-resolution irradiance and load data into the simulations for obtaining accurate results. We investigated the following four scenarios:

- Scenario 1, low (actual) penetration of small PV w/ 2 MW PV installation: The number and ratings of the PV generators are based on what is installed in the system today (based on data provided by the host utility). The total capacity of the PV generators is 2.295 MW (about 20% of the total load MW rating) with 0.298 MW coming from small PVs and 2 MW from two large PV installations near a hospital.
- Scenario 2, low (actual) penetration of small PV w/o 2 MW PV installation: Same as scenario 1 with the exception that we removed the 2 MW PV installations near the hospital to achieve a more homogenous distribution of the PV generators that is more representative of a typical distributed generation scenario. This scenario results in a total PV capacity of 0.298 MW (about 2.47% of the total load MW rating) with only small PVs in the system.
- Scenario 3, high penetration of small PV w/ 2 MW PV installation: This scenario represents a hypothetical future scenario in which a large number of residential and commercial customers have PV generators operating on their premises. The small PV generators were duplicated nine times and the duplicated PVs were connected randomly to load buses on the feeder. No load bus has more than one PV. All original PV locations from Scenario 1 were retained. The large 2 MW PV installations were retained and not duplicated (that is, the amount of centralized PV in the system was not changed). This scenario results in a total PV capacity of 4.973 MW (about 41% of the total load MW rating) with 0.298 MW coming from small PVs and 2 MW from two large PV installations near a hospital.
- Scenario 4, high penetration of small PV w/o 2 MW PV installation: Same as scenario 2 with the exception that we removed the 2 MW PV installations near the hospital to achieve a more homogenous distribution of the PV generators that is more representative of a typical distributed generation scenario. This scenario results in a total PV capacity of 2.975 MW (about 25% of the total load MW rating) with only small PVs in the system.

We run seven cases for each of the three scenarios described above. The first six cases varied with regards to (1) aggregating/disaggregating the loads, (2) the temporal resolution of the input data (1 hour for the low-resolution cases and 30 seconds for the high-resolution cases), and (3)

aggregating/disaggregating the PV generation during a cloudy day. The last case was for a day with a clear sky with disaggregated loads and high temporal resolution. Note that for the clear-sky case, disaggregation is not required to obtain realistic results as all PV generators are exposed to the same irradiance levels. Based on the simulation results, we draw the following conclusions:

1. **PV reduces line losses:** The presence of PVs significantly reduces line losses on the feeder. In the low PV penetration Scenario 1, line losses are reduced by about 8% during cloudy days and 14% during a clear day. In the high PV penetration Scenario 3, line losses are reduced by about 11% and 19% during clear days and cloudy days, respectively. The losses are even further reduced when confining the time frame of the comparison to the daylight hours (up to 50% for the high PV penetration Scenario 3 during a clear day). We attribute the reduction of line losses to the fact the PV generation is much closer to the load compared to the no PV scenarios in which the power is supplied from the substation. On the other hand, the line losses for the low PV penetration Scenario 2 are very similar to the line losses for the no PV scenario. Note that our simulations do not account for transmissions losses that occur during the transfer of power from the plant to the substation. Accounting for these losses would increase the absolute difference between losses without PV on the system and losses with PV on the system even more. Investigating the value of PV for loss reduction on transmission systems versus the value for loss reduction on distribution systems is a worthy undertaking for future research. Transmission lines are normally longer than distribution lines, which increases the losses and, thereby, the value of PV for loss reduction. On the other hand, the higher transmission level voltages reduce losses, which decreases the value of PV for loss reduction.
2. **Distributed PV vs. centralized PV:** The PV penetration levels in Scenario 1 and Scenario 4 are similar (20% and 25%, respectively). The main difference is that Scenario 1 has two large 1 MW PV systems located close together which constitute nearly 90% of the total PV generation in the system. On the other hand, Scenario 4 does not contain large PV installations and the numerous smaller PV installations were more-or-less evenly distributed along the feeder. For the centralized PV Scenario 1, the tap changing operations were slightly more frequent and the line losses were larger compared to the distributed PV Scenario 4. It is important to note that this tendency is not necessarily a general conclusion that applies to all feeders, but it shows that the distribution of the PV on the feeder has a significant impact on both the tap changing operations and the losses. The maximum voltage on the feeder for the no PV scenarios and the PV scenarios without the large PV installations (Scenarios 2 and 4) are essentially identical (1.05 pu). On the other hand, the maximum voltages in the centralized PV Scenarios 1 and 3 are significantly higher than in the no PV / distributed PV Scenarios (up to 1.08 pu). This indicates that the voltage regulators deployed on the investigated feeder are capable of keeping the voltages along the feeder within permissible limits – even if the number of distributed PV is increased tenfold. On the other hand, centralized PV on the feeder is much more prone

to cause overvoltages – in particular if voltage regulators are not strategically placed to accommodate the PV concentration on the feeder. Note that, technically, PV inverters can be utilized to regulate the voltage on the feeder thereby potentially alleviating over and undervoltage issues on the feeder. However, IEEE 1547 does currently not permit distributed generation to actively regulate voltage (see Section 3.2).

3. **PV increases operation of tap changers significantly – in particular during cloudy days:** Tap changers during cloudy days in the high PV penetration Scenario 3 (41% penetration) are operating about 70 to 80 times each day (depending on the simulation case) which is significantly higher than the number of tap changer operations for the no PV and low PV penetration Scenario 2 (about 13 operation for both scenarios) and the clear-day simulation case 6 (between 12 and 19 operations, depending on the scenario). This indicates that tap changing operations during cloudy days will significantly increase if PV penetration levels are high, which will substantially increase maintenance costs and life-cycle costs of voltage regulators. On the other hand, for low PV penetration levels and during clear days, the tap changing operations is not impacted much. Note that the conclusions above came out of results from our simulations that utilize data with high temporal resolution (30 seconds). Our simulations with low-resolution (one hour) data were not suitable to resolve any of these differences – in fact the number of tap changing operations from the low-resolution results were around five for <u>all</u> PV penetration scenarios, which results in a large error for the high PV penetration scenarios where the number of tap changing operations reached above 80 (based on the more realistic simulation results that utilize high-resolution data).
4. **Low temporal resolution data vs. high temporal resolution data:** Using low resolution data underestimates tap changing operations significantly in high PV penetration scenarios. In our simulations, the increase in tap changing operations for high PV penetration levels was only observed when more accurate high resolution data (30 second time step) were used as input to the model. Simulations with low-resolution data (one hour time step) did not show the increase in tap changing operations. This indicates that it is important to use high resolution data when evaluating tap changing operations for high PV penetration scenarios.
5. **Effect of disaggregating PV irradiances:** For the >20% PV penetration Scenarios 1, 3 and 4, a comparison of the number of tap changing operations for cases 1 and 3 (aggregated/disaggregated PV; loads aggregated in both cases) and cases 2 and 4 (aggregated/disaggregate PV; loads disaggregated in both cases) shows that disaggregation of the PV generation does reduce the number of tap changing operations significantly (30 to 70%). This indicates that aggregating PV generation curves in simulations overestimates the actual tap changing operations that occurs on the real world system substantially.
6. **Effect of disaggregating load profiles:** For the >20% PV penetration Scenarios 1, 3 and 4, a comparison of the number of tap changing operations for cases 1 and 2

(aggregated/disaggregated loads; PV aggregated in both cases) and cases 3 and 4 (aggregated/disaggregate loads; PV disaggregated in both cases) shows that load disaggregation impacts the number of tap changing operations. However, there is no clear trend regarding whether disaggregating the load curves results in an increase or a decrease of the number of tap changing operations.

7. **Net consumption of active power:** For the >20% PV penetration Scenarios 1, 3 and 4, the active power net consumption of the distribution feeder, that is, the active power that needs to be supplied from the substation to supply the load demand on the feeder, is significantly reduced. For example, for the high PV penetration Scenario 3, the daily reduction of net consumption due to the presence of PV leads to about 8-15% less energy demand for the feeder, depending on the sky condition. In other words, generation sources outside the feeder need to supply about 8-15% less energy to the feeder (not accounting for losses associated with transferring the power from the plant to the substation). If these generation sources are fueled by conventional non-renewable resources (i.e., fossil and radioactive fuels), then this reduction leads to significant savings of these non-renewable resources.
8. **Net consumption of reactive power:** Conversely to the previous conclusion, the reactive power net consumption of the distribution feeder is increased, that is, more reactive power is consumed on the feeder, which has to be supplied by generation sources or reactive compensation outside the feeder or at the substation. This is because the PVs, in particular at high penetration levels, increase the voltages on the feeder, which results in more power consumed by the loads on the feeder. The PVs in our simulation operate at unity power factor, that is, they provide active power, but no reactive power. Consequently, the net consumption of reactive power is increased. On the other hand, the net consumption of active power is reduced because the additional active power (due to the voltage increase) is supplied by the PV. Note that this result depends strongly on the load mix on the feeder – we modeled all loads as ZIP loads with 70% active power and 30% reactive power. Our interpretation of this result is that PVs can decrease the operating efficiency of loads if the utility does not make adjustments. However, the increased voltages on the feeder due to the PV gives the utility the opportunity to apply energy saving measures such as conservation voltage reduction, that is, the utility can lower the voltage at the substation during times of PV production and the power generated by the PV will keep the voltages along the feeder within permissible limits. This practice would be particularly effective if (1) the PV is evenly distributed along the feeder as this will avoid localized regions on the feeder that have undervoltage when the voltage at the substation is reduced and (2) the PV generation is supported with sufficient storage or power factor control capability as this would avoid sudden undervoltage conditions due to clouds. Lowering the voltage at the substation will decrease the reactive power net consumption and further reduce the active power that needs to be supplied from outside generation sources.

Table of Contents

EXECUTIVE SUMMARY **II**

TABLE OF CONTENTS **VII**

TABLE OF FIGURES **IX**

TABLE OF TABLES **XVI**

1 INTRODUCTION **1**

2 CURRENT STATE OF IEEE 1547 **2**

3 POWER QUALITY AND UTILITY OPERATION ISSUES CAUSED BY PHOTOVOLTAICS **3**

3.1 Voltage Fluctuations *3*
3.2 Voltage Regulation Requirements *6*
3.3 Harmonics *8*
3.4 Islanding *10*

4 FIELD EXPERIENCE WITH HIGH-PENETRATION PV **12**

4.1 USA *12*
4.2 Japan *13*
4.3 Germany *14*
4.4 Australia *15*
4.5 Netherlands *15*
4.6 Greece *15*
4.7 Canada *16*

5 DISTRIBUTION FEEDER MODEL **17**

5.1 General Description and Selection of Distribution Feeder *17*
5.2 Modeling Approach, Assumptions, and Validation *18*
5.3 Adding PV Generators *28*
5.4 Description of Completed Model *33*

6 SOLAR GENERATION PROFILES **40**

6.1 General Procedure for Determining Irradiance Profiles at Each PV Location *40*
6.2 Solar Irradiance Levels and PV Output Power used in our Simulations *42*
6.3 Considerations for the Impact of Clouds on PV Generation Profiles *48*

7 LOAD PROFILES **51**

7.1 Example of Four-Load Scenario *51*
7.2 Example of Ten-Load Scenario *54*

7.3 Example of One-Hundred-load scenario *55*
7.4 Load Profiles Used in Our Simulations *57*
8 CASE STUDIES AND SIMULATION RESULTS **63**
8.1 Description of Simulated Scenarios and Cases *63*
8.2 Summary of Each Scenario *66*
8.3 Case Study Summary *76*
9 DISCUSSION AND CONCLUSIONS **86**
WORKS CITED **90**

Table of Figures

Figure 5-1: Short circuit comparison of simulation results from OpenDSS and SynerGEE.....20
Figure 5-2: Short circuit comparison of simulation results from OpenDSS and SynerGEE. PV generators are included in the OpenDSS simulation. 21
Figure 5-3: Comparison of power flow results from initial OpenDSS runs and customer-provided results from SynerGEE simulation runs, active power.....22
Figure 5-4: Comparison of power flow results from initial OpenDSS runs and customer-provided results from SynerGEE simulation runs, reactive power. 23
Figure 5-5: Comparison of power flow results from OpenDSS runs and customer-provided results from SynerGEE simulation runs with all capacitor banks removed from the system, reactive power. 24
Figure 5-6: Comparison of power flow results from OpenDSS runs and customer-provided results from SynerGEE simulation runs with all capacitor banks removed from the system and adjusted load kVAr ratings, reactive power.....25
Figure 5-7: Comparison of power flow results from OpenDSS runs and customer-provided results from SynerGEE simulation runs after matching active power.....26
Figure 5-8: Comparison of power flow results from initial OpenDSS runs and customer-provided results from SynerGEE simulation runs after matching reactive power.....27
Figure 5-9: Locations of PV generators and their rated output. The rated output power is logarithmically proportional to the area of the circles representing the PV generators. 28
Figure 5-10: Locations and ratings of PV Generators 1 through 24.....30
Figure 5-11: Locations and ratings of PV Generators 25 through 45.....31
Figure 5-12: Source in the utility system, its OpenDSS representation, and its representation as a Matlab object. The OpenDSS simulation of the utility system includes a single source object.....34
Figure 5-13: Lines in the utility system and their OpenDSS representations. The OpenDSS model of the utility system includes 2455 line objects and 87 different line types. 35
Figure 5-14: Transformers in the utility system and OpenDSS representations of (1) a three-phase transformer and (2) a three-phase voltage regulator. The OpenDSS model of the utility system includes seven transformer objects. 36
Figure 5-15: Loads in the utility system and OpenDSS representations of three selected loads. The OpenDSS model of the utility system includes 1733 load objects.....37
Figure 5-16: PV generators in the utility system and OpenDSS representations of three selected PV generators. The OpenDSS model of the utility system includes 45 PV generator objects.....38
Figure 5-17: Capacitor banks in the utility system and OpenDSS representations of two selected capacitor banks. The OpenDSS model of the utility system includes 4 capacitor bank objects. 39
Figure 6-1: Shadow map for Feeder B captured at 10:00 am on December 14, 2012. White-shaded areas are areas with cloud cover. The feeder map is colored in green and overlaid on a Google satellite image. 43
Figure 6-2: Comparison of modeled GHI at the PV generator and measured irradiance from one of the sensor at UC San Diego for December 14, 2012.....44

Figure 6-3: Comparison of modeled GHI at the PV generator and measured irradiance from one of the sensor at UC San Diego for a two hour period on December 14th. 44
Figure 6-4: GHI profiles from 6:00 PST to 18:00 PST on December 14th 2012 at three PV sites. 46
Figure 6-5: GHI profiles from 10 PST to 12:00 PST on December 14th 2012 at three PV sites. 46
Figure 6-6: Power output profiles for three PV sites with different sizes derived from irradiance measured on December 14, 2012 at UC San Diego, two hour time frame. 47
Figure 6-7: Power output profiles during a clear day. The profiles were obtained from filtered irradiance levels measured on December 14, 2012 at UC San Diego. 47
Figure 7-1: Aggregate load factors, all load factors, and disaggregate loads, 4 loads.....53
Figure 7-2: Comparison of aggregated load profile with sum of individual load profiles, 4 loads...53
Figure 7-3: Aggregate load factors, all load factors, and disaggregate loads, 10 loads.....54
Figure 7-4: Comparison of aggregated load profile with sum of individual load profiles, 10 loads.55
Figure 7-5: Aggregate load factors, all load factors, and disaggregate loads, 100 loads. 56
Figure 7-6: Comparison of aggregated load profile with sum of individual load profiles, 100 loads. 56
Figure 7-7: Aggregated load factors for residential, small-commercial, medium-commercial and hospital load types. 58
Figure 7-8: Aggregate load factors, all load factors, and disaggregate loads, residential. 58
Figure 7-9: Comparison of aggregated load profile with sum of individual load profiles, residential. 59
Figure 7-10: Aggregate load factors, all load factors, and disaggregate loads, small-commercial. .60
Figure 7-11: Aggregate load factors, all load factors, and disaggregate loads, small-commercial. .60
Figure 7-12: Aggregate load factors, all load factors, and disaggregate loads, medium commercial. 61
Figure 7-13: Aggregate load factors, all load factors, and disaggregate loads, medium commercial. 62
Figure 8-1: Locations of 432 PV systems used in scenario 2 and their rated output. The rated output power is logarithmically proportional to the area of the circles representing the PV generators. 64
Figure 8-2: Summary of total regulator events for all scenarios and cases.....76
Figure 8-3: Summary of maximum voltages for all scenarios and cases. 77
Figure 8-4: Summary of maximum voltage average margins for all scenarios and cases. 78
Figure 8-5: Summary of minimum voltage average margins for all scenarios and cases.....79
Figure 8-6: Summary of MW daily total losses for all scenarios and cases. 80
Figure 8-7: Summary of MVAr daily total losses for all scenarios and cases. 80
Figure 8-8: Summary of MW daylight total losses for all scenarios and cases. 81
Figure 8-9: Summary of MVar daylight total losses for all scenarios and cases. 82
Figure 8-10: Summary of MW daily total net consumption for all scenarios and cases. 83
Figure 8-11: Summary of MVArh daily total net consumption for all scenarios and cases.....83
Figure 8-12: Summary of MW daylight total net consumption for all scenarios and cases. 84
Figure 8-13: Summary of MVArh daylight total net consumption for all scenarios and cases. 85

Figure A-1: Daily voltage profile for scenario 1 and case 0. 92
Figure A-2: Daily total real power profile for scenario 1 and case 0. 93
Figure A-3: Daily current profiles for scenario 1 and case 0. 94
Figure A-4: Maximum and minimum voltages for scenario 1 and case 0. 95
Figure A-5: MW and MVAr losses for scenario 1 and case 0. 95
Figure A-6: MW and MVAr net consumption for scenario 1 and case 0. 96
Figure A-7: MW net consumption and total PV generation for scenario 1 and case 0. 96
Figure A-8: Daily voltage profile for scenario 1 case 1. 97
Figure A-9: Daily total real power profile for scenario 1 and case 1. 98
Figure A-10: Daily current profiles for scenario 1 and case 1. 99
Figure A-11: Maximum and minimum voltages for scenario 1 and case 1. 100
Figure A-12: MW and MVAr losses for scenario 1 and case 1. 100
Figure A-13: MW and MVAr net consumption for scenario 1 and case 1. 101
Figure A-14: MW net consumption and total PV generation for scenario 1 and case 1. 101
Figure A-15: Daily voltage profile for scenario 1 and case 2. 102
Figure A-16: Daily total real power profile for scenario 1 and case 2. 103
Figure A-17: Daily current profiles for scenario 1 and case 2. 104
Figure A-18: Maximum and minimum voltages for scenario 1 and case 2. 105
Figure A-19: MW and MVAr losses for scenario 1 and case 2. 105
Figure A-20: MW and MVAr net consumption for scenario 1 and case 2. 106
Figure A-21: MW net consumption and total PV generation for scenario 1 and case 2. 106
Figure A-22: Daily voltage profile for scenario 1 case 3. 107
Figure A-23: Daily total real power profile for scenario 1 and case 3. 108
Figure A-24: Daily current profiles for scenario 1 and case 3. 109
Figure A-25: Maximum and minimum voltages for scenario 1 and case 3. 110
Figure A-26: MW and MVAr losses for scenario 1 and case 3. 110
Figure A-27: MW and MVAr net consumption for scenario 1 and case 3. 111
Figure A-28: MW net consumption and total PV generation for scenario 1 and case 3. 111
Figure A-29: Daily voltage profile for scenario 1 case 4. 112
Figure A-30: Daily total real power profile for scenario 1 and case 4. 113
Figure A-31: Daily current profiles for scenario 1 and case 4. 114
Figure A-32: Maximum and minimum voltages for scenario 1 and case 4. 115
Figure A-33: MW and MVAr losses for scenario 1 and case 4. 115
Figure A-34: MW and MVAr net consumption for scenario 1 and case 4. 116
Figure A-35: MW net consumption and total PV generation for scenario 1 and case 4. 116
Figure A-36: Daily voltage profile for scenario 1 case 5. 117
Figure A-37: Daily total real power profile for scenario 1 and case 5. 118
Figure A-38: Daily current profiles for scenario 1 and case 5. 119
Figure A-39: Maximum and minimum voltages for scenario 1 and case 5. 120
Figure A-40: MW and MVAr losses for scenario 1 and case 5. 120
Figure A-41: MW and MVAr net consumption for scenario 1 and case 5. 121

Figure A-42: MW net consumption and total PV generation for scenario 1 and case 5. 121
Figure A-43: Daily voltage profile for scenario 1 case 6. 122
Figure A-44: Daily total real power profile for scenario 1 and case 6. 123
Figure A-45: Daily current profiles for scenario 1 and case 6. 124
Figure A-46: Maximum and minimum voltages for scenario 1 and case 6. 125
Figure A-47: MW and MVAr losses for scenario 1 and case 6. 125
Figure A-48: MW and MVAr net consumption for scenario 1 and case 6. 126
Figure A-49: MW net consumption and total PV generation for scenario 1 and case 6. 126
Figure B-1: Daily voltage profile for scenario 2 case 0. 127
Figure B-2: Daily total real power profile for scenario 2 and case 0. 128
Figure B-3: Daily current profiles for scenario 2 and case 0. 129
Figure B-4: Maximum and minimum voltages for scenario 2 and case 0. 130
Figure B-5: MW and MVAr losses for scenario 2 and case 0. 130
Figure B-6: MW and MVAr net consumption for scenario 2 and case 0. 131
Figure B-7: MW net consumption and total PV generation for scenario 2 and case 0. 131
Figure B-8: Daily voltage profile for scenario 2 case 1. 132
Figure B-9: Daily total real power profile for scenario 2 and case 1. 133
Figure B-10: Daily current profiles for scenario 2 and case 1. 134
Figure B-11: Maximum and minimum voltages for scenario 2 and case 1. 135
Figure B-12: MW and MVAr losses for scenario 2 and case 1. 135
Figure B-13: MW and MVAr net consumption for scenario 2 and case 1. 136
Figure B-14: MW net consumption and total PV generation for scenario 2 and case 1. 136
Figure B-15: Daily voltage profile for scenario 2 case 2. 137
Figure B-16: Daily total real power profile for scenario 2 and case 2. 138
Figure B-17: Daily current profiles for scenario 2 and case 2. 139
Figure B-18: Maximum and minimum voltages for scenario 2 and case 2. 140
Figure B-19: MW and MVAr losses for scenario 2 and case 2. 140
Figure B-20: MW and MVAr net consumption for scenario 2 and case 2. 141
Figure B-21: MW net consumption and total PV generation for scenario 2 and case 2. 141
Figure B-22: Daily voltage profile for scenario 2 case 3. 142
Figure B-23: Daily total real power profile for scenario 2 and case 3. 143
Figure B-24: Daily current profiles for scenario 2 and case 3. 144
Figure B-25: Maximum and minimum voltages for scenario 2 and case 3. 145
Figure B-26: MW and MVAr losses for scenario 2 and case 3. 145
Figure B-27: MW and MVAr net consumption for scenario 2 and case 3. 146
Figure B-28: MW net consumption and total PV generation for scenario 2 and case 3. 146
Figure B-29: Daily voltage profile for scenario 2 case 4. 147
Figure B-30: Daily total real power profile for scenario 2 and case 4. 148
Figure B-31: Daily current profiles for scenario 2 and case 4. 149
Figure B-32: Maximum and minimum voltages for scenario 2 and case 4. 150
Figure B-33: MW and MVAr losses for scenario 2 and case 4. 150

Figure B-34: MW and MVAr net consumption for scenario 2 and case 4. 151
Figure B-35: MW net consumption and total PV generation for scenario 2 and case 4. 151
Figure B-36: Daily voltage profile for scenario 2 case 5. 152
Figure B-37: Daily total real power profile for scenario 2 and case 5. 153
Figure B-38: Daily current profiles for scenario 2 and case 5. 154
Figure B-39: Maximum and minimum voltages for scenario 2 and case 5. 155
Figure B-40: MW and MVAr losses for scenario 2 and case 5. 155
Figure B-41: MW and MVAr net consumption for scenario 2 and case 5. 156
Figure B-42: MW net consumption and total PV generation for scenario 2 and case 5. 156
Figure B-43: Daily voltage profile for scenario 2 case 6. 157
Figure B-44: Daily total real power profile for scenario 2 and case 6. 158
Figure B-45: Daily current profiles for scenario 2 and case 6. 159
Figure B-46: Maximum and minimum voltages for scenario 2 and case 6. 160
Figure B-47: MW and MVAr losses for scenario 2 and case 6. 160
Figure B-48: MW and MVAr net consumption for scenario 2 and case 6. 161
Figure B-49: MW net consumption and total PV generation for scenario 2 and case 6. 161
Figure C-1: Daily voltage profile for scenario 3 case 0. 162
Figure C-2: Daily total real power profile for scenario 3 and case 0. 163
Figure C-3: Daily current profiles for scenario 3 and case 0. 164
Figure C-4: Maximum and minimum voltages for scenario 3 and case 0. 165
Figure C-5: MW and MVAr losses for scenario 3 and case 0. 165
Figure C-6: MW and MVAr net consumption for scenario 3 and case 0. 166
Figure C-7: MW net consumption and total PV generation for scenario 3 and case 0. 166
Figure C-8: Daily voltage profile for scenario 3 case 1. 167
Figure C-9: Daily total real power profile for scenario 3 and case 1. 168
Figure C-10: Daily current profiles for scenario 3 and case 1. 169
Figure C-11: Maximum and minimum voltages for scenario 3 and case 1. 170
Figure C-12: MW and MVAr losses for scenario 3 and case 1. 170
Figure C-13: MW and MVAr net consumption for scenario 3 and case 1. 171
Figure C-14: MW net consumption and total PV generation for scenario 3 and case 1. 171
Figure C-15: Daily voltage profile for scenario 3 case 2. 172
Figure C-16: Daily total real power profile for scenario 3 and case 2. 173
Figure C-17: Daily current profiles for scenario 3 and case 2. 174
Figure C-18: Maximum and minimum voltages for scenario 3 and case 2. 175
Figure C-19: MW and MVAr losses for scenario 3 and case 2. 175
Figure C-20: MW and MVAr net consumption for scenario 3 and case 2. 176
Figure C-21: MW net consumption and total PV generation for scenario 3 and case 2. 176
Figure C-22: Daily voltage profile for scenario 3 case 3. 177
Figure C-23: Daily total real power profile for scenario 3 and case 3. 178
Figure C-24: Daily current profiles for scenario 3 and case 3. 179
Figure C-25: Maximum and minimum voltages for scenario 3 and case 3. 180

Figure C-26: MW and MVAr losses for scenario 3 and case 3. 180
Figure C-27: MW and MVAr net consumption for scenario 3 and case 3. 181
Figure C-28: MW net consumption and total PV generation for scenario 3 and case 3. 181
Figure C-29: Daily voltage profile for scenario 3 case 4. 182
Figure C-30: Daily total real power profile for scenario 3 and case 4. 183
Figure C-31: Daily current profiles for scenario 3 and case 4. 184
Figure C-32: Maximum and minimum voltages for scenario 3 and case 4. 185
Figure C-33: MW and MVAr losses for scenario 3 and case 4. 185
Figure C-34: MW and MVAr net consumption for scenario 3 and case 4. 186
Figure C-35: MW net consumption and total PV generation for scenario 3 and case 4. 186
Figure C-36: Daily voltage profile for scenario 3 case 5. 187
Figure C-37: Daily total real power profile for scenario 3 and case 5. 188
Figure C-38: Daily current profiles for scenario 3 and case 5. 189
Figure C-39: Maximum and minimum voltages for scenario 3 and case 5. 190
Figure C-40: MW and MVAr losses for scenario 3 and case 5. 190
Figure C-41: MW and MVAr net consumption for scenario 3 and case 5. 191
Figure C-42: MW net consumption and total PV generation for scenario 3 and case 5. 191
Figure C-43: Daily voltage profile for scenario 3 case 6. 192
Figure C-44: Daily total real power profile for scenario 3 and case 6. 193
Figure C-45: Daily current profiles for scenario 3 and case 6. 194
Figure C-46: Maximum and minimum voltages for scenario 3 and case 6. 195
Figure C-47: MW and MVAr losses for scenario 3 and case 6. 195
Figure C-48: MW and MVAr net consumption for scenario 3 and case 6. 196
Figure C-49: MW net consumption and total PV generation for scenario 3 and case 6. 196
Figure D-1: Daily voltage profile for scenario 4 case 0. 197
Figure D-2: Daily total real power profile for scenario 4 and case 0. 198
Figure D-3: Daily current profiles for scenario 4 and case 0. 199
Figure D-4: Maximum and minimum voltages for scenario 4 and case 0. 200
Figure D-5: MW and MVAr losses for scenario 4 and case 0. 200
Figure D-6: MW and MVAr net consumption for scenario 4 and case 0. 201
Figure D-7: MW net consumption and total PV generation for scenario 4 and case 0. 201
Figure D-8: Daily voltage profile for scenario 4 case 1. 202
Figure D-9: Daily total real power profile for scenario 4 and case 1. 203
Figure D-10: Daily current profiles for scenario 4 and case 1. 204
Figure D-11: Maximum and minimum voltages for scenario 4 and case 1. 205
Figure D-12: MW and MVAr losses for scenario 4 and case 1. 205
Figure D-13: MW and MVAr net consumption for scenario 4 and case 1. 206
Figure D-14: MW net consumption and total PV generation for scenario 4 and case 1. 206
Figure D-15: Daily voltage profile for scenario 4 case 2. 207
Figure D-16: Daily total real power profile for scenario 4 and case 2. 208
Figure D-17: Daily current profiles for scenario 4 and case 2. 209

Figure D-18: Maximum and minimum voltages for scenario 4 and case 2. 210
Figure D-19: MW and MVAr losses for scenario 4 and case 2. 210
Figure D-20: MW and MVAr net consumption for scenario 4 and case 2. 211
Figure D-21: MW net consumption and total PV generation for scenario 4 and case 2. 211
Figure D-22: Daily voltage profile for scenario 4 case 3. 212
Figure D-23: Daily total real power profile for scenario 4 and case 3. 213
Figure D-24: Daily current profiles for scenario 4 and case 3. 214
Figure D-25: Maximum and minimum voltages for scenario 4 and case 3. 215
Figure D-26: MW and MVAr losses for scenario 4 and case 3. 215
Figure D-27: MW and MVAr net consumption for scenario 4 and case 3. 216
Figure D-28: MW net consumption and total PV generation for scenario 4 and case 3. 216
Figure D-29: Daily voltage profile for scenario 4 case 4. 217
Figure D-30: Daily total real power profile for scenario 4 and case 4. 218
Figure D-31: Daily current profiles for scenario 4 and case 4. 219
Figure D-32: Maximum and minimum voltages for scenario 4 and case 4. 220
Figure D-33: MW and MVAr losses for scenario 4 and case 4. 220
Figure D-34: MW and MVAr net consumption for scenario 4 and case 4. 221
Figure D-35: MW net consumption and total PV generation for scenario 4 and case 4. 221
Figure D-36: Daily voltage profile for scenario 4 case 5. 222
Figure D-37: Daily total real power profile for scenario 4 and case 5. 223
Figure D-38: Daily current profiles for scenario 4 and case 5. 224
Figure D-39: Maximum and minimum voltages for scenario 4 and case 5. 225
Figure D-40: MW and MVAr losses for scenario 4 and case 5. 225
Figure D-41: MW and MVAr net consumption for scenario 4 and case 5. 226
Figure D-42: MW net consumption and total PV generation for scenario 4 and case 5. 226
Figure D-43: Daily voltage profile for scenario 4 case 6. 227
Figure D-44: Daily total real power profile for scenario 4 and case 6. 228
Figure D-45: Daily current profiles for scenario 4 and case 6. 229
Figure D-46: Maximum and minimum voltages for scenario 4 and case 6. 230
Figure D-47: MW and MVAr losses for scenario 4 and case 6. 230
Figure D-48: MW and MVAr net consumption for scenario 4 and case 6. 231
Figure D-49: MW net consumption and total PV generation for scenario 4 and case 6. 231

Table of Tables

Table 3-1: Flicker levels according to IEEE Std. 1453. 4
Table 3-2: Range A and Range B service voltage limits according to ANSI C84.1. 7
Table 3-3: IEEE 519-1992 individual and total odd harmonic current limits given in percent of load current. Even harmonics are limited to 25% of the odd harmonic limits. 9
Table 5-1: Characteristics of five distribution feeders as provided by the host utility. 17
Table 5-2: List of PV locations and ratings on circuit B. 29
Table 5-3: Main characteristics of circuit B. 33
Table 8-1: Summary of the simulation cases 65
Table 8-2: Summary of the voltage regulators tap change operations increase for the individual cases, Scenario 1. 66
Table 8-3: Summary of the daily maximum per unit voltage values for the individual cases, Scenario 1. 66
Table 8-4: Summary of the minimum and maximum voltage average margin between simulations with PV and without PV for the individual cases, Scenario 1. 67
Table 8-5: Summary of the MWh and MVArh daily losses, Scenario 1. 67
Table 8-6: Summary of the MWh and MVArh daylight losses, Scenario 1. 67
Table 8-7: Summary of the MWh and MVArh daily net consumption, Scenario 1. 68
Table 8-8: Summary of the MWh and MVArh daylight net consumption, Scenario 1. 68
Table 8-9: Summary of the voltage regulators tapchange operations increase for the individual cases, Scenario 2. 68
Table 8-10: Summary of the daily maximum per unit voltage values for the individual cases, Scenario 2. 69
Table 8-11: Summary of the minimum and maximum voltage average margin between simulations with PV and without PV for the individual cases, Scenario 2. 69
Table 8-12: Summary of the MWh and MVArh daily losses, Scenario 2. 69
Table 8-13: Summary of the MWh and MVArh daylight losses, Scenario 2. 70
Table 8-14: Summary of the MWh and MVArh daily net consumption, Scenario 2. 70
Table 8-15: Summary of the MWh and MVArh daylight net consumption, Scenario 2. 70
Table 8-16: Summary of the voltage regulators tap change operations for the individual cases, Scenario 3. 71
Table 8-17: Summary of the daily maximum per unit voltage values for the individual cases, Scenario 3. 71
Table 8-18: Summary of the minimum and maximum voltage average margin between simulations with PV and without PV for the individual cases, Scenario 3. 71
Table 8-19: Summary of the MWh and MVArh daily losses, Scenario 3. 72
Table 8-20: Summary of the MWh and MVArh daylight losses, Scenario 3. 72
Table 8-21: Summary of the MWh and MVArh daily net consumption, Scenario 3. 72
Table 8-22: Summary of the MWh and MVArh daylight net consumption, Scenario 3. 73

Table 8-23: Summary of the voltage regulators tap change operations increase for the individual cases, Scenario 4. 73
Table 8-24: Summary of the daily maximum per unit voltage values for the individual cases, Scenario 4. 73
Table 8-25: Summary of the minimum and maximum voltage average margin between simulations with PV and without PV for the individual cases, Scenario 4. 74
Table 8-26: Summary of the MWh and MVArh daily losses, Scenario 4. 74
Table 8-27: Summary of the MWh and MVArh daylight losses, Scenario 4. 74
Table 8-28: Summary of the MWh and MVArh daily net consumption, Scenario 4. 75
Table 8-29: Summary of the MWh and MVArh daylight net consumption, Scenario 4. 75
Table 8-30: Summary of the voltage regulators tap changing operations increase, shown as percentage increase between simulations with PV and without PV, for the individual cases and scenarios 77
Table 8-31: Summary of the daily maximum per unit voltage values, shown as percentage margins between simulations with PV and without PV, for the individual cases and scenarios 78
Table 8-32: Summary of the minimum and maximum voltage average margin between simulations with PV and without PV for the individual cases and scenarios 79
Table 8-33: Summary of the MWh and MVArh daily losses, shown as percentage increase between simulations with PV and without PV, for the individual cases and scenarios 81
Table 8-34: Summary of the MWh and MVArh daylight losses, shown as percentage increase between simulations with PV and without PV, for the individual cases and scenarios 82
Table 8-35: Summary of the MWh and MVArh daily net consumption, shown as percentage margins between simulations with PV and without PV, for the individual cases and scenarios 84
Table 8-36: Summary of the MWh and MVArh daylight net consumption 85

1 Introduction

Small scale renewable generation and non-renewable generation are being incentivized in California and nationwide. Currently 1% of San Diego Gas & Electric's (SDG&E's) customers have installed distributed solar PV systems. Pacific Gas & Electric (PG&E) leads the nation with the highest number of interconnected PV. Southern California Edison (SCE) reports PV penetration levels of up to 70% for some of their distribution feeder circuits. Small numbers of PV generation systems cause few or no problems on the grid, but as the percentage of PV generation grows, a number of issues begin to appear.

This study focuses on the integration and economic impacts of Distributed Renewable Generation on grid operation. Specifically, we investigated (1) how the distribution feeder loading changes with PV penetration level, (2) the impact of increased PV penetration on system losses, and (3) the effect of voltage fluctuation due to changing generation levels of PV on voltage regulator operation. This report documenting the results of our study is structured as follows:

- Chapter 2 briefly reviews the current state (as of March 2013) of IEEE Std. 1547-2008, which is the "Standard for Interconnecting Distributed Resources with Electric Power Systems".
- Chapter 3 documents (1) concerns and potential issues caused by the presence of high-penetration solar in distribution systems and (2) requirements imposed by IEEE 1547 and other interconnection standards.
- Chapter 4 reviews reports that document the experience with high-penetration PV that US utilities and utilities in other countries had.
- Chapter 5 gives detailed information of the distribution feeder circuit we used in our simulations, and explains how we modeled the PVs in the system.
- In Chapter 6, we (1) describe the instruments and the process we used to obtain the cloud map and irradiance data, (2) present examples for irradiance profiles we used in our simulations, and (3) discuss the impact of clouds on PV output power and describe our process for generating solar generation profiles from the measured irradiance data and cloud maps.
- In Chapter 7, we develop a stochastic algorithm to create individual load profiles based on aggregated load curves.
- In Chapter 8, we describe the investigated PV penetration scenarios and the different simulation assumptions/settings we use to simulate these scenarios. We also present summaries of our simulation results for each scenario and for all scenarios combined. Detailed simulation results for each scenario are included in the Appendix
- Chapter 9 discusses our simulations results and summarizes our findings.

2 Current State of IEEE 1547

IEEE Std. 1547-2008 is the "Standard for Interconnecting Distributed Resources with Electric Power Systems". This standard was initially approved in 2003, and re-affirmed with no changes in 2008. This standard is technically voluntary, but has been referenced in the Federal Energy Policy Act of 2005 and by many state regulatory commissions. Many utility tariffs also specifically reference the standard. One of the limitations is that IEEE Std. 1547 only applies to generation up to 10 MVA in size, at the point of interconnection. There is a gap between this level and the 20-MVA limit on "small generation" defined by FERC and many other agencies. In addition to the main standard, there are currently seven sub-parts published or under development as of January 2013.

1. IEEE Std. 1547.1-2005: IEEE Standard Conformance Test Procedures for Equipment Interconnecting Distributed Resources With Electric Power Systems (active)
2. IEEE Std. 1547.2-2008: IEEE Application Guide for IEEE Std 1547 (active)
3. IEEE Std. 1547.3-2007: IEEE Guide for Monitoring, Information Exchange, and Control of Distributed Resources Interconnected With Electric Power Systems (active)
4. IEEE Std. 1547.4-2011: IEEE Guide for Design, Operation, and Integration of Distributed Resource Island Systems with Electric Power Systems
5. Withdrawn: IEEE Std. 1547.5: Draft Technical Guidelines for Interconnection of Electric Power Sources Greater than 10MVA to the Power Transmission Grid (under development)
6. IEEE Std. 1547.6-2011: IEEE Recommended Practice For Interconnecting Distributed Resources With Electric Power Systems Distribution Secondary Networks
7. IEEE Std. 1547.7: Draft Guide to Conducting Distribution Impact Studies for Distributed Resource Interconnection (under development)
8. 7. IEEE Std. 1547.7: Draft Recommended Practice for Establishing Methods and Procedures that Provide Supplemental Support for Implementation Strategies for Expanded Use of IEEE Standard 1547

IEEE Std. 1547.5 was withdrawn in December 2011 and material from it is being folded into IEEE 1547.8. IEEE Std. 1547.7 is nearing completion and ready to go to ballot in early 2013 (as of January 2013). Additionally, IEEE Std. 1547 is being amended in 2013 to address voltage regulation and response to area electric power systems abnormal conditions of voltage and frequency. A major revision of IEEE Std. 1547 will follow by 2018.

In Chapter 3, we review the requirement imposed by IEEE 1547 and other interconnection standards.

3 Power Quality and Utility Operation Issues caused by Photovoltaics

In general, PV generators are connected to the utility grid or a micro grid in three different ways – (1) large PV plants that are composed of a number of PV generators that connect to the transmission grid via a dedicated collector system, (2) individual PV generators that connect directly to the distribution grid or to a microgrid,, and (3) PV generators that are connected "on the other side of the utility meter". [1] PV generators connected directly to the distribution grid (connection type 2 above) can be fairly large (100s of kW) and, if so, are often referred to as centralized PV. PV generators connected "on the other side of the meter" (connection type 3 above) are usually small (a few kW) that are installed on rooftops or next to residential, commercial, or industrial buildings. However, the aggregated generation of a large number of these small PV generators installed on a feeder can still be large. In general, these small PV generators are more dispersed and, consequently, are often referred to as Distributed Generation (DG). The connection type of the PV generators does have an impact on the issues that are of concern. In this section, we give an overview of potential detrimental effects that PV connected in distribution systems (connection types 2 and 3 above) have on power quality and utility operation, and list applicable standards.

3.1 Voltage Fluctuations

Changing PV generation levels and changing generation levels from other distributed resources can produce voltage fluctuations on the electric power system. Conventional generation may also switch on or off at any time, but less frequently. Distributed wind generation is varying, but changes in wind speed are not as fast as changes in irradiance levels and the impact of the wind speed change is "smoothened" by the wind turbine inertia. On the other hand, cloud shading may cause fast changes of irradiance levels, which results in immediate changes of the generated power from the inertialess PV. These changes will result in low-frequency voltage fluctuations on the distribution system, which is perceived by the customer in the form of changing light intensity and commonly referred to as "flicker".

Flicker impacts may be quantified using one of the metrics listed below:

- The short term flicker coefficient P_{ST} is used to quantify voltage fluctuations due to disturbances with a short duty cycle or disturbances that produce continuous fluctuations. The observation period for short-term flicker is typically a 10 minutes time interval.
- The long term flicker coefficient P_{LT} is used to quantify voltage fluctuations due to disturbances with a long duty cycle. The observation period for long-term flicker is typically two hours. Note that in the absence of short duty cycle disturbances, the values for P_{ST} and P_{LT} are equal.

- Maximum step voltage change in percent, for infrequent events.
- Increased number of regulator tap change operations in a period.
- Increased number of capacitor switching operations in a period.
- Comparison to curves that indicate voltage variation such as the Information Technology Industry Council (ITIC) curve.

The most accurate method for measuring flicker is to use so-called flicker meters. Generally, a flicker meter is composed of three sections. In the first section, the input waveform is demodulated, thus removing the carrier signal. As a result of the demodulator, the dc offset and higher frequency terms (sidebands) are produced. The second section removes these unwanted terms using filters, thus leaving only the modulating (flicker) signal remaining. The second section also consists of filters that weigh the modulating signal according to the particular meter's specifications. The last section usually consists of a statistical analysis of the measured flicker [2].

Applicable Standards

IEEE Std. 1453-2004 adopts the flicker evaluation and measurement methods in IEC Std. 61000-3-3, -3-5, -3-7, and -4-15. In fact, IEC 61000-4-15, the flicker meter specification, was adopted as a normative annex of IEEE 1453. The IEC flicker meter measures voltage fluctuations, weighted as a function of frequency to produce one output value, but it also embeds the characteristics of incandescent lamps. Newer lamp types, and other load types, should probably weigh the voltage fluctuations differently to evaluate the impact. The P_{ST} output is defined for a 10-minute period. A long-term flicker severity, P_{LT}, is defined over a 2-hour period by the cubic geometric mean of 12 consecutive P_{ST} samples. This method produces an output for any voltage fluctuation within the previous 2 hours, albeit weighted for incandescent lamps.

The main body of IEEE Std. 1453 adopts flicker compatibility limits and planning levels. The compatibility limit is the severity level at which customer complaints are likely to occur. The planning level is used to set limits on new loads (or DER), which have to be coordinated with other fluctuating loads on the system. These levels are listed in Table 3-1.

Table 3-1: Flicker levels according to IEEE Std. 1453.

Flicker Severity Level	Compatibility Level	Planning Level, Medium Voltage	Planning Level, High Voltage and Extra High Voltage
P_{ST} [10-minute]	1.0	0.9	0.8
P_{LT} [120-minute]	1.0	0.7	0.6

For distributed generation applied on medium-voltage systems, the applicable planning limits would be P_{ST} = 0.9 and P_{LT} = 0.7. Some types of equipment, in particular wind turbines, require vendor test reports for a complete flicker evaluation. For wind turbines, the applicable standard is IEC 61400-21, on power quality characteristics of grid-connected wind turbines. Members of the 1453 Task Force have published panel session summaries and a tutorial on applying the standard, including aggregation of sources, transfer to lower voltage levels, and other application topics.

IEEE Std. 1453-2004 supersedes most of IEEE Std. 141-1993, and the flicker sections of IEEE Std. 519-1992. This change has been noted in the reaffirmed Std. 1547, and the recently adopted 1547.2. The main body of 1453 states that limitations from 141-1993 are still useful for infrequent events, because the IEC flicker meter works best for periods of one hour or less. An informative annex gives the percent voltage dip from 141-1993 as 2.7% for perception and 6% for irritation, at 1 dip per hour. In IEC terms, these would be equivalent to 5.4% and 12%, respectively, at 0.017 changes per minute.

Maximum Step-Voltage Change

As with a large motor starting, a large distributed resource switching on or off would produce a step voltage change, which depends on the short-circuit strength at the point of common coupling, and on the distributed resource's operating point (real and reactive power). This may be compared against a hard limit, such as 3%, if already established by the utility. Section 4.1.3 of Std. 1547 imposes a hard limit equal to 5% of the prevailing voltage at the PCC. The IEC flicker meter will also produce a non-zero output during such operations, which may be compared to the planning and compatibility levels for P_{ST} and P_{LT}.

Voltage Control Operations

If the voltage fluctuations yield more capacitor switching and tap change operations, equipment wear would increase and equipment life may decrease. Additional capacitor switching operations may also cause utility customers to experience more transient overvoltage events. The power system voltage control system can be simulated over the normal load profile for a defined period (e.g., one day, one week, or one year), and the number of switching / tap change events noted. Then a repeat of the simulation with distributed resource-induced voltage fluctuations would show the expected increase in switching / tap change events. The capacitor switches and tap changers may have a rated number of operations for comparison to this number. Capacitor banks might normally switch twice daily, once on and a second time off, but in any case, a percentage increase in switching operations could occur from distributed resource-induced voltage fluctuations, and this could have a power quality impact on power system loads. The level

of transient overvoltage depends on capacitor switch characteristics (e.g., synchronous closing, pre-insertion impedance) and random effects of the pole closing instants. [3]

3.2 Voltage Regulation Requirements

Over-/undervoltages can occur during (1) steady-state operation and (2) during momentary disturbance, such as utility switching operation, fault clearing, large motor starts, lightning strikes, etc.. In this section, we discuss sustained (steady-state) over-/undervoltages.

The voltage provided to utility customers must be kept within certain limits (1) to ensure correct operation of the customers' equipment that is supplied by the voltage and (2) to prevent safety hazards due to overvoltages. Detrimental effects of sustained over-/undervoltage include

- inhibiting the correct operation of the customers' equipment (e.g., machines running too fast or too slow),
- tripping of sensitive load,
- overheating of induction motors (induction motors operated below rated voltage draw more current, which increases heating losses),
- premature failure (e.g., the life cycle of incandescent lights operated at higher-than-rated voltage decreases), and
- increased losses during overvoltage conditions.

Most regulatory entities and utilities in the USA adhere to the voltage limits specified in ANSI C84.1. The standard specifies two different tolerances for two different locations in the power systems. The preferred, more restrictive, voltage range is 'Range A' and the less restrictive voltage range is 'Range B'. 'Range B' voltages that are outside 'Range A' may be acceptable in "problem systems" but, according to the standard "… corrective measures shall be undertaken within a reasonable time to improve voltages to meet Range A requirements." Both ranges allow for voltages that are outside the specified limits, but these excursions "should be infrequent". ANSI C84.1 specifies limits for the service voltage and the utilization voltages. The service voltage is the voltage at the point where the customer connects to the system (usually at the meter) – maintaining the service voltage within acceptable limits is the utility's responsibility. The utilization voltage is the voltage that is supplied to the customer's equipment (for instance, the voltage at the outlet). The utilization voltage is typically less than the service voltage due to the voltage drop caused by the wiring of the facility, but, if the service voltage is within acceptable limits and the wiring is done according to building codes, which is the customer's responsibility, then the utilization voltage is expected to be within acceptable limits as well. Table 3-2 lists the ANSI C84.1 service voltage limits for Range A and Range B.

Table 3-2: Range A and Range B service voltage limits according to ANSI C84.1.

	120 V to 600 V		above 600 V	
	Min	Max	Min	Max
Range A	-5%	+5%	-2.5%	+5%
Range B	-8.3%	+5.8%	-5%	+5.8%

Most utilities control the voltage on the secondary distribution circuit (the low-voltage circuit the customer is directly connected to) by regulating the voltage on the primary circuit (the distribution feeder circuit with typical voltage levels between 4 kV and 35 kV). The service voltage is the stepped-down feeder voltage minus the losses (i.e., service transformer losses and wiring losses). Based on the expected load, utilities can design service transformer sizes and the size and length of a service connection so that the service voltage stays within acceptable limits. Equipment that is at the utilities disposal for regulating the primary circuit voltage include (1) Load Tap-Changing transformers (LTCs) at the substation and on the line and (2) shunt capacitor banks. In general, any control operation of the voltage regulation equipment (changing of the taps or switching of capacitor steps) is detrimental to the lifetime of the regulation equipment and an excessive number of control operations can dramatically reduce the equipment lifetime.

Inverters used in many DGs usually have power factor correction capabilities. However, IEEE 1547 forbids the DG to actively regulate voltage, which is a somewhat controversial requirement. Opponents of this requirement argue that this restriction is counter innovative in the sense that it curbs the full potential of DG inverter technology. A consequence of IEEE 1547 restriction is that on systems that require active regulation to meet the area service voltage requirements (see Table 3-2), equipment other than the DG must be employed to change the reactive power in direct response to measured voltage conditions. Active regulation can come from, for instance, D-STACOMs, which typically use inverter technology that is similar to the inverter technology employed in modern DGs. The opponents of the IEEE 1547 requirement point out that it is inefficient to use DG inverters to force operation at constant power factor (in response to varying environmental conditions) and then employ D-STATCOMs to provide dynamic power factor control (in response to the measured voltage fluctuations) instead of using the DG alone to control the power factor in response to varying environmental conditions AND system voltage fluctuations.

There is consensus in the standard-developing community that employing DG for active regulation of the PCC voltage is (1) technically feasible, (2) requires coordination between the DG operator and the area Electric Power System (EPS) operator in order to ensure proper operation of regulation equipment operated by the area EPS, and (3) violates the IEEE 1547 requirement

and is therefore currently not an option on systems that follow IEEE 1547. This current status quo is in place because the working group that developed the IEEE 1547 standard decided that, at the time the standard was written, the problems associated with active regulation from the DG outweigh the obvious benefits of DG providing active regulation of the PCC voltage. Some of the arguments that led to the acceptance of this IEEE 1547 requirement are listed below:

- The current market structure makes it difficult to provide ancillary services to the area EPS operators due to the need of uniform rules for the public utilities.
- Since IEEE 1547 was published, many manufacturers designed their products to meet IEEE 1547 requirements. Consequently, many current installations that employ these products do not have the capability to actively regulate the area EPS voltage and will not benefit from lifting the IEEE 1547 requirement.
- Active regulation could lead to communication and control interactions between utilities and DG owners, which some DG proponents wished to avoid at the time 1547 was adopted.

3.3 Harmonics

Harmonics are sinusoidal voltages and currents with frequencies that are integer multiples of the fundamental frequency (60 Hz in the United States). The value of the multiplier corresponds to the harmonic order. Undesirable effects of harmonics include:

- Nuisance tripping of breakers and fuses
- Transformer overheating resulting in the shortening of the expected lifetime
- Degrade meter accuracy due to uncertainties on how to measure active power and reactive power of a distorted signal
- Failed capacitor cans due to excessive harmonic currents or overvoltage stress on dielectrics
- Overloaded neutral conductors (third harmonic currents do not cancel in the neutral conductor)
- Increased ohmic losses and shortened lifetime of cables
- Motor heating
- Control misoperation
- Communication system interference

The measure for the degree of harmonic contamination of a waveform by a single harmonic is the Individual Harmonic Distortion (IHD) level, which is the ratio of the magnitude of a given harmonic to the magnitude of the fundamental multiplied by 100%. The measure for the degree of harmonic contamination of a waveform by all harmonics is the Total Harmonic Distortion (THD)

level. The THD is the ratio of RMS of the individual harmonic content of a signal to the fundamental multiplied by 100%:

$$THD = \frac{\sqrt{\sum_{i=2}^{n} {H_i}^2}}{H_1} \cdot 100\%$$

where H1 is the fundamental harmonic (e.g., 60-Hz voltage or current) and H_i is the ith harmonic. IEEE 519-1992 recommends limiting the voltage THD at the Point of Common Coupling to below 5%. The IEEE 1547 limits for harmonic current distortion are based upon the limits provided in IEEE 519-1992, utilizing the most stringent current injection limits for distribution systems. The current IHD and THD limits are based on load size (quantified by the load current IL) with respect to the size of the power system to which the load is connected (quantified by the short-circuit current ISC). The IEEE 519 recommended current distortion values for single consumers for various short-circuit current to load current ratios are shown in Table 3-3. Harmonic current and voltage distortion limits are also specified in the IEC standards 61000 parts 3-2 and 3-4 for equipment with rated currents of below 16 A and above 16 A, respectively.

Table 3-3: IEEE 519-1992 individual and total odd harmonic current limits given in percent of load current. Even harmonics are limited to 25% of the odd harmonic limits.

I_{SC}/I_L	IHD for Odd Harmonic Currents					THD for Odd Harmonic Currents
	h < 11	11 ≤ h < 17	17 ≤ h < 23	23 ≤ h < 35	35 ≤ h	
<20	4.0%	2.0%	1.5%	0.6%	0.3%	5.0%
20-50	7.0%	3.5%	2.5%	1.0%	0.5%	8.0%
50-100	10.0%	4.5%	4.0%	1.5%	0.7%	12.0%
100-1000	12.0%	5.5%	5.0%	2.0%	1.0%	15.0%
>1000	15.0%	7.0%	6.0%	2.5%	1.4%	20.0%

Note that IEEE 519 is not a standard but rather a document that provides information on recommended practices for engineers to control harmonics in order to avoid a number of undesirable effects and impacts on the operation of loads and system equipment. According to IEEE 519, the responsibility to limit harmonics lies both with the end-user and utilities. The end-user has control over the harmonic current through the load the user connects to the system; the resulting harmonic voltage is typically the responsibility of the utility. However, what complicates things is that the harmonic distortion present in the system is determined by both the injected harmonic current and the system impedance, which is a function of the injected harmonic current

and vice versa. Consequently, harmonic current on some equipment in the power system such as transformers and capacitors may need to be limited during, for instance, resonant conditions even if the harmonic voltage is within IEEE 519 limits. Vice versa, exceeding the harmonic current distortion limits does not always result in a violation of harmonic voltage limits – a single user may exceed the harmonic current distortion limits without causing excessive harmonic voltages in the system. Consequently, the recommended harmonic current limits in IEEE 519 can be overly restrictive in some situations, which is important to be aware of when utilizing the current limits to govern decisions regarding the installation of expensive mitigation equipment to limit harmonic currents. [4]

Harmonic distortion in distribution systems predominately originates from loads in which the current is not linearly related to the voltage. However, harmonics can also be generated on the generation side. All distributed generation technologies that generate either dc or non-power frequency ac must use an electronic power inverter to interface with the electric power system. The early thyristor-based, line-commutated inverters quickly developed a reputation for being undesirable on the power system. These inverters produced harmonic currents in similar proportion to loads. To achieve better control and to avoid harmonics problems, the inverter technology has changed to switched, pulse-width modulated (PWM) technologies with high switching frequencies, which do not produce low-order harmonics and are therefore not expected to cause low-order harmonic problems. However, unexpectedly high harmonic levels have been observed in systems with a high penetration of inverter-based PVs [5]. This was apparently due to the interaction of the inverters in the system, which presumably resulted in a significant increase of harmonic emission. Interaction may be due to (1) resonance conditions created by the dc capacitor employed in inverters and/or (2) poorly-designed control schemes that do not sufficiently filter the harmonic pollution from the system.

3.4 Islanding

Islanding refers to the condition where the DG is isolated on a portion of the power system and operates as an "island" separate from the power system. Islanding is often referred to as “loss-of-mains”. One concern of islanding is the safety to utility workers and customers as the lines in the islanded system are still energized whereas it is assumed otherwise. The other concern is that equipment may be damaged when the utility power is restored due to (1) limited voltage and frequency control and (2) power quality issues of electric service to utility customers

Most of the time, islanding on distribution system is unintentional and undesirable. Islanding often occurs for a brief period following the opening of a utility breaker to clear a fault. There will be a few cycles during which an island exists while the DG interconnection relaying detects the

problem and clears the fault. The existence of a fault gives the DG protection (relaying and/or inverter abnormal voltage/frequency protection) advance warning that the utility breaker is about to open and the DG can disconnect to avoid an island. However, of concern is the case when there is an inadvertent trip of the utility breaker without a fault. The question is: Will the resulting voltage and frequency deviate enough to detect the island promptly? Simulation of the system dynamics is required to provide the answer. If the answer is "no", other means of detecting the inadvertent island must be implemented.

In certain cases, islanding is desirable and can result in an autonomously operating system. For instance, a microgrid is a collection of distributed resources serving one or more loads that, when required, can operate autonomously. Ideally, microgrids have the capability to disconnect seamlessly from the local utility and operate in islanded mode. Islanding detection technology is a critical component in a microgrid. It is important that the microcrid can reliably detect a loss of utility mains to facilitate the transition into islanded mode.

Applicable codes and standards, such as IEEE 1547, UL 1741, and IEC 62116 demand that DG does not energize any portion of the host utility system during islanding. According to IEEE 1547, the DG "shall cease to energize the area EPS within two seconds after the formation of an unintentional island". This requirement is difficult to achieve if there is generation-load balance in the microgrid, because the changes in voltage and frequency during loss-of-main may be too small to reliably detect the islanded state. No information about intentional islanding is given in IEEE 1547-2003. The topic is under consideration for a future revision of the standard. The guide IEEE 1547.4-2011 addresses the topic of operation of DR island systems and includes information about the ability of a DG to separate from and reconnect to the grid while providing power to a local island.

4 Field Experience with High-Penetration PV

In the following sections, we identify, discuss, and summarize selected reports that document the experience with high-penetration PV that US utilities and utilities in other countries had.

4.1 USA

During the October 2012 UVIG DG User Group meeting, Pepco reported on the grid impact of PVs in their system [6]. The number of PV installations has been increasing rapidly on their system since 2006 and reached 124 MW total installed capacity as of October 2012. In addition, PV projects with a total capacity of 97 MW are pending. Pepco categorizes their PV installations in 'Large PV' (>3 MW), 'Medium PV' (250 kW – 3 MW), and 'Small PV' (<250 kW). The utility reported the following experiences with PV in their system:

- For a system with a large 10 MW solar installation, Pepco reported up to 1.05 pu voltage levels due to the voltage rise caused by PV. In addition, asymmetric 1.3 kHz harmonic oscillations were observed that resonated with the impedance of the utility system. The combined effect caused inverter tripping, which was mitigated by adding capacitance to the inverters.
- Pepco reported on two systems with medium-size PV installation (1.7 MW and 1.3 MW) for which the PV generation changed the load profiles in that the load curve during time of PV peak production on clear days was flattened significantly. Large fluctuations in the load curve were observed during cloudy days at times of PV peak production. Pepco observed the general tendency of PV causing load peaks to flatten and shifting peaks towards later hours.
- For a 1.9 MW PV system, Pepco observed voltages exceeding the state-required ±4%, voltage range. The utility mitigated these overvoltages with the low-cost solution of changing the unity power factor to 0.97 leading (absorbing).
- Reverse power flow was observed for a 1.3 MW PV system installed in a 12.47 kV circuit with a peak load of 8.5 MVA resulting in 15% PV penetration. The reverse flow caused operation of the regulators with non-reversible control located at the substation, which raised the voltage on the line side. This resulted in large enough overvoltages to damage some customer equipment. Inverters tripped after the fact.

In 2012, Mather and Neal [7] reported on a five-year project approved in 2010 of installing a total of 500 MW[1] of PV in the service territory of Southern California Edison (SCE). At this stage of the project, no technical issues have been reported by SCE – instead SCE had to deal with non-

[1] The 500 MW target has been revised later on to 250 MW of PV.

technical challenges related to handling the large number of interconnection requests and conducting system impact studies for a system that is in flux.

Coddington et al. [8] report on the deployment of 5.2 MW of PV on the Colorado State University Foothills Campus in Fort Collins, Colorado, for which Xcel Energy supplies power. The feeder's average daily peak load was 7.5 MVA in 2010 (maximum: 9.1 MVA, minimum daytime load: 3.1 MVA) resulting in a PV penetration level of approximately 47%. Despite this high penetration level, Xcel Energy has not reported any major power quality or reliability issues, although the tightly-programmed voltage regulators experienced more frequent operation leading to greater maintenance requirements.

Braun et al. [9] document a number of case studies of PV integration in the US, Europe, Japan, and Australia. Inverter tripping due to abnormal voltages and frequency appears to be an issue in small isolated grids and/or feeder circuits with high PV penetration. For instance, (1) feeders in Belgium reportedly experienced problems with the disconnection of PV due to overvoltages and (2) an isolated feeder in Australia (3 MW of PV on a system with a 60 MW peak load) experienced disconnecting PV systems due to underfrequency, which the Northern Territory's Power and Water Authority mitigated by relaxing the disconnect requirements due to abnormal frequency. The Hawaiian Electric and Light Company (HELCO) operates several distribution circuits with PV penetration levels above 50%. HELCO requires that all distributed PV is installed with adjustable voltage and frequency trip points, which suggests that customized PV trip settings are necessary to avoid tripping. The Kauai Island Utility Cooperative (KIUC) installed a 1-MW PV system on a small distribution circuit that, during sunny days, feeds power back to the substation transformer.

SCE reported to EnerNex that the highest PV penetration feeder in their service territory has 70% of rated power coming from PV – specifically, three large utility-scale PV installation with a total rated power of about 7 MW. SCE reported reverse power flow on this feeder during low-load conditions and high solar irradiance levels.

4.2 Japan

Ota City is an industrial city in Japan with approximately 220,000 inhabitants. 553 PV systems were installed on newly built houses in the area. The total capacity of the PV systems was 2,130 MW. The Total Harmonic Distortion (THD) increased by 2% after the number of PV generators in the system increased by a factor of seven. It was identified that voltage rise due to PV penetration was a major limiting factor to PV penetration level. Hence, power conditioners for PV systems were designed to control the voltage rise and keep the voltage magnitude within permissible

limits. However, a major initial set-back with this approach was that the PV power output was curbed in order to control the voltage, thereby leading to a lower yield of the PV installations. This problem was somewhat alleviated by storing excess PV generation in storage devices, such as batteries. [10]

The grid-connected PV project in Gunma, Japan, has over 550 houses with rooftop systems. The overall capacity of the clustered-PV system is about 2.2 MW of PV generation distributed in a 1-km^2 area. Groups of 5 to 15 PV-integrated houses were connected to a low-voltage (LV) feeder and supplied by a LV transformer. Continuous measurements, monitoring and analysis of the PV system operation for a one month period led to (1) an increase in the daily global solar irradiation of above 5 kWh/m^2 resulted in about a 2% increase in the output voltage of each PV-inverter, and (2) periods of light loading shifted up the voltage profile of a feeder by 1.5% - 2% above the maximum limit. [11]

4.3 Germany

[10] and [11] report on the experience of a community in Germany that has 50 condominium apartments with a total PV installed capacity of about 300 kW. The PV systems and buildings are distributed over two radial feeders supplied from a 400 kVA transformer. A series of measurements and power quality studies were performed when 40 PV systems composed of 100 inverters were operating. The results showed that voltage THD and current THD levels were below the permissible limits of 8% (EN61000-3-2 standard). However, violation of the maximum voltage level and power flow reversal were observed, mainly during high solar irradiation. Also increased phase voltage unbalance was observed due to uneven distribution of the PV inverters on the different phases. The report stated that the reason for the imbalance was uneven distribution of inverters over the three phases.

[12] investigated the effect of PV generators on flicker on a high PV penetration feeder (an average of 5 kW per house connection) in southern Germany. Ten-minute average data were recorded from January 2011 to December 2012 by 560 smart meters that were primarily installed at houses with PV systems. Findings from the data analysis are summarized as below. Note that the conclusions only apply to the studied feeder– investigations on feeder with different characteristics (short circuit capacity, PV penetration, feeder topology, load characteristics, etc.) may yield different conclusions.

- A small fraction of the recorded flicker values (0.2%) were outside the permissible long term flicker limit ($P_{lt} < 0.5$).

- The analysts had difficulty to find a correlation between variations in PV generation due to clouds and flicker levels – apparently because the effect of PV on flicker is very small.
- The observation that similarly high flicker levels occurred on days without rapid changes of PV generation (i.e., clear sky days and days with a thick cloud cover) and days with rapid changes of PV variation (cloud transients due to fluctuating cloudiness) suggests that the effect of PV on flicker is much smaller than the effect of loads on flicker.

4.4 Australia

The solar village at the Sidney Olympic Village in Australia consists of 629 homes, with each home having a 1-kW rooftop PV system connected to a low voltage (240/415V) underground distribution system. Prior to the Sydney 2000 Olympic Games, a series of voltage/current distortion measurements for large scale PV-inverter installations in the vicinity of each other showed that grid voltage total harmonic distortion was below 3%. It was reported that the main reasons for low THD of voltage were low grid impedance, short distance between houses, and adequate cable size. [11]

4.5 Netherlands

The Nieuwland project in the Netherlands consists of 500 houses with roof-mounted PV installations covering an effective area of 12 km^2 with 1-GWh annual generation capacity. The Vroonermeer-Zuid project in the Netherlands consists of 197 houses with PV arrays and inverters. In both projects, the PV system installation for each house varied from 1 to 3 kW with typically 30 houses connected to a single 220V distribution feeder, supplied by a 10kV/0.22kV transformer. Data measurement and investigation showed an increase in the harmonic pollution level which could violate the Dutch power quality standard (measurement results not reported). Some cases of undesirable inverter switch-off were also reported, which were believed to be caused by either harmonic activities or a rise in the feeder voltage. [11]

4.6 Greece

There are several PV projects in the Greek islands, including Arki, Antikythira, and Gavdos. The harmonic measurements from multiple field tests at different times of the day (and under various load conditions) showed that the THD measurements for voltage in Antikthira was well below 2%, but in Arki PV project, current harmonic injections from the loads increased the THD of the voltage above the standard level of 5% (Arki and Antikthira PV networks are weak grids). The current harmonics injected by nonlinear and reactive loads caused significant voltage and current distortions in the mini-grid. [11]

4.7 Canada

In a PV project in Canada it was observed that during light-load conditions and high PV penetration/generation, the feeder voltage at the PCC increased by 2-3% above the no-load voltage level. The voltage rise was higher when a PV cluster was sited far from a distribution substation or a transformer location. For instance, under similar loading conditions, the PV cluster at the end of a feeder segment resulted in 1% voltage increase at the PCC whereas 0.4% voltage increase was obtained when PV cluster was placed close to the substation. The rate of voltage rise was also reported to increase as load net consumptions in the PV neighborhood decreased. The study suggests that in order to limit the voltage profile to permissible levels, the voltage at the substation has to be regulated and the feeder has to be appropriately sized and configured. [11]

5 Distribution Feeder Model

The simulation tool we selected for this study is Open Distribution System Simulator (OpenDSS) developed by the Electric Power Research Institute (EPRI). This open source frequency-domain analysis software application tool was developed for special distribution analysis applications, such as the investigation of DG impacts and the integration of user interfaces, GIS and other databases. For this study, OpenDSS was selected as our main simulation tool since this text based simulation software allows the construction and batch processing of large (thousands of buses) highly-detailed distribution network simulations. The key features of OpenDSS in the context of this study are as follows:

- Multi-phase unbalanced power flow, short-circuit, and dynamics analysis.
- Time-sequenced simulation of overcurrent protective devices, regulator controls, and capacitor controls.
- Duration curve, duty cycle, and Monte Carlo simulation modes for variable load and generation.

5.1 General Description and Selection of Distribution Feeder

Simulations were performed in OpenDSS on one distribution feeder that is representative of California feeders. The focus as stated in the Statement of Work was on modeling an urban feeder. The host utility provided us with data for five distribution feeders located in Southern California (see Table 5-1). From these five feeders, we selected Feeder B because (1) the circuit has a large number of customer per feeder length, which is a typical characteristic of an urban feeder and (2) the circuit has a high number of voltage regulation equipment (two capacitors and six voltage regulators) and it is of interest to investigate the effect PV has on their operations (see Section 3).

Table 5-1: Characteristics of five distribution feeders as provided by the host utility.

Circuit	Substation Xfmr Size (MVA)	Feeder Length (ft)		# of Customers	# of Distribution Capacitors	# of Voltage Regs
		Underground	Overhead			
A	2x28	8993	27989	3770	2	0
B	28	444	132811	2219	2	6
C	28	249	131679	1063	1	1
D	28,13	2795	52827	445	1	1
E	2x28	2856	19646	1474	1	0

Table 5-1 lists the general characteristics of all five feeders as provided by the host utility including the characteristics of Circuit B, which we selected for our analysis. Detailed feeder data that were required to build the OpenDSS model were provided in the form of SynerGEE models

for each circuit along with short circuit data and power flow data from SynerGEE model runs. Even though the SynerGEE models contained much information, some information was still missing for building the OpenDSS model. We constructed an OpenDSS model of Circuit B by (1) using the information from the SynerGEE model, (2) incorporating additional information provided by the host utility through email and conversations, and (3) making reasonable assumptions. This process is described in detail in the following sections.

5.2 Modeling Approach, Assumptions, and Validation

5.2.1 Modeling Approach

The system information the host utility provided to EnerNex was generated from SynerGEE and resides in a Microsoft Access database. The database contains the following information:

- Network topology: information on buses, equipment settings, and which types of equipment are connected to the buses,
- Equipment characteristics: specifications of capacitors, voltage regulators, and other utility equipment
- Load locations and characteristics

EnerNex developed Matlab code that (1) pulls the system information from the Microsoft Access database, (2) processes the information to generate all parameters needed for the OpenDSS, and (3) creates files that can be used as input to the OpenDSS. In addition, we developed a visualization tool that yields information about the location and properties of each object in the system.

5.2.2 Assumptions

Some information was not included in the customer-provided Microsoft Access database. In addition, the database information was not entirely consistent with the feeder characteristics listed in Table 5-1. For instance, the number of customers as stated in the table is 2219 and, based on the SynerGEE model, this number is 1733. We decided to deal with these inconsistencies by using the customer-provided short circuit currents and power flow results from SynerGEE model runs as a benchmark for our OpenDSS simulations, that is, our priority was to match our OpenDSS results to the SynerGEE results[1]. This required some adjustments to the converted OpenDSS model, which we sanity checked to ensure that the parameters used in the

[1] The better approach is to verify our simulation results using measured data, but since these were not available to us we believe that achieving consistency with the host utility's simulation results is the second best approach, which is in line with the conceptual nature of this study.

converted OpenDSS circuit, such as load impedances, source impedances, reactive compensation etc. are within the parameter ranges that are typical for actual feeder. Our assumptions we had to make due to missing information and inconsistencies of the customer-provided data set are listed below:

- Cable types used on the feeder and the lengths of the line segments were specified, but no electrical characteristics nor information on tower/underground cable geometry were provided. We based the line impedances used in our OpenDSS model on typical values for the specified cable impedances and used typical line geometries.
- The provided SynerGEE model for the feeder includes one large two MW PV generation site, but it does not include information about other PV generators connected to the host utility's system[1]. The host utility provided additional information regarding PV generators on their system in the form of a one-line diagram with PV site locations and PV ratings indicated (no information on whether the PV generators are single phase or three phase was provided). We mapped these PV locations to the buses and made assumptions regarding the phasing of these generators as described in detail in Section 5.3.
- The characteristics of individual service transformers were not included in the database[2]. Consequently, we were not able to place residential PV generators at their actual location on the service transformer's secondary side and instead connected the PV generators directly to the load. This resulted in the PV generators being effectively connected to the primary side of the service transformer. Consequences of this approach are that (1) transformer losses resulting from excessive power generated by the PV and fed back into the grid are not captured and (2) power generated by the PV and fed to the local loads are subjected to transformer losses even though, in reality, it would not flow through the transformer. We believe that the effects of these limitations are minor and do not impact the validity of the conclusions we draw from our simulation results. We describe our approach in more detail in Section 5.3.
- We made a number of assumptions that were needed to produce a good match between the customer-provided power flow results from SynerGEE simulation runs and the results from our OpenDSS simulation runs. These assumptions are detailed in Section 5.2.4.

5.2.3 Validation of Short Circuit Behavior

In this section, we validate the consistency of the short circuit current behavior of our OpenDSS model with the SynerGEE model. We do this by comparing the short circuit results provided by host utility from their SynerGEE simulations and simulation result from OpenDSS in "fault study"

[1] The host utility typically does not model small PV systems as the absence of PV is a conservative assumption with regards to the amount of power they need to supply to their residential customers.
[2] It is common practice at the host utility to aggregate loads and other components, such as service transformers, to reduce the model complexity. Consequently, the transformer impedances are not resolved in the SynerGEE models but are rather incorporated in the load impedances.

mode. As mentioned in section 5.1, Feeder B has six regulators. It should be noted that there is a fundamental difference in the way SynerGEE and OpenDSS simulate regulator behavior. In SynerGEE, the regulator itself is a complete device that includes a transformer internally to do voltage regulation. This integrated transformer has a very low impedance. On the other hand, the OpenDSS regulator object is a dedicated controller, which observes the voltage and, if a set voltage threshold is exceeded, sends a signal to the OpenDSS transformer object to do the actual tap changing operation that changes the voltage. As such, in our effort to convert the model from SynerGEE to OpenDSS, six transformers are added to the corresponding regulators. These transformers however have non-negligible impedance that affects the results of the OpenDSS short circuit analysis. In order to make the OpenDSS short circuit results comparable to the SynerGEE results, we replaced these transformers by low-impedance line segments. The regulating transformers are, however, present in all OpenDSS simulations conducted in later sections. Figure 5-1 shows a comparison of short circuit current between the provided SynerGEE results and results from our OpenDSS simulation. The short circuit results match fairly well except for some mismatch at the end of the feeder. We are speculating that this mismatch is due to our assumption we made regarding the cable impedances (see Section 5.2.2).

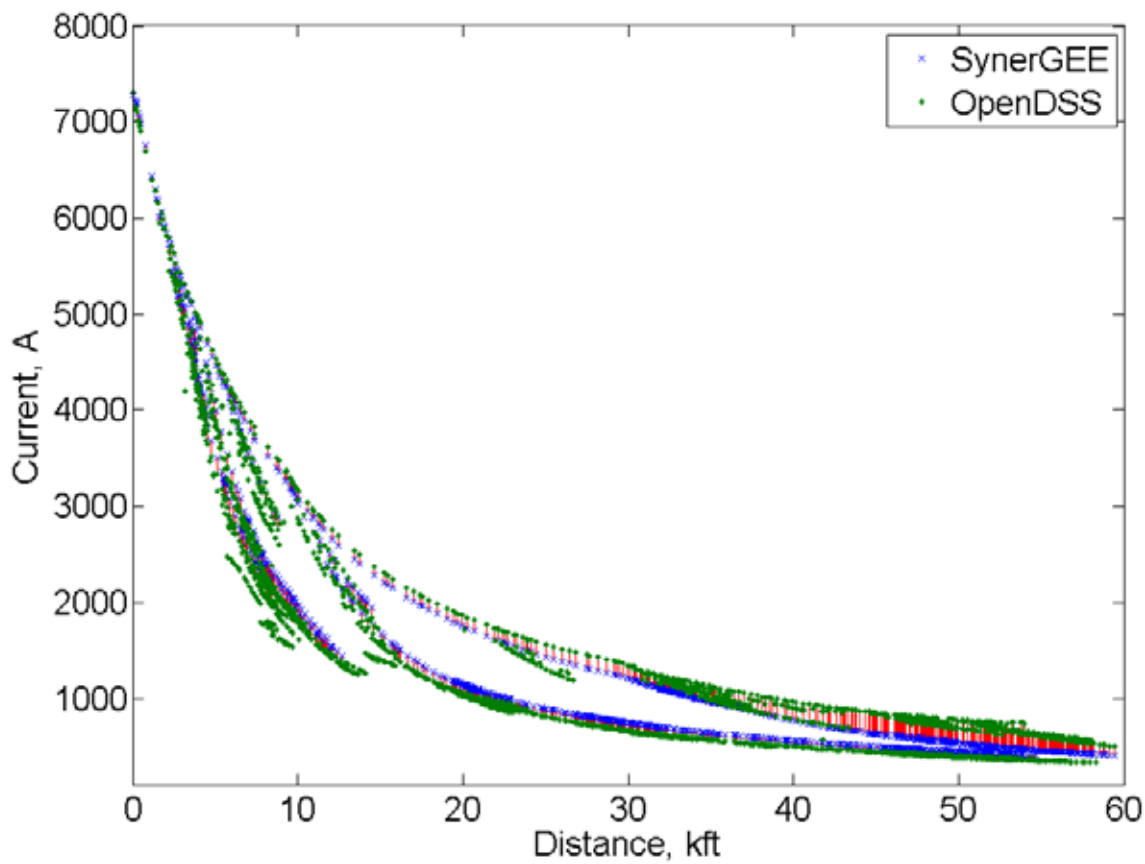

Figure 5-1: Short circuit comparison of simulation results from OpenDSS and SynerGEE.

Various changes were made to the original converted OpenDSS circuit to fill in missing data, to match the power flow result given, and to add PV systems that exist on the feeder, but are not accounted for in the provided SynerGEE model. Section 5.3 explains these changes in detail. We were interested to see if the short-circuit behavior of the modified OpenDSS is still similar to the short-circuit behavior of the SynerGEE model or if our changes to the original OpenDSS model caused significant changes with regards to the short-circuit currents. Figure 5-2 compares the short-circuit results from the SynerGEE model with the short-circuit results from the modified OpenDSS model. A comparison of Figure 5-1 and Figure 5-2 shows that the match close to the substation gets slightly worse and the match near locations at the feeder end slightly improves, but overall we can conclude that the original OpenDSS model and the modified OpenDSS produce very similar short-circuit currents.

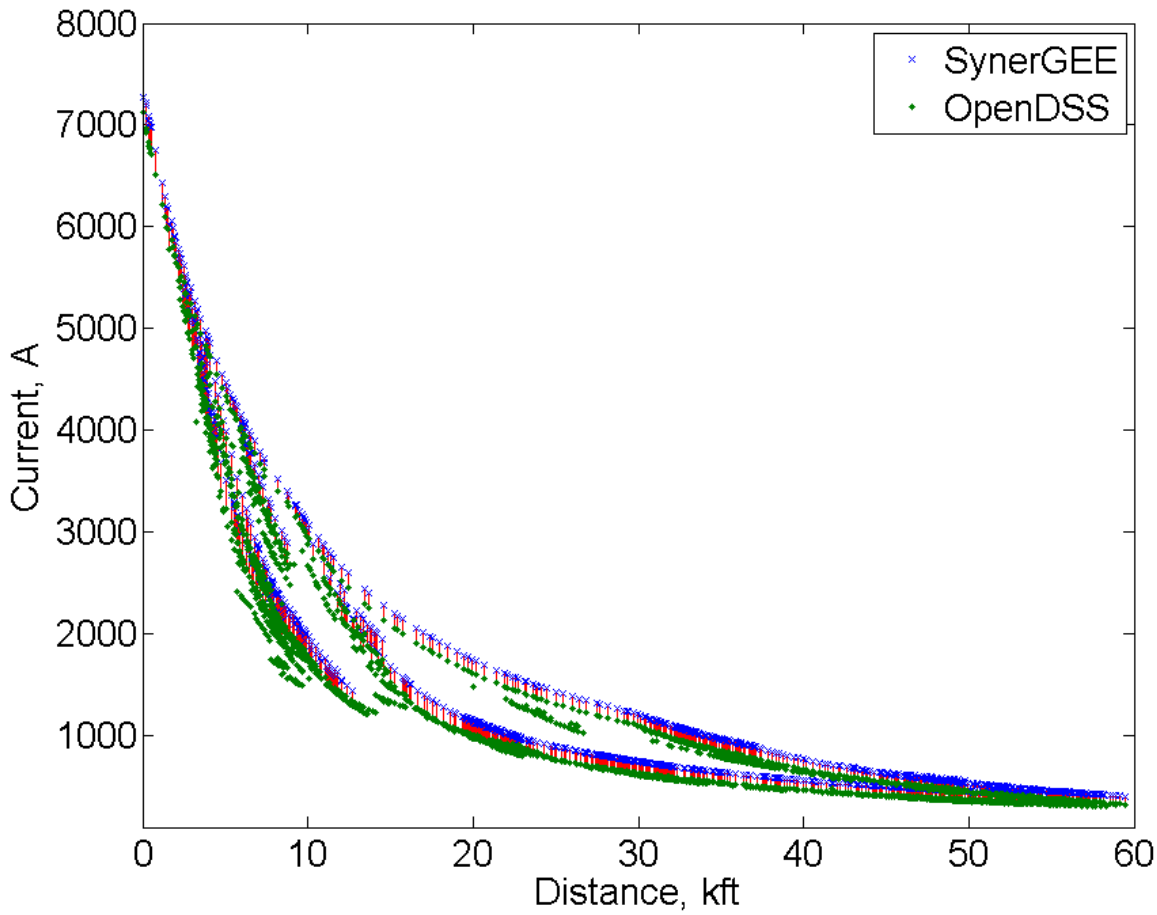

Figure 5-2: Short circuit comparison of simulation results from OpenDSS and SynerGEE. PV generators are included in the OpenDSS simulation.

5.2.4 Validation of Power Flow Behavior

The initial power flow results of the OpenDSS system we created are illustrated in Figure 5-3 and Figure 5-4 and compared to the customer-provided results from SynerGEE simulation runs. It is apparent from the figures that there is a large mismatch between the OpenDSS and SynerGEE data sets. We think that this mismatch is in part due to (1) incompleteness and inconsistencies of the information that has been provided to us (see Section 5.2.2) and (2) differences that are attributable to the simulation software application[1].

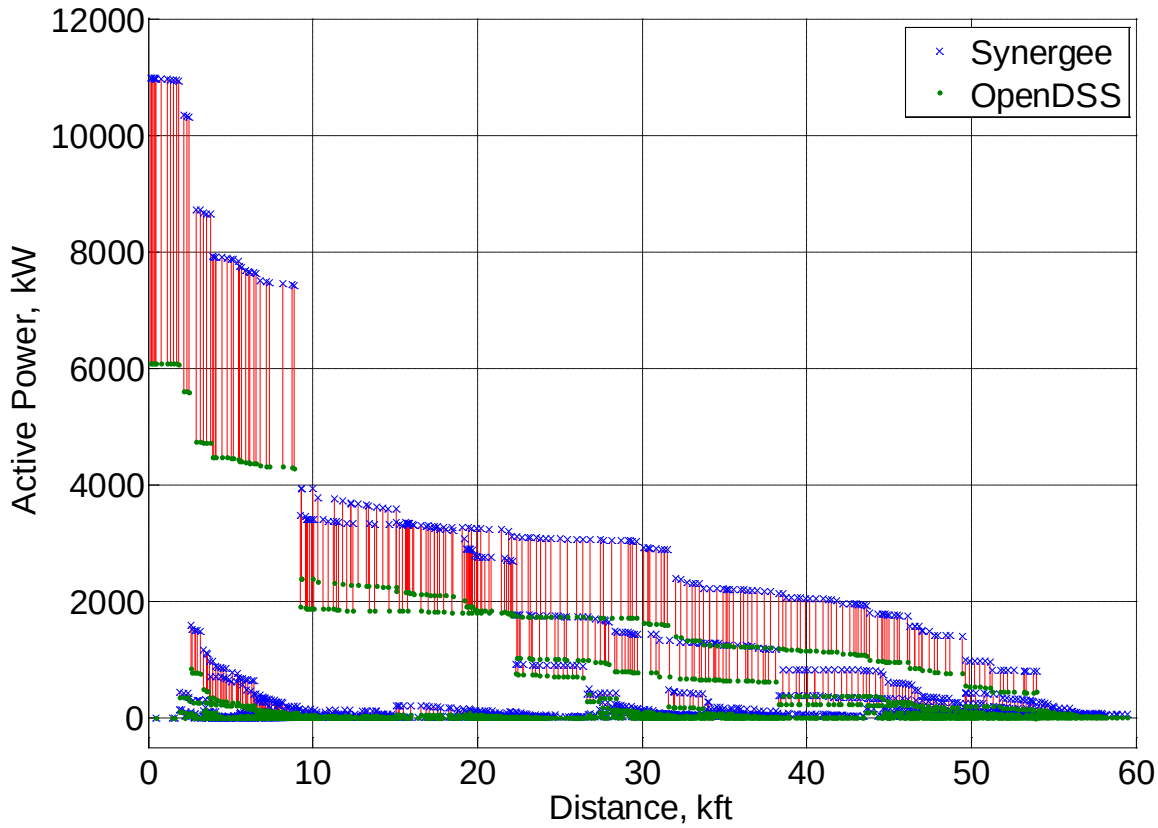

Figure 5-3: Comparison of power flow results from initial OpenDSS runs and customer-provided results from SynerGEE simulation runs, active power.

[1] It is not uncommon that different simulation software applications produce different results. This can be due to differences in (1) power flow solution techniques, (2) line and load models, (3) techniques to account for the ground return path, (4) balanced vs. unbalanced power flow solutions, etc.

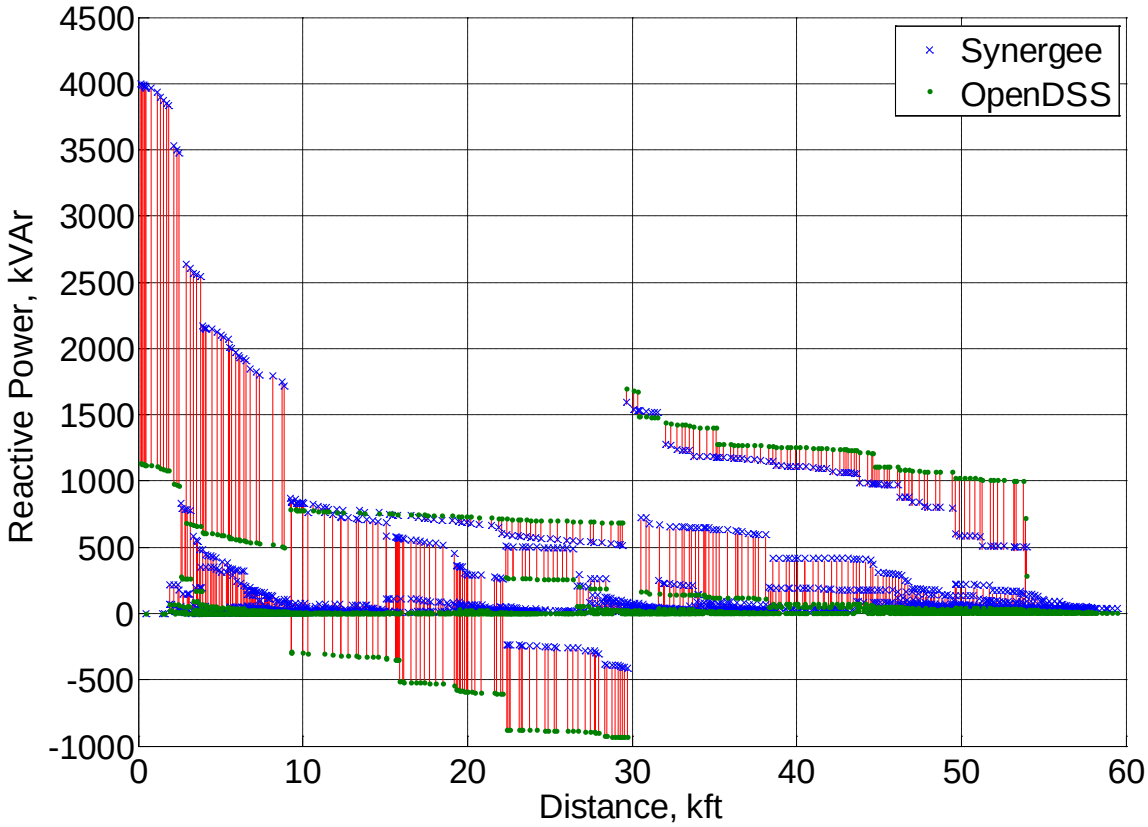

Figure 5-4: Comparison of power flow results from initial OpenDSS runs and customer-provided results from SynerGEE simulation runs, reactive power.

As stated previously, we decided to use the customer-provided results from SynerGEE runs as a benchmark for our OpenDSS simulations and adjusted our OpenDSS model to the SynerGEE results. The adjustments to the converted OpenDSS model are listed below:

1) We increased the kVAr ratings of all but the four biggest loads (i.e., 1,223.4 kVAr, 473.7 kVAr, 208.8 kVAr, and 189.6 kVAr) in the system, 2.5 times. The reason for doing this is what appears to be over-compensation at lower kVAr level (load level) after removing all capacitor banks from the simulation (see Figure 5-5) [1]. In other words, even without the capacitors some buses show kVAr values that are lower than the kVAr values obtained from the SynerGEE simulation. Addition of capacitor banks to the circuit would further decrease the kVAr values preventing a satisfactory match between OpenDSS and SynerGEE simulated reactive power results. Red circles, in Figure 5-5, mark the areas of concern. After increasing the kVAr ratings of 1729 loads in the system, the lower level kVAr values increased to a point

[1] Removing the cap banks from the OpenDSS circuit during the parameterization allowed us to assess the overall reactive power flow in the circuit without local compensation.

where further reactive power parameterization efforts could be completed by adding appropriately sized capacitor banks. Figure 5-6 shows the simulated reactive power values after the load kVAr ratings were increased.

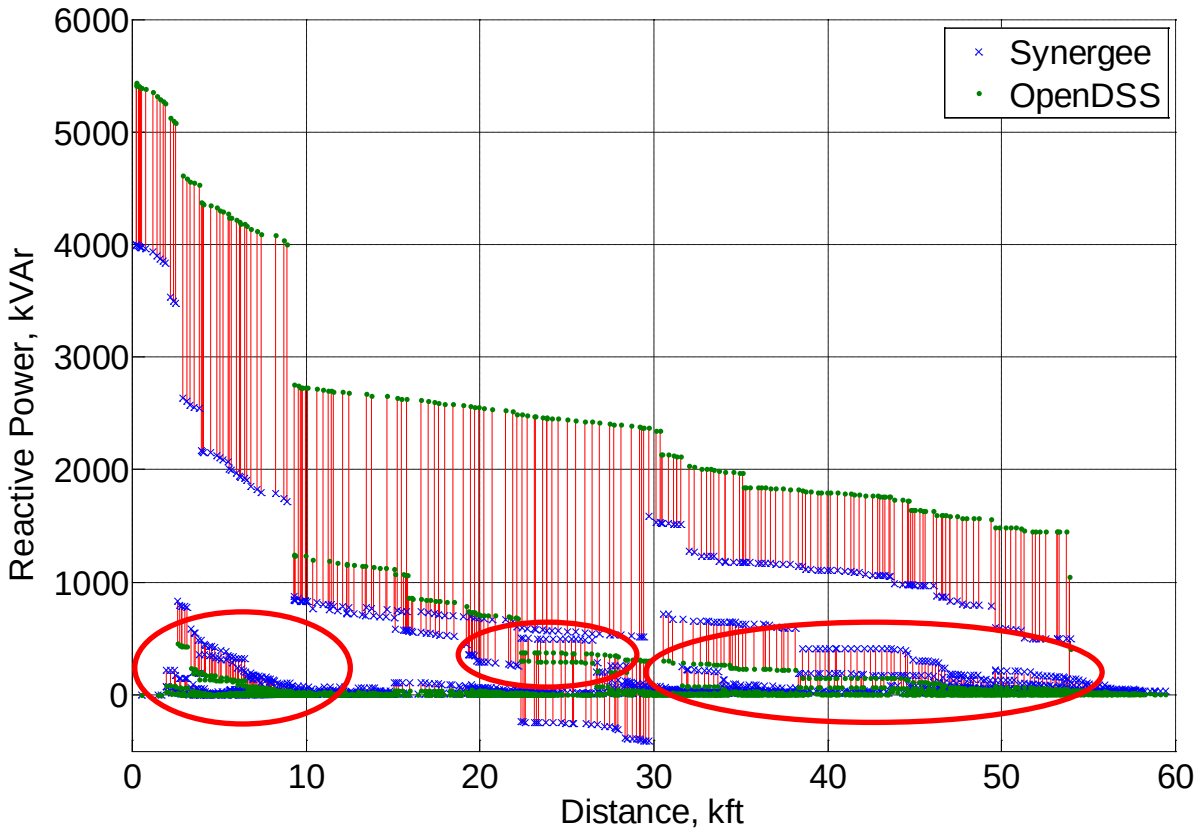

Figure 5-5: Comparison of power flow results from OpenDSS runs and customer-provided results from SynerGEE simulation runs with all capacitor banks removed from the system, reactive power.

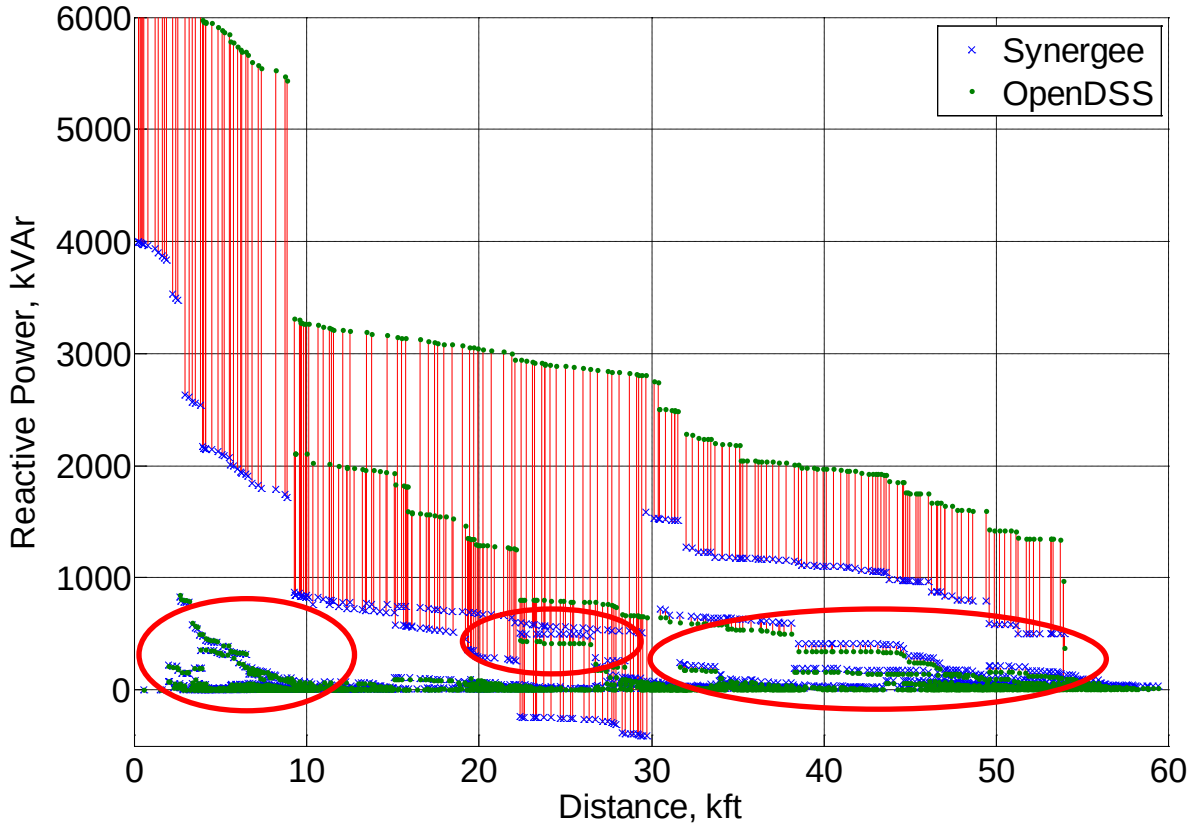

Figure 5-6: Comparison of power flow results from OpenDSS runs and customer-provided results from SynerGEE simulation runs with all capacitor banks removed from the system and adjusted load kVAr ratings, reactive power.

2) We adjusted the values of the two existing capacitor banks and added two additional ones:
   - Capacitor bank at bus 05201314: Old value 1200 kVAr, adjusted value 1600 kVAr
   - Capacitor bank at bus 05202234: Old value 1200 kVAr, adjusted value 1500 kVAr
   - New capacitor bank at bus 05201643A: Value 1230 kVAr
   - New capacitor bank at bus 05201644A: Value 100 kVAr
3) We added a load tap changing (LTC) substation transformer between the transmission line representing 'SourceBus' and the first system bus '0520'. The tap position settings of the LTC control were set to maintain the low voltage side at 12 kV.
4) We adjusted the tap positions for the six regulators to maintain the voltages at the buses the regulators are connected to at 12.48 kV[1].

[1] This value is only relevant for the system validation process. In our later simulation runs we used min and max voltage thresholds for the regulators to maintain appropriate voltage levels at the monitored buses.

Figure 5-7 and Figure 5-8 show and compare the active and reactive powers, respectively, after incorporating all the changes mentioned above. As apparent from the figures, the active and reactive powers from the OpenDSS simulation match the customer-provided results obtained from SynerGEE simulation runs well.

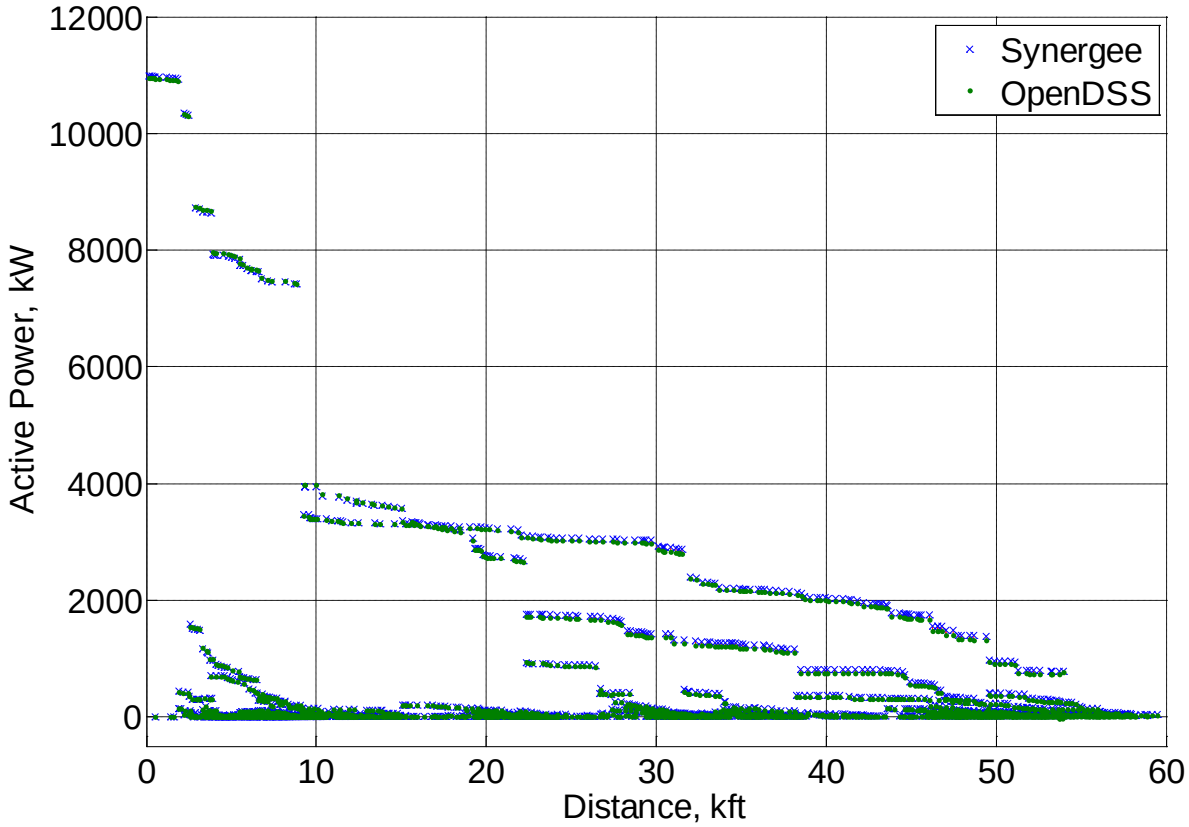

Figure 5-7: Comparison of power flow results from OpenDSS runs and customer-provided results from SynerGEE simulation runs after matching active power.

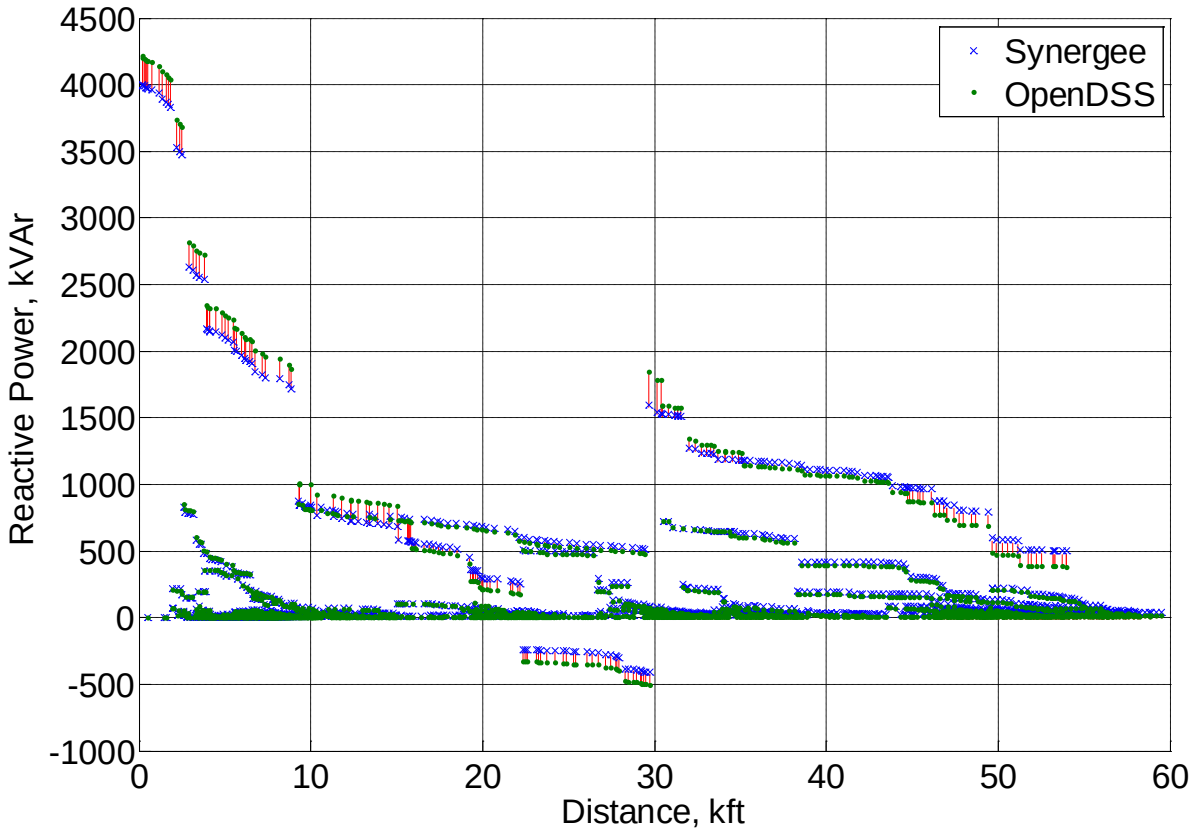

Figure 5-8: Comparison of power flow results from initial OpenDSS runs and customer-provided results from SynerGEE simulation runs after matching reactive power.

5.3 Adding PV Generators

5.3.1 PV Locations and Connections

Information on the residential-sized PV generators were not given in the customer-provided Microsoft Access database – only one large two MW PV generation site was included in the database. The host utility provided information on PV generators that included generators not in the database in the form of one-line diagrams with PV site locations and PV ratings indicated. We manually mapped the PV locations for feeder B indicated in the respective one-line diagram to the locations of the buses specified in the database. Figure 5-9 illustrates the results of our mapping effort. In the figure, the location of each of the mapped PV sites is illustrated by circles. The size (with regards to rated output power) of the PV sites can be gleaned from (1) the color, based on the logarithmic color scale in the figure, and (2) the size of the circle with the area of the circle being proportional to log of the rated output power.

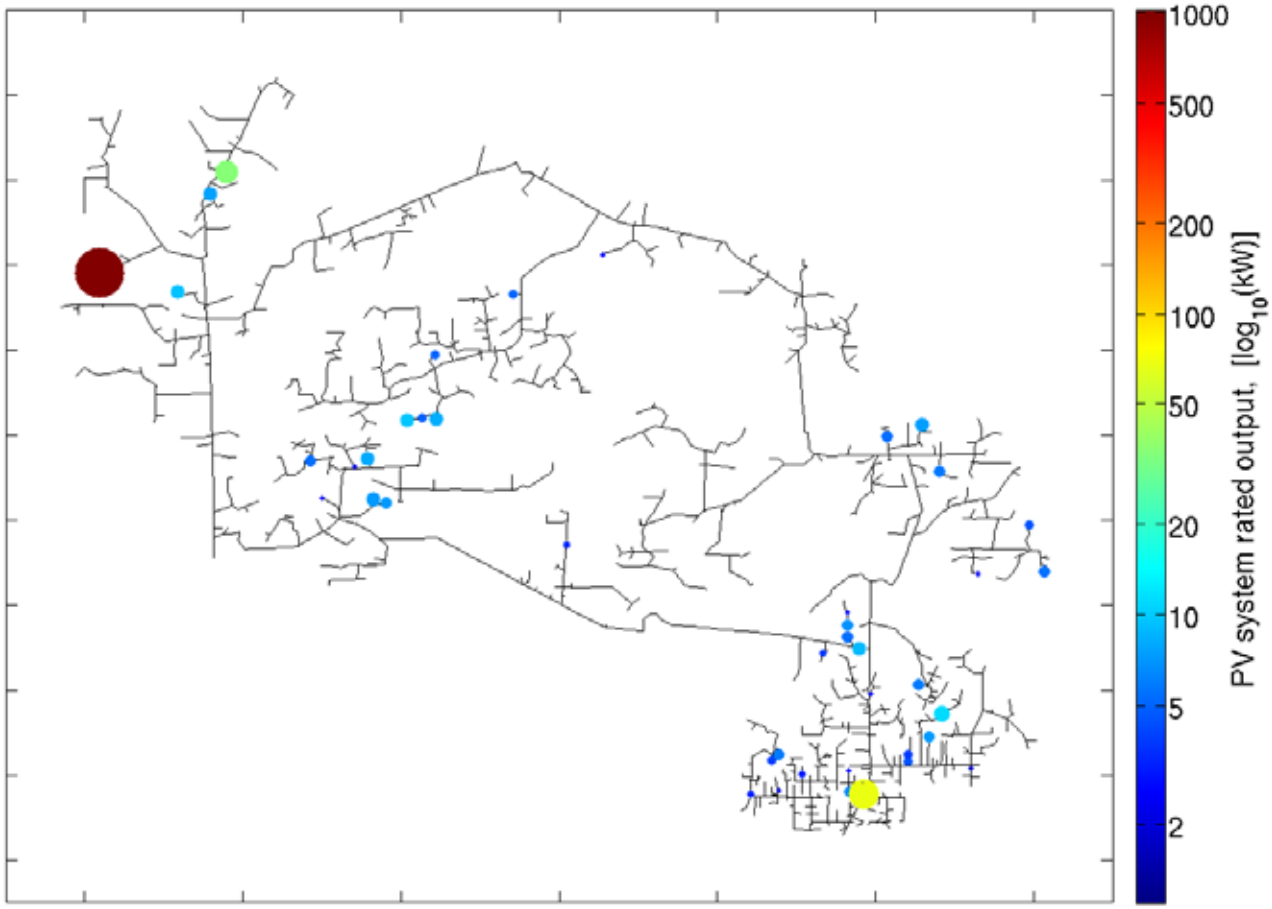

Figure 5-9: Locations of PV generators and their rated output. The rated output power is logarithmically proportional to the area of the circles representing the PV generators.

Table 5-2 lists each of the 45 PV sites and the rated power of the PV generators. Note that in the table, the large PV site included in the database as a single two MW unit, is listed, based on information from the one-line diagram, as two closely-located one MW PV generators. In addition to the large PV site, Feeder B has two medium-size PV units (one 65 kW PV generator and one 33 kW generator) and 41 small PV units with rated powers ranging from 1 kW to 10 kW.

Table 5-2: List of PV locations and ratings on circuit B.

PV ID	Rated Power, kW	PV ID	Rated Power, kW
1	3	24	5
2	1.9	25	2.5
3	3.7	26	2.5
4	5.4	27	7.5
5	6	28	6.835
6	2.4	29	6.8
7	65	30	9.2
8	1.1	31	4.68
9	4.3	32	7.8
10	3.6	33	3.152
11	1.5	34	5
12	2.9	35	7
13	3.5	36	5.4
14	5	37	4.3
15	6.472	38	999
16	2.4	39	998.9
17	8.28	40	8.8
18	2.5	41	7.1
19	5.4	42	4.8
20	6.7	43	4.8
21	10.4	44	2.4
22	2.2	45	33.2
23	5.1		

Information on the phasing of the PV generators was not provided. The mapping process sometimes identified a three phase bus without a load directly connected to it as the one that is closest to the small/medium/large PV site. While large- and medium-sized PV generators are typically connected three-phase, the typical connection for the small-size PV generators would be single phase. Furthermore, the small-size mostly rooftop-mounted PV sites connect directly to a residential load (i.e., the aggregate of the electrical devices in the building) and, therefore, the PV generators should be connected to a bus to which a load is connected as well. Consequently, there was a need to reassign some of the small-size PV generators to single-phase buses to which a load is connected to. Due to the lack of information regarding the specific bus the small-PV site is connected to, we had to reassign the PV generator to an arbitrary nearby single-phase bus to which a load was connected. Figure 5-10 and Figure 5-11 document the location and rating of each of the PV generators we included in the OpenDSS model.

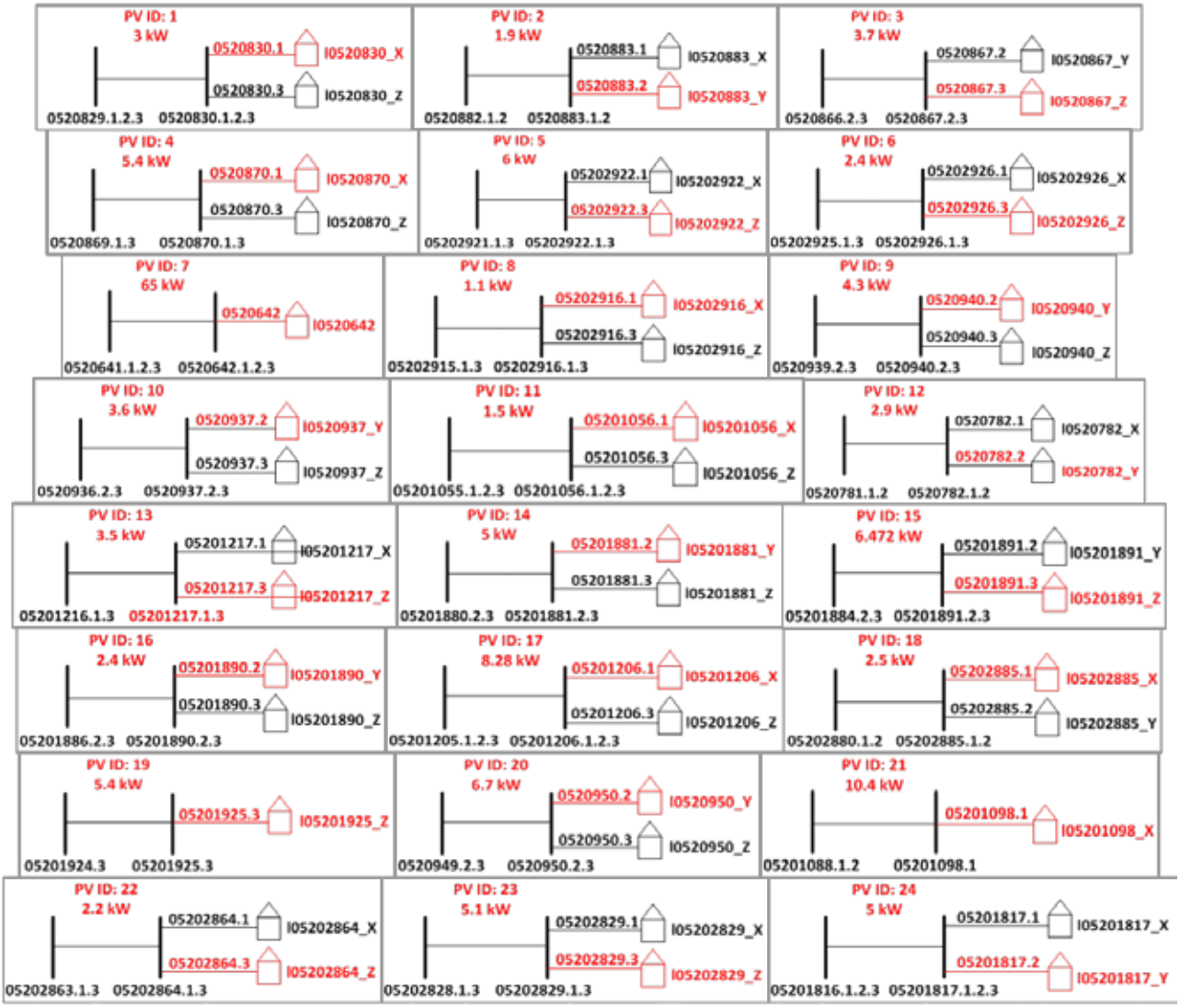

Figure 5-10: Locations and ratings of PV Generators 1 through 24.

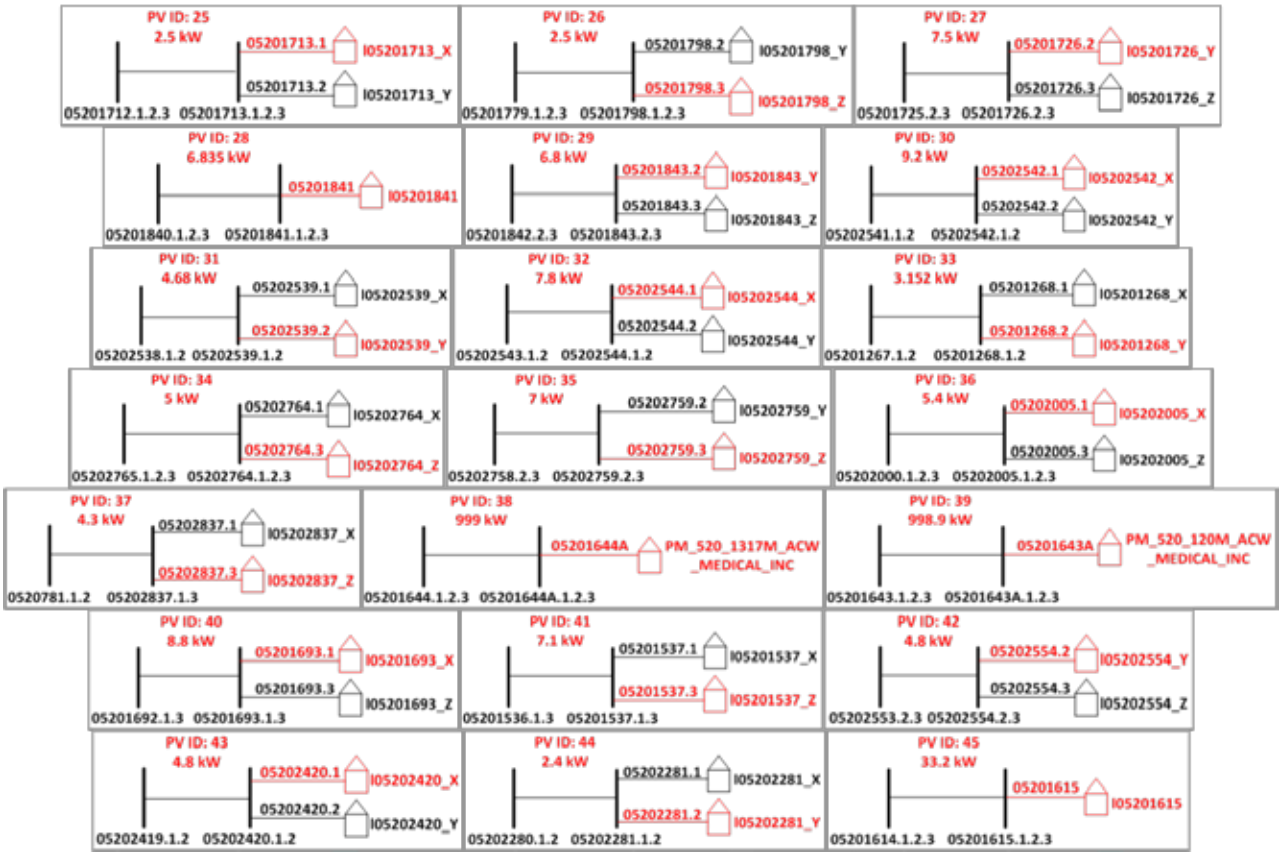

Figure 5-11: Locations and ratings of PV Generators 25 through 45.

5.3.2 PV Model

We represented the PV generators in our simulations using the OpenDSS PVSystem device model. This device model is available in OpenDSS V7.4.1 or later and is composed of elements that represent the PV array and the PV inverter. The PVSystem component is suitable for steady-state and quasi-steady-state analysis and, consequently, is sufficient for the investigation of most interconnection impact issues.

A limitation of the PVSystem model is that it is unsuitable for transient and dynamic studies that require time-domain modeling, such as transient fault studies, detailed investigation of inverter behavior, flicker, etc. This is an inherent limitation of OpenDSS as this software application tool is only capable of frequency-domain analysis. Another limitation is that the inverter protection (e.g., inverter tripping on over- /undervoltage) is not inherently part of the PVSystem model. The inverter protection would need to be modeled separately.

The properties, capabilities, and assumptions of the PVSystem device models are summarized below [13]:

- Applicable for simulations that have time steps larger than 1 second.
- A model assumption is that the inverter finds the Maximum Power Point (MPP) of the panel quickly.
- The active power is a function of (1) the irradiance, (2) temperature, (3) rated power at the MPP at a selected temperature and irradiance of 1.0 kW/m^2, and (4) the efficiency of the inverter at the operating power and voltage.
- The irradiance and temperature can be varied with each simulation step in a quasi-steady state analysis. This is achieved through the Loadshape and Tshape objects, which assign multiplication factors to the rated irradiance and rated temperature, respectively, at each simulation step. The result is that the output power of the PVSystem device varies with each step.
- XYcurve objects are used to describe how the active power at the MPP varies with temperature. The XYcurve is an object that is composed of x and y values that correlate two parameters – for the case above, power at the MPP and temperature. Values that lie between user-specified points are filled in through interpolation.
- XYcuve objects to correlate the inverter efficiency and dc bus voltage may be used in future versions of the PVSystem device. The current version uses only a single efficiency curve that is based on the typical operating voltage of a given array.
- The reactive power is specified separately from the active power. The PVSystem device can be set to either (1) constant VAr or (2) constant Power Factor (PF). In constant VAr mode, the VAr output of the inverter fixed at the set value unless this value exceeds the rated VA value of the inverter – in this case the VAr output is reduced.

  The PVSystem device is not able to adjust VArs dynamically to regulate voltage – a capability that many PV inverters have, but that is not permitted according to IEEE 1547 (see Section 3.2). Future version of the PVSystem device may incorporate voltage regulation modeling capability. A workaround for the current version of the PVSystem is to utilize the "kVAr" property of the PVSystem, which, when set, forces the inverter to operate in constant reactive power mode while the active power is changing based on the irradiance intensity. Voltage regulation can be simulated by pre-calculating the reactive compensation required from the PV generator and manually setting the kVAR value of the PVSystem object to this value. However, this method does not allow for dynamic voltage regulation, that is, in the real world the reactive power that needs to be provided by PV generators with voltage regulation capability will change with changing load and generation conditions. OpenDSS can simulate the changing conditions with its quasi-steady state simulation mode, but the reactive power provided by the PVSystem will remain on its pre-set value and not dynamically adjust based on the changing load conditions.

5.4 Description of Completed Model

The system information the host utility provided to EnerNex was generated from SynerGEE. EnerNex developed Matlab code that (1) pulls the system information from the SynerGEE files, (2) processes the information to generate all parameters needed for the OpenDSS, and (3) creates files that can be used as input to the OpenDSS. In addition, we developed a visualization tool that yields information about the location and properties of each object in the system. We used the visualization tool to create Figure 5-12 through Figure 5-17, which illustrate distribution Feeder B and its components. Table 5-3 summarizes the main characteristics of this feeder.

Table 5-3: Main characteristics of circuit B.

Feeder Parameters		Values
General	Buses	2463
	Nodes	6125
	Devices	6831
Conductors	Length of three-phase lines	312 kft / 95.1 km
	Length of two-phase lines	253 kft/ 77.1 km
	Length of single-phase lines	18.5 kft/ 5.6 km
Substation	Voltage level	12 kV_{RMS} (LL)
	Rating	28 MVA
Loads	Total active power	12.023 MW
	Number of three-phase loads	223
	Number of single-phase loads	1510
PV	Number of PV generators	45
	Total rating	2.295 MW
Transformers	Number of transformers	1 (substation)
	Number of voltage regulators	6
Capacitor Banks	Total number of capacitor banks	4
	Rating	4.430 MVAr

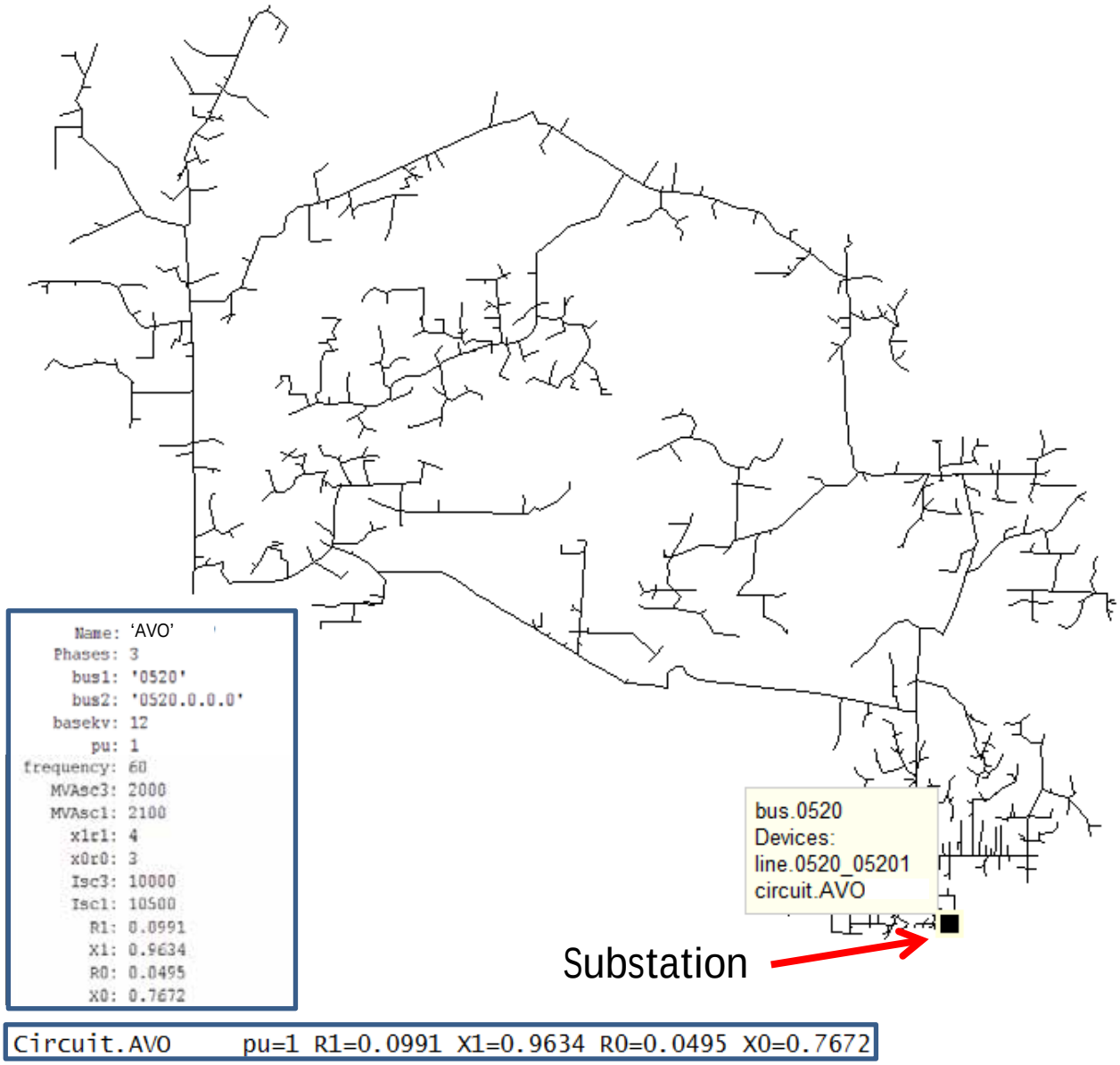


```
Circuit.AVO      pu=1 R1=0.0991 X1=0.9634 R0=0.0495 X0=0.7672
```

Figure 5-12: Source in the utility system, its OpenDSS representation, and its representation as a Matlab object. The OpenDSS simulation of the utility system includes a single source object.

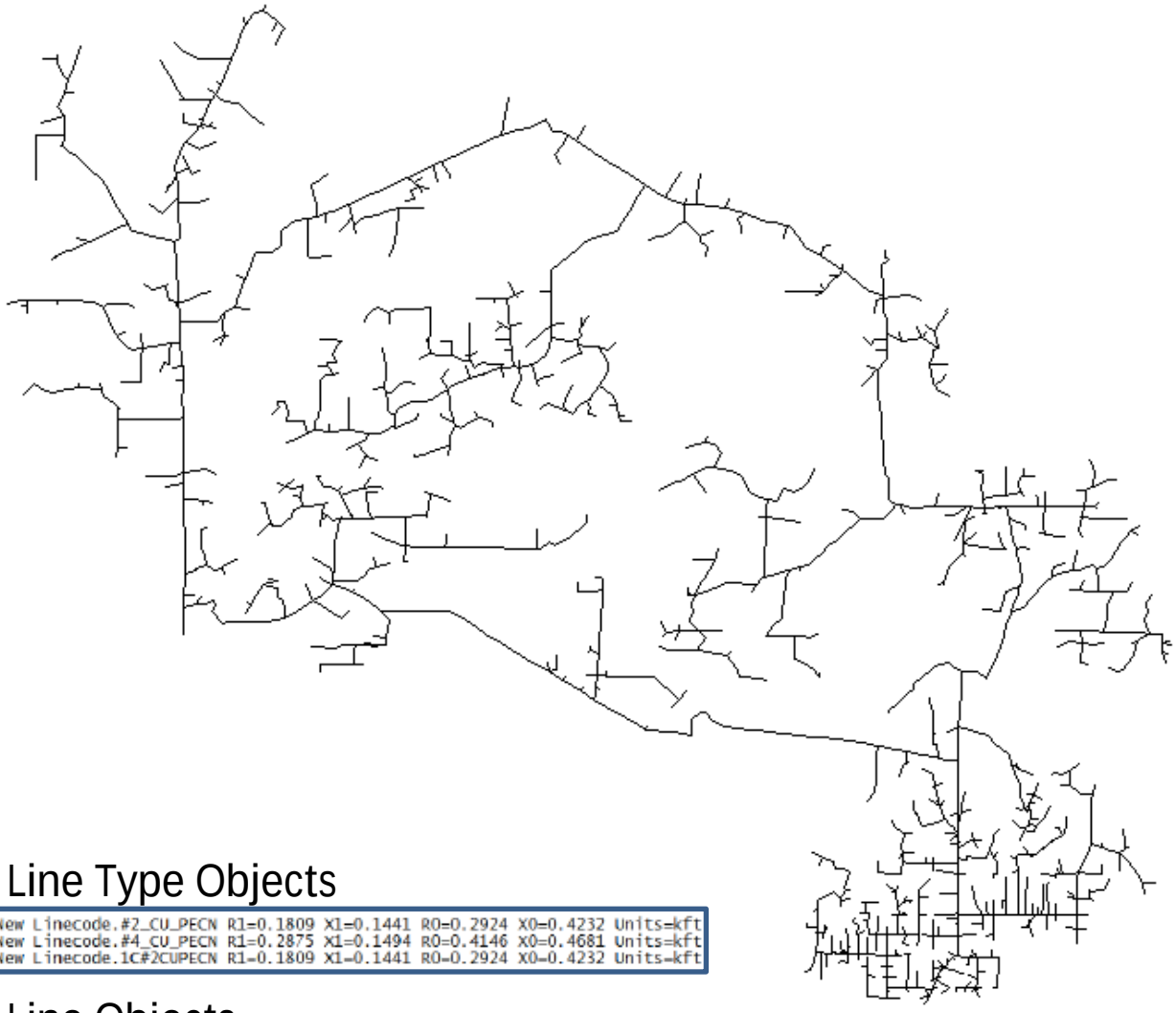

Line Type Objects

```
New Linecode.#2_CU_PECN R1=0.1809 X1=0.1441 R0=0.2924 X0=0.4232 Units=kft
New Linecode.#4_CU_PECN R1=0.2875 X1=0.1494 R0=0.4146 X0=0.4681 Units=kft
New Linecode.1C#2CUPECN R1=0.1809 X1=0.1441 R0=0.2924 X0=0.4232 Units=kft
```

Line Objects

```
New Line.05201008_05201009 LineCode=3_#6_CU_C Phases=3 bus1=05201008.1.2.3 bus2=05201009.1.2.3 Units=Ft Length=310.4
New Line.05201009_05201010 LineCode=3_#6_CU_C Phases=3 bus1=05201009.1.2.3 bus2=05201010.1.2.3 Units=Ft Length=292.7
New Line.05201010_05201011 LineCode=3_#6_CU_C Phases=3 bus1=05201010.1.2.3 bus2=05201011.1.2.3 Units=Ft Length=348.2
```

Figure 5-13: Lines in the utility system and their OpenDSS representations. The OpenDSS model of the utility system includes 2455 line objects and 87 different line types.

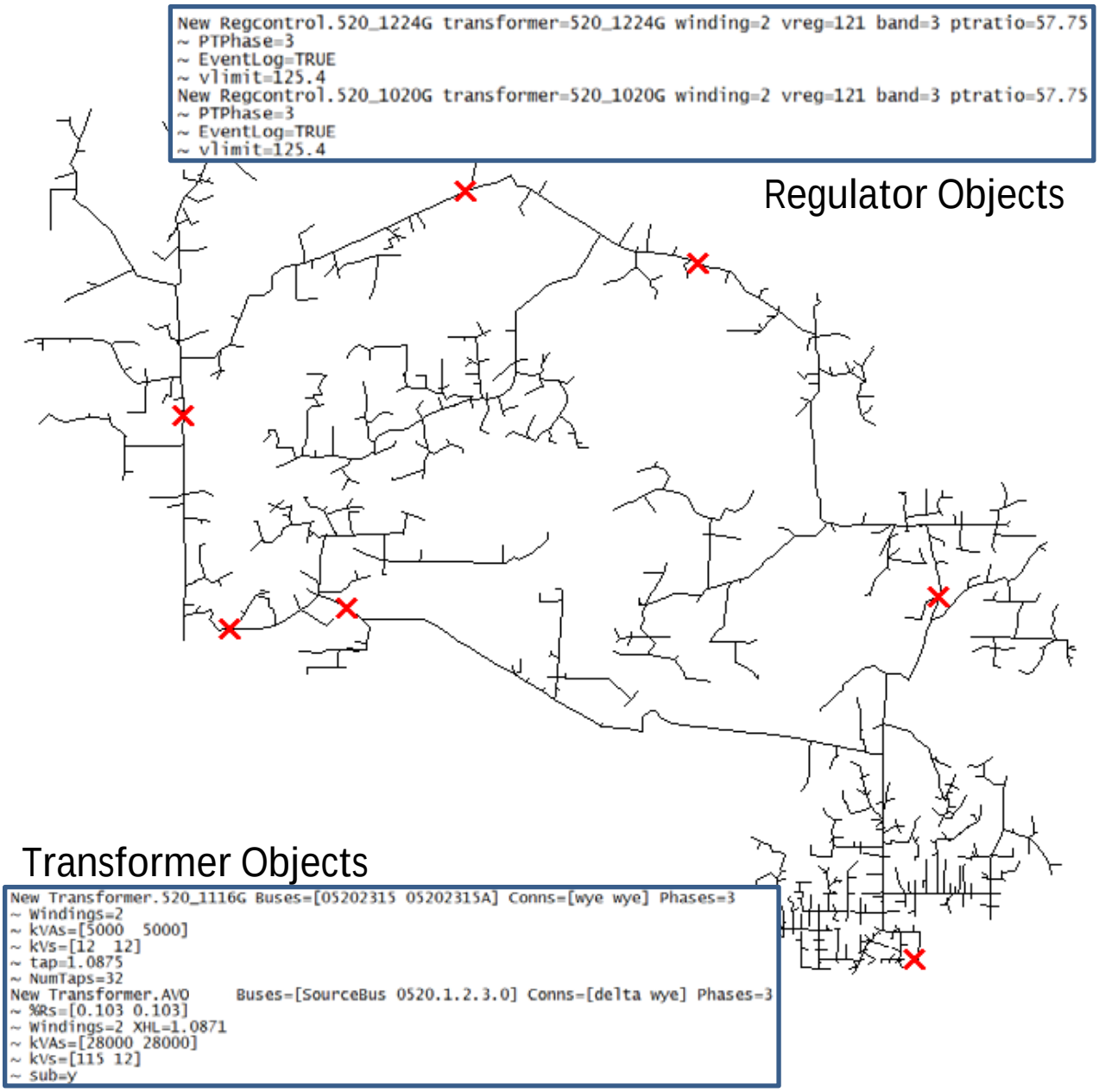

Figure 5-14: Transformers in the utility system and OpenDSS representations of (1) a three-phase transformer and (2) a three-phase voltage regulator. The OpenDSS model of the utility system includes seven transformer objects.

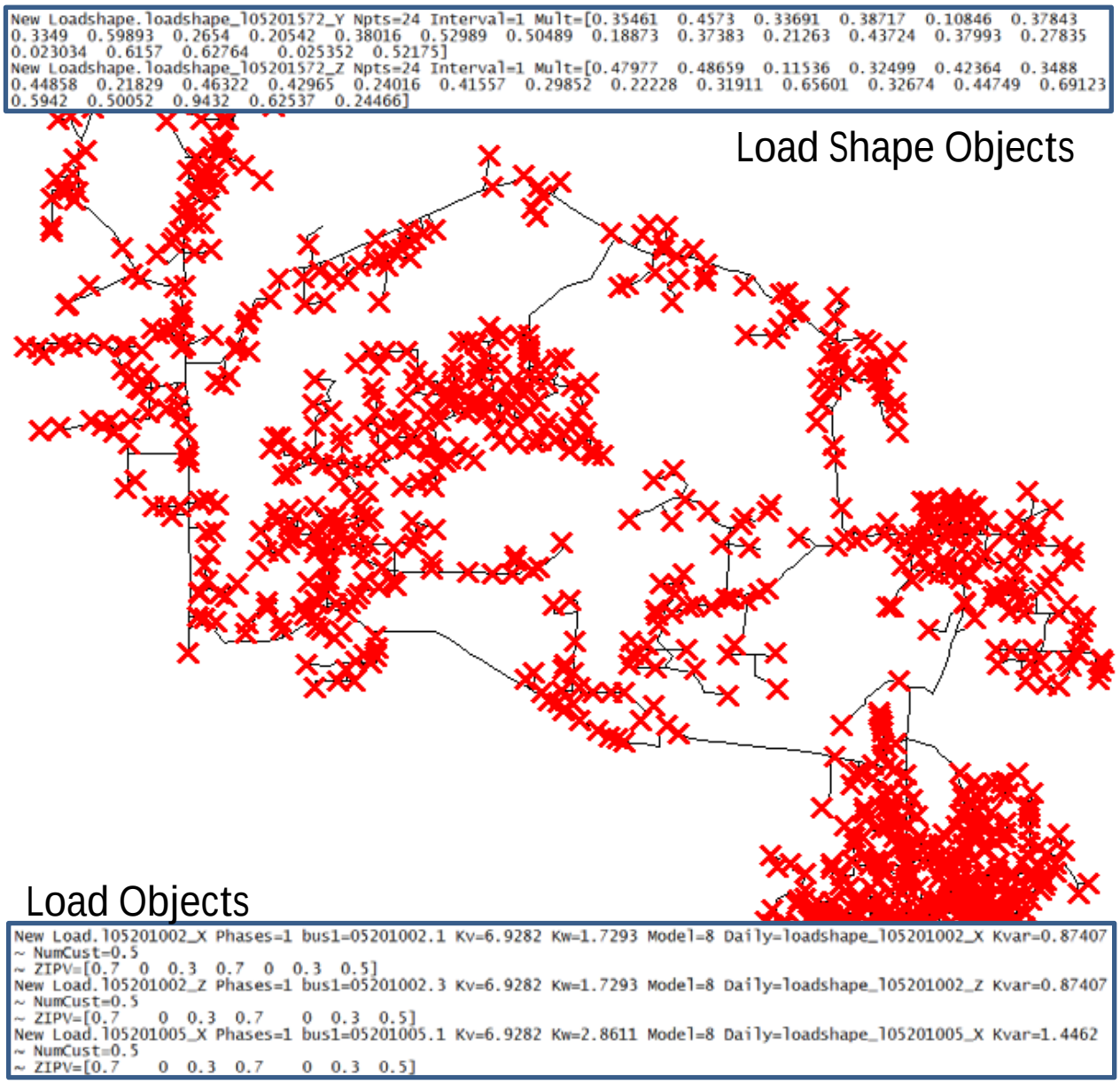

Figure 5-15: Loads in the utility system and OpenDSS representations of three selected loads. The OpenDSS model of the utility system includes 1733 load objects.

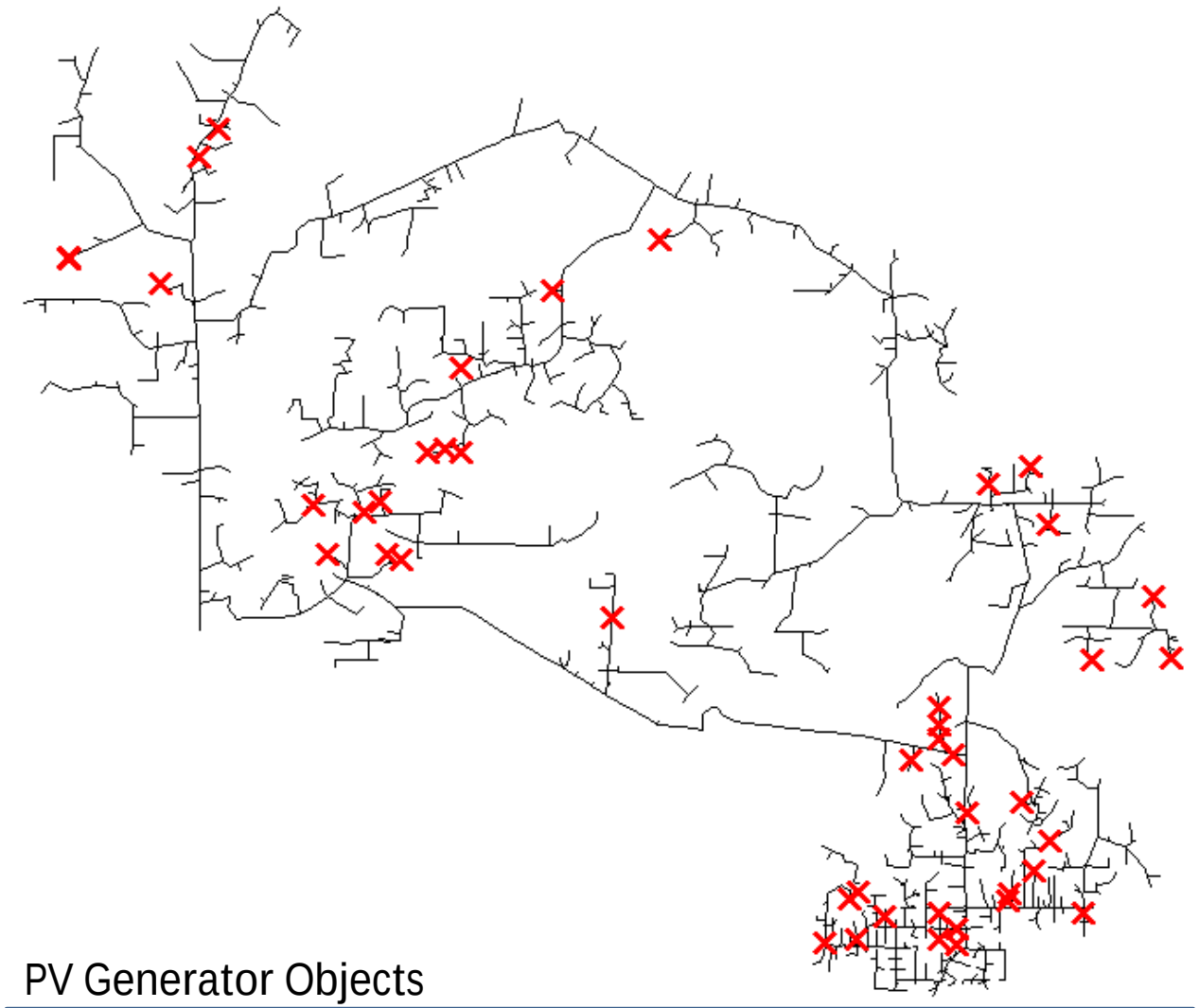


```
New Pvsystem.7          phases=1 bus1=0520830.1 kv=6.9282 pf=1 conn=wye kVA=3 daily=pv
New Pvsystem.6         phases=1 bus1=0520883.2 kv=6.9282 pf=1 conn=wye kVA=1.9 daily=pv
New Pvsystem.11         phases=1 bus1=0520867.3 kv=6.9282 pf=1 conn=wye kVA=3.7 daily=pv
```

Figure 5-16: PV generators in the utility system and OpenDSS representations of three selected PV generators. The OpenDSS model of the utility system includes 45 PV generator objects.

```
New Capcontrol.capctrl_520_1228CF Element=line.05201313_05201314 Capacitor=cap_520_1228CF
~ Type=voltage
~ CTRatio=100
~ EventLog=TRUE
~ OFFsetting=125
~ ONsetting=117
~ PTPhase=3
~ PTRatio=57.75
~ Vmax=126
~ Vmin=116
~ VoltOverride=False
```

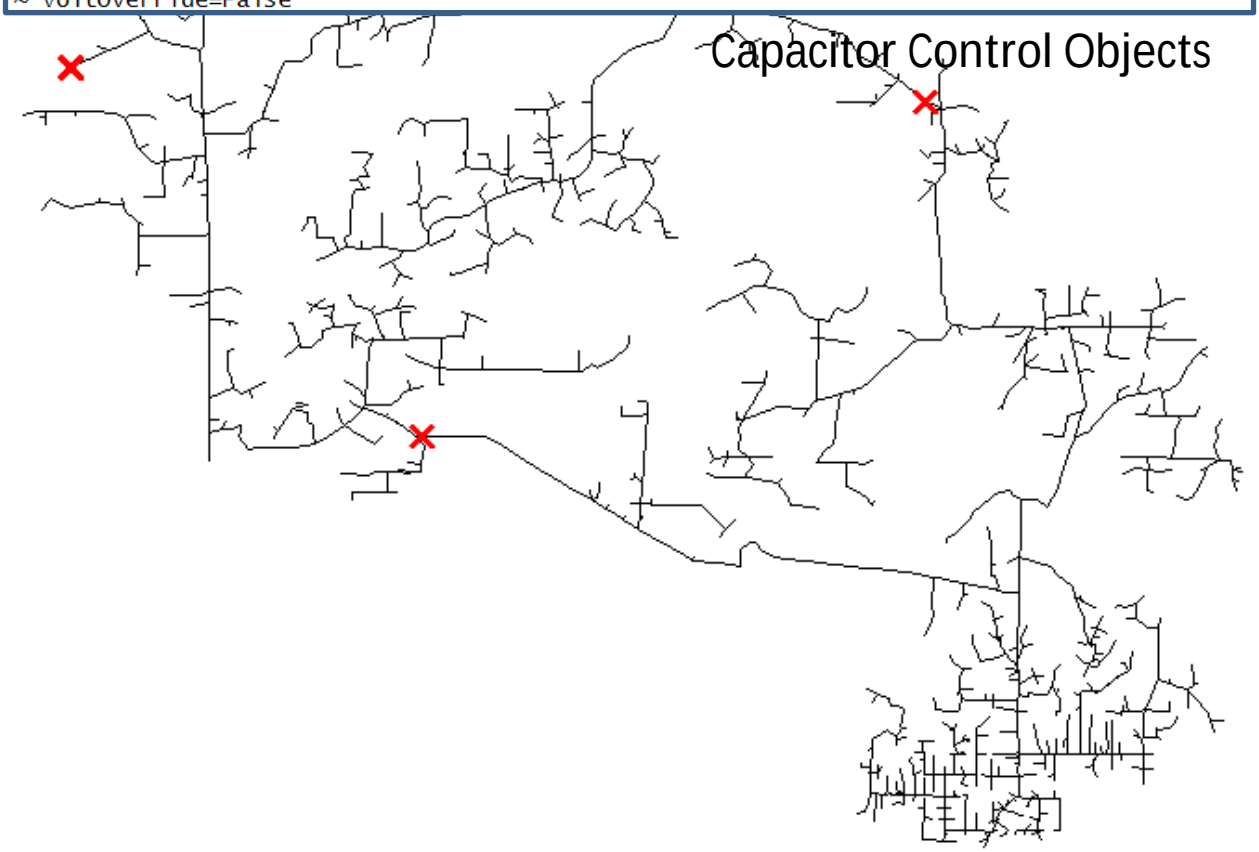

Capacitor Bank Objects

```
New Capacitor.cap_520_1228CF Phases=3 Bus1=05201314 Kvar=1600 Kv=12 Conn=wye states=1
New Capacitor.cap_520_121CW Phases=3 Bus1=05202234 Kvar=1500 Kv=12 Conn=wye states=1
```

Figure 5-17: Capacitor banks in the utility system and OpenDSS representations of two selected capacitor banks. The OpenDSS model of the utility system includes 4 capacitor bank objects.

6 Solar Generation Profiles

A key objective and unique aspect of our study is that we realistically represent the solar-generated power in our simulations by disaggregating the solar generation profiles. This is a significant improvement from typical PV system impact studies, which, for simplicity and lack of irradiance data, use the same aggregated solar generation profile for all PV generators in the system. In this study, we do not do this and instead incorporated the actual solar irradiance conditions at each PV site in our simulations, which we obtained from (1) a sequence of high temporal and spatial resolution cloud maps that we captured with a sky imager system and (2) measured irradiance levels.

In this section, we (1) describe the instruments and the process we used to obtain cloud maps and irradiance data, (2) present examples for irradiance profiles we used in our simulations, and (3) discuss the impact of clouds on PV output power and describe our process for generating solar generation profiles from the measured irradiance data and cloud maps.

6.1 General Procedure for Determining Irradiance Profiles at Each PV Location

<u>Cloud and Shadow Maps</u>

We obtained cloud maps from a whole-sky imager deployed at the UC San Diego campus. This instrument is a fisheye-lens sky camera that captures an image of the sky every 30 seconds. Each image is processed to determine the location of clouds and, based on this information, the locations of the cloud shadows on the ground are calculated and used to create a shadow map, which shows shaded and unshaded regions on the feeder. The sky image covers a total circular cloud area with a radius of several kilometers to tens of kilometers, depending on the height of the clouds. The spatial resolution of a given area on the shadow maps depends on how close this area is from the center of the sky image – it is about 10 meters near the center to about 100 meters near the edge of the sky image. Combining these shadow maps with the known locations of the PV generators on the feeder allows us to determine every 30 seconds (the temporal resolution of the sequence of cloud maps) whether or not a given PV generators is shaded by a cloud. Unshaded areas on the shadow map receive a high level of irradiance and cloudy areas receive a lower level of irradiance that depends on the type of cloud condition. Note that unshaded areas do not necessarily receive 100% of “clear sky” irradiance due to effects such as aerosol scattering and, similarly, shaded areas can receive considerably more than zero irradiance, just as there is still considerable daylight from diffuse horizontal irradiance even on cloudy days.

Solar Irradiance Profiles

A network of irradiance sensors (DEMROES) at UCSD is used to collect irradiance data and calculate the clear sky indices, which are a measure for how much irradiation from the sun reaches the Earth surface under different cloud conditions. We define three categories for the cloud conditions – (1) no cloud (or clear sky), (2) thin cloud, and (3) thick cloud. This categorization is used for converting the shadow map to realistic irradiance profiles, as described in the next paragraph:

Clear sky index is defined as the amount of irradiation (counting both direct normal irradiance DNI and diffuse horizontal irradiance DHI) reaching the ground for each cloud condition. kt is calculated from a histogram of the measured irradiance data obtained directly from GHI sensors. The measured value is normalized with respect to the clear-sky irradiance level, which is determined by the clear sky irradiance model for the atmospheric condition at the location of interest. Historical data going back two hours are used for constructing the histogram. For instance, for a forecast at 12 pm, the histogram is constructed from data collected from 10 am to 12 pm. From the histogram, three values at three peaks are chosen for clear, thin clouds, thick clouds. Using measurements right before the time of forecast ensures that the forecast is based on the most relevant sky indices. If some cloud conditions are not present for the last two hours (e.g., the sky is clear for the last two hours), then default sky indices are used. The default values are 1.057 for clear sky, 0.7 for thin cloud and 0.418 for thick cloud.

Calculating GHI Profiles from Cloud Maps and Irradiance Profiles

A Global Horizontal Irradiance (GHI) profile yields information about the irradiance level at a given location as a function of time. We calculated GHI profiles for each PV location from (1) the series of cloud maps captured by the sky camera and (2) the irradiance data measured at the irradiance sensor locations. Specifically, we calculated the GHI level at each time step as follows:

1) Calculate the clear sky index value, kt, which contains three values: one for clear sky (0.9-1.1), one for thin cloud (0.6-0.9), and one for thick cloud (0.1-0.5).
2) Determine the cloud condition (clear/thin/thick) for all the pixels on the ground using the cloud map information and assign the corresponding clear sky index value to all pixels.
3) Calculate the sky index value (k_{pv}) for a PV system at this time step: If the PV system's footprint has only one pixel then just assign the sky index value of this pixel to the PV system ($k_{pv} = k_i$). If the PV system's footprint has multiple pixels, then calculate an average sky index value for this PV system by taking the mean of the indices from all the pixels (k_{pv} = sum(k_i)/n with n being the total number of pixels representing the PV system's footprint).

4) Calculate GHI for this PV system: $GHI_{pv}(t)= k_{pv} * GHI_{clear}(t)$ where $GHI_{clear}(t)$ is the clear sky GHI at time t.
5) Calculate the power output: $P_{pv} = GHI_{pv}/1000\ W\ m^2 * P_{pv_rated}$ where 1000 is consider the rated GHI value and P_{pv_rated} is the rated power output of the PV system.

Note that the sky camera and irradiance sensors were not located at the simulated feeder and, consequently, we virtually displaced the cloud maps and irradiance data to the area of the analyzed distribution feeder (Feeder B) to generate GHI profiles at the PV locations on the feeder. We consider this a valid approach because the experimentally determined sky conditions, even though they were determined for the UC San Diego Campus area, are representative for coastal California in which Feeder B is located in.

6.2 Solar Irradiance Levels and PV Output Power used in our Simulations

The cloud maps we used in our simulations were measured on December 14, 2012 using the Sky Camera located at the UCSD campus. For this day, a low and thick cloud layer with large coverage and average moving speed was observed. The partly cloudy condition causes large ramps in the morning but the overcast sky in the afternoon reduced both the magnitude and variability of the PV power output. Figure 6-1 shows a shadow map in which the cloud shadows determined from a processed sky image are overlaid on a map of our analyzed feeder (Feeder B) – the figure shows a single snapshot from a sequence of shadow maps recorded every 30 seconds. Note that in the snapshot, over half of the feeder circuit area is covered by clouds, while the remaining area is clear, which illustrates that there are large location-dependent differences in irradiance levels and the importance of individually determining the solar irradiance level at each PV site. Figure 6-2 and Figure 6-3 compare the irradiance levels measured by the irradiance sensor (DEMROES) station at UC San Diego and the irradiance levels at one of the PV sites on Feeder B, which were derived as described in Section 6.1. Figure 6-2, which shows the irradiance levels on a 12-hour time scale, illustrate that during this day large and frequent fluctuations in GHI occurred, which were attributable to highly variable cloud conditions. It is apparent from Figure 6-3, which shows the irradiance levels on a two-hour time scale, that the measured GHI measured by the sensor fluctuates more than the GHI at the PV location. The larger fluctuation of the sensor data is difficult to explain, but might be partly attributable to the following reasons: (1) Our forecast system has three levels of irradiance output (clear/thin/thick) while the actual irradiance output measured by the sensors could be anywhere between 0 and 1.1. Consequently, the sensor data has a higher level of vertical resolution resulting in more fluctuation. (2) Our cloud detection is not perfect, that is, the cloud map (to determine cloud condition for a ground pixel) introduces

an error. For instance, a thin cloud condition might be classified as clear sky and that error would cause the forecast to miss a ramp in the GHI profile.

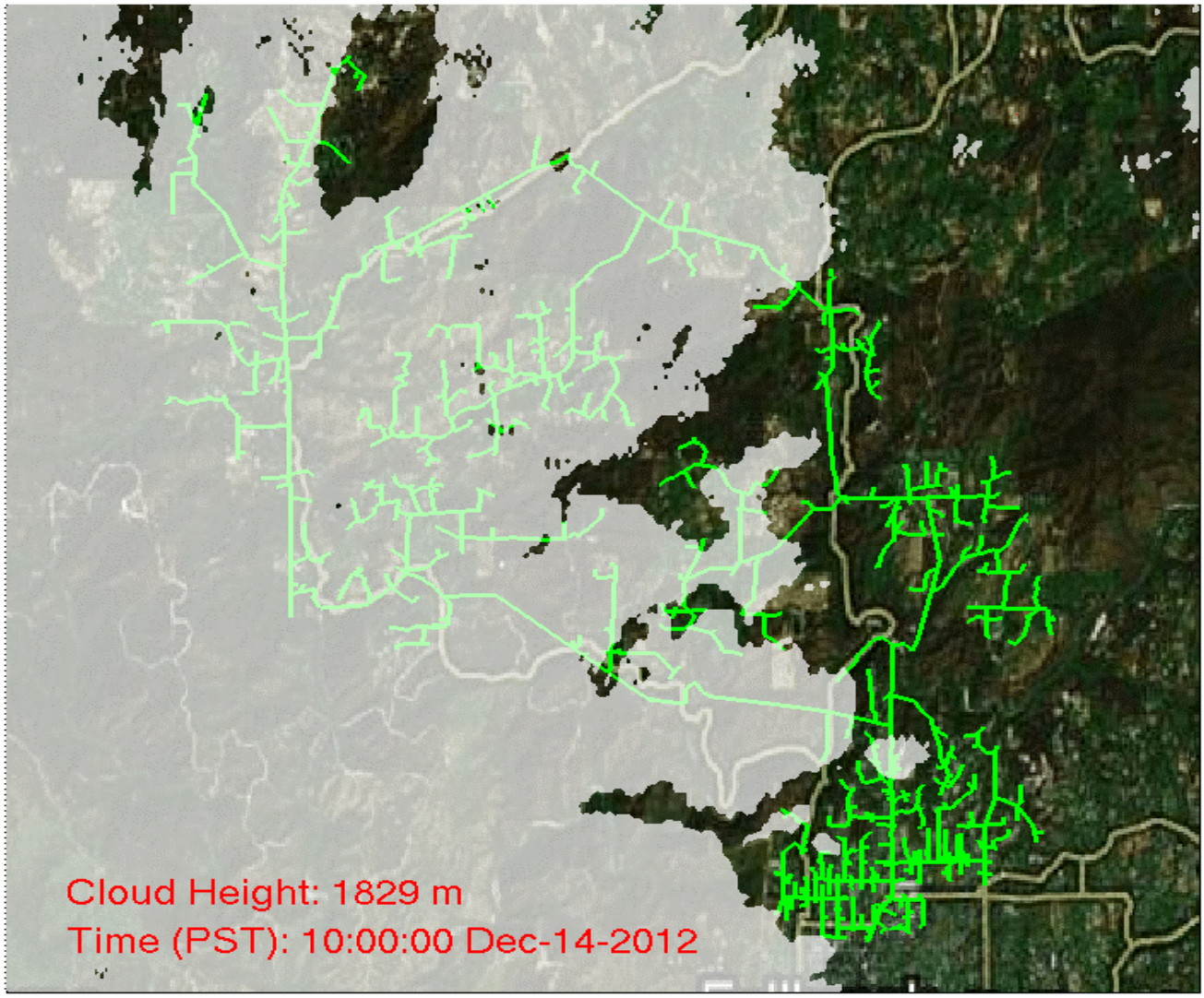

Figure 6-1: Shadow map for Feeder B captured at 10:00 am on December 14, 2012. White-shaded areas are areas with cloud cover. The feeder map is colored in green and overlaid on a Google satellite image.

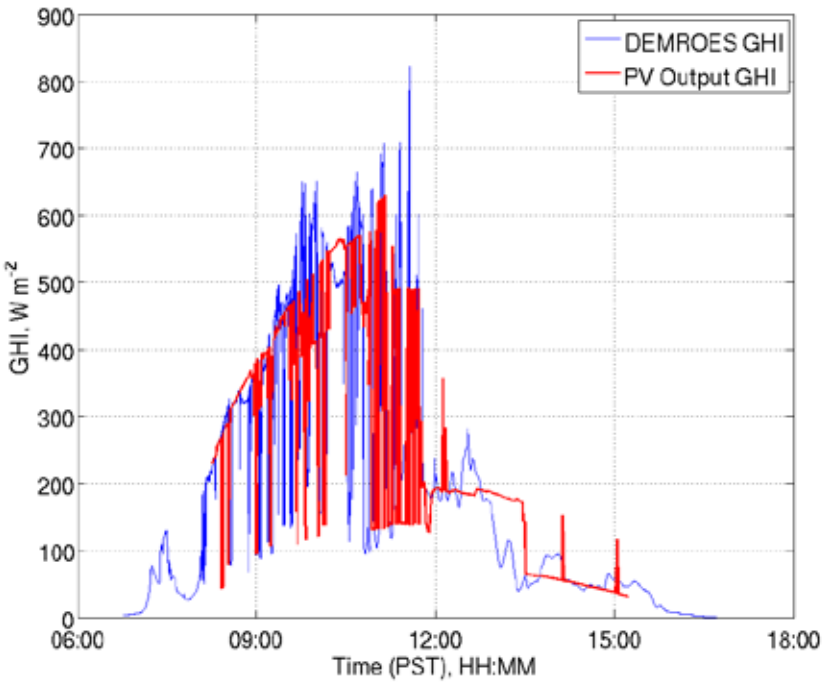

Figure 6-2: Comparison of modeled GHI at the PV generator and measured irradiance from one of the sensor at UC San Diego for December 14, 2012.

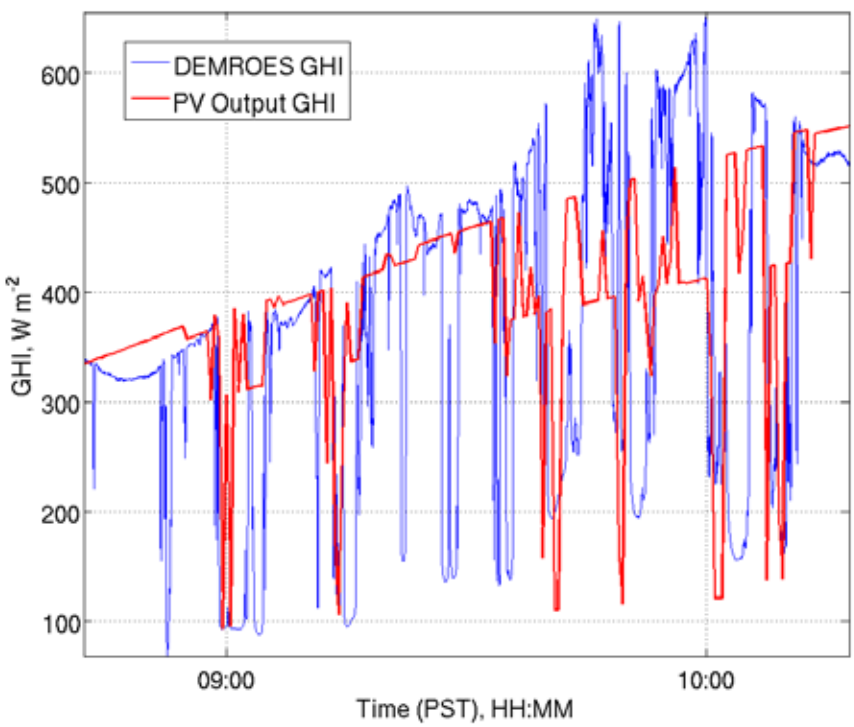

Figure 6-3: Comparison of modeled GHI at the PV generator and measured irradiance from one of the sensor at UC San Diego for a two hour period on December 14th.

Figure 6-4 and Figure 6-5 show a 12-hour GHI profile and a two-hour GHI profile, respectively, for three different PV sites calculated as described in Section 6.1. Figure 6-4 shows that the GHI profile varies between clear sky conditions (maximum values of irradiance levels before noon), thick cloud cover (irradiance levels between noon and 3pm) and isolated thick clouds (sharp dips in the irradiance levels before noon). It is apparent from Figure 6-5 that there are location-dependent differences in irradiance levels between the three GHI profiles. For instance, PV site #15 exhibits a dip in the irradiance level at 10:30am, due to an isolated thick cloud shading at this location, while the other two sites experience clear-sky conditions. On the other hand, the overcast condition in the afternoon (12am to 3pm) results in very similar GHI profiles (see Figure 6-4).

We calculated the power output of each PV generator in the system from the GHI profile at the respective PV site and the rated power output of the respective PV generator. For example, the GHI profiles from the three generators shown in Figure 6-5 resulted in the power output profiles shown Figure 6-6 after scaling the GHI profiles by the rated power output of the PV generators (3 kW, 6 kW, and 33 kW). Again, the effect of disaggregation is apparent from Figure 6-6 – the spatial separation of the location of the three PVs and the moving clouds during the 'partly cloudy' conditions in the morning result in three distinguished generation profiles with regards to variability of the power.

We also used irradiance profiles in our simulations that are typical for a clear day in order to facilitate a comparison between PV impacts during a clear-sky day and a cloudy day. We constructed the 'perfectly clear day' irradiance levels by removing the effect of clouds from the irradiance levels measured during December 14, 2012 at UC San Diego, which resulted in the smooth power output curves shown in Figure 6-7. Note that this clear-sky scenario is hypothetical for this particular day, but, in general, clear periods are common in California.

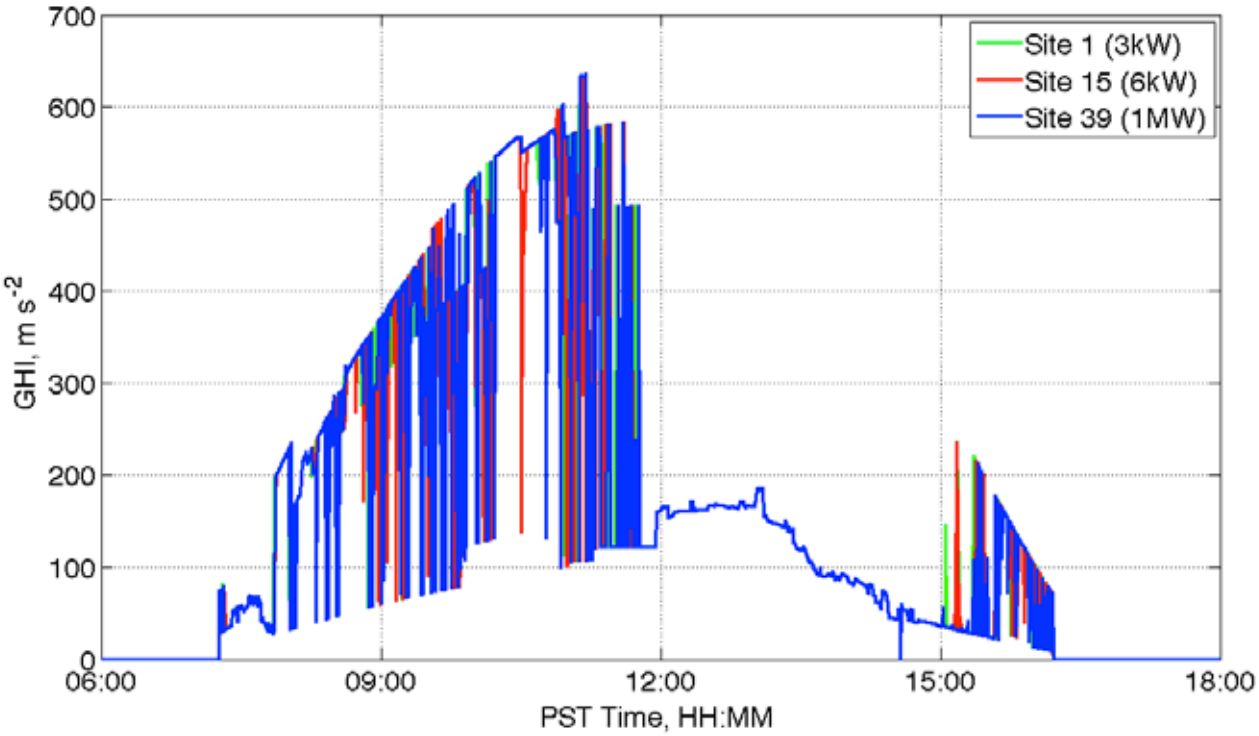

Figure 6-4: GHI profiles from 6:00 PST to 18:00 PST on December 14th 2012 at three PV sites.

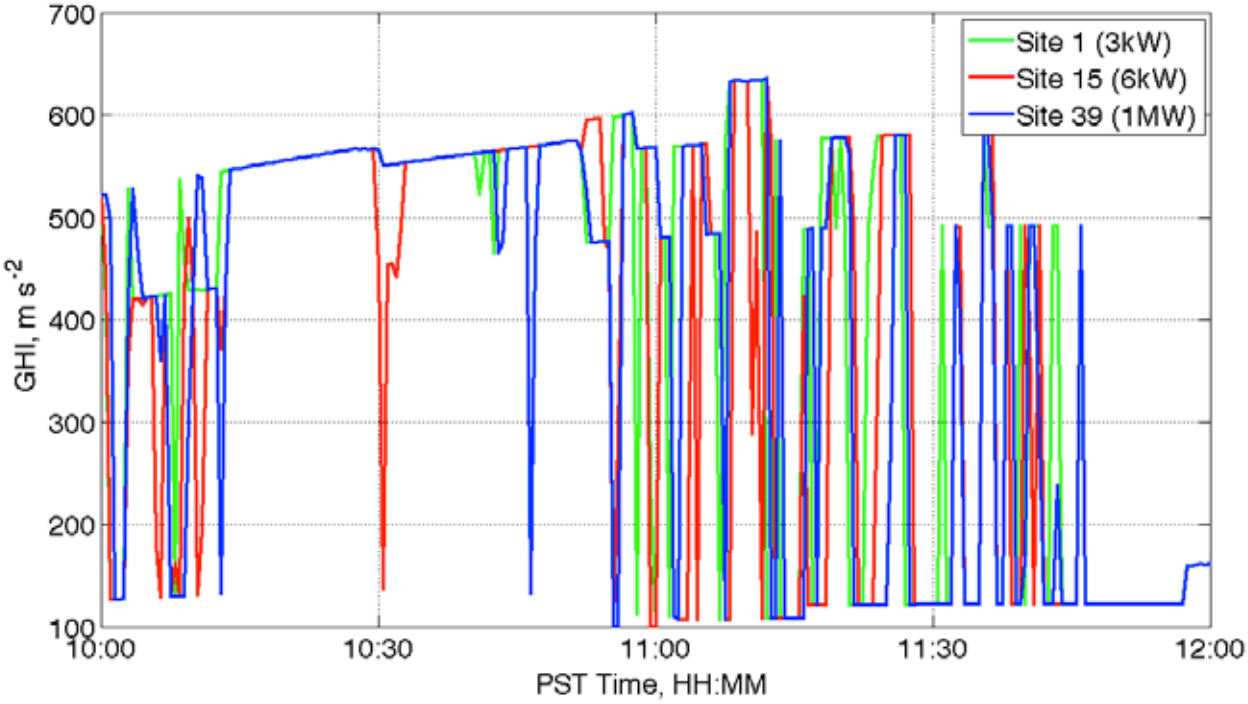

Figure 6-5: GHI profiles from 10 PST to 12:00 PST on December 14th 2012 at three PV sites.

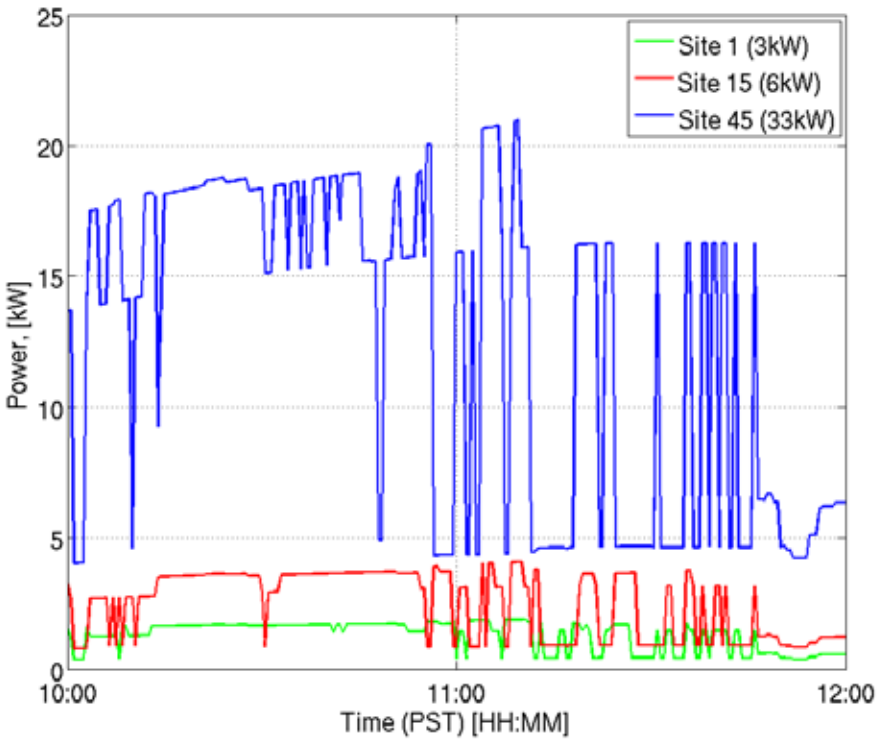

Figure 6-6: Power output profiles for three PV sites with different sizes derived from irradiance measured on December 14, 2012 at UC San Diego, two hour time frame.

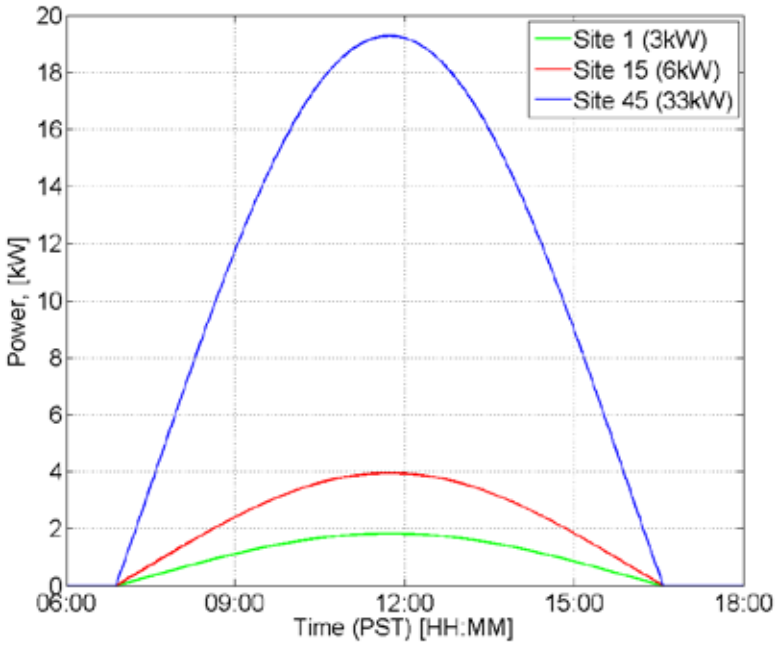

Figure 6-7: Power output profiles during a clear day. The profiles were obtained from filtered irradiance levels measured on December 14, 2012 at UC San Diego.

6.3 Considerations for the Impact of Clouds on PV Generation Profiles

Realistic PV generation profiles must account for actual irradiance conditions at the PV locations, which, during partly cloudy days, can be very different at different locations. Moving clouds affect the generated power on two scales – (1) clouds shade part of an array causing shaded and unshaded areas on the same array and (2) clouds shade part of the feeder causing shaded and unshaded PV sites on the same feeder. The following paragraphs elaborate upon these two cases.

<u>Clouds shading part of a PV array</u>

The area the PV generator occupies on the ground depends on the power ratings, that is, PV generators with a higher rating generally have more PV panels that cover a larger area than the area covered by PV generators with a smaller rating (this dependency is illustrated in Figure 5-9). At a given time, some area of an array of a PV generator may be shaded by clouds while another part of the same array may have clear-sky conditions – a scenario that is more likely to occur on large PV generators due their larger footprint. The net effect of a partially shaded PV array is highly dependent on the connection type of the solar panel strings that constitutes the array and the solar modules in the panel – the power output of partially shaded array in which the strings are connected in series can be substantially lower than the power output of a panel of the same size and the same shaded area, but with the strings connected in parallel[1]. [14] [15] For instance, if 50% of the array area is shaded, the parallel-connected array may generate at 50% of the rated power while the series-connected array may generate at well below 50% of the rated power. Either way, the generation output of a large PV generator will not be interrupted immediately when a small cloud begins to move over the array gradually shading the array. Instead, there will be an averaging effect and the cloud-caused variation of the PV power output will be "smooth" instead of a sharp step change. On the other hand, the time frame between maximum generation (clear sky) and low generation (array completely covered by cloud) tends to be much shorter for arrays with a smaller area as it takes less time for a cloud to cover the entire array area. The maximum resolution of the cloud maps we employed is 18 m by 18 m for each pixel in the map and the largest PV site is the site with the two 1 MW PV generators located at close proximity, which has a combined estimated footprint of 5 pixels by 10 pixels. We accounted for partial shading of the PV array in our simulations for each simulation time step by

[1] In general, shading has a less detrimental effect on parallel-connected strings. However, series connections are still necessary to achieve desired voltage levels, so a real-world PV array is typically composed of both parallel and series connected strings.

1) estimating the size of the PV area based on its rating,
2) setting up the footprint of the PV system on the ground based on its size and location,
3) determining the shaded and unshaded areas of the PV footprint based on the cloud map,
4) calculating the power output for the shaded and unshaded areas of the PV footprint based on the GHI profile for this location, and
5) calculating the total power output for each PV system by summing up the power outputs from the PV system's shaded and unshaded areas.[1]

The PV power generated at a PV site of this size will experience some smoothing effect, but the PV site area is relatively small compared to the area of the whole feeder. Consequently, the smoothing effect will be more significant when accounting for the effect of clouds on the total PV generation [16], as explained in the following paragraph.

Cloud shading part of a feeder

Some PV sites on the feeder may be shaded by clouds, while others experience clear sky conditions. The shaded and unshaded regions are in a continuous flux due to cloud movement. Similar to the above case (cloud shading part of a PV array) the net effect will be that the total PV generated power is smoothened due to the spatial diversity of the PV sites. Figure 6-6 demonstrates the dependency of PV generation on location. The figure shows the power output for the same two-hour time frame for three sites at different locations and with different output ratings. It is apparent from the figure that cloud transients (i.e., sharp changes of irradiance levels that cause spikes or dips of the PV output power) occur at different times – e.g., the PV output power of generator #45 dips sharply at about 10:50am while the other two generators generate at full power at this time. We are capturing this effect in our simulation by

1) overlaying the cloud map at a given time t_1 over the feeder area,
2) determining shaded and unshaded PV sites based on the cloud map at time t_1,
3) assigning different power outputs for unshaded PV generators and shaded PV generators based on the GHI profile for each PV site, that is determined from algorithm presented in Section 6.1,
4) solving the OpenDSS circuit for time step t_1,
5) moving on to time $t_2=t_1+\Delta t$, where Δt is the simulation time step, and
6) repeating the process, noting that the cloud map at time t_2 will be different due to cloud movement, until the simulation end time is reached.

[1] Steps 4) and 5) implicitly assume that the shaded area and the unshaded area can be treated independently as two separate arrays, that is, the power produced by the unshaded area does not affect the power produced by the shaded area. This is the case if parallel-connected PV strings are used, as explained above.

Depending on the cloud conditions, this elaborate process for determining PV generation levels may or may not be necessary, as discussed in the following paragraph.

Impact of different cloud conditions on PV generation

During clear days, PV generation can be easily and accurately determined from location, size, and tilt angle of the PV systems. On overcast days when the sun is rarely seen in the sky, the PV output is generally low and can be predicted without much error. PV generation is fluctuating most and is hardest to predict during partly cloudy days. Power output can drop to 20% of clear sky power or less if a thick cloud covers the whole PV system. Clouds can be classified into different categories depending on many parameters such as their shape, height, and velocity. For the purpose of investigating the impact of clouds on the PV generation, we limit these parameters to three key factors: 1) cloud thickness, 2) cloud velocity, and 3) cloud size. These parameters will impact cloud-caused variation of PV output power as follows:

- The first factor, cloud thickness, determines how much sunlight the solar panel receives. Cloud thickness will impact the magnitude of fluctuation of the PV output power, such as the magnitude of cloud-caused ramps. For instance, cirrus cloud with thin and wispy characteristics are more transparent causing slower ramps compared to cumulus clouds, which are thick and have clearly defined edges.
- The second factor, cloud velocity, together with the cloud height determines how fast shaded and unshaded areas on the feeders are changing. This factor impacts the width of the cloud-caused ramp. For instance, slow cloud at low altitude will cause more rapid ramps compared to a fast cloud at high altitude.
- The third factor, cloud size, together with cloud height determines the size of the shaded area cast by the cloud. This will impact the frequency of power fluctuations. For instance, for the same cloud cover fraction, large, isolated clouds will cause less frequent ramps compared to smaller and more scattered clouds

Furthermore, the impact of clouds on PV output power also depends on the PV generator "density". For instance, a medium-size cloud may provide a overcast cloud cover for a small-size feeder with a large number of PV generators while the same cloud conditions may be seen as 'scattered' (causing more variation in PV output power) for a large feeder and a smaller number of PV generators.

7 Load Profiles

In this section, we develop a stochastic algorithm to create individual load profiles based on aggregated load curves. The algorithm takes the variability of individual loads into account by assuming that they vary based on a normal distribution. The procedure we used to generate the individual load profiles is as follows:

1) Read in the daily aggregated load factor and ratings of individual loads.
2) Randomly generate individual load factors for each individual load based on normal distribution, which takes the respective aggregated load factor as mean and a user-defined standard deviation.
3) Compute individual load profiles using the ratings of individual loads and individual load factors.

In order to evaluate the effect of disaggregation, the total power supplied to all loads for the disaggregated case should be similar to the total power supplied to all loads for the aggregated case. This is important because any changes with regards to tap changing operations, feeder voltage profiles, etc. would be attributable to making the simulation more realistic by disaggregating the loads and not to changing the overall load demand. However, due to the random variation of the individual load factors, there will be a mismatch between the load demand for the disaggregated case and the aggregated case. This mismatch will be larger for larger values of the standard deviation and for smaller numbers of loads. We quantify this mismatch by calculating the discrepancy between the total load demand for the disaggregated case and the aggregated case at each hour. In the following sections, we demonstrate the procedure in three examples (i.e., four loads, ten loads, 100 loads) and document the load profiles created for our simulations, in which we applied the same methodology to all loads.

7.1 Example of Four-Load Scenario

In this example, four individual loads are considered. The ratings of the loads are: 0.57 kW, 2.86 kW, 6.88 kW, and 17.17 kW. We demonstrate the algorithm we developed for disaggregating the loads below:

1. Select the Aggregated Load Factor (ALF) at Hour 1:
   ALF = 26.6%
2. Input Ratings of Individual Loads (RIL):
   $RIL_1 = 0.57kW, RIL_2 = 2.86kW, RIL_3 = 6.88kW, RIL_4 = 17.17kW$
3. Calculate the Aggregated Load Demand (ALD):
   $ALD = ALF \cdot (RIL_1 + RIL_2 + RIL_3 + RIL_4) = 7.3097\ kW$

4. Generate n random values $(x_1, x_2, x_3, \ldots\ x_n)$ based on a normal distribution with a selected standard deviations and a mean value of zero. n is the number of loads.
   In our example for the four-load scenario the randomly generated values are
   $x_1 = 0.0421, \quad x_2 = 0.1008, \quad x_3 = 0.1992, \quad x_4 = 0.1605$
5. Calculate Individual Load Factors (ILF) – one for each load:
   $ILF_n = ALF \times x_n$
   In our example for the four-load scenario the ILFs are
   $ILF_1 = 25.48\%, \qquad ILF_2 = 23.92\%, \qquad ILF_3 = 21.3\%, \qquad ILF_4 = 22.33\%$
6. Calculate Individual Load Demands (ILDs) for Hour 1 as follows:
   $ILD_n = ILF_n \times RIL_n$
   In our example for the four-load scenario the ILDs are
   $ILD_1 = 0.1452kW, \quad ILD_2 = 0.6843kW, \quad ILD_3 = 1.4653kW, \quad ILD_4 = 3.8336kW$
7. Assess the discrepancy between the aggregated load demand and the sum of the individual load demands by computing the relative error. The relative error is the difference between these two values with respect to the sum of the rated loads.
   $$Error = \frac{ALD - \sum_1^n ILD_n}{\sum_1^n RIL_n} \times 100\%$$
   In our example for the four-load scenario the error is
   $$Error = \frac{ALD - (ILD_1 + ILD_2 + ILD_3 + ILD_4)}{RIL_1 + RIL_2 + RIL_3 + RIL_4} \times 100\% = 4.30\%$$
8. Repeat Steps 1 through 7 for the remaining 23 hours.

The steps 1 through 8 documented above will result in a number of series – each series containing 24 values (one value for each hour of the day) and describing the variation of parameters such as ILDs, ILFs, errors, etc. throughout the day.

The daily aggregated load factor curve is shown in Figure 7-1a. Figure 7-1b shows the individual load factor curves, which are derived from the aggregated load factor curve. The aggregated load factor curve is included in Figure 7-1b for comparison purpose. The individual load factors vary around the aggregated load factor. In Figure 7-1c, four individual load profiles are generated based on the stochastic algorithm as explained above. We selected a standard deviation of 0.2. Note that for the four-load scenario, we selected a relatively small number for the standard deviation in order to keep the error due to the stochastic variation of a small number of loads within reason. In Figure 7-2a, the sum of the individual load profiles is compared

to the aggregated load profile. The percentage errors, as shown in Figure 7-2b, vary between -7.2% and 4.3%.

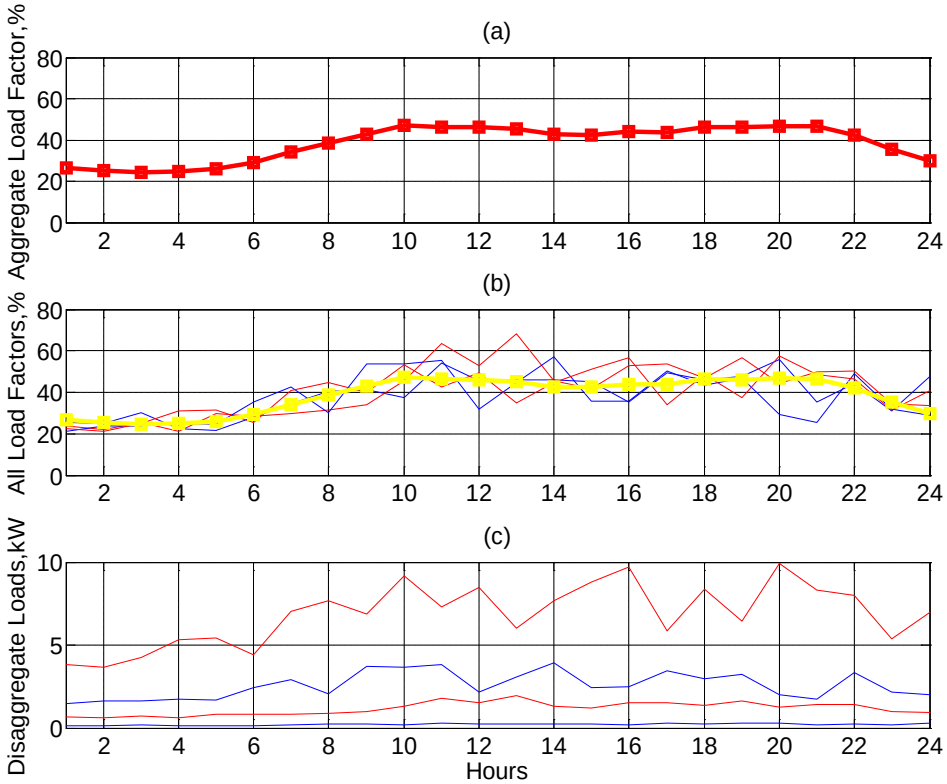

Figure 7-1: Aggregate load factors, all load factors, and disaggregate loads, 4 loads.

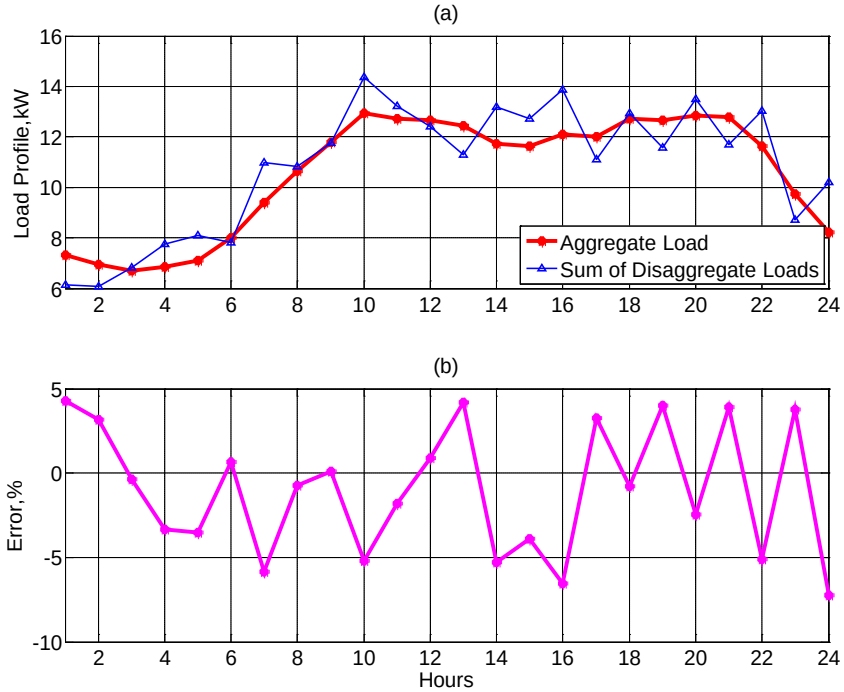

Figure 7-2: Comparison of aggregated load profile with sum of individual load profiles, 4 loads.

7.2 Example of Ten-Load Scenario

In this example, ten individual loads are considered. The ratings of the loads are: 0.57 kW, 1.13 kW, 1.73 kW, 3.44 kW, 4.6 kW, 5.7 kW, 6.88 kW, 7.99 kW, 10.34 kW, and 25.78 kW. The daily aggregated load factor curve is shown in Figure 7-3a. Figure 7-3b shows individual load factor curves, which were derived from the aggregated load factor curve. The aggregated load factor curve is included in Figure 7-3b for comparison purpose. The individual load factors vary around the aggregated load factor. In Figure 7-3c, ten individual load profiles are generated based on the stochastic algorithm described in Section 7.1. We selected a standard deviation of 0.2. Note that for the ten-load scenario, we selected a relatively small number for the standard deviation in order to keep the error due to the stochastic variation of a small number of loads within reason. In Figure 7-4a, the sum of the individual load profiles is compared to the aggregated load profile. The percentage errors, as shown in Figure 7-4b, vary between -7.9% and 6.1%.

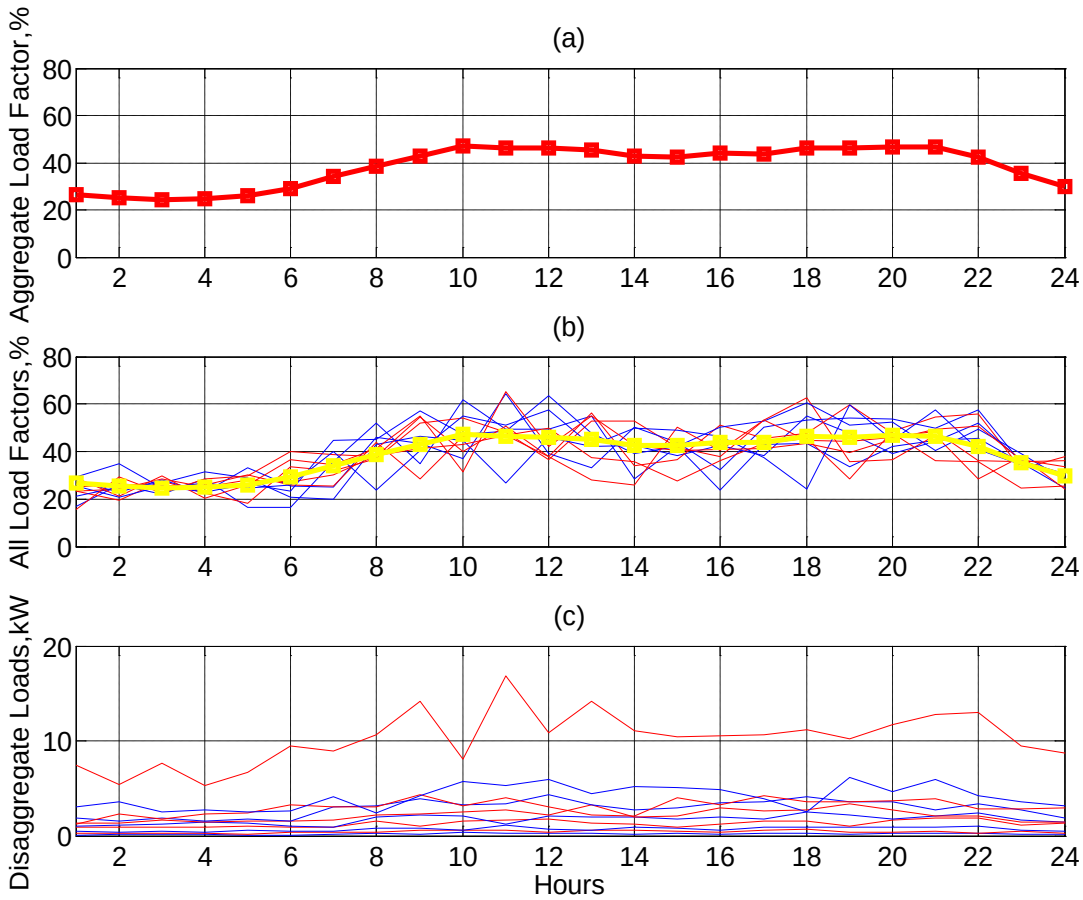

Figure 7-3: Aggregate load factors, all load factors, and disaggregate loads, 10 loads.

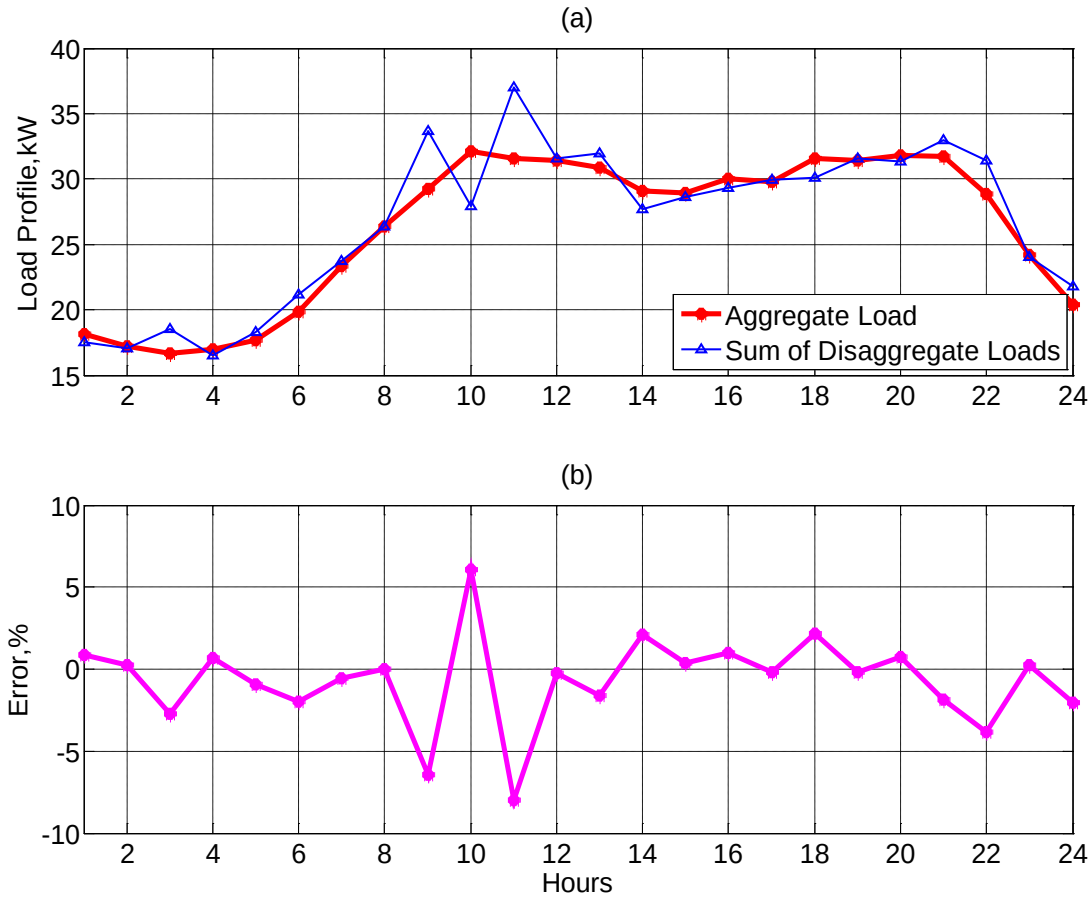

Figure 7-4: Comparison of aggregated load profile with sum of individual load profiles, 10 loads.

7.3 Example of One-Hundred-load scenario

In this example, a total of hundred individual loads are considered. The ratings of loads are: ten 0.57 kW loads, ten 1.13 kW loads, ten 1.73 kW loads, ten 3.44 kW loads, ten 4.6 kW loads, ten 5.7 kW loads, ten 6.88 kW loads, ten 7.99 kW loads, ten 10.34 kW loads, and ten 25.78 kW loads. The daily aggregated load factor curve is shown in Figure 7-5a. Figure 7-5b shows individual load factor curves, which were derived from the aggregated load factor curve. The aggregated load factor curve is included in Figure 7-5b for comparison purpose. The individual load factors vary around the aggregated load factor. In Figure 7-5c, a hundred individual load profiles are generated based on a normal distribution with a standard deviation of 0.5 (see Section 7.1). In Figure 7-6a, the sum of the individual load profiles is compared to the aggregated load profile. The percentage errors, as shown in Figure 7-6b, vary between -7.9% and 6.1%.

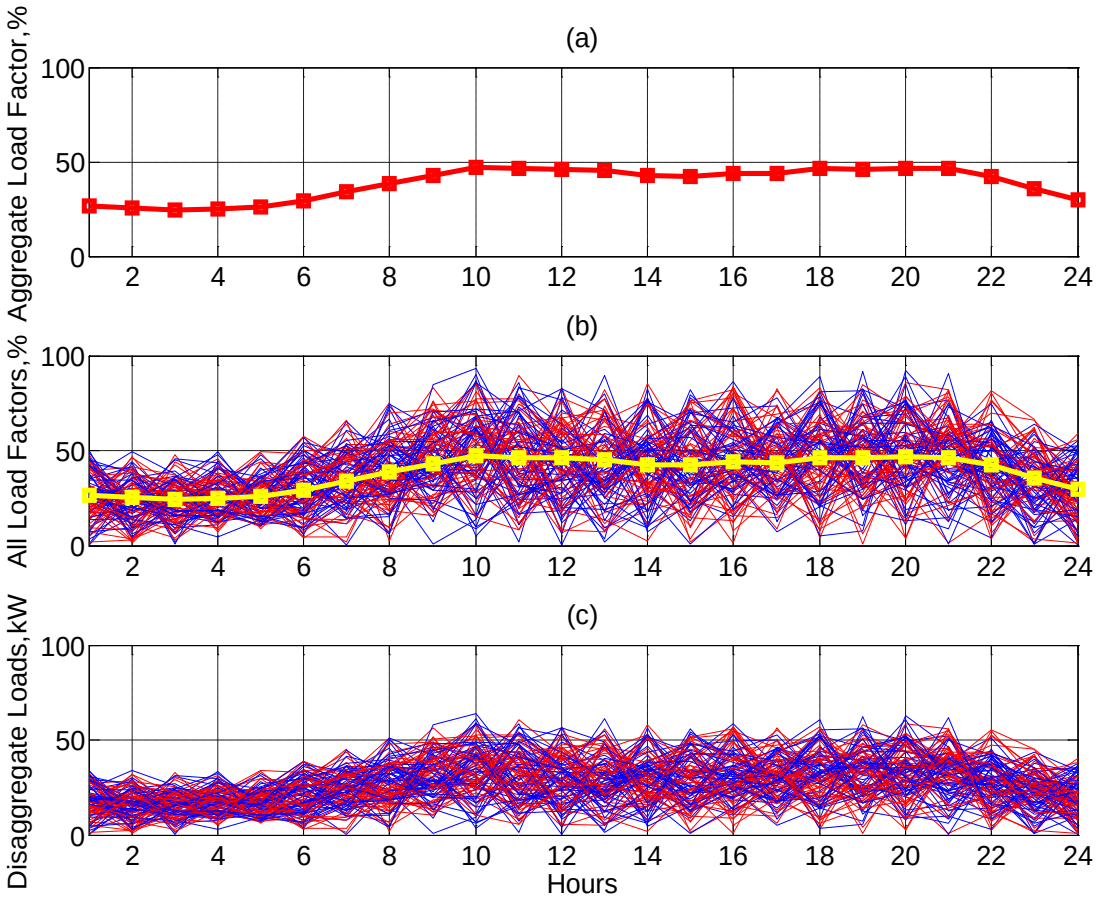

Figure 7-5: Aggregate load factors, all load factors, and disaggregate loads, 100 loads.

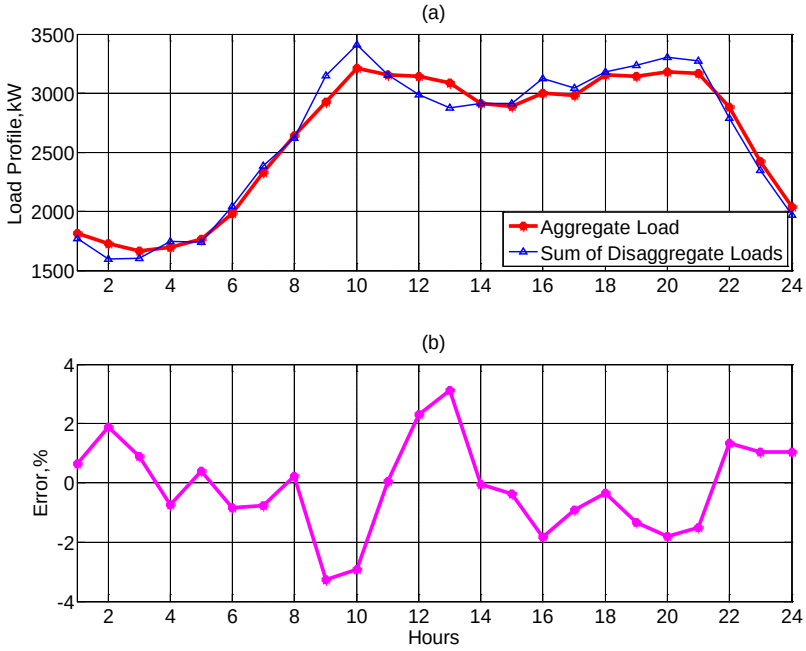

Figure 7-6: Comparison of aggregated load profile with sum of individual load profiles, 100 loads.

7.4 Load Profiles Used in Our Simulations

The system loads provided in the SynerGEE simulation files provided by the host utility were divided into four different load groups consisting of 1699 residential loads ($0.344 \leq kW \leq 30$), 30 small-commercial loads ($30 < kW \leq 100$), 4 medium-commercial loads ($100 < kW \leq 800$), and one hospital load (1,974 kW). The corresponding aggregated 24 hour load factors for residential, small-commercial, medium-commercial, and industrial loads were obtained from data that are publicly available on Southern California Edison's (SCE) website[1]. SCE stores averaged static hourly load profiles for different rate groups. We obtained hourly data for each of the four groups covering the same time period in December as the solar irradiation profiles (see Section 6). The stochastic algorithm was applied to the first three aggregated load factors to generate individual 24 hour profiles for every single load in the circuit. We assumed that the hospital load behaves similar to an industrial load in that both load profiles have significant demand during night hours. Based on this assumption, we selected the industrial load profile to represent the hospital load. The hospital load was not disaggregated since this group contains only a single load. Figure 7-7 shows the normalized and aggregated 24 hour profiles for the identified groups, as obtained from SCE.

<u>Residential Loads</u>

For the 1699 residential loads, the daily aggregated load factor curve is shown in Figure 7-8a. Figure 7-8b shows individual load factors. The aggregated load factor curve is included in Figure 7-8b for comparison purpose. The individual load factors vary around the aggregated load factor. In Figure 7-8c, individual load profiles are generated based on a normal distribution with a standard deviation of 0.5 (see Section 7.1). In Figure 7-9a, the sum of individual load profiles is compared with the residential aggregated load profile. The percentage error, as shown in Figure 7-9b, varies between -1.3% and 1.1%.

[1] **Regulatory Information - SCE Load Profiles (https://www.sce.com/wps/portal/home/regulatory/load-profiles/historical/)**

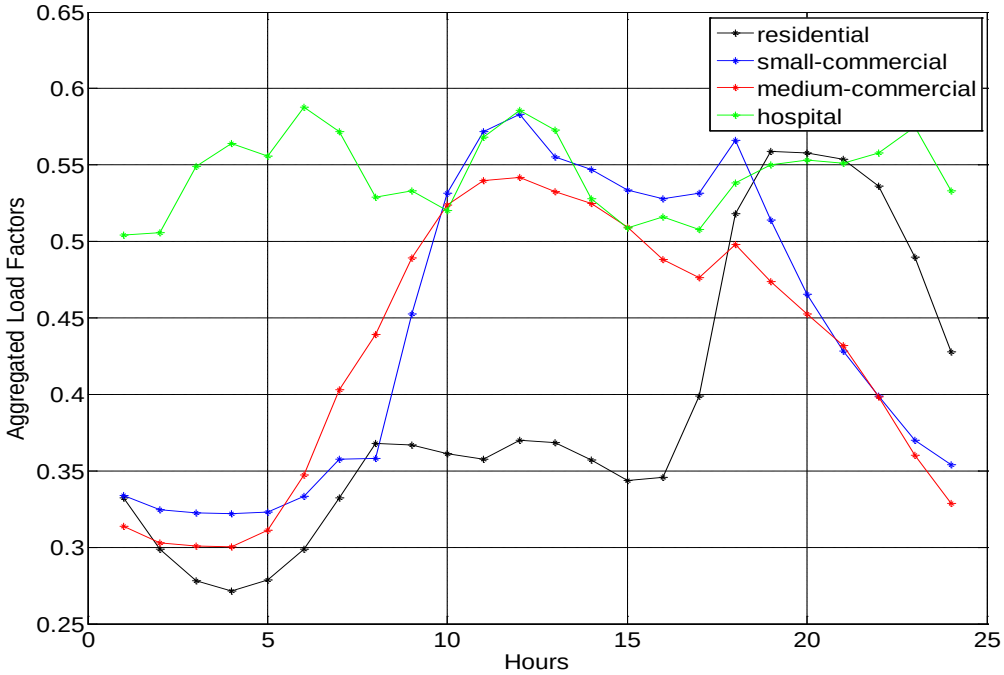

Figure 7-7: Aggregated load factors for residential, small-commercial, medium-commercial and hospital load types.

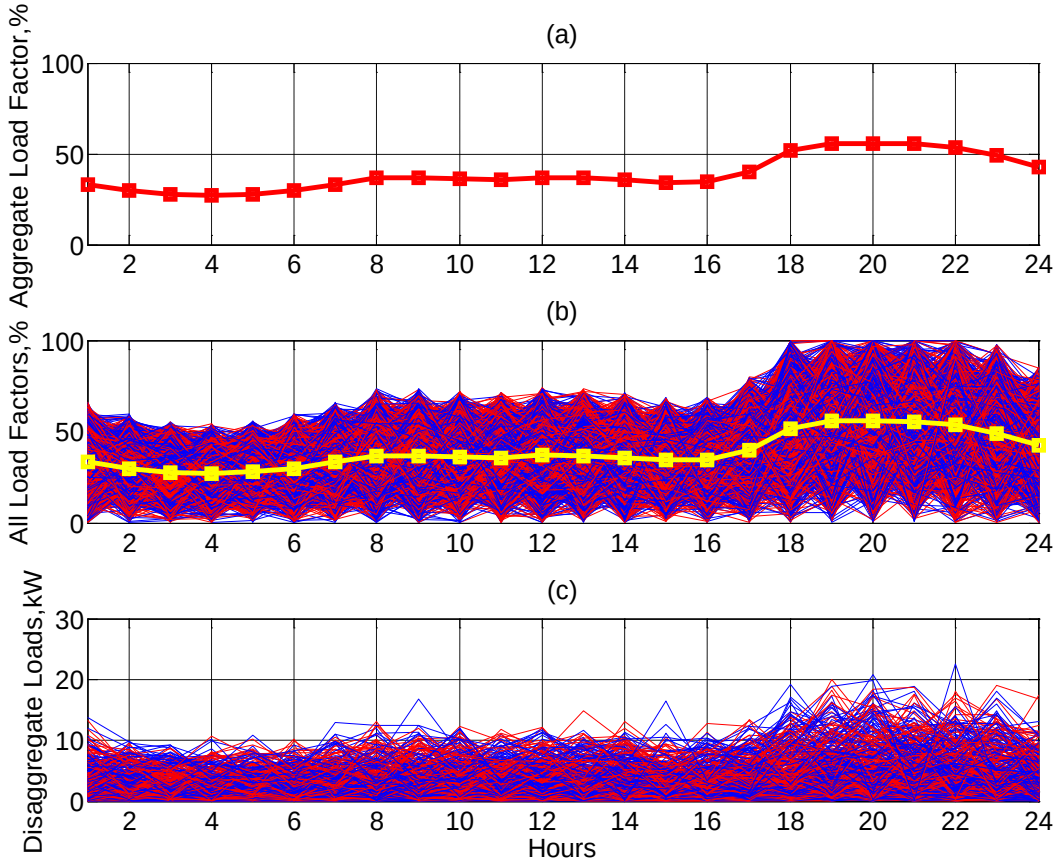

Figure 7-8: Aggregate load factors, all load factors, and disaggregate loads, residential.

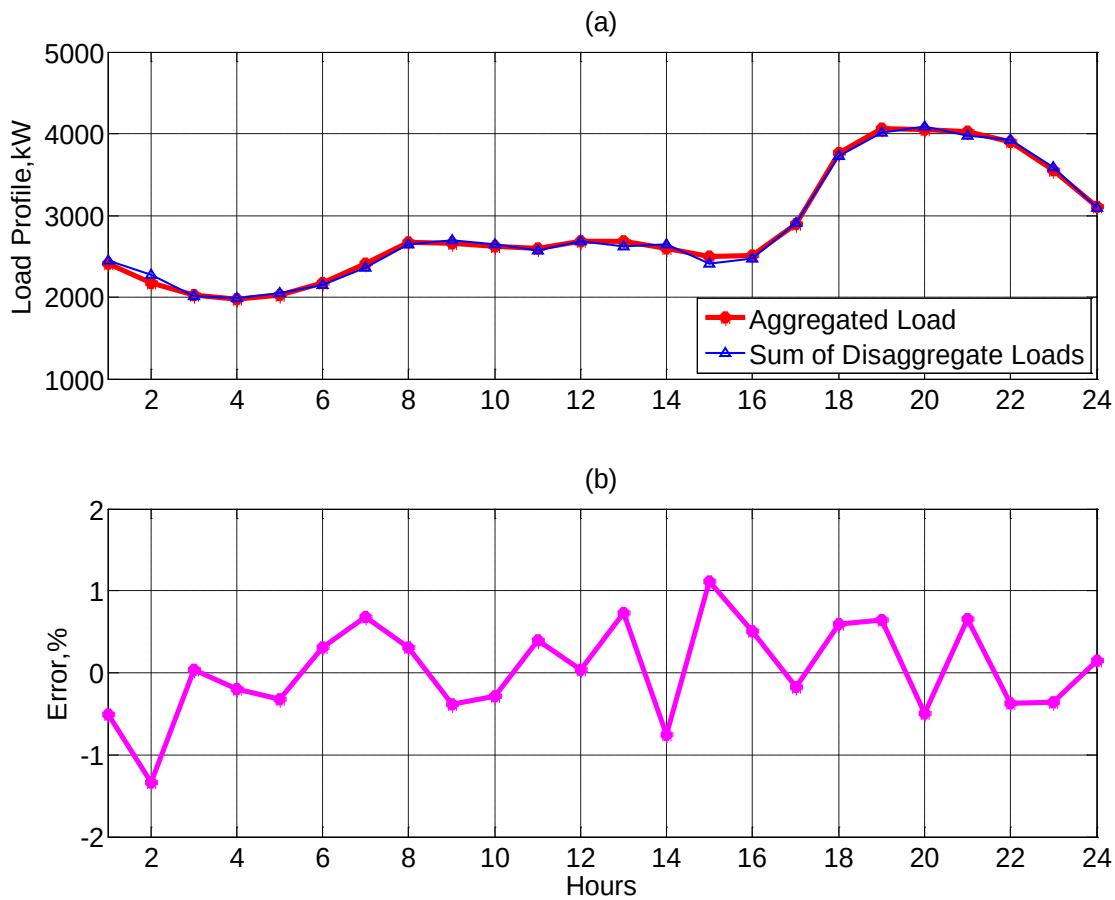

Figure 7-9: Comparison of aggregated load profile with sum of individual load profiles, residential.

Small Commercial Loads

For the 30 small-commercial loads, the daily aggregated load factor curve is shown in Figure 7-10a. Figure 7-10b shows individual load factor curves. The aggregated load factor curve is included in Figure 7-10b for comparison purpose. The individual load factors vary around the aggregated load factor. In Figure 7-10c, individual load profiles are generated based on a normal distribution with a standard deviation of 0.5 (see Section 7.1). In Figure 7-11a, the sum of individual load profiles is compared with the small-commercial aggregated load profile. The percentage error, as shown in Figure 7-11b, varies between -2.4% and 2.2%.

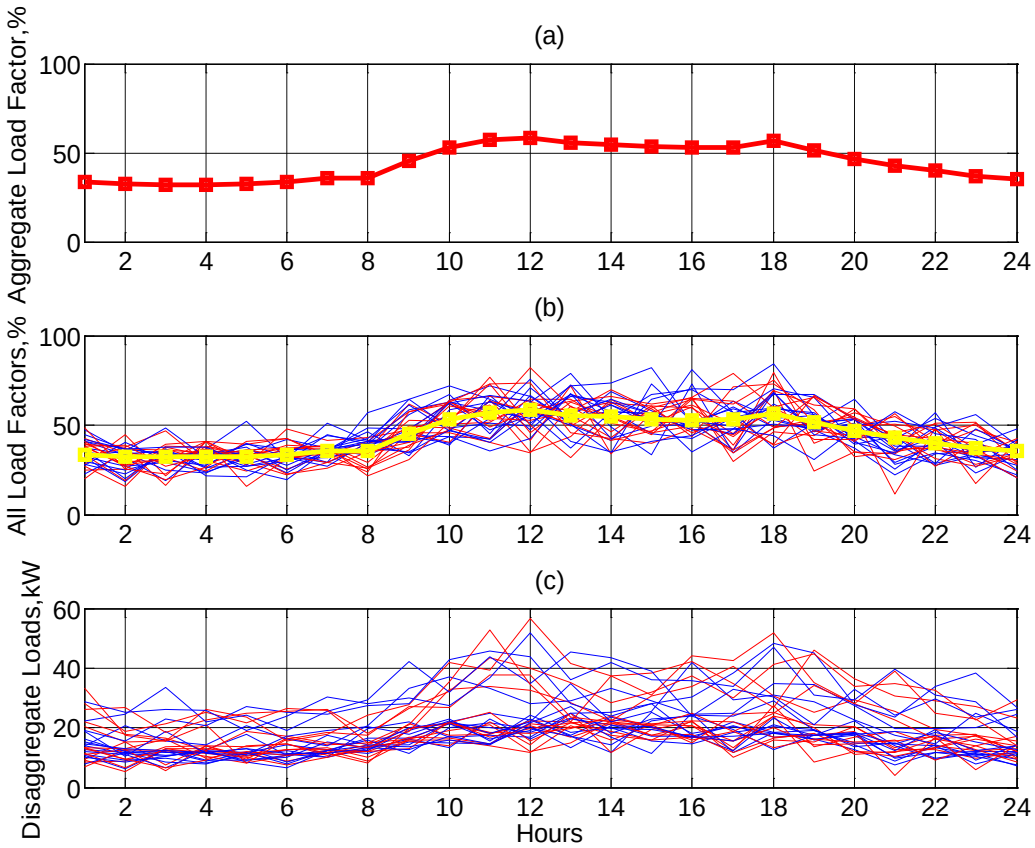

Figure 7-10: Aggregate load factors, all load factors, and disaggregate loads, small-commercial.

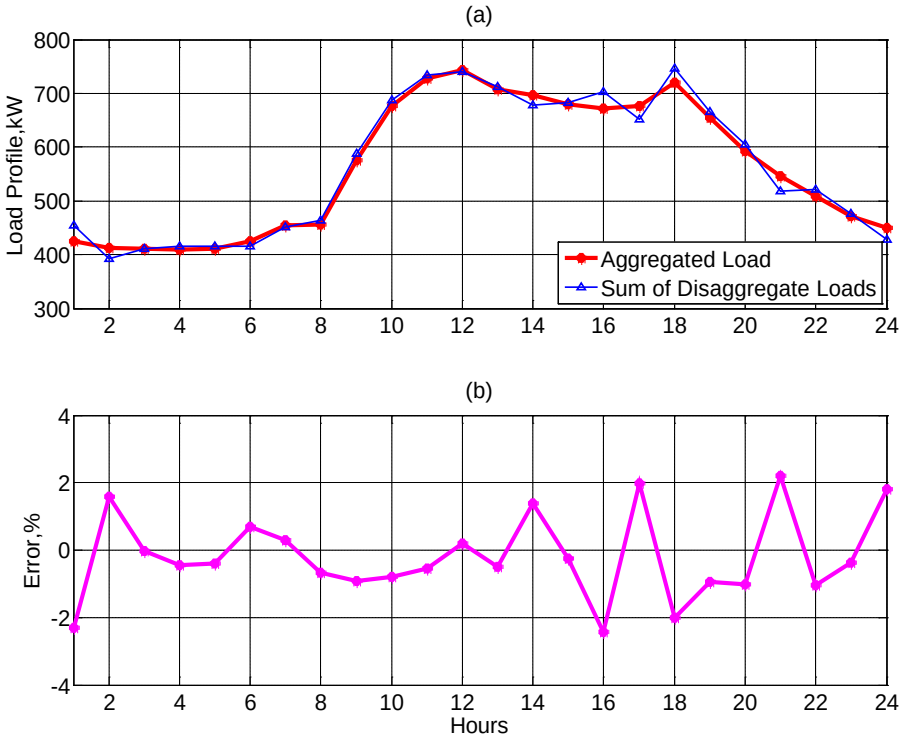

Figure 7-11: Aggregate load factors, all load factors, and disaggregate loads, small-commercial.

Medium Commercial Loads

For the four medium-commercial loads, the daily aggregated load factor curve is shown in Figure 7-12a. Figure 7-12b shows individual load factors. The aggregated load factor curve is included in Figure 7-12b for comparison purpose. The individual load factors vary around the aggregated load factor. In Figure 7-12c, individual load profiles are generated based on the stochastic algorithm described in Section 7.1. We selected a standard deviation of 0.2. Note that for this four-load scenario, we selected a relatively small number for the standard deviation in order to keep the error due to the stochastic variation of a small number of loads within reason. We also think that it is reasonable to select a small number for the standard deviation as large loads have a tendency to have less variation. In Figure 7-13a, the sum of individual load profiles is compared with the medium-commercial aggregated load profile. The percentage error, as shown in Figure 7-13b, varies between -10% and 6.9%.

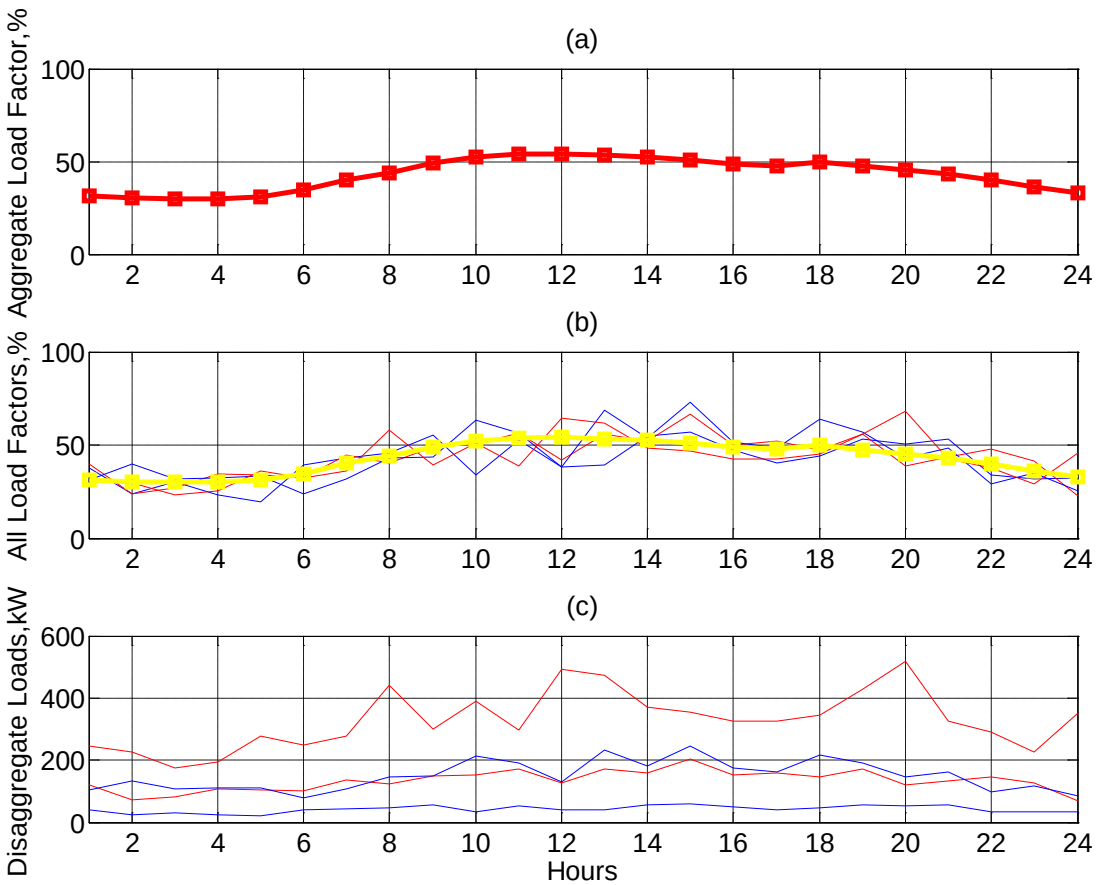

Figure 7-12: Aggregate load factors, all load factors, and disaggregate loads, medium commercial.

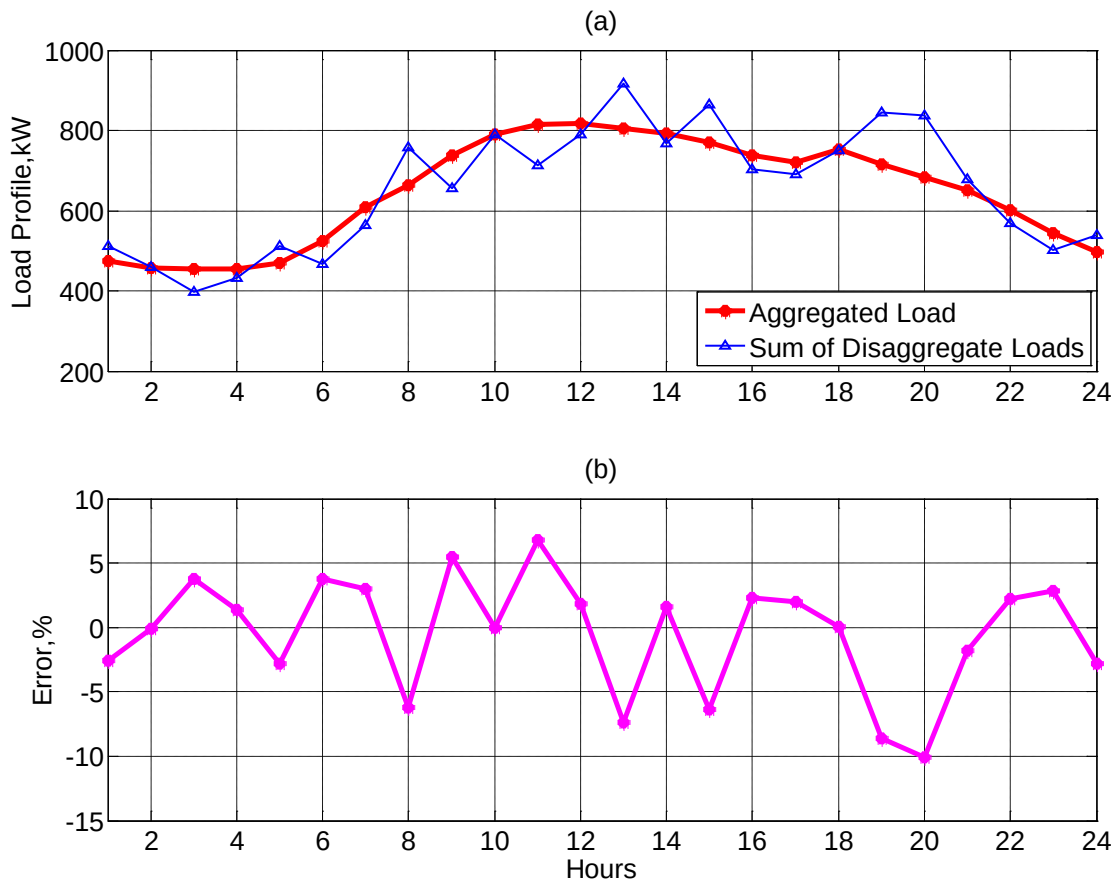

Figure 7-13: Aggregate load factors, all load factors, and disaggregate loads, medium commercial.

8 Case Studies and Simulation Results

In this section, we describe the investigated PV penetration scenarios and the different simulation assumptions/settings we use to simulate these scenarios. We also present summaries of our simulation results for each scenario and for all scenarios combined. Detailed simulation results for each scenario are included in Appendix A through Appendix D.

8.1 Description of Simulated Scenarios and Cases

In order to investigate the impacts of PV generation on the system under study, we defined four scenarios with different PV penetration levels. These scenarios represent a 24 hour simulation involving solar irradiation profiles and load profiles described in Section 6 and Section 7, respectively. The scenarios were defined as follows:

- Scenario 1, low (actual) penetration of small PV w/ 2 MW PV installation: The number and ratings of the PV generators are based on what is installed in the system today (based on data provided by the host utility). The total capacity of the PV generators is 2.295 MW (about 20% of the total load MW rating) with 0.298 MW coming from small residential/industrial/commercial PVs and 2 MW from two large PV installations near a hospital. This PV scenario is described in detail in Section 5.3.1.
- Scenario 2, low (actual) penetration of small PV w/o 2 MW PV installation: Same as scenario 1 with the exception that we removed the 2 MW PV installations near the hospital to achieve a more homogenous distribution of the PV generators that is more representative of a typical distributed generation scenario. This scenario results in a total PV capacity of 0.298 MW (about 2.47% of the total load MW rating) with only small residential/industrial/commercial PVs in the system.
- Scenario 3, high penetration of small PV w/ 2 MW PV installation: This scenario represents a hypothetical future scenario in which a large number of residential and commercial customers have PV generators operating on their premises. The small PV generators were duplicated nine times and the duplicated PVs were connected randomly to load buses on the feeder. No load bus has more than one PV. All original PV locations from Scenario 1 were retained. The large 2 MW PV installations were retained and not duplicated (that is, the amount of centralized PV in the system was not changed). This scenario results in a total PV capacity of 4.973 MW (about 41% of the total load MW rating) with 0.298 MW coming from small residential/industrial/commercial PVs and 2 MW from two large PV installations near a hospital. Figure 8-1 shows a detailed map of all PV generators used in this scenario.
- Scenario 4, high penetration of small PV w/o 2 MW PV installation: Same as scenario 2 with the exception that we removed the 2 MW PV installations near the hospital to achieve a more homogenous distribution of the PV generators that is more representative of a typical distributed generation scenario. This scenario results in a total PV capacity of

2.975 MW (about 25% of the total load MW rating) with only small residential/industrial/commercial PVs in the system.

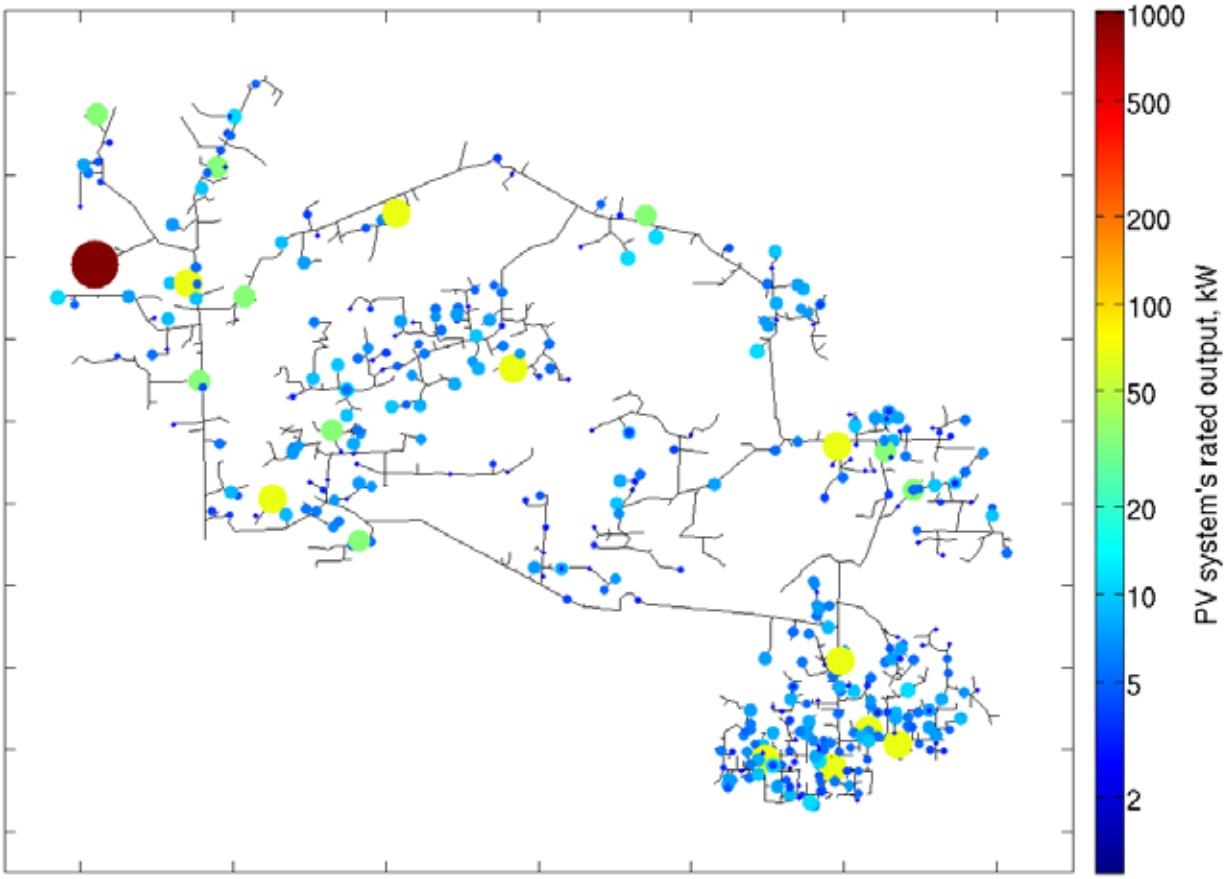

Figure 8-1: Locations of 432 PV systems used in scenario 2 and their rated output. The rated output power is logarithmically proportional to the area of the circles representing the PV generators.

Additionally to different levels of PV penetration, we defined sub-cases for each of the three scenarios that show the importance (or insignificance) of high-resolution temporary variation (i.e., hours vs. seconds) and spatial variation (i.e., different loads or PV generators use same generation profiles vs. each load or PV generator uses an individual generation profile) of the PV and load data. The seven cases are defined below. The characteristics of each case are summarized in Table 8-1.

- Case 0: a single load profile for each of the four defined load groups (i.e., residential, small-commercial, medium-commercial, and hospital) and a single generation profile for all PV generators. Time resolution is one hour.
- Case 1: Same load profiles as Case 0, with the time resolution being 30 seconds.
- Case 2: Every load follows an individual load profile (see Section 7.4) but the PV generators still share a single profile. Time resolution is 30 seconds.

- Case 3: Same load profiles as Cases 0 and 1 but the PV generators follow individual generator profiles (see Section 6). Time resolution is 30 seconds.
- Case 4: Both loads and PV generators follow individual profiles. Time resolution is 30 seconds.
- Case 5: Same as Case 4 but the time resolution is one hour.
- Case 6: PV generators follow a single generation profile on a clear day (Figure 6-7). This case is representative for a situation in which the PV generation varies slowly due to time-of-day variation. Fast cloud-induced ramps do not occur in the scenario. The time resolution is 30 seconds.

Table 8-1: Summary of the simulation cases

Case #	Load Aggregated	PV Aggregated	Resolution	Sky Condition
0	Yes	Yes	1 h	Cloudy to Overcast
1	Yes	Yes	30 sec	Cloudy to Overcast
2	No	Yes	30 sec	Cloudy to Overcast
3	Yes	No	30 sec	Cloudy to Overcast
4	No	No	30 sec	Cloudy to Overcast
5	No	No	1 h	Cloudy to Overcast
6	No	Yes	30 sec	Clear

The simulation results are presented in two different formats –3D plots and 2D plots. The 3D plots show phase voltages, currents, and real power values over the studied period as a function of distance from the substation. While the currents are split into three figures showing the individual phases, all three phase voltages are integrated into a single figure for each scenario and case. The real power figures show the total three-phase power for a given point in time and distance. The 2D plots show following feeder properties:

- Maximum and minimum bus voltages: highest and lowest measured voltage across the entire feeder for every time step (i.e., 1 hour or 30 seconds) of the simulated 24 hour profile.
- Total losses: combined MW and MVAr losses across the entire feeder for every time step (i.e., 1 hour or 30 seconds) of the simulated 24 hour profile.
- Total power: total MW and MVAr net consumption for the entire feeder for every time step (i.e., 1 hour or 30 seconds) of the simulated 24 hour profile.
- Voltage regulator events: total raising or lowering operations (tap changes) for all of the six voltage regulators and the substation transformer for every time step (i.e., 1 hour or 30 seconds) of the simulated 24 hour profile.

8.2 Summary of Each Scenario

In this section, we present the simulation results for each of the four scenarios summarized in Table 8-2 through Table 8-36. The summary includes margins of minimum and maximum voltage averages between simulations with PV and without PV (Table 8-4, Table 8-11, Table 8-18, and Table 8-25). The margins in the tables were calculated using following equations:

$$\text{Average}_{\text{MAX}} = \frac{\sum_{i=n}^{m}\left(MAX_{PV_i} - MAX_{NoPV_i}\right)}{m-n} \cdot 100\%$$

$$\text{Average}_{\text{MIN}} = \frac{\sum_{i=n}^{m}\left(MIN_{PV_i} - MIN_{NoPV_i}\right)}{m-n} \cdot 100\%$$

$$\text{Daylight} \begin{cases} n = 7am \\ m = 4pm \end{cases}$$

8.2.1 Scenario 1 Summary

Table 8-2: Summary of the voltage regulators tap change operations increase for the individual cases, Scenario 1.

Case #	Increase
0	0.00%
1	378.54%
2	324.64%
3	308.78%
4	277.73%
5	-8.33%
6	10.90%

Table 8-3: Summary of the daily maximum per unit voltage values for the individual cases, Scenario 1.

Case #	Without PV	With PV	Difference
0	1.038	1.048	1.00%
1	1.038	1.052	1.40%
2	1.05	1.065	1.50%
3	1.038	1.052	1.40%
4	1.05	1.065	1.50%
5	1.05	1.059	0.90%
6	1.05	1.063	1.30%

Table 8-4: Summary of the minimum and maximum voltage average margin between simulations with PV and without PV for the individual cases, Scenario 1.

Case #	Average_MAX	Average_MIN
0	0.44%	1.00%
1	0.49%	1.37%
2	0.87%	1.25%
3	0.48%	1.40%
4	0.86%	1.26%
5	0.75%	1.01%
6	1.92%	2.09%

Table 8-5: Summary of the MWh and MVArh daily losses, Scenario 1.

Case #	Without PV		With PV		Difference	
	MWh	MVArh	MWh	MVArh	MWh	MVArh
0	14.53	11.99	13.34	10.89	-8.19%	-9.17%
1	14.53	11.98	13.28	10.83	-8.60%	-9.60%
2	12.77	10.28	11.72	9.32	-8.22%	-9.34%
3	14.53	11.98	13.28	10.83	-8.60%	-9.60%
4	12.77	10.28	11.72	9.32	-8.22%	-9.34%
5	12.80	10.31	11.77	9.38	-8.05%	-9.02%
6	12.77	10.28	10.96	8.62	-14.17%	-16.15%

Table 8-6: Summary of the MWh and MVArh daylight losses, Scenario 1.

Case #	Without PV		With PV		Difference	
	MWh	MVArh	MWh	MVArh	MWh	MVArh
0	5.97	4.86	4.78	3.76	-19.93%	-22.63%
1	5.41	4.41	4.17	3.26	-22.92%	-26.08%
2	4.75	3.78	3.70	2.83	-22.11%	-25.13%
3	5.41	4.41	4.17	3.27	-22.92%	-25.85%
4	4.75	3.78	3.70	2.83	-22.11%	-25.13%
5	5.24	4.17	4.22	3.24	-19.47%	-22.30%
6	4.75	3.78	2.96	2.14	-37.68%	-43.39%

Table 8-7: Summary of the MWh and MVArh daily net consumption, Scenario 1.

Case #	Without PV		With PV		Difference	
	MWh	MVArh	MWh	MVArh	MWh	MVArh
0	138.55	26.18	133.45	27.90	-3.68%	6.57%
1	138.52	26.23	133.19	28.09	-3.85%	7.09%
2	125.35	35.93	120.15	37.55	-4.15%	4.51%
3	138.52	26.23	133.20	28.09	-3.84%	7.09%
4	125.35	35.93	120.15	37.55	-4.15%	4.51%
5	125.42	35.90	120.41	37.44	-3.99%	4.29%
6	125.35	35.93	115.73	38.80	-7.67%	7.99%

Table 8-8: Summary of the MWh and MVArh daylight net consumption, Scenario 1.

Case #	Without PV		With PV		Difference	
	MWh	MVArh	MWh	MVArh	MWh	MVArh
0	57.02	11.23	51.93	12.95	-8.93%	15.32%
1	51.70	9.88	46.39	11.73	-10.27%	18.72%
2	46.87	13.45	41.70	15.06	-11.03%	11.97%
3	51.70	9.88	46.40	11.74	-10.25%	18.83%
4	46.87	13.45	41.71	15.06	-11.01%	11.97%
5	51.70	15.17	46.69	16.71	-9.69%	10.15%
6	46.87	13.45	37.34	16.29	-20.33%	21.12%

8.2.2 Scenario 2 Summary

Table 8-9: Summary of the voltage regulators tapchange operations increase for the individual cases, Scenario 2.

Case #	Increase
0	0.00%
1	2.93%
2	4.74%
3	2.93%
4	7.11%
5	0.00%
6	-1.90%

Table 8-10: Summary of the daily maximum per unit voltage values for the individual cases, Scenario 2.

Case #	Without PV	With PV	Difference
0	1.038	1.038	0.00%
1	1.038	1.038	0.00%
2	1.05	1.05	0.00%
3	1.038	1.038	0.00%
4	1.05	1.05	0.00%
5	1.05	1.05	0.00%
6	1.05	1.05	0.00%

Table 8-11: Summary of the minimum and maximum voltage average margin between simulations with PV and without PV for the individual cases, Scenario 2.

Case #	$Average_{_MAX}$	$Average_{_MIN}$
0	0.01%	0.06%
1	0.00%	0.07%
2	0.02%	-0.02%
3	0.00%	0.07%
4	0.02%	-0.02%
5	0.02%	-0.01%
6	0.04%	-0.01%

Table 8-12: Summary of the MWh and MVArh daily losses, Scenario 2.

Case #	Without PV		With PV		Difference	
	MW	MVAr	MW	MVAr	kW	kVAr
0	14.53	11.99	14.47	11.92	-0.41%	-0.58%
1	14.53	11.98	14.47	11.92	-0.41%	-0.50%
2	12.77	10.28	12.72	10.22	-0.39%	-0.58%
3	14.53	11.98	14.47	11.91	-0.41%	-0.58%
4	12.77	10.28	12.72	10.22	-0.39%	-0.58%
5	12.80	10.31	12.74	10.24	-0.47%	-0.68%
6	12.77	10.28	12.67	10.16	-0.78%	-1.17%

Table 8-13: Summary of the MWh and MVArh daylight losses, Scenario 2.

Case #	Without PV		With PV		Difference	
	MWh	MVArh	MWh	MVArh	MWh	MVArh
0	5.97	4.86	5.91	4.79	-1.01%	-1.44%
1	5.41	4.41	5.35	4.34	-1.11%	-1.59%
2	4.75	3.78	4.70	3.72	-1.05%	-1.59%
3	5.41	4.41	5.35	4.34	-1.11%	-1.59%
4	4.75	3.78	4.69	3.72	-1.26%	-1.59%
5	5.24	4.17	5.19	4.10	-0.95%	-1.68%
6	4.75	3.78	4.65	3.66	-2.11%	-3.17%

Table 8-14: Summary of the MWh and MVArh daily net consumption, Scenario 2.

Case #	Without PV		With PV		Difference	
	MWh	MVArh	MWh	MVArh	MWh	MVArh
0	138.55	26.18	137.99	26.28	-0.40%	0.38%
1	138.52	26.23	137.93	26.34	-0.43%	0.42%
2	125.35	35.93	124.74	36.02	-0.49%	0.25%
3	138.52	26.23	137.92	26.34	-0.43%	0.42%
4	125.35	35.93	124.73	36.01	-0.49%	0.22%
5	125.42	35.90	124.81	35.99	-0.49%	0.25%
6	125.35	35.93	124.20	36.09	-0.92%	0.45%

Table 8-15: Summary of the MWh and MVArh daylight net consumption, Scenario 2.

Case #	Without PV		With PV		Difference	
	MWh	MVArh	MWh	MVArh	MWh	MVArh
0	57.02	11.23	56.46	11.34	-0.98%	0.98%
1	51.70	9.88	51.10	9.99	-1.16%	1.11%
2	46.87	13.45	46.27	13.53	-1.28%	0.59%
3	51.70	9.88	51.10	9.99	-1.16%	1.11%
4	46.87	13.45	46.26	13.53	-1.30%	0.59%
5	51.70	15.17	51.09	15.25	-1.18%	0.53%
6	46.87	13.45	45.73	13.61	-2.43%	1.19%

8.2.3 Scenario 3 Summary

Table 8-16: Summary of the voltage regulators tap change operations for the individual cases, Scenario 3.

Case #	Increase
0	4.65%
1	507.32%
2	497.63%
3	438.05%
4	435.07%
5	-3.70%
6	33.18%

Table 8-17: Summary of the daily maximum per unit voltage values for the individual cases, Scenario 3.

Case #	Without PV	With PV	Difference
0	1.038	1.063	2.50%
1	1.038	1.069	3.10%
2	1.05	1.083	3.30%
3	1.038	1.069	3.10%
4	1.05	1.08	3.00%
5	1.05	1.076	2.60%
6	1.05	1.08	3.00%

Table 8-18: Summary of the minimum and maximum voltage average margin between simulations with PV and without PV for the individual cases, Scenario 3.

Case #	$Average_{_MAX}$	$Average_{_MIN}$
0	0.89%	1.08%
1	1.03%	1.28%
2	1.44%	1.28%
3	1.02%	1.26%
4	1.45%	1.30%
5	1.30%	1.01%
6	3.10%	2.42%

Table 8-19: Summary of the MWh and MVArh daily losses, Scenario 3.

Case #	Without PV		With PV		Difference	
	MW	MVAr	MW	MVAr	kW	kVAr
0	14.53	11.99	12.92	10.45	-11.08%	-12.84%
1	14.53	11.98	12.83	10.38	-11.70%	-13.36%
2	12.77	10.28	11.34	8.94	-11.20%	-13.04%
3	14.53	11.98	12.81	10.35	-11.84%	-13.61%
4	12.77	10.28	11.32	8.91	-11.35%	-13.33%
5	12.80	10.31	11.38	8.97	-11.09%	-13.00%
6	12.77	10.28	10.37	8.02	-18.79%	-21.98%

Table 8-20: Summary of the MWh and MVArh daylight losses, Scenario 3.

Case #	Without PV		With PV		Difference	
	MWh	MVArh	MWh	MVArh	MWh	MVArh
0	5.97	4.86	4.36	3.32	-26.97%	-31.69%
1	5.41	4.41	3.73	2.81	-31.05%	-36.28%
2	4.75	3.78	3.33	2.44	-29.89%	-35.45%
3	5.41	4.41	3.71	2.78	-31.42%	-36.96%
4	4.75	3.78	3.31	2.42	-30.32%	-35.98%
5	5.24	4.17	3.83	2.83	-26.91%	-32.13%
6	4.75	3.78	2.38	1.55	-49.89%	-58.99%

Table 8-21: Summary of the MWh and MVArh daily net consumption, Scenario 3.

Case #	Without PV		With PV		Difference	
	MWh	MVArh	MWh	MVArh	MWh	MVArh
0	138.55	26.18	128.42	28.68	-7.31%	9.55%
1	138.52	26.23	127.86	28.87	-7.70%	10.06%
2	125.35	35.93	114.89	38.27	-8.34%	6.51%
3	138.52	26.23	127.73	28.90	-7.79%	10.18%
4	125.35	35.93	114.76	38.30	-8.45%	6.60%
5	125.42	35.90	115.05	38.19	-8.27%	6.38%
6	125.35	35.93	105.94	40.06	-15.48%	11.49%

Table 8-22: Summary of the MWh and MVArh daylight net consumption, Scenario 3.

Case #	Without PV		With PV		Difference	
	MWh	MVArh	MWh	MVArh	MWh	MVArh
0	57.02	11.23	46.90	13.74	-17.75%	22.35%
1	51.70	9.88	41.08	12.51	-20.54%	26.62%
2	46.87	13.45	36.46	15.77	-22.21%	17.25%
3	51.70	9.88	40.96	12.54	-20.77%	26.92%
4	46.87	13.45	36.34	15.80	-22.47%	17.47%
5	51.70	15.17	41.32	17.45	-20.08%	15.03%
6	46.87	13.45	27.63	17.53	-41.05%	30.33%

8.2.4 Scenario 4 Summary

Table 8-23: Summary of the voltage regulators tap change operations increase for the individual cases, Scenario 4.

Case #	Increase
0	-4.65%
1	305.85%
2	280.09%
3	249.76%
4	249.29%
5	-0.93%
6	0.00%

Table 8-24: Summary of the daily maximum per unit voltage values for the individual cases, Scenario 4.

Case #	Without PV	With PV	Difference
0	1.038	1.038	0.00%
1	1.038	1.038	0.00%
2	1.05	1.051	0.10%
3	1.038	1.04	0.20%
4	1.05	1.05	0.00%
5	1.05	1.05	0.00%
6	1.05	1.05	0.00%

Table 8-25: Summary of the minimum and maximum voltage average margin between simulations with PV and without PV for the individual cases, Scenario 4.

Case #	Average_MAX	Average_MIN
0	0.17%	-0.10%
1	0.20%	-0.21%
2	0.42%	-0.08%
3	0.21%	-0.24%
4	0.41%	-0.08%
5	0.38%	-0.17%
6	0.89%	-0.13%

Table 8-26: Summary of the MWh and MVArh daily losses, Scenario 4.

Case #	Without PV		With PV		Difference	
	MW	MVAr	MW	MVAr	kW	kVAr
0	14.53	11.99	13.93	11.34	-4.13%	-5.42%
1	14.53	11.98	13.89	11.30	-4.40%	-5.68%
2	12.77	10.28	12.22	9.69	-4.31%	-5.74%
3	14.53	11.98	13.87	11.28	-4.54%	-5.84%
4	12.77	10.28	12.20	9.67	-4.46%	-5.93%
5	12.80	10.31	12.23	9.70	-4.45%	-5.92%
6	12.77	10.28	11.78	9.21	-7.75%	-10.41%

Table 8-27: Summary of the MWh and MVArh daylight losses, Scenario 4.

Case #	Without PV		With PV		Difference	
	MWh	MVArh	MWh	MVArh	MWh	MVArh
0	5.97	4.86	5.37	4.21	-10.05%	-13.37%
1	5.41	4.41	4.78	3.73	-11.65%	-15.42%
2	4.75	3.78	4.20	3.19	-11.58%	-15.61%
3	5.41	4.41	4.76	3.71	-12.01%	-15.87%
4	4.75	3.78	4.19	3.17	-11.79%	-16.14%
5	5.24	4.17	4.68	3.56	-10.69%	-14.63%
6	4.75	3.78	3.77	2.72	-20.63%	-28.04%

Table 8-28: Summary of the MWh and MVArh daily net consumption, Scenario 4.

Case #	Without PV		With PV		Difference	
	MWh	MVArh	MWh	MVArh	MWh	MVArh
0	138.55	26.18	132.82	27.17	-4.14%	3.78%
1	138.52	26.23	132.49	27.28	-4.35%	4.00%
2	125.35	35.93	119.37	36.89	-4.77%	2.67%
3	138.52	26.23	132.35	27.32	-4.45%	4.16%
4	125.35	35.93	119.23	36.91	-4.88%	2.73%
5	125.42	35.90	119.33	36.89	-4.86%	2.76%
6	125.35	35.93	114.14	37.70	-8.94%	4.93%

Table 8-29: Summary of the MWh and MVArh daylight net consumption, Scenario 4.

Case #	Without PV		With PV		Difference	
	MWh	MVArh	MWh	MVArh	MWh	MVArh
0	57.02	11.23	51.30	12.22	-10.03%	8.82%
1	51.70	9.88	45.69	10.93	-11.62%	10.63%
2	46.87	13.45	40.92	14.40	-12.69%	7.06%
3	51.70	9.88	45.56	10.97	-11.88%	11.03%
4	46.87	13.45	40.79	14.42	-12.97%	7.21%
5	51.70	15.17	45.61	16.15	-11.78%	6.46%
6	46.87	13.45	35.76	15.20	-23.70%	13.01%

8.3 Case Study Summary

In order to investigate the impacts of PV generation on the system under study, we defined four scenarios with different PV penetration levels. These scenarios represent a 24 hour simulation involving solar irradiation profiles and load profiles described in Section 6 and Section 7, respectively. The scenarios were defined as follows:

- Scenario 1: 2.295 MW (about 20% of the total load MW rating)
- Scenario 2: 0.298 MW (about 2.47% of the total load MW rating)
- Scenario 3: 4.973 MW (about 41% of the total load MW rating)
- Scenario 4: 2.975 MW (about 25% of the total load MW rating)

The results of our simulations are summarized in Table 8-30 through Table 8-36 and illustrated in Figure 8-2 through Figure 8-13.

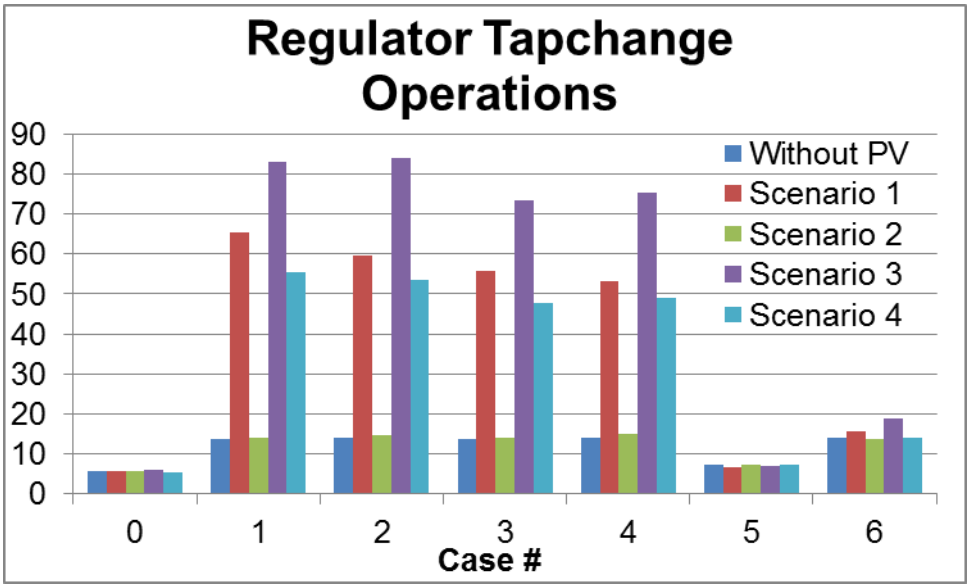

Figure 8-2: Summary of total regulator events for all scenarios and cases.

Table 8-30: Summary of the voltage regulators tap changing operations increase, shown as percentage increase between simulations with PV and without PV, for the individual cases and scenarios

Case #	Scenario 1	Scenario 2	Scenario 3	Scenario 4
0	0.00%	0.00%	4.65%	-4.65%
1	378.54%	2.93%	507.32%	305.85%
2	324.64%	4.74%	497.63%	280.09%
3	308.78%	2.93%	438.05%	249.76%
4	277.73%	7.11%	435.07%	249.29%
5	-8.33%	0.00%	-3.70%	-0.93%
6	10.90%	-1.90%	33.18%	0.00%

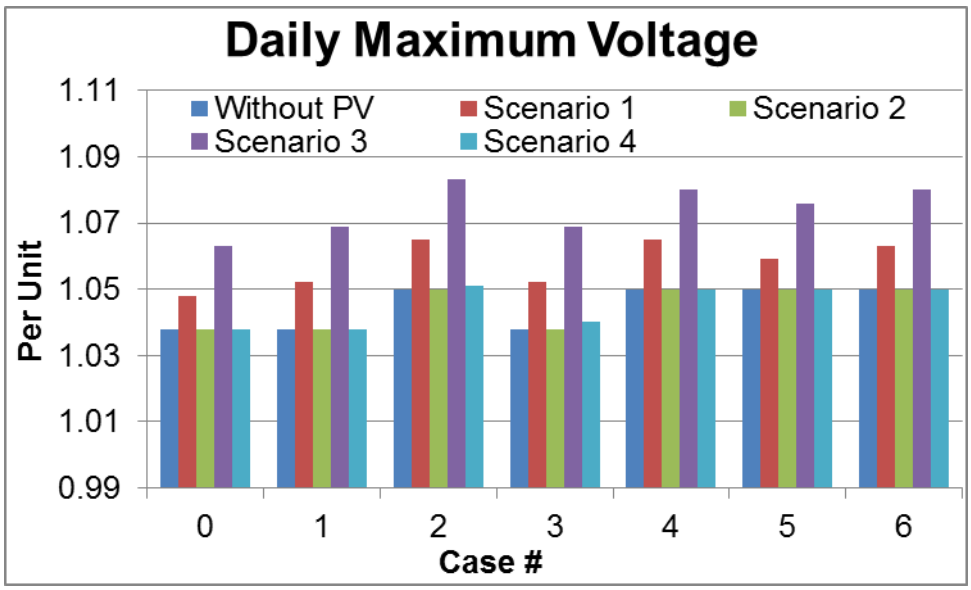

Figure 8-3: Summary of maximum voltages for all scenarios and cases.

Table 8-31: Summary of the daily maximum per unit voltage values, shown as percentage margins between simulations with PV and without PV, for the individual cases and scenarios

Case #	Scenario 1	Scenario 2	Scenario 3	Scenario 4
0	1.00%	0.00%	2.50%	0.00%
1	1.40%	0.00%	3.10%	0.00%
2	1.50%	0.00%	3.30%	0.10%
3	1.40%	0.00%	3.10%	0.20%
4	1.50%	0.00%	3.00%	0.00%
5	0.90%	0.00%	2.60%	0.00%
6	1.30%	0.00%	3.00%	0.00%

Figure 8-4, Figure 8-5, and Table 8-32 summarize the margins of minimum and maximum voltage averages between simulations with PV and without for the individual cases and scenarios. The margins were calculated using following equations:

$$\text{Average}_{\text{MAX}} = \frac{\sum_{i=n}^{m}\left(MAX_{PV_i} - MAX_{NoPV_i}\right)}{m-n} \cdot 100\%$$

$$\text{Average}_{\text{MIN}} = \frac{\sum_{i=n}^{m}\left(MIN_{PV_i} - MIN_{NoPV_i}\right)}{m-n} \cdot 100\%$$

$$\text{Daylight} \begin{cases} n = 7am \\ m = 4pm \end{cases}$$

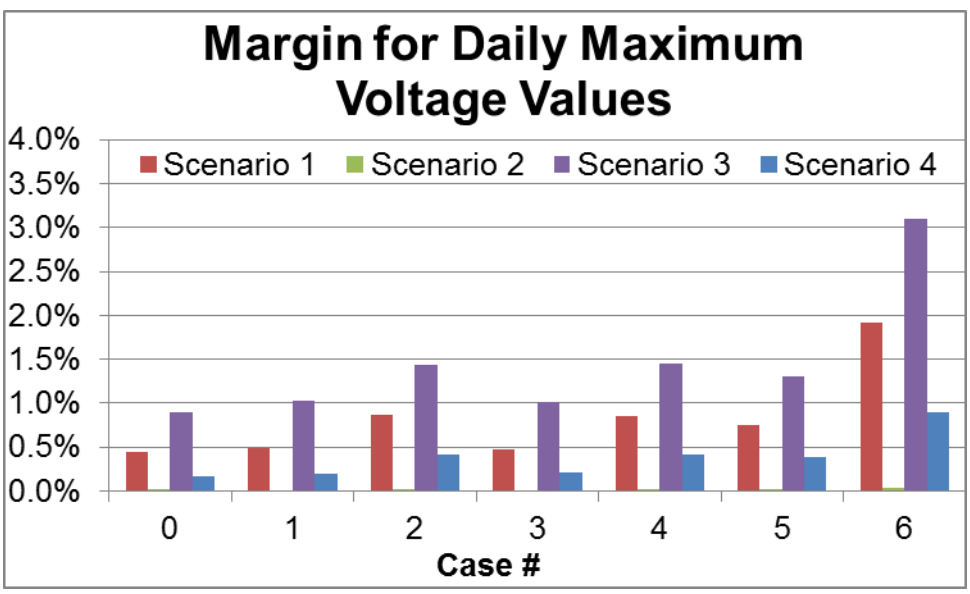

Figure 8-4: Summary of maximum voltage average margins for all scenarios and cases.

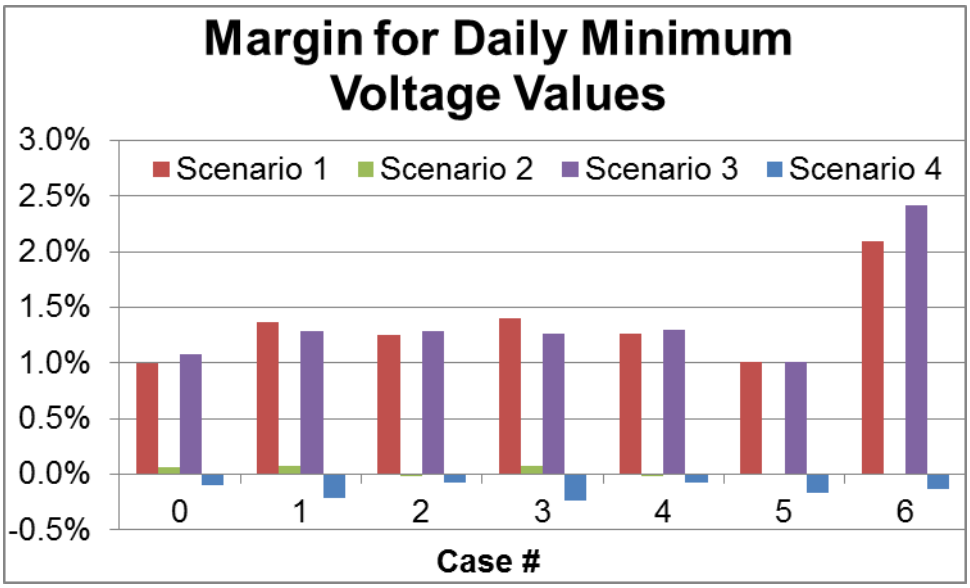

Figure 8-5: Summary of minimum voltage average margins for all scenarios and cases.

Table 8-32: Summary of the minimum and maximum voltage average margin between simulations with PV and without PV for the individual cases and scenarios

Case #	Scenario 1		Scenario 2		Scenario 3		Scenario 4	
	Max	Min	Max	Min	Max	Min	Max	Min
0	0.44%	1.00%	0.01%	0.06%	0.89%	1.08%	0.17%	-0.10%
1	0.49%	1.37%	0.00%	0.07%	1.03%	1.28%	0.20%	-0.21%
2	0.87%	1.25%	0.02%	-0.02%	1.44%	1.28%	0.42%	-0.08%
3	0.48%	1.40%	0.00%	0.07%	1.02%	1.26%	0.21%	-0.24%
4	0.86%	1.26%	0.02%	-0.02%	1.45%	1.30%	0.41%	-0.08%
5	0.75%	1.01%	0.02%	-0.01%	1.30%	1.01%	0.38%	-0.17%
6	1.92%	2.09%	0.04%	-0.01%	3.10%	2.42%	0.89%	-0.13%

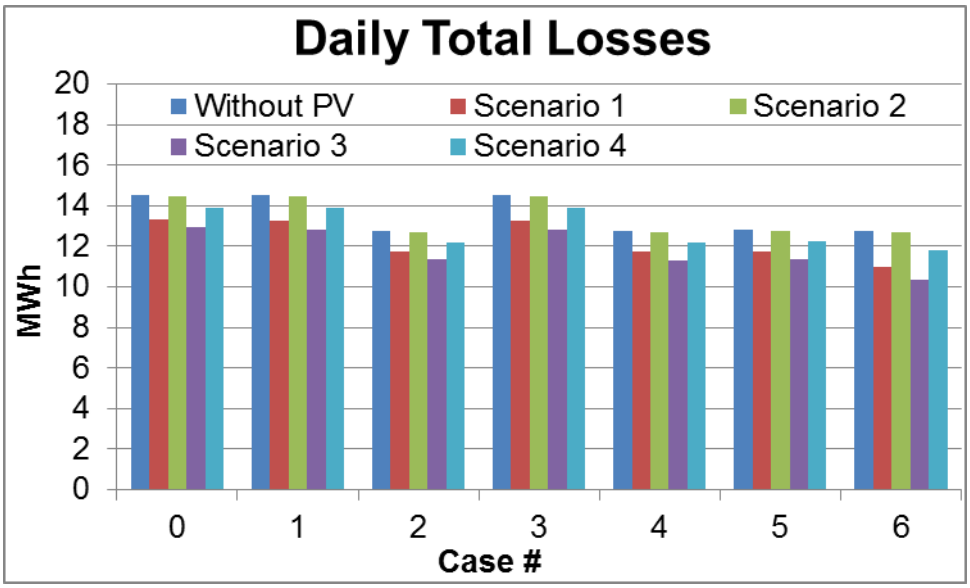

Figure 8-6: Summary of MW daily total losses for all scenarios and cases.

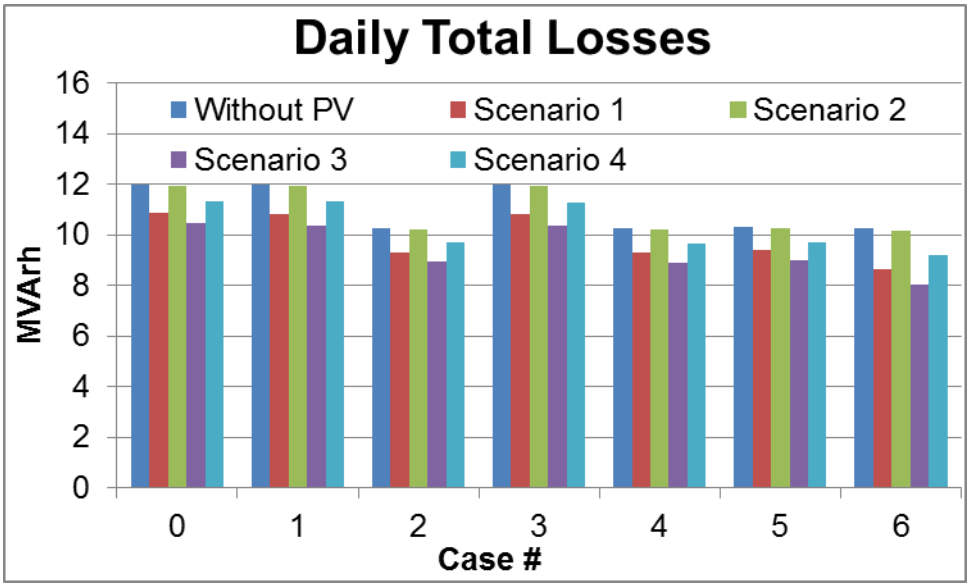

Figure 8-7: Summary of MVAr daily total losses for all scenarios and cases.

Table 8-33: Summary of the MWh and MVArh daily losses, shown as percentage increase between simulations with PV and without PV, for the individual cases and scenarios

Case #	Scenario 1		Scenario 2		Scenario 3		Scenario 4	
	MWh	MVArh	MWh	MVArh	MWh	MVArh	MWh	MVArh
0	-8.19%	-9.17%	-0.41%	-0.58%	-11.08%	-12.84%	-4.13%	-5.42%
1	-8.60%	-9.60%	-0.41%	-0.50%	-11.70%	-13.36%	-4.40%	-5.68%
2	-8.22%	-9.34%	-0.39%	-0.58%	-11.20%	-13.04%	-4.31%	-5.74%
3	-8.60%	-9.60%	-0.41%	-0.58%	-11.84%	-13.61%	-4.54%	-5.84%
4	-8.22%	-9.34%	-0.39%	-0.58%	-11.35%	-13.33%	-4.46%	-5.93%
5	-8.05%	-9.02%	-0.47%	-0.68%	-11.09%	-13.00%	-4.45%	-5.92%
6	-14.17%	-16.15%	-0.78%	-1.17%	-18.79%	-21.98%	-7.75%	-10.41%

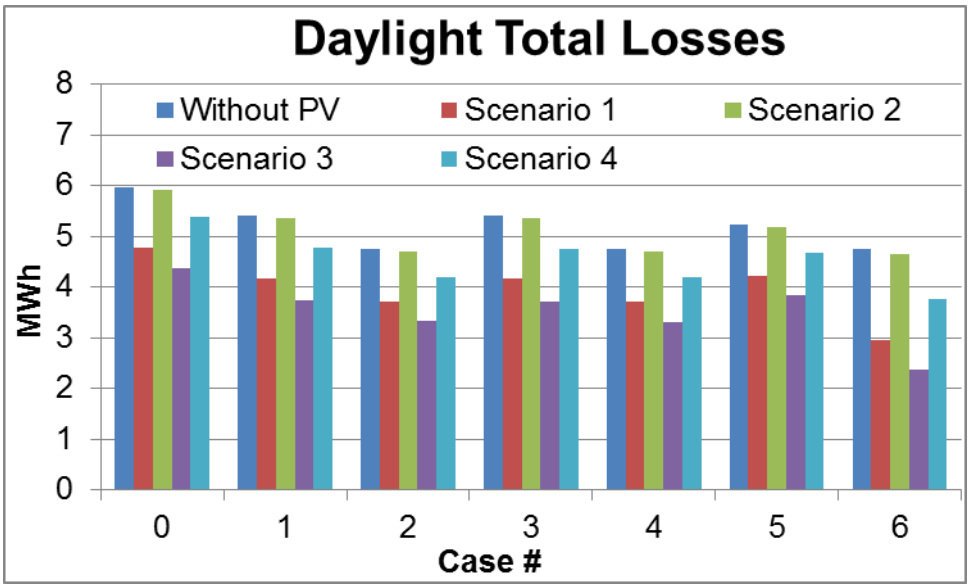

Figure 8-8: Summary of MW daylight total losses for all scenarios and cases.

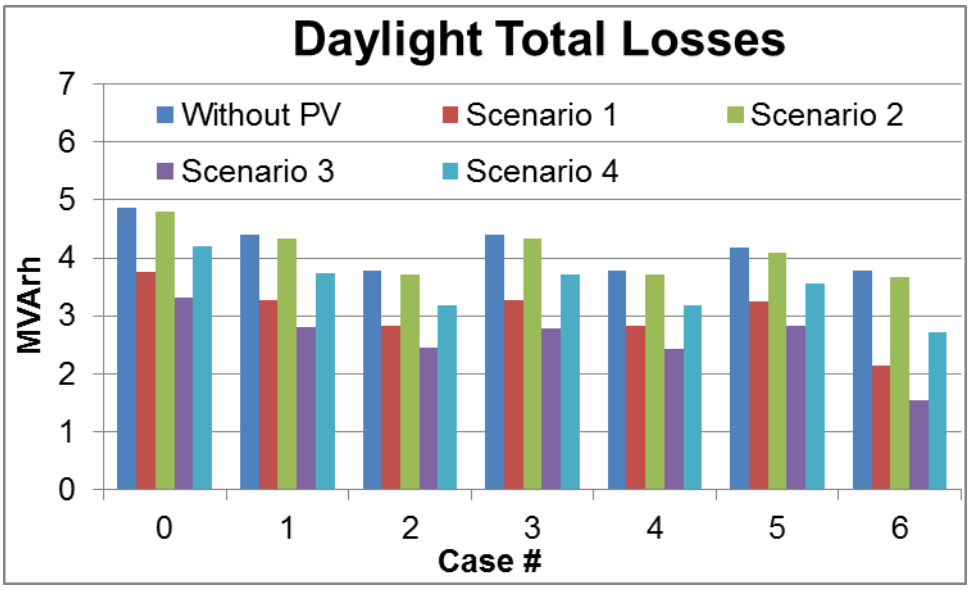

Figure 8-9: Summary of MVar daylight total losses for all scenarios and cases.

Table 8-34: Summary of the MWh and MVArh daylight losses, shown as percentage increase between simulations with PV and without PV, for the individual cases and scenarios

Case #	Scenario 1		Scenario 2		Scenario 3		Scenario 4	
	MWh	MVArh	MWh	MVArh	MWh	MVArh	MWh	MVArh
0	-19.93%	-22.63%	-1.01%	-1.44%	-26.97%	-31.69%	-10.05%	-13.37%
1	-22.92%	-26.08%	-1.11%	-1.59%	-31.05%	-36.28%	-11.65%	-15.42%
2	-22.11%	-25.13%	-1.05%	-1.59%	-29.89%	-35.45%	-11.58%	-15.61%
3	-22.92%	-25.85%	-1.11%	-1.59%	-31.42%	-36.96%	-12.01%	-15.87%
4	-22.11%	-25.13%	-1.26%	-1.59%	-30.32%	-35.98%	-11.79%	-16.14%
5	-19.47%	-22.30%	-0.95%	-1.68%	-26.91%	-32.13%	-10.69%	-14.63%
6	-37.68%	-43.39%	-2.11%	-3.17%	-49.89%	-58.99%	-20.63%	-28.04%

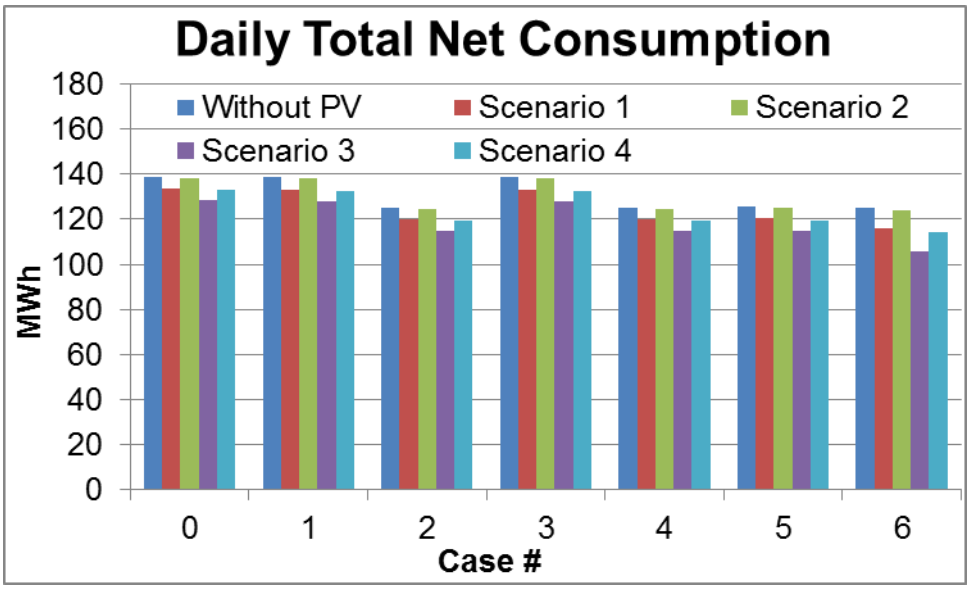

Figure 8-10: Summary of MW daily total net consumption for all scenarios and cases.

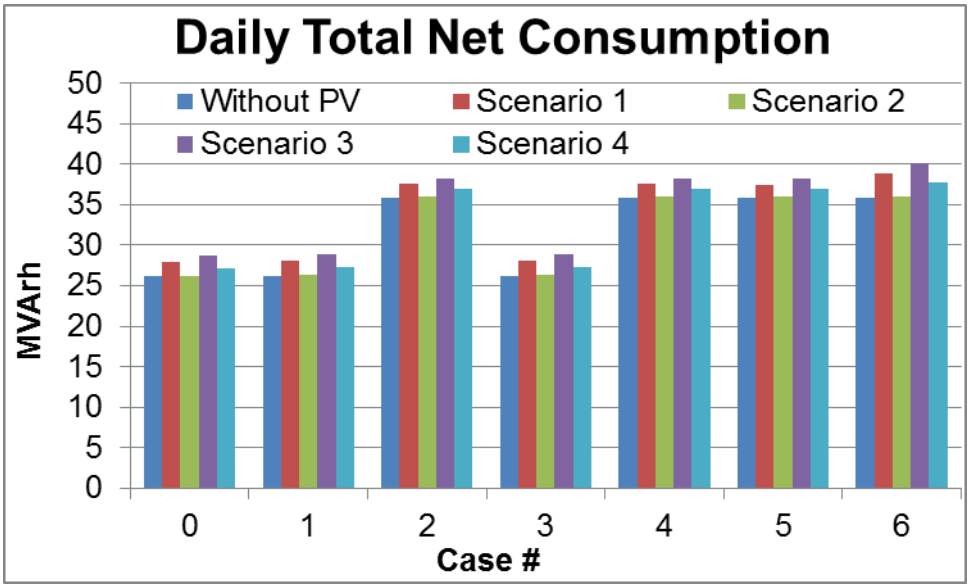

Figure 8-11: Summary of MVArh daily total net consumption for all scenarios and cases.

Table 8-35: Summary of the MWh and MVArh daily net consumption, shown as percentage margins between simulations with PV and without PV, for the individual cases and scenarios

Case #	Scenario 1		Scenario 2		Scenario 3		Scenario 4	
	MWh	MVArh	MWh	MVArh	MWh	MVArh	MWh	MVArh
0	-3.68%	6.57%	-0.40%	0.38%	-7.31%	9.55%	-4.14%	3.78%
1	-3.85%	7.09%	-0.43%	0.42%	-7.70%	10.06%	-4.35%	4.00%
2	-4.15%	4.51%	-0.49%	0.25%	-8.34%	6.51%	-4.77%	2.67%
3	-3.84%	7.09%	-0.43%	0.42%	-7.79%	10.18%	-4.45%	4.16%
4	-4.15%	4.51%	-0.49%	0.22%	-8.45%	6.60%	-4.88%	2.73%
5	-3.99%	4.29%	-0.49%	0.25%	-8.27%	6.38%	-4.86%	2.76%
6	-7.67%	7.99%	-0.92%	0.45%	-15.48%	11.49%	-8.94%	4.93%

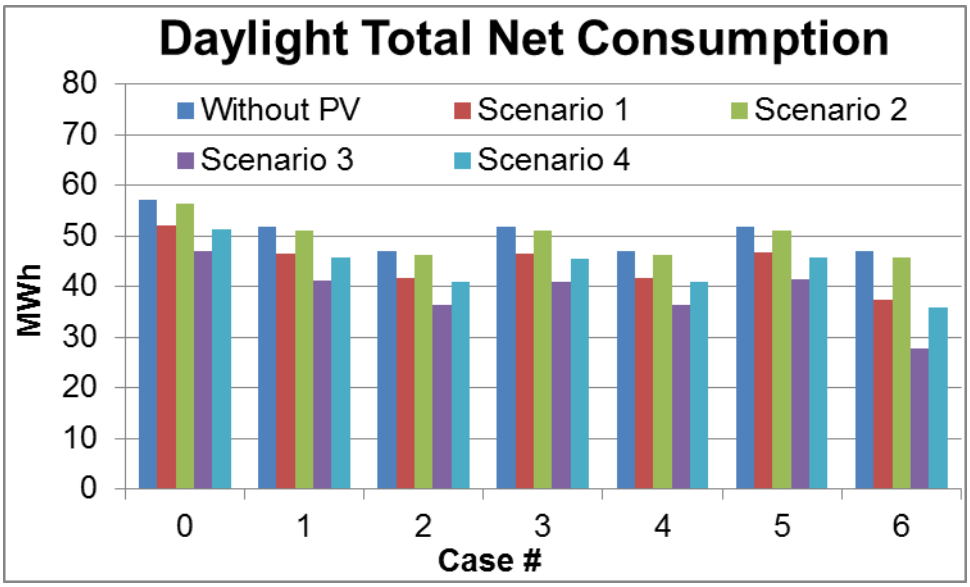

Figure 8-12: Summary of MW daylight total net consumption for all scenarios and cases.

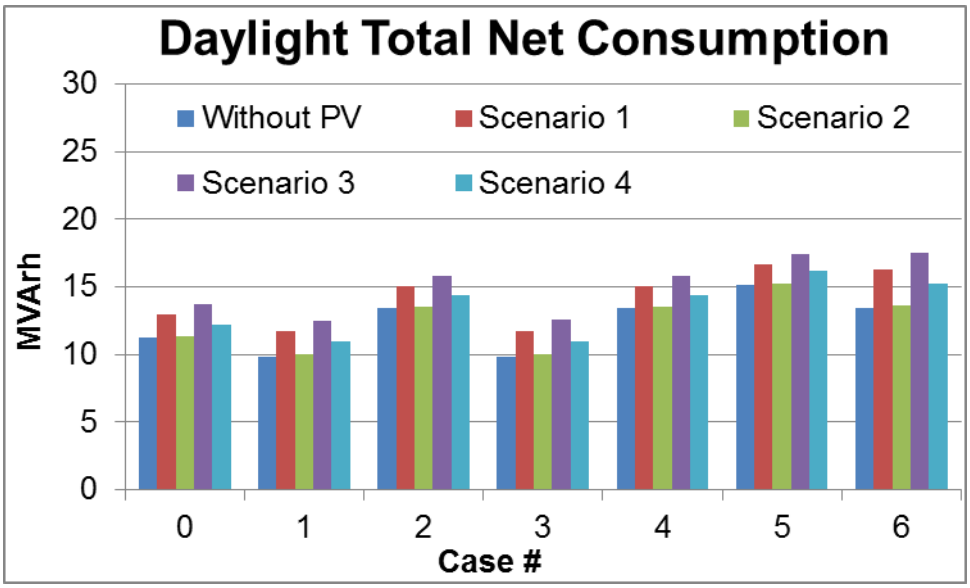

Figure 8-13: Summary of MVArh daylight total net consumption for all scenarios and cases.

Table 8-36: Summary of the MWh and MVArh daylight net consumption

Case #	Scenario 1		Scenario 2		Scenario 3		Scenario 4	
	MWh	MVArh	MWh	MVArh	MWh	MVArh	MWh	MVArh
0	-8.93%	15.32%	-0.98%	0.98%	-17.75%	22.35%	-10.03%	8.82%
1	-10.27%	18.72%	-1.16%	1.11%	-20.54%	26.62%	-11.62%	10.63%
2	-11.03%	11.97%	-1.28%	0.59%	-22.21%	17.25%	-12.69%	7.06%
3	-10.25%	18.83%	-1.16%	1.11%	-20.77%	26.92%	-11.88%	11.03%
4	-11.01%	11.97%	-1.30%	0.59%	-22.47%	17.47%	-12.97%	7.21%
5	-9.69%	10.15%	-1.18%	0.53%	-20.08%	15.03%	-11.78%	6.46%
6	-20.33%	21.12%	-2.43%	1.19%	-41.05%	30.33%	-23.70%	13.01%

9 Discussion and Conclusions

We run a large number of simulations to study the potential issues related to different levels of PV penetration and the importance of high-resolution temporary variation and spatial variation of the PV and load data. We investigated the following three scenarios:

- Scenario 1, low (actual) penetration of small PV w/ 2 MW PV installation: The number and ratings of the PV generators are based on what is installed in the system today (based on data provided by the host utility). The total capacity of the PV generators is 2.295 MW (about 20% of the total load MW rating) with 0.298 MW coming from small PVs and 2 MW from two large PV installations near a hospital.
- Scenario 2, low (actual) penetration of small PV w/o 2 MW PV installation: Same as scenario 1 with the exception that we removed the 2 MW PV installations near the hospital to achieve a more homogenous distribution of the PV generators that is more representative of a typical distributed generation scenario. This scenario results in a total PV capacity of 0.298 MW (about 2.47% of the total load MW rating) with only small PVs in the system.
- Scenario 3, high penetration of small PV w/ 2 MW PV installation: This scenario represents a hypothetical future scenario in which a large number of residential and commercial customers have PV generators operating on their premises. The small PV generators were duplicated nine times and the duplicated PVs were connected randomly to load buses on the feeder. No load bus has more than one PV. All original PV locations from Scenario 1 were retained. The large 2 MW PV installations were retained and not duplicated (that is, the amount of centralized PV in the system was not changed). This scenario results in a total PV capacity of 4.973 MW (about 41% of the total load MW rating) with 0.298 MW coming from small PVs and 2 MW from two large PV installations near a hospital.
- Scenario 4, high penetration of small PV w/o 2 MW PV installation: Same as scenario 3 with the exception that we removed the 2 MW PV installations near the hospital to achieve a more homogenous distribution of the PV generators that is more representative of a typical distributed generation scenario. This scenario results in a total PV capacity of 2.975 MW (about 25% of the total load MW rating) with only small PVs in the system.

We run seven cases for each of the three scenarios described above. The first six cases varied with regards to (1) aggregating/disaggregating the loads, (2) the temporal resolution of the input data (1 hour for the low-resolution cases and 30 seconds for the high-resolution cases), and (3) aggregating/disaggregating the PV generation during a cloudy day. The last case was a day with a clear sky with disaggregated loads and high temporal resolution (30 seconds). Note that for the clear-sky case, disaggregation is not required to obtain realistic results as all PV generators are exposed to the same irradiance levels. Based on the simulation results, we draw the following conclusions:

1. **PV reduces line losses:** The presence of PVs significantly reduces line losses on the feeder. In the low PV penetration Scenario 1, line losses are reduced by about 8% during cloudy days and 14% during a clear day. In the high PV penetration Scenario 3, line losses are reduced by about 11% and 19% during clear days and cloudy days, respectively. The losses are even further reduced when confining the time frame of the comparison to the daylight hours (up to 50% for the high PV penetration Scenario 3 during a clear day). We attribute the reduction of line losses to the fact the PV generation is much closer to the load compared to the no PV scenarios in which the power is supplied from the substation. On the other hand, the line losses for the low PV penetration Scenario 2 are very similar to the line losses for the no PV scenario. Note that our simulations do not account for transmissions losses that occur during the transfer of power from the plant to the substation. Accounting for these losses would increase the absolute difference between losses without PV on the system and losses with PV on the system even more. Investigating the value of PV for loss reduction on transmission systems versus the value for loss reduction on distribution systems is a worthy undertaking for future research. Transmission lines are normally longer than distribution lines, which increases the losses and, thereby, the value of PV for loss reduction. On the other hand, the higher transmission level voltages reduce losses, which decreases the value of PV for loss reduction.
2. **Distributed PV vs. centralized PV:** The PV penetration levels in Scenario 1 and Scenario 4 are similar (20% and 25%, respectively). The main difference is that Scenario 1 has two large 1 MW PV systems located close together which constitute nearly 90% of the total PV generation in the system. On the other hand, Scenario 4 does not contain large PV installations and the numerous smaller PV installations were more-or-less evenly distributed along the feeder. For the centralized PV Scenario 1, the tap changing operations were slightly more frequent and the line losses were larger compared to the distributed PV Scenario 4. It is important to note that this tendency is not necessarily a general conclusion that applies to all feeders, but it shows that the distribution of the PV on the feeder has a significant impact on both the tap changing operations and the losses. The maximum voltage on the feeder for the no PV scenarios and the PV scenarios without the large PV installations (Scenarios 2 and 4) are essentially identical (1.05 pu). On the other hand, the maximum voltages in the centralized PV Scenarios 1 and 3 are significantly higher than in the no PV / distributed PV Scenarios (up to 1.08 pu). This indicates that the voltage regulators deployed on the investigated feeder are capable of keeping the voltages along the feeder within permissible limits – even if the number of distributed PV is increased tenfold. On the other hand, centralized PV on the feeder is much more prone to cause overvoltages – in particular if voltage regulators are not strategically placed to accommodate the PV concentration on the feeder. Note that, technically, PV inverters can be utilized to regulate the voltage on the feeder thereby potentially alleviating over and undervoltage issues on the feeder. However, IEEE 1547 does currently not permit distributed generation to actively regulate voltage (see Section 3.2).

3. **PV increases operation of tap changers significantly – in particular during cloudy days:** Tap changers during cloudy days in the high PV penetration Scenario 3 (41% penetration) are operating about 70 to 80 times each day (depending on the simulation case) which is significantly higher than the number of tap changer operations for the no PV and low PV penetration Scenario 2 (about 13 operation for both scenarios) and the clear-day simulation case 6 (between 12 and 19 operations, depending on the scenario). This indicates that tap changing operations during cloudy days will significantly increase if PV penetration levels are high, which will substantially increase maintenance costs and life-cycle costs of voltage regulators. On the other hand, for low PV penetration levels and during clear days, the tap changing operations is not impacted much. Note that the conclusions above came out of results from our simulations that utilize data with high temporal resolution (30 seconds). Our simulations with low-resolution (one hour) data were not suitable to resolve any of these differences – in fact the number of tap changing operations from the low-resolution results were around five for <u>all</u> PV penetration scenarios, which results in a large error for the high PV penetration scenarios where the number of tap changing operations reached above 80 (based on the more realistic simulation results that utilize high-resolution data).
4. **Low temporal resolution data vs. high temporal resolution data:** Using low resolution data underestimates tap changing operations significantly in high PV penetration scenarios. In our simulations, the increase in tap changing operations for high PV penetration levels was only observed when more accurate high resolution data (30 second time step) were used as input to the model. Simulations with low-resolution data (one hour time step) did not show the increase in tap changing operations. This indicates that it is important to use high resolution data when evaluating tap changing operations for high PV penetration scenarios.
5. **Effect of disaggregating PV irradiances:** For the >20% PV penetration Scenarios 1, 3 and 4, a comparison of the number of tap changing operations for cases 1 and 3 (aggregated/disaggregated PV; loads aggregated in both cases) and cases 2 and 4 (aggregated/disaggregate PV; loads disaggregated in both cases) shows that disaggregation of the PV generation does reduce the number of tap changing operations significantly (30 to 70%). This indicates that aggregating PV generation curves in simulations overestimates the actual tap changing operations that occurs on the real world system substantially.
6. **Effect of disaggregating load profiles:** For the >20% PV penetration Scenarios 1, 3 and 4, a comparison of the number of tap changing operations for cases 1 and 2 (aggregated/disaggregated loads; PV aggregated in both cases) and cases 3 and 4 (aggregated/disaggregate loads; PV disaggregated in both cases) shows that load disaggregation impacts the number of tap changing operations. However, there is no clear trend regarding whether disaggregating the load curves results in an increase or a decrease of the number of tap changing operations.

7. **Net consumption of active power:** For the >20% PV penetration Scenarios 1, 3 and 4, the active power net consumption of the distribution feeder, that is, the active power that needs to be supplied from the substation to support the load demand on the feeder, is significantly reduced. For example, for the high PV penetration Scenario 3, the daily reduction of net consumption due to the presence of PV leads to about 8-15% less energy demand for the feeder, depending on the sky condition. In other words, generation sources outside the feeder need to supply about 8-15% less energy to the feeder (not accounting for losses associated with the transfer of power from the plant to the substation). If these outside generation sources are fueled by conventional non-renewable resources (i.e., fossil and radioactive fuels), then this reduction leads to significant savings of these non-renewable resources.
8. **Net consumption of reactive power:** Conversely to the previous conclusion, the reactive power net consumption of the distribution feeder is increased, that is, more reactive power is consumed on the feeder, which has to be supplied by generation sources or reactive compensation outside the feeder or at the substation. This is because the PVs, in particular at high penetration levels, increase the voltages on the feeder, which results in more power consumed by the loads on the feeder. The PVs in our simulation operate at unity power factor, that is, they provide active power, but no reactive power. Consequently, the net consumption of reactive power is increased. On the other hand, the net consumption of active power is reduced because the additional active power (due to the voltage increase) is supplied by the PV. Note that this result depends strongly on the load mix on the feeder – we modeled all loads as ZIP loads with 70% active power and 30% reactive power. Our interpretation of this result is that PVs can decrease the operating efficiency of loads if the utility does not make adjustments. However, the increased voltages on the feeder due to the PV gives the utility the opportunity to apply energy saving measures such as conservation voltage reduction, that is, the utility can lower the voltage at the substation during times of PV production and the power generated by the PV will keep the voltages along the feeder within permissible limits. This practice would be particularly effective if (1) the PV is evenly distributed along the feeder as this will avoid localized regions on the feeder that have undervoltage when the voltage at the substation is reduced and (2) the PV generation is supported with sufficient storage or power factor control capability as this would avoid sudden undervoltage conditions due to clouds. Lowering the voltage at the substation will decrease the reactive power net consumption and further reduce the active power that needs to be supplied from outside generation sources.

Works Cited

[1] F. Katiraei and J. R. Aguero, "Solar PV Integration Challenges," *IEE Power & Energy Magazine*, pp. 62-71, May/June 2011.

[2] J.W. Smith, "Analytical Evaluation of Flicker Meter Algorithms," 1998.

[3] T.E. McDermott, "Voltage Control and Voltage Fluctuations in Distributed Resource Interconnection Projects," in *IEEE PES Transmission and Distribution Conference and Exposition*, New Orleans, LA, 19-22 April 2010.

[4] P. F. Riberio, "Common Misapplications of the IEEE 519 Harmonic Standard: Voltage or Current Limits," , 2008.

[5] J.H.R. Enslin and P.J.M. Heskes, "Harmonic interaction between a large number of distributed power inverters and the distribution network," *IEEE Transaction on Power Electronics*, vol. 19, No. 6, November 2004.

[6] S. Steffel, "Electric Grid Impact of PV and Mitigation Strategies," in *UVIG 2012 Fall Technical Workshop*, Omaha, Nebraska, October 2012.

[7] B. Mather and R. Neal, "Integrating High Penetrations of PV into Southern California: Year 2 Project Update," in *IEEE Photovoltaic Specialists Conference*, Austin, Texas, June 3–8, 2012.

[8] M.H. Coddington, D. Baca, B.D. Kroposki, and T. Basso, "Deploying high penetration photovoltaic systems - A case study," in *37th IEEE Photovoltaic Specialists Conference (PVSC)*, Seattle, WA, June 2011.

[9] M. Braun et al., "Is the distribution grid ready to accept large-scale photovoltaic deployment? State of the art, progress, and future prospects," in *26th EU PVSEC*, Hamburg, Germany, November 2011.

[10] S. Cobben, B. Gaiddon, and H. Laukamp, "Impact of Photovoltaic Generation on Power Quality in Urban Areas with High PV Population," Intelligent Energy Europe, EIE/05/171/SI2.420208, 2008.

[11] F. Katiraei, K. Mauch, and L. Dinard-Bailey, "Integration of Photovoltaic Power Systems in High-Penetration Clusters for Distribution Networks and Mini-Grids," *International Journal of Distributed Energy Resources*, vol. Volume 3, no. Number 3, 2007.

[12] A. Spring et al., "Effects of Flicker in a Distribution Grid with high PV Penetration," in *28th European Photovoltaic Solar Energy Conference and Exhibition*, Paris, France, September/October 2013.

[13] Electric Power Research Institude (EPRI), "OpenDSS PVSystem Element Model, Version 1," February 23, 2011.

[14] L. Gao, R.A. Dougal, S. Liu, and A.P. Iotova, "Parallel-Connected Solar PV System to Address Partial and Rapidly Fluctuating Shadow Conditions," *IEEE Transactions on Industrial Electronics*, vol. 56, no. 5, May 2009.

[15] R. Ramabadran and B. Mathur, "Effect of Shading on Series and Parallel Connected Solar PV Modules," *Modern Applied Science*, vol. 3, no. 10, October 2009.

[16] M. Lave, J. Kleissl, and E. Arias-Castro, "High-frequency irradiance fluctuations and geographic smoothing," *Solar Energy*, vol. Volume 86, no. Issue 8, pp. 2190-2199, August 2012.

[17] J.W. Smith, R.C. Dugan, and W. Sunderman, "Distribution Modeling and Analysis of High Penetration PV," in *IEEE/PES GM*, Detroit, 2011.

[18] National Renewable Energy Laboratory (NREL), "Southern California Edison High-Penetration Photovoltaic Project – Year 1," NREL/TP-5500-50875, 2011.

[19] Joakim Widen, "Distributed Photovoltaics in the Swedish Energy System: Model Development and Simulations," Uppsala Universitet, Uppsala, Sweden, Thesis 2009.

Appendix A - Scenario 1

In this Section we present the simulation results obtained for scenario 1 – all PV generators are kept at their original rating totaling 2.295 MW (~ 20 % of the total load MW rating).

A.1 Case 0

Figure A-1 through Figure A-7 show simulation results for scenario 1 and case 0.

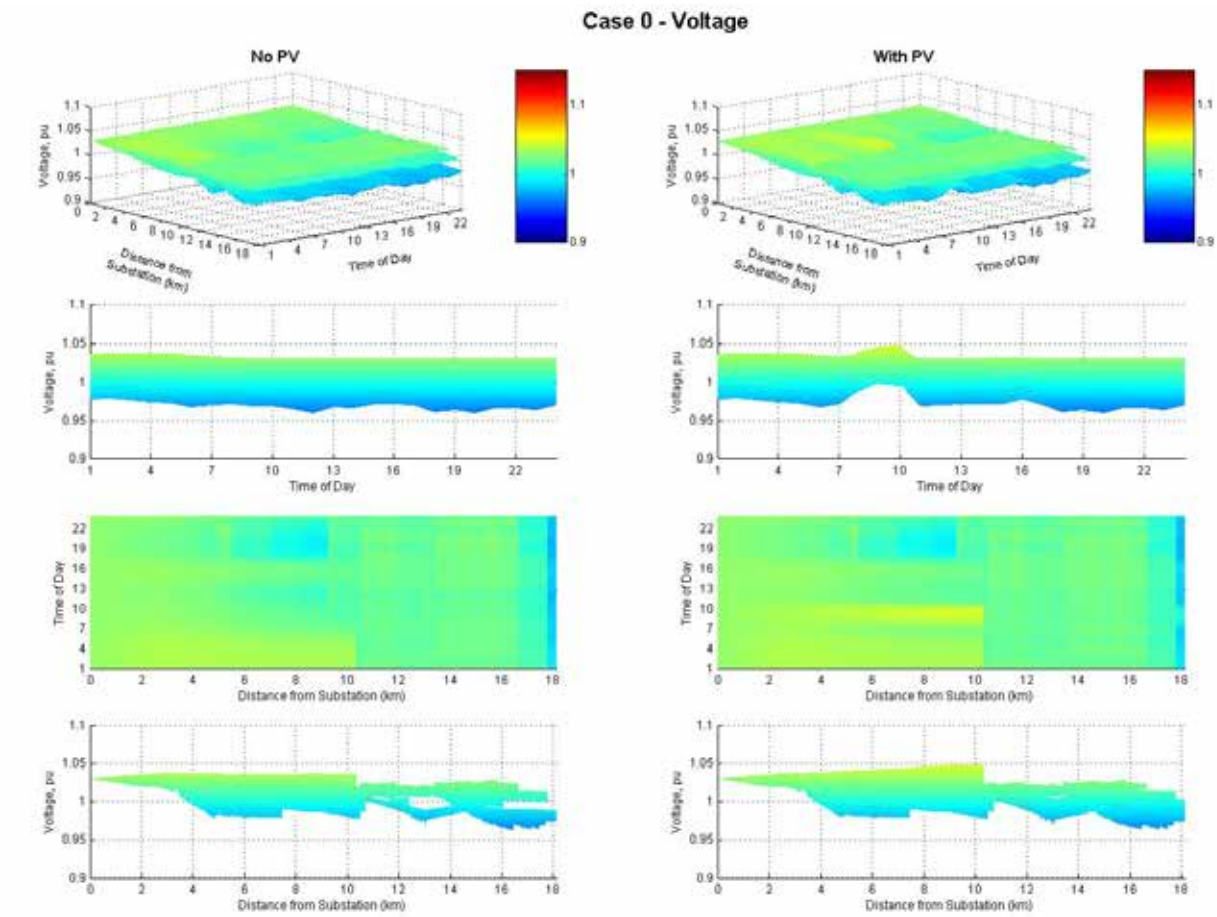

Figure A-1: Daily voltage profile for scenario 1 and case 0.

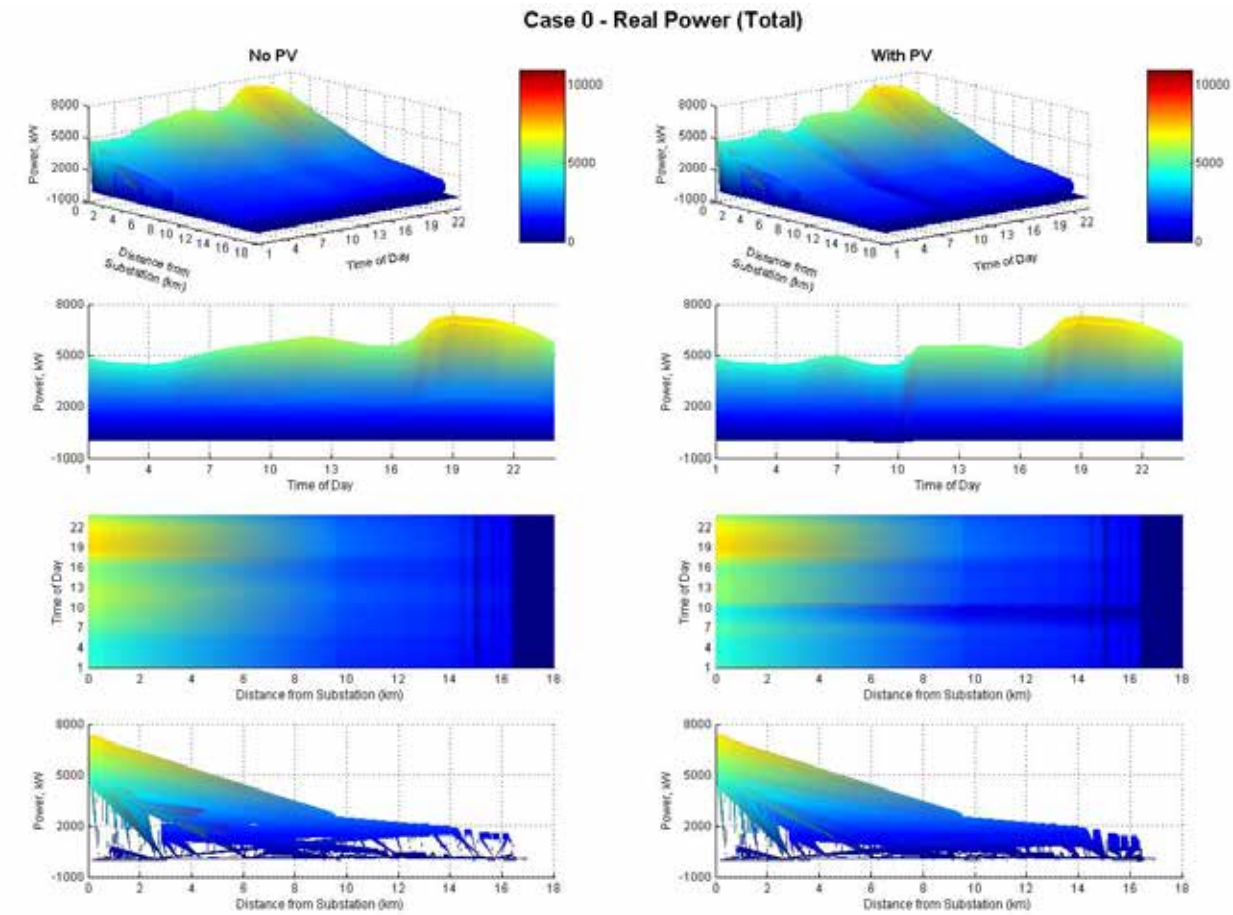

Figure A-2: Daily total real power profile for scenario 1 and case 0.

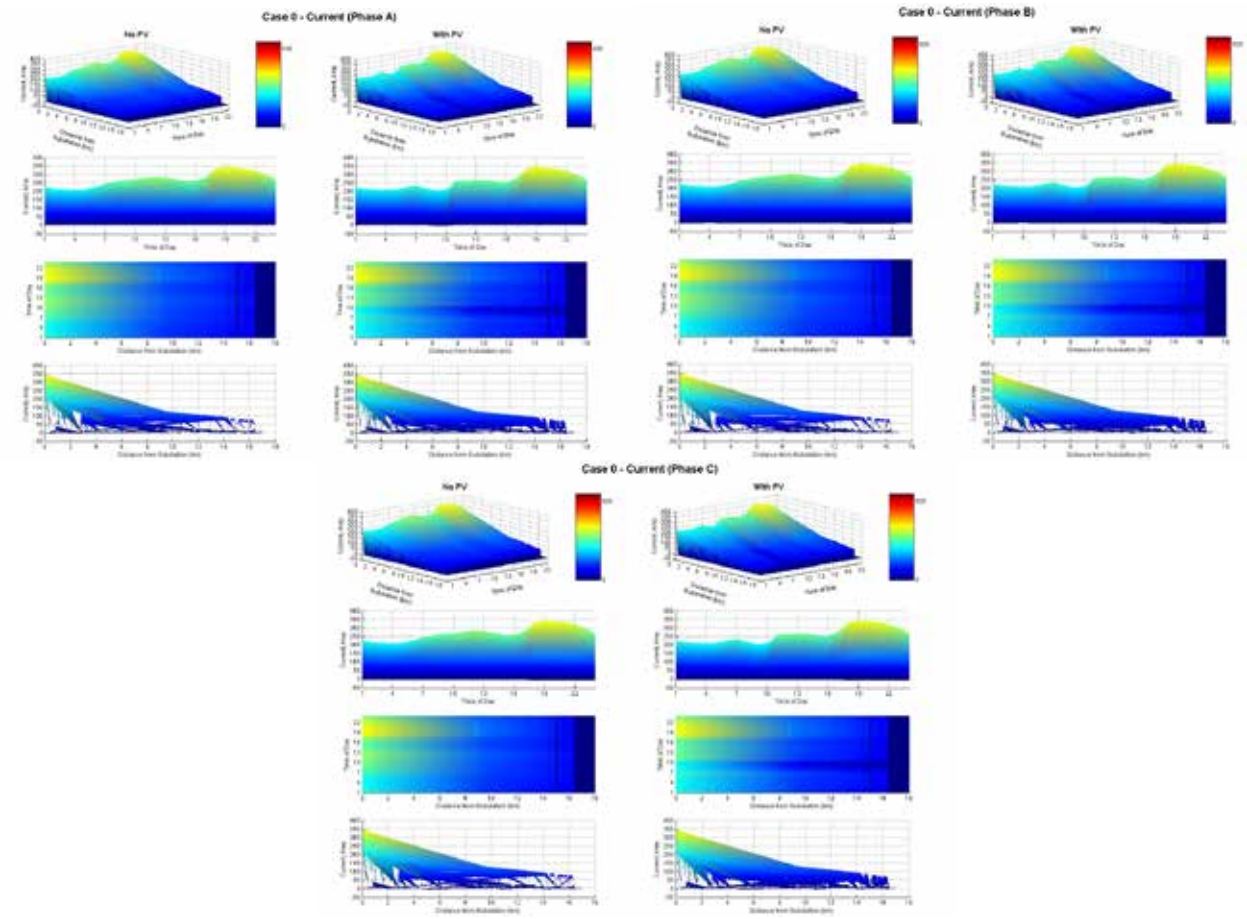

Figure A-3: Daily current profiles for scenario 1 and case 0.

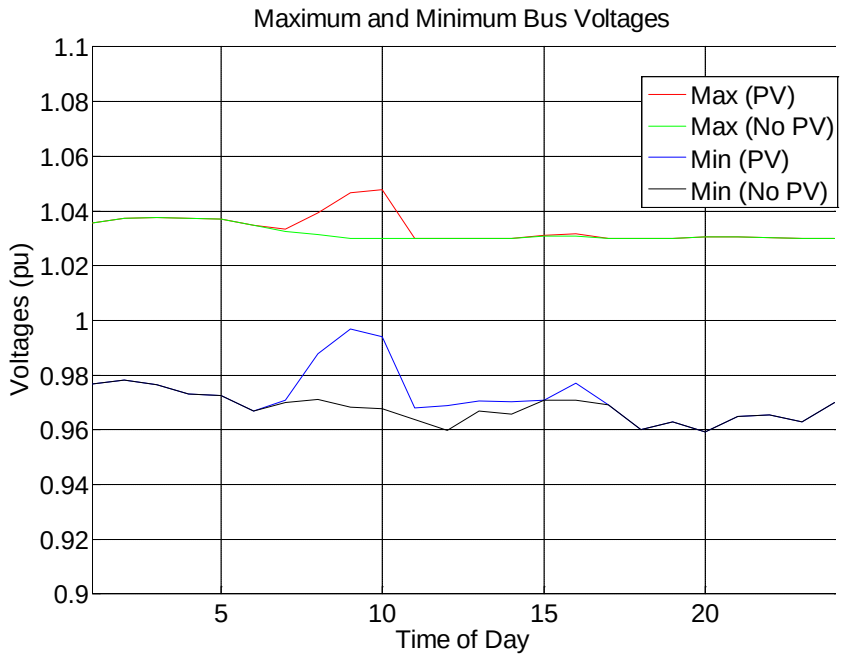

Figure A-4: Maximum and minimum voltages for scenario 1 and case 0.

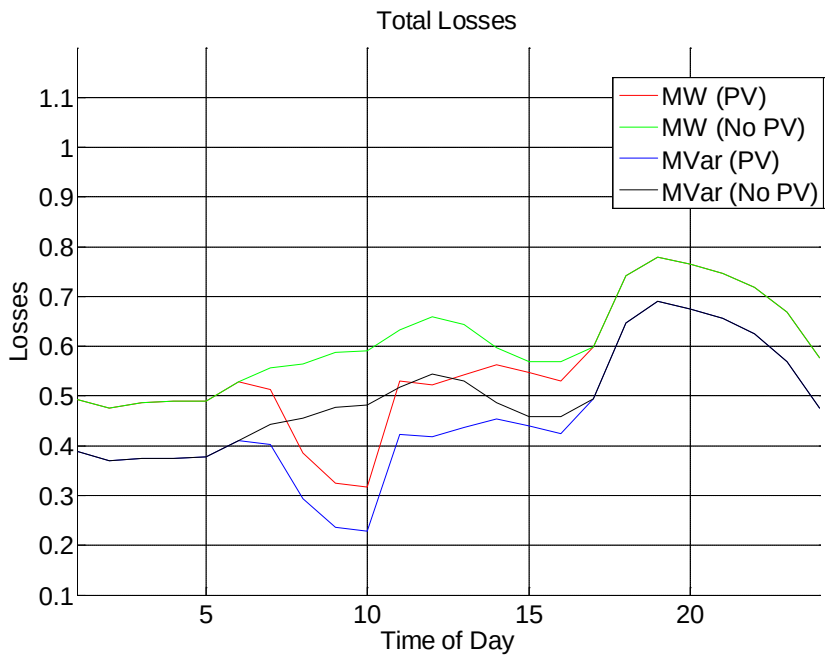

Figure A-5: MW and MVAr losses for scenario 1 and case 0.

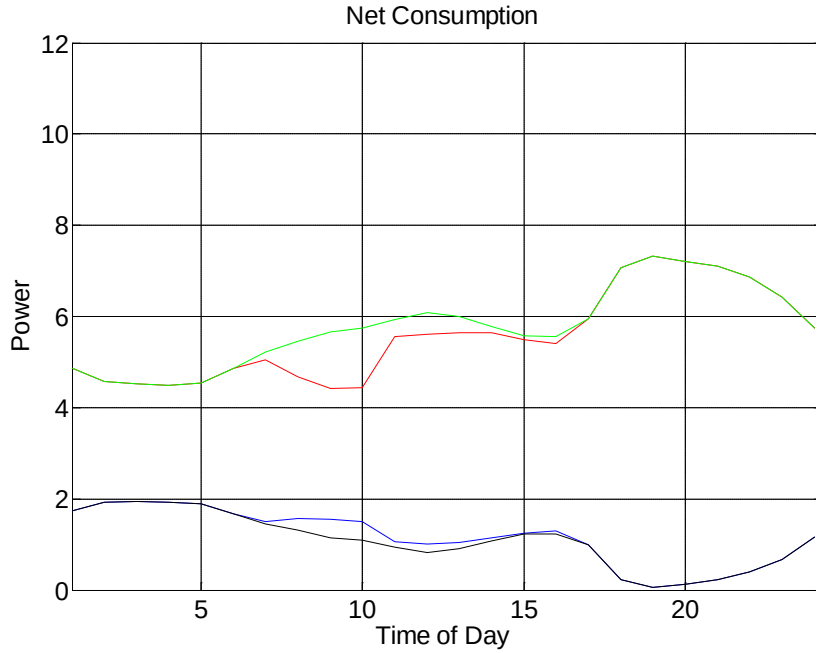

Figure A-6: MW and MVAr net consumption for scenario 1 and case 0.

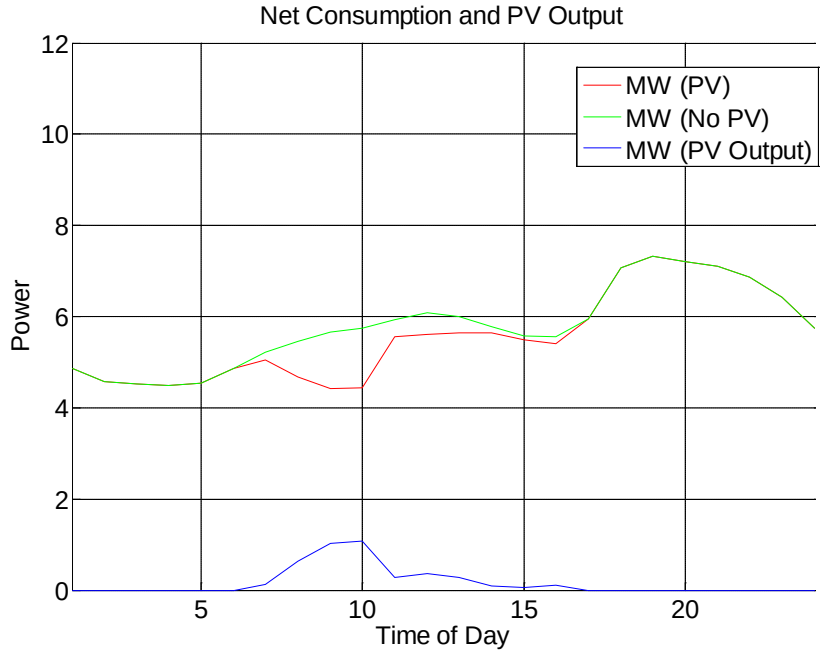

Figure A-7: MW net consumption and total PV generation for scenario 1 and case 0.

A.2 Case 1

Figure A-8 through Figure A-14 show simulation results for scenario 1 and case 1.

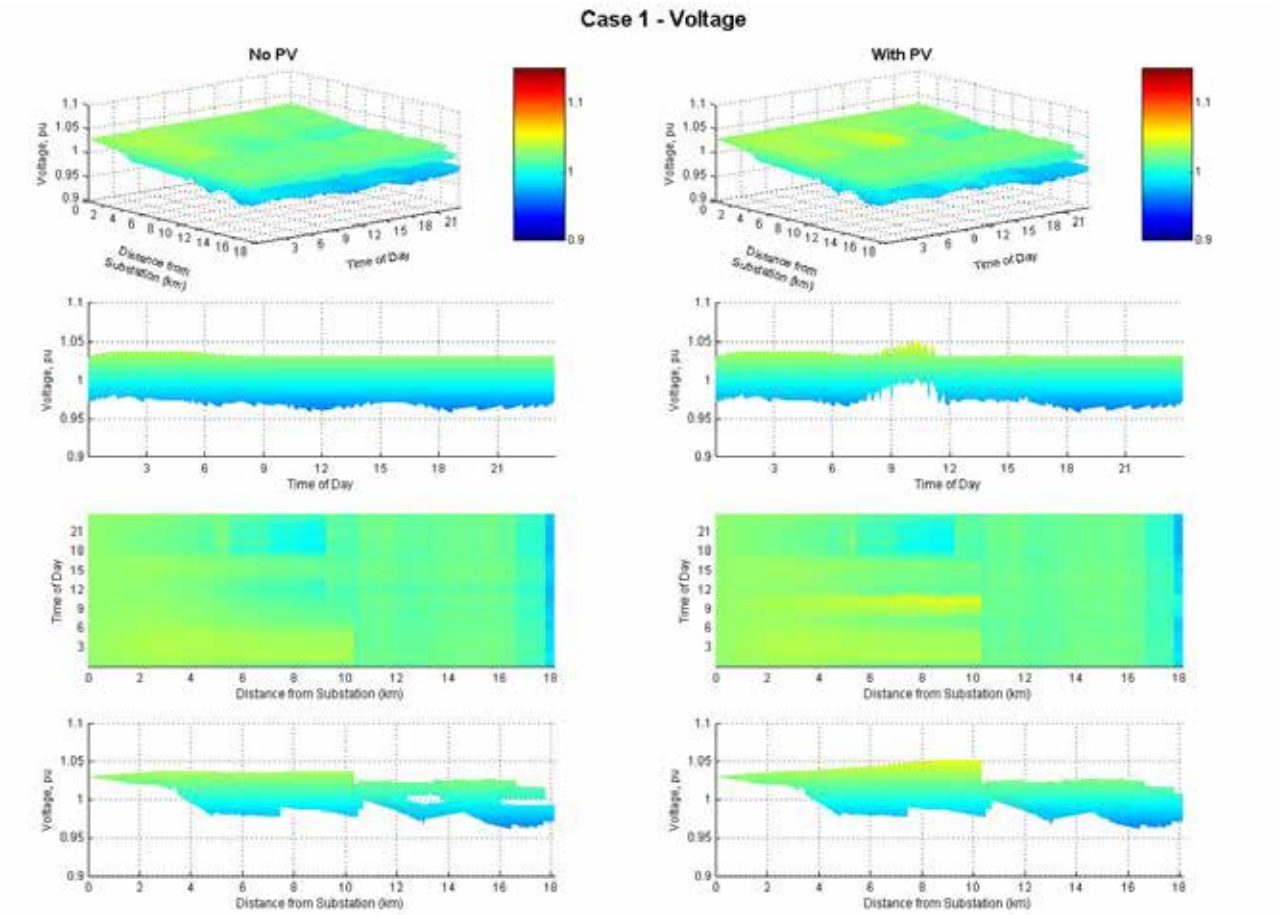

Figure A-8: Daily voltage profile for scenario 1 case 1.

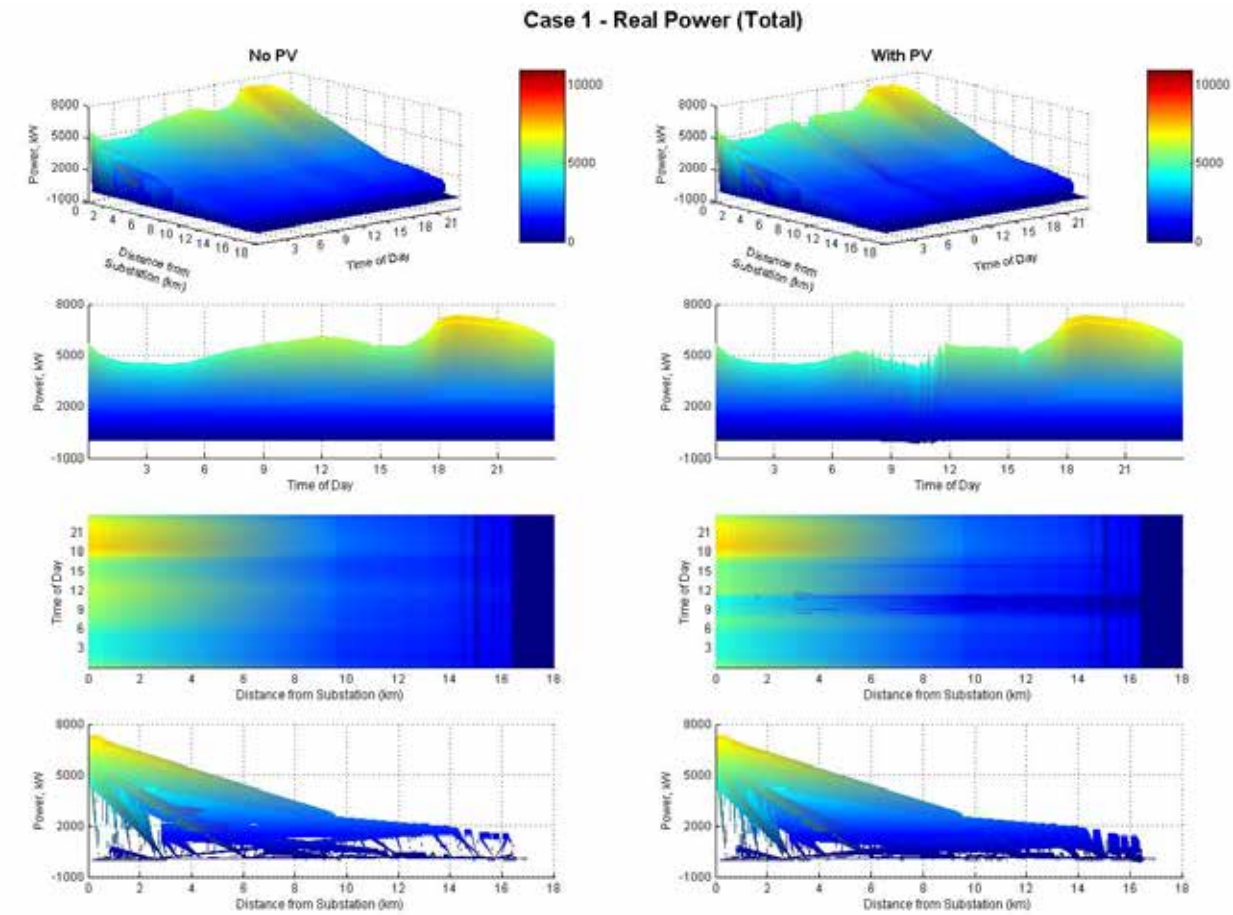

Figure A-9: Daily total real power profile for scenario 1 and case 1.

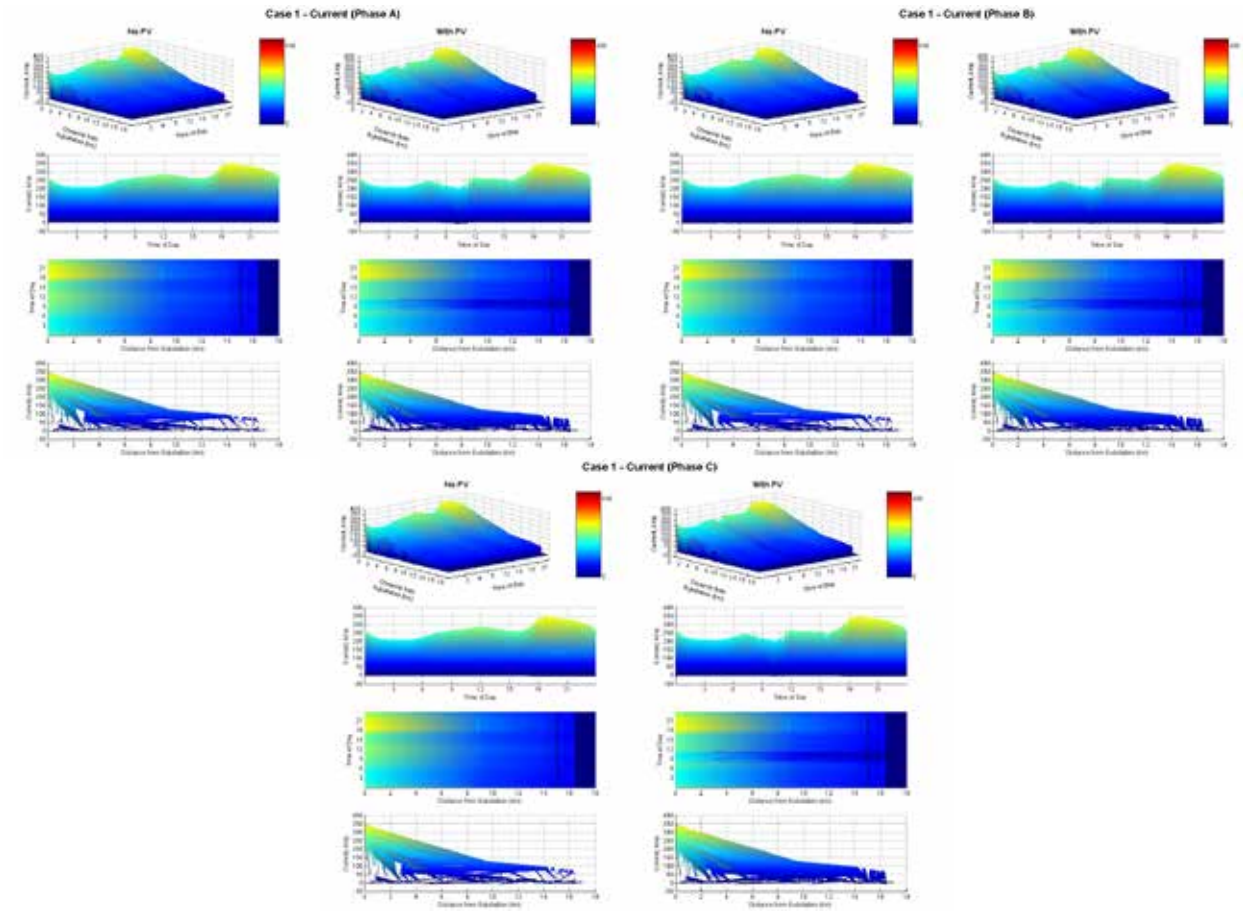

Figure A-10: Daily current profiles for scenario 1 and case 1.

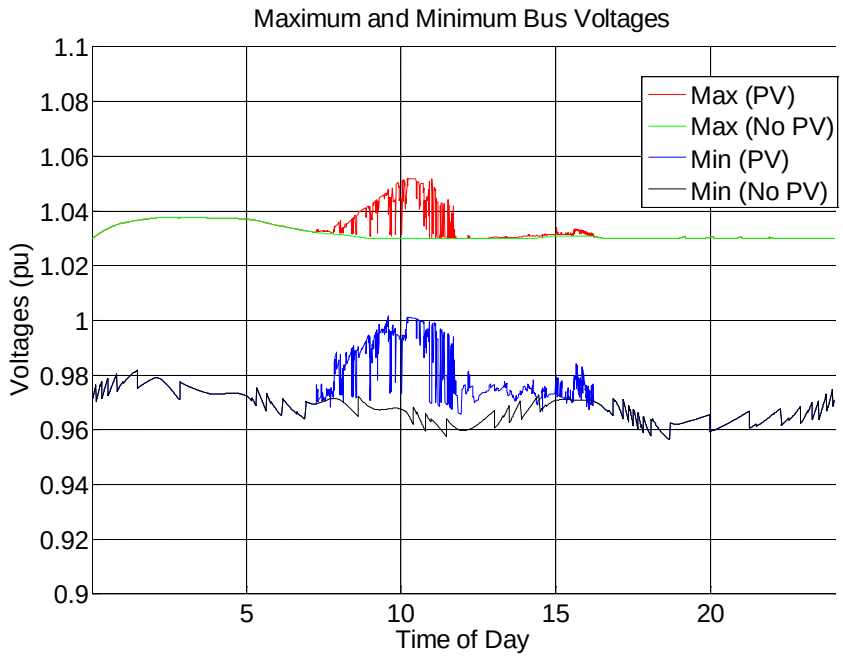

Figure A-11: Maximum and minimum voltages for scenario 1 and case 1.

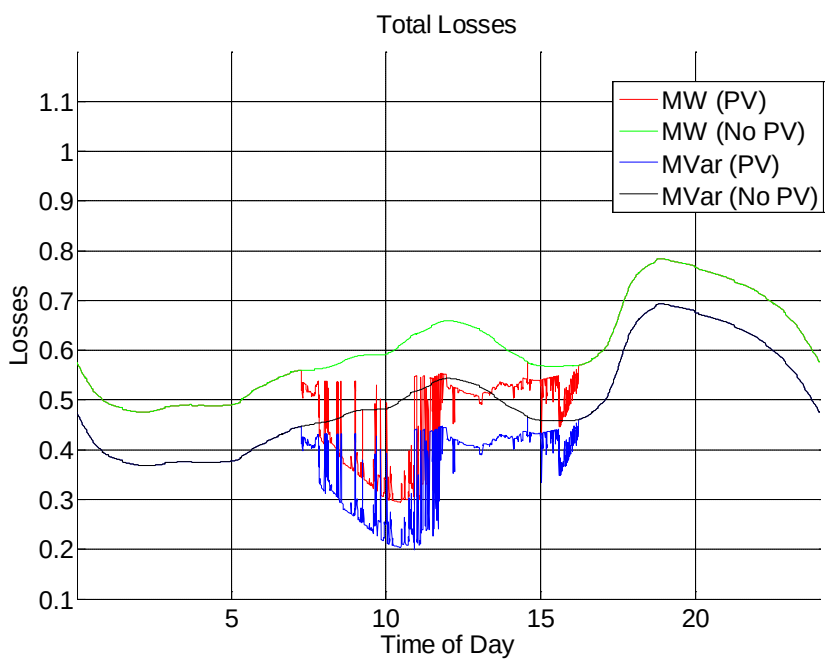

Figure A-12: MW and MVAr losses for scenario 1 and case 1.

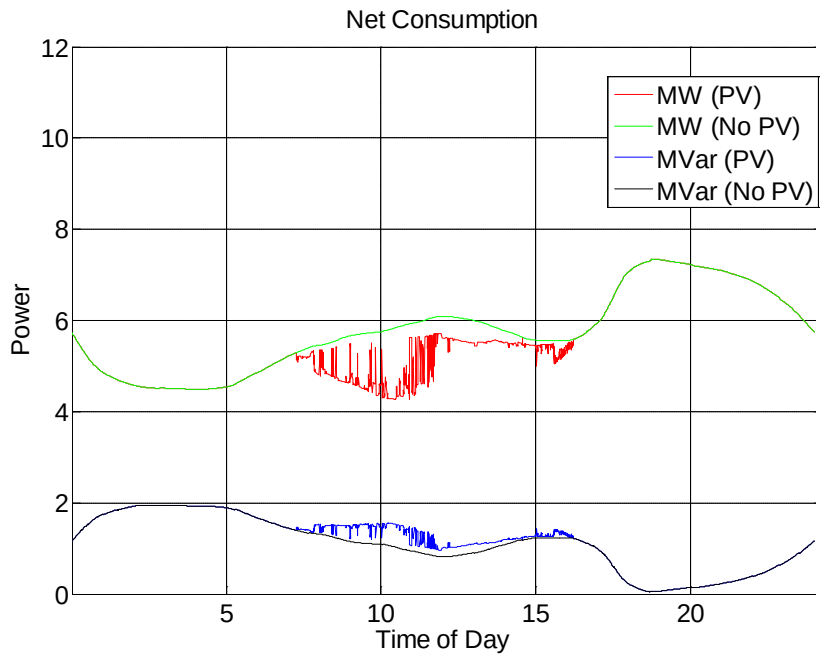

Figure A-13: MW and MVAr net consumption for scenario 1 and case 1.

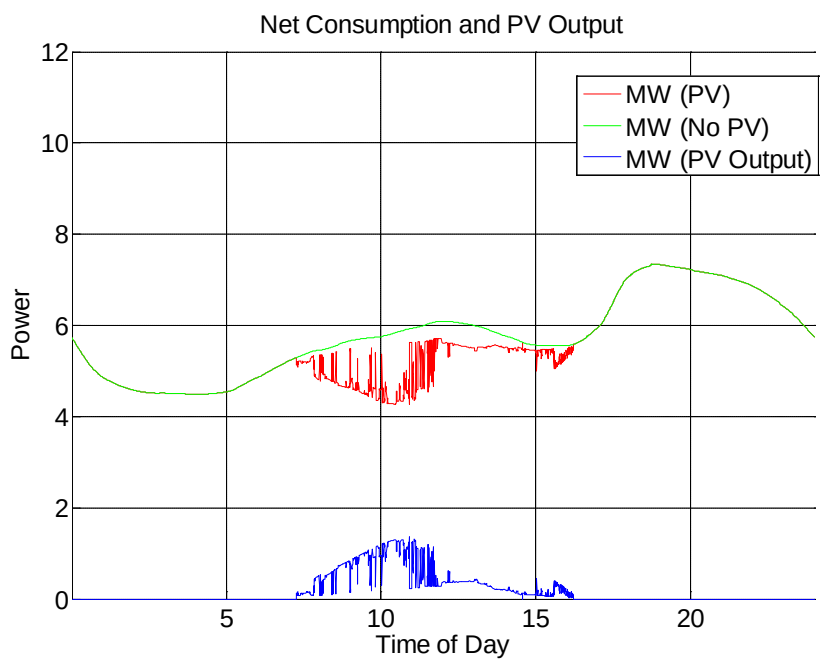

Figure A-14: MW net consumption and total PV generation for scenario 1 and case 1.

A.3 Case 2

Figure A-15 through Figure A-21 show simulation results for scenario 1 and case 2.

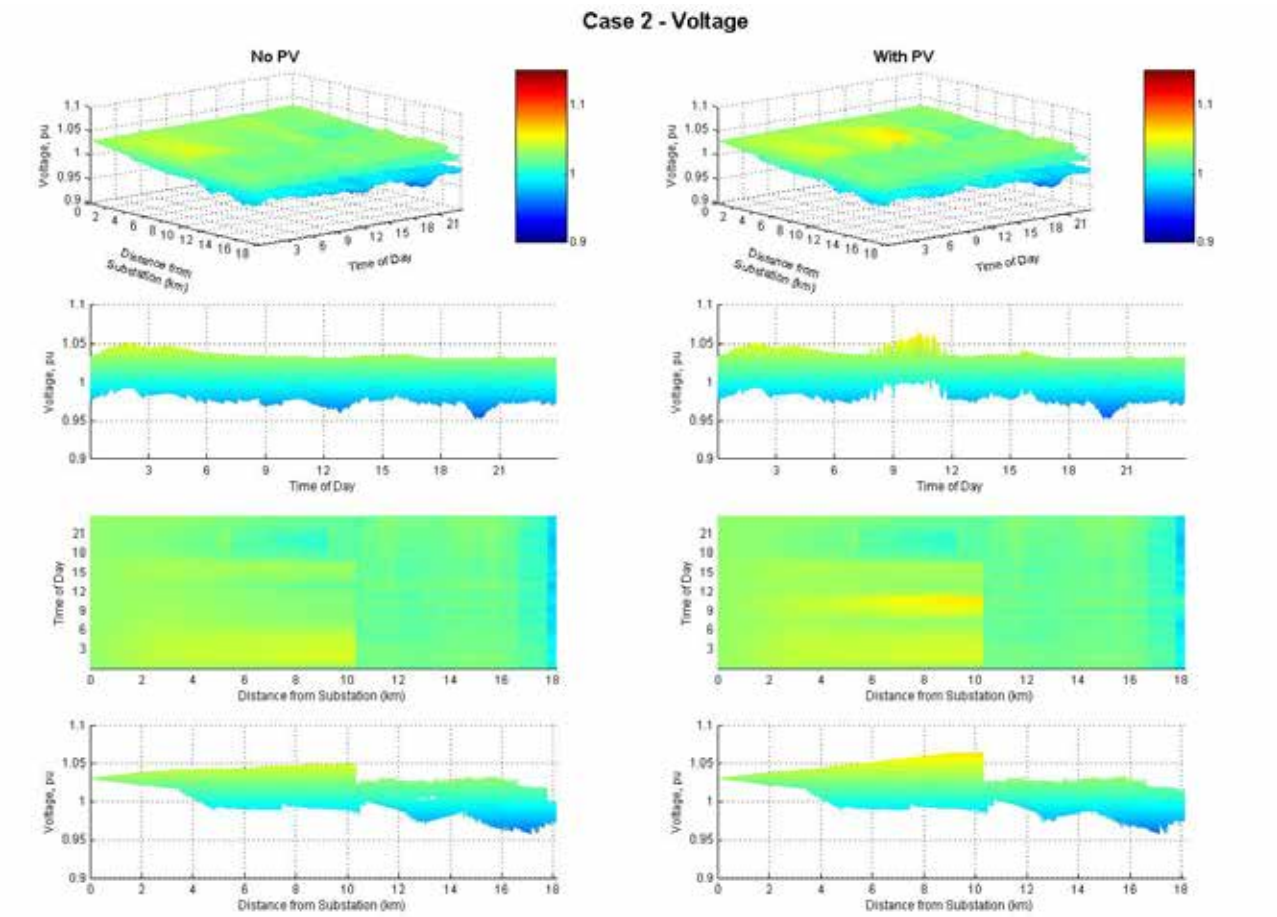

Figure A-15: Daily voltage profile for scenario 1 and case 2.

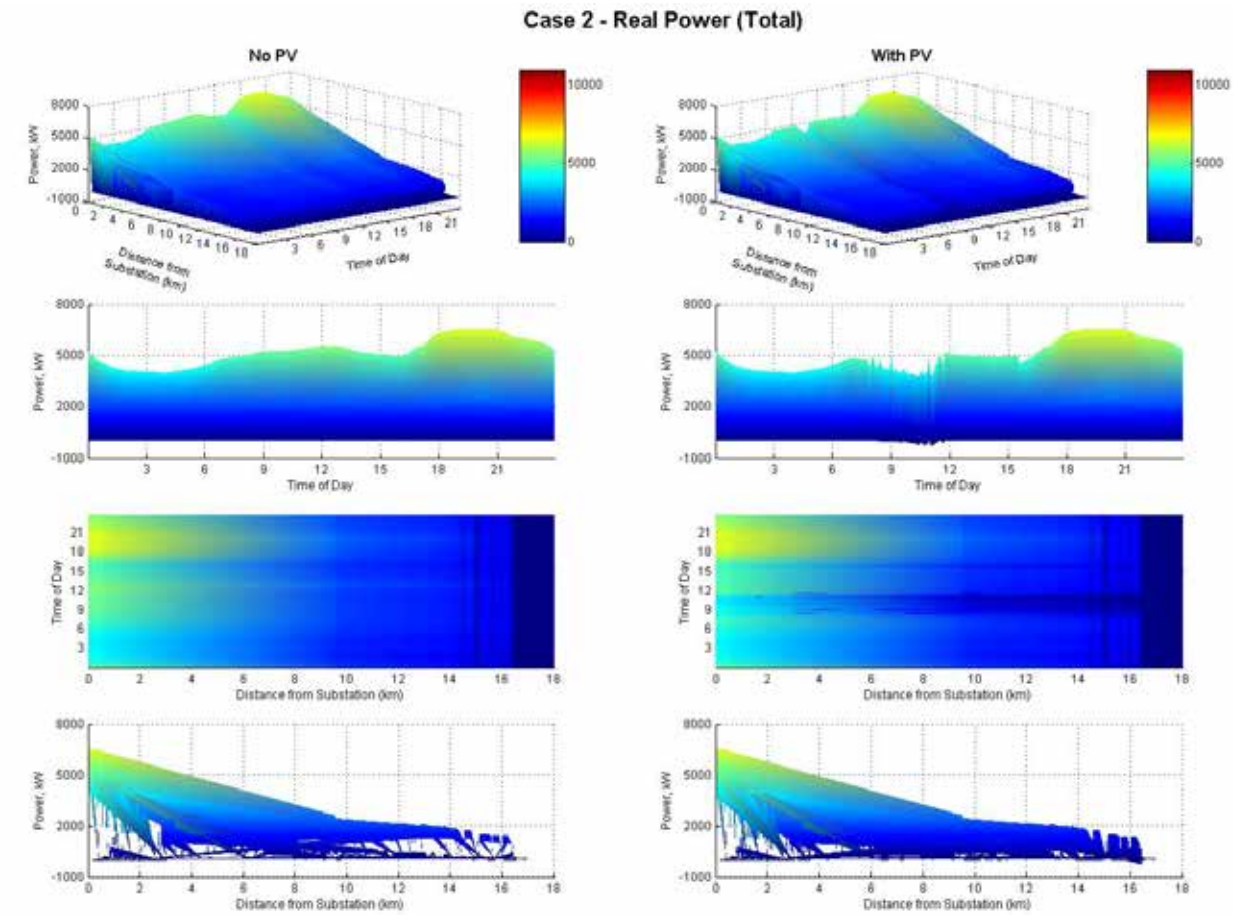

Figure A-16: Daily total real power profile for scenario 1 and case 2.

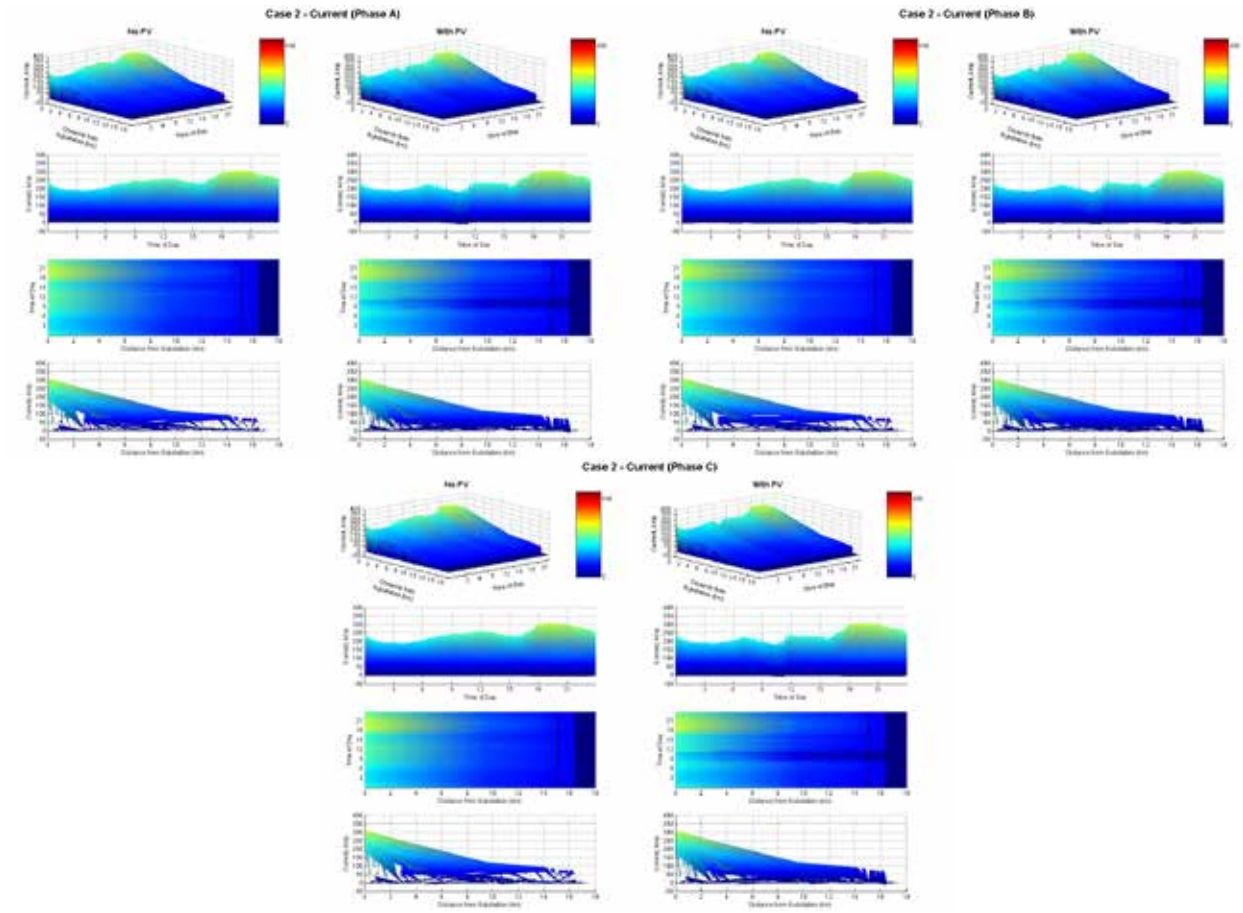

Figure A-17: Daily current profiles for scenario 1 and case 2.

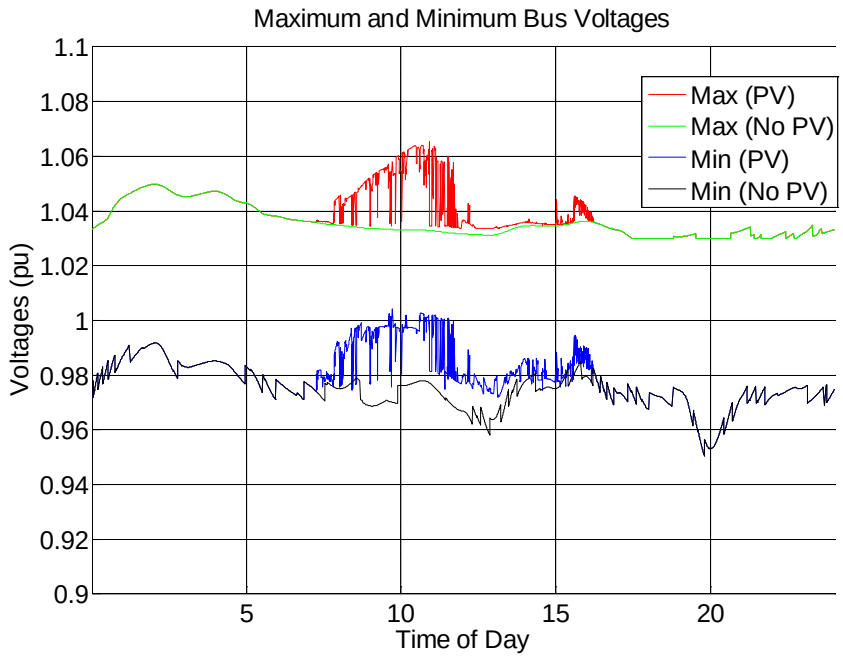

Figure A-18: Maximum and minimum voltages for scenario 1 and case 2.

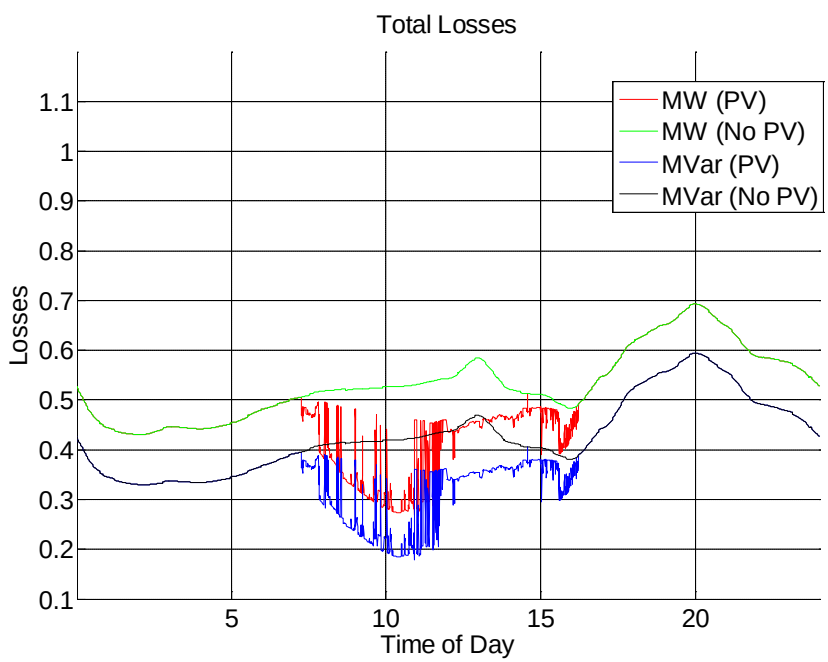

Figure A-19: MW and MVAr losses for scenario 1 and case 2.

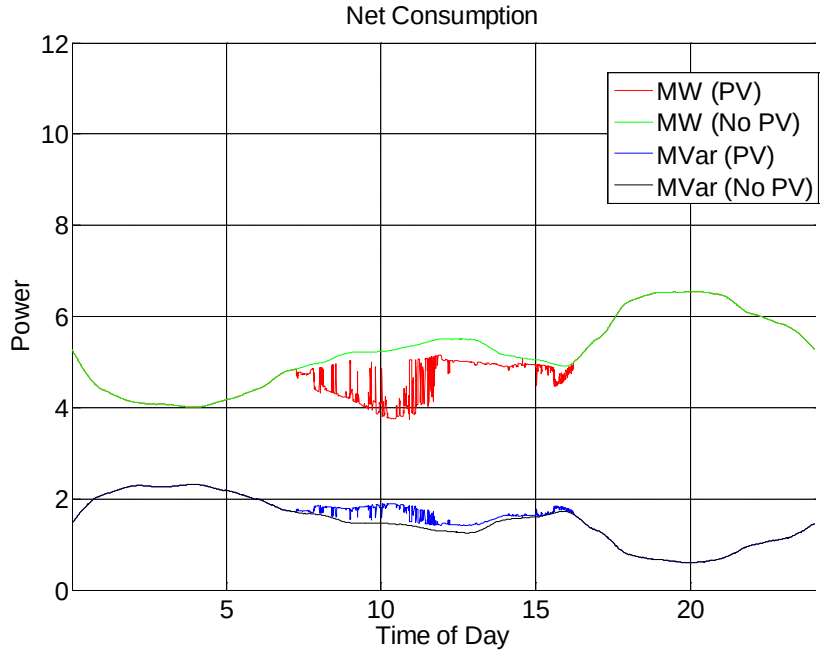

Figure A-20: MW and MVAr net consumption for scenario 1 and case 2.

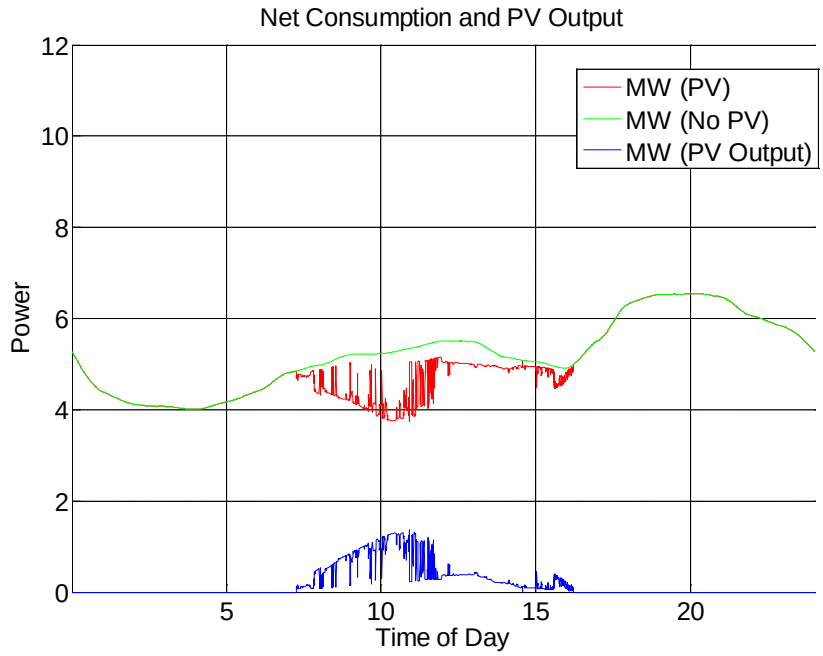

Figure A-21: MW net consumption and total PV generation for scenario 1 and case 2.

A.4 Case 3

Figure A-22 through Figure A-28 show simulation results for scenario 1 and case 3.

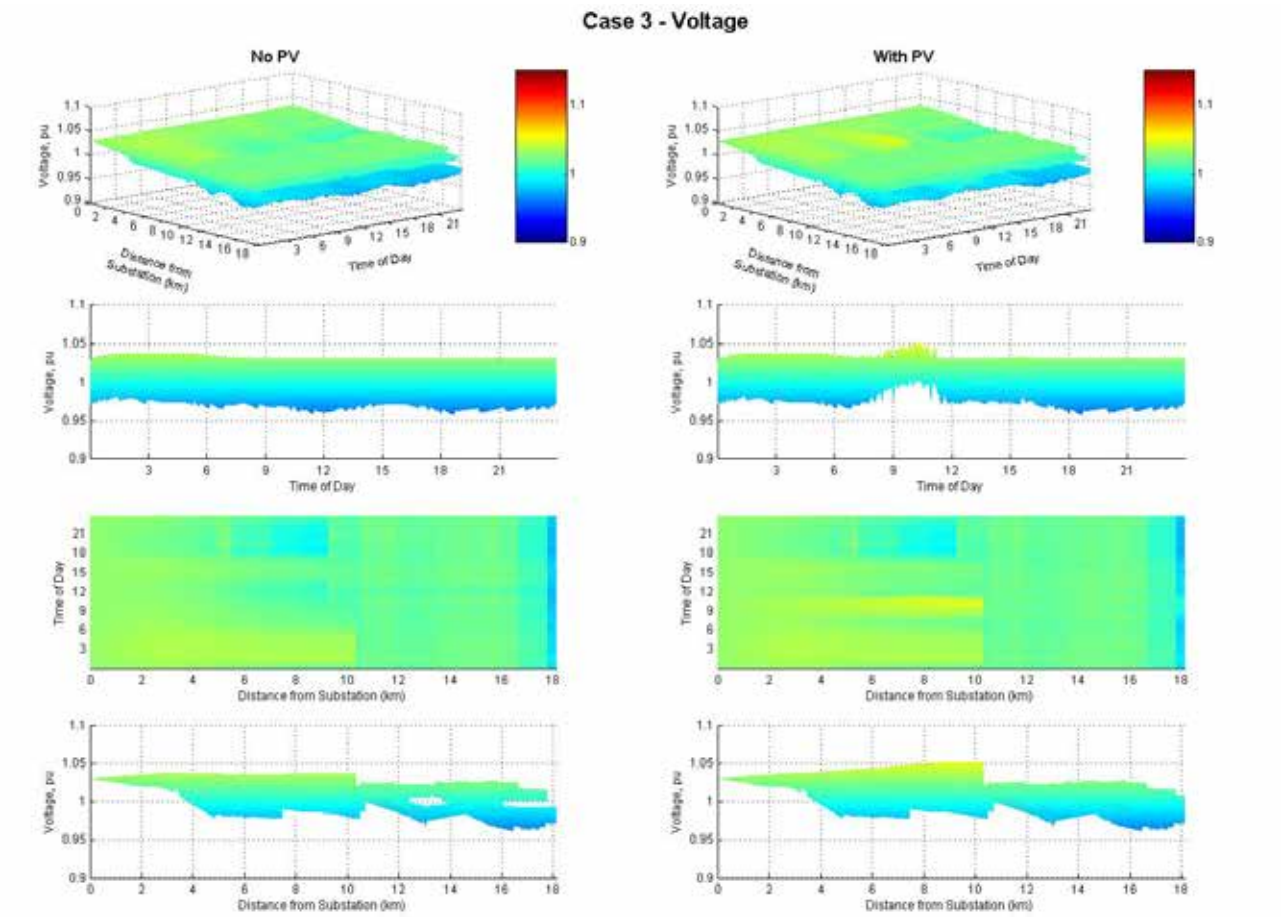

Figure A-22: Daily voltage profile for scenario 1 case 3.

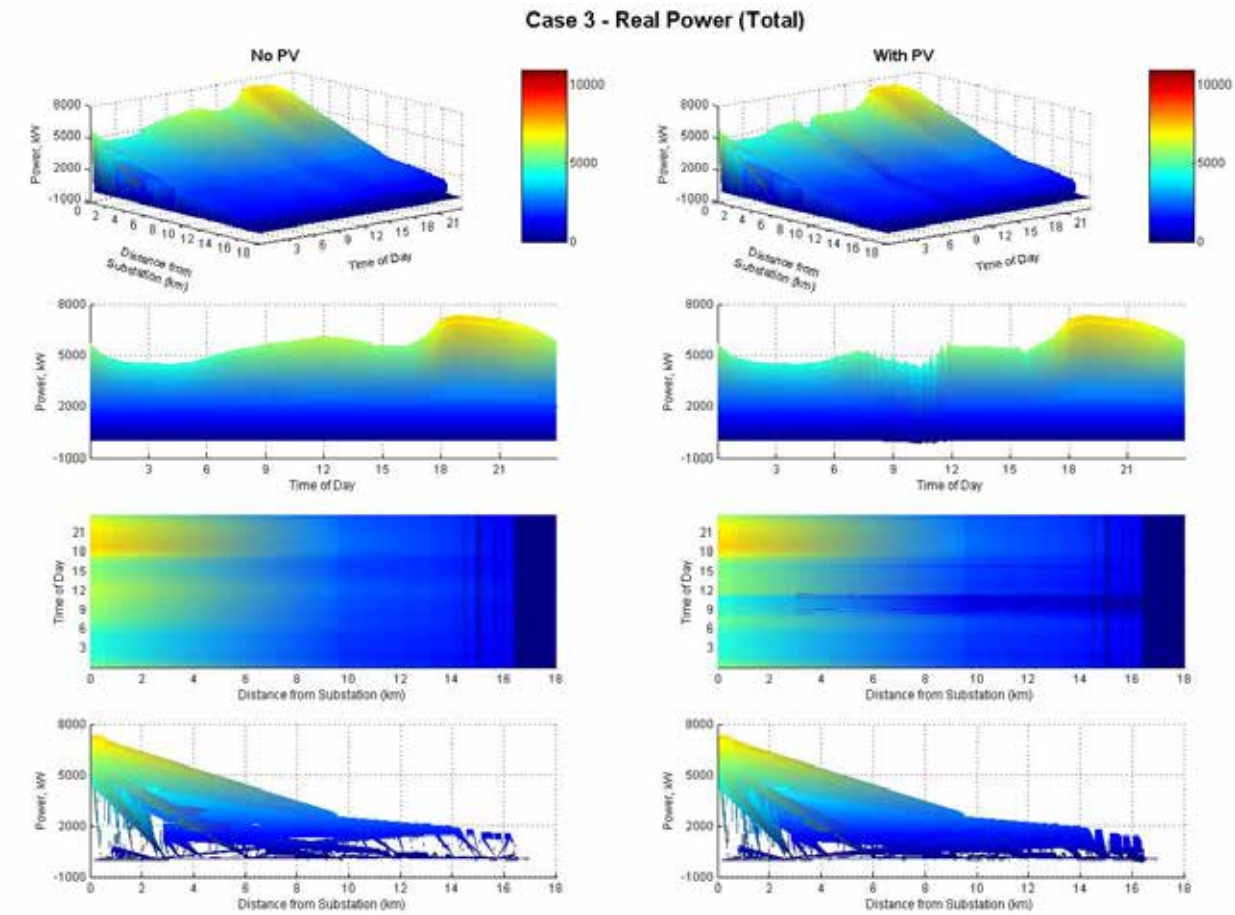

Figure A-23: Daily total real power profile for scenario 1 and case 3.

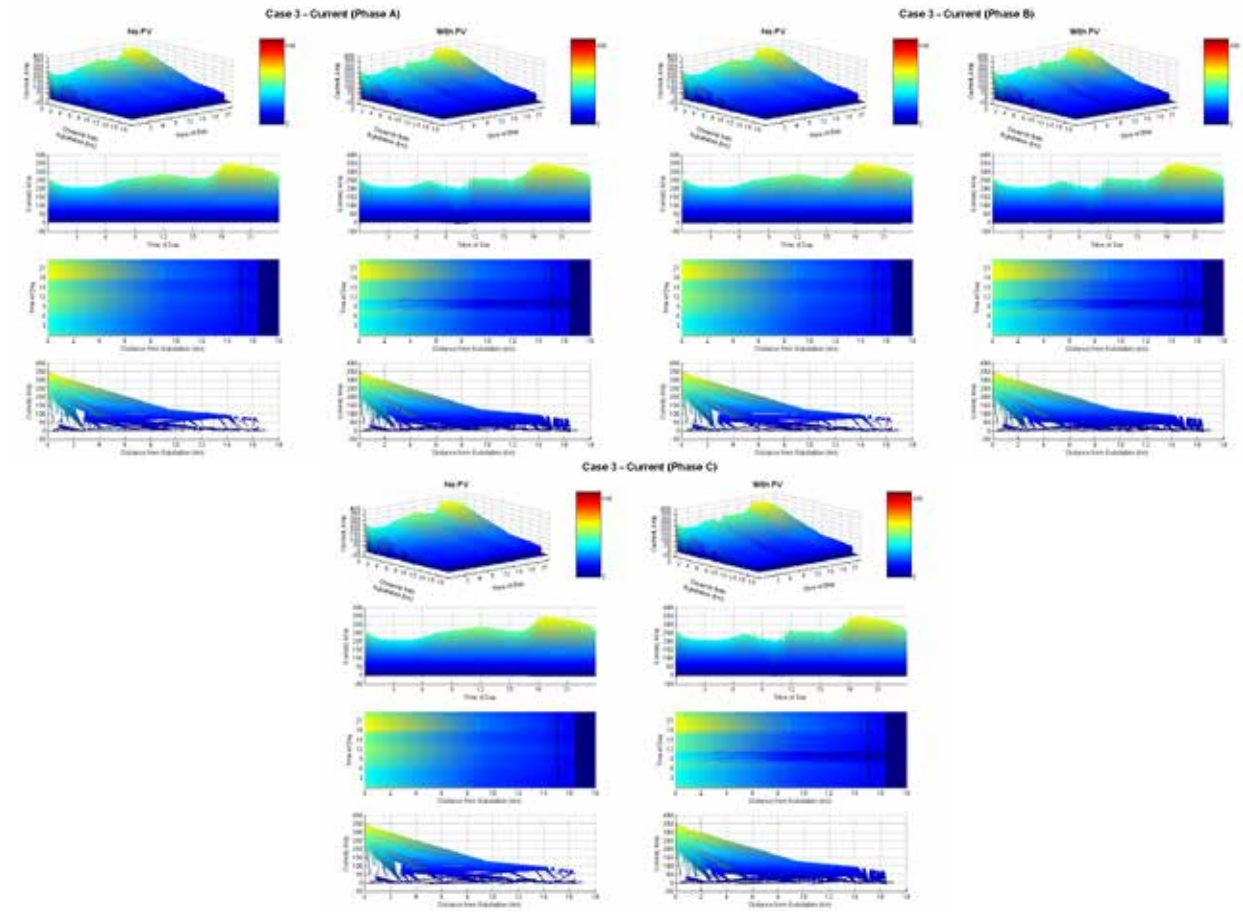

Figure A-24: Daily current profiles for scenario 1 and case 3.

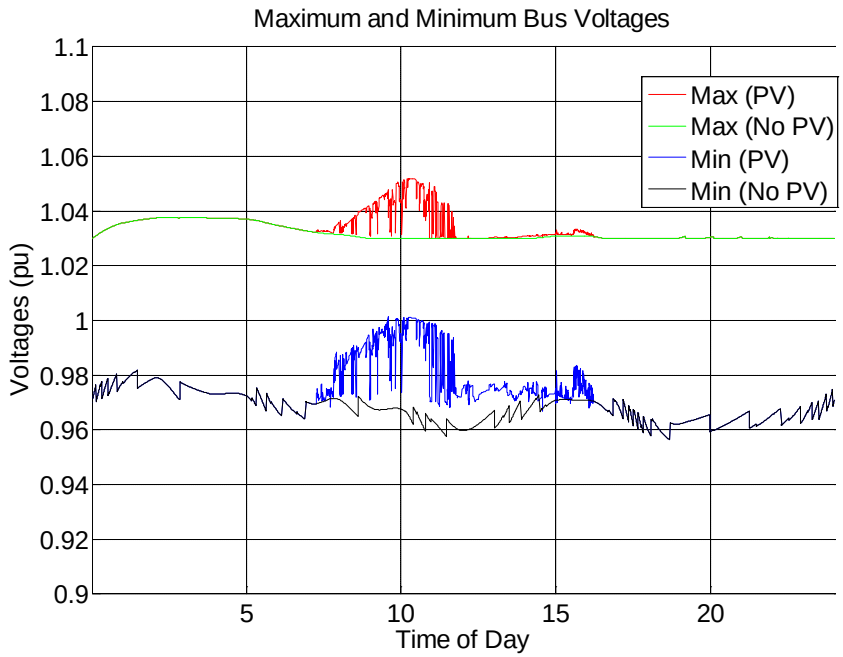

Figure A-25: Maximum and minimum voltages for scenario 1 and case 3.

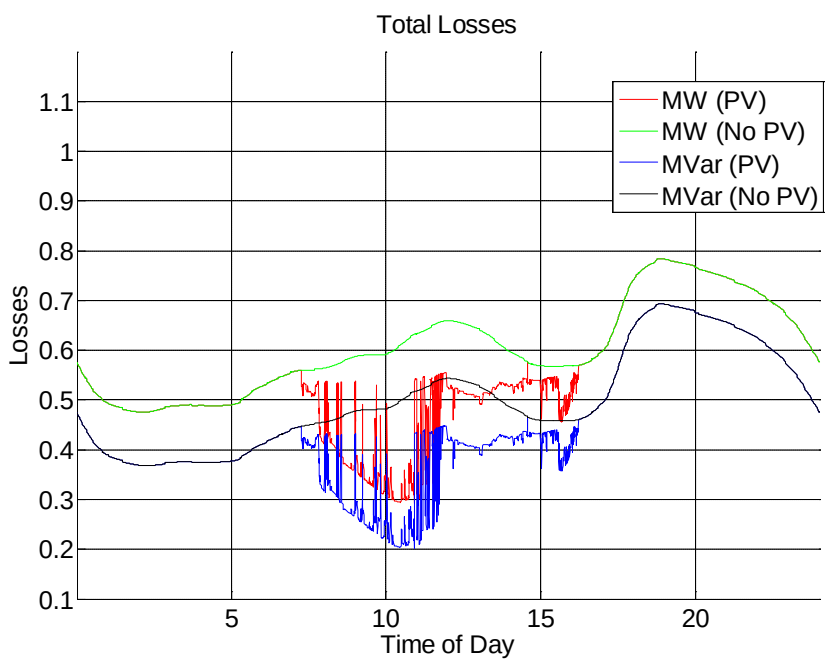

Figure A-26: MW and MVAr losses for scenario 1 and case 3.

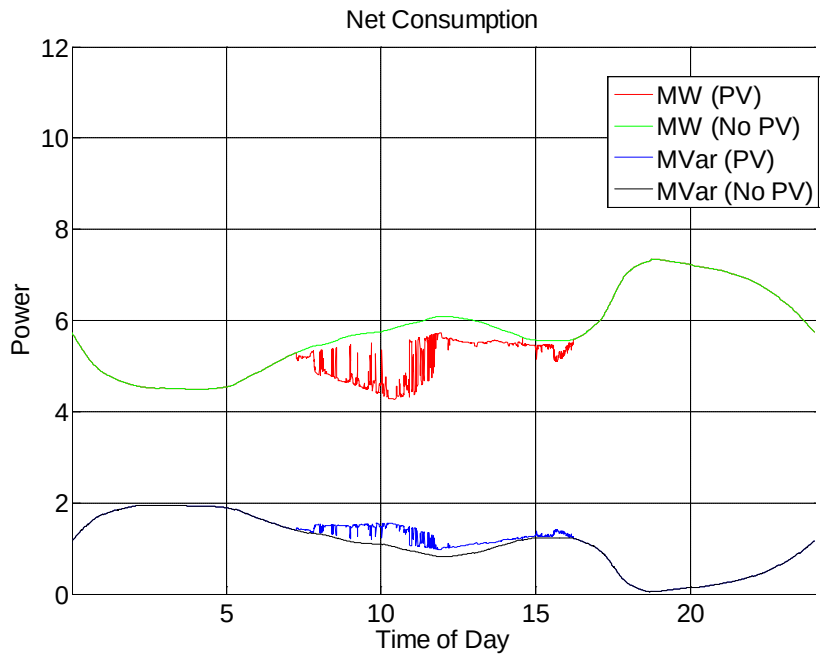

Figure A-27: MW and MVAr net consumption for scenario 1 and case 3.

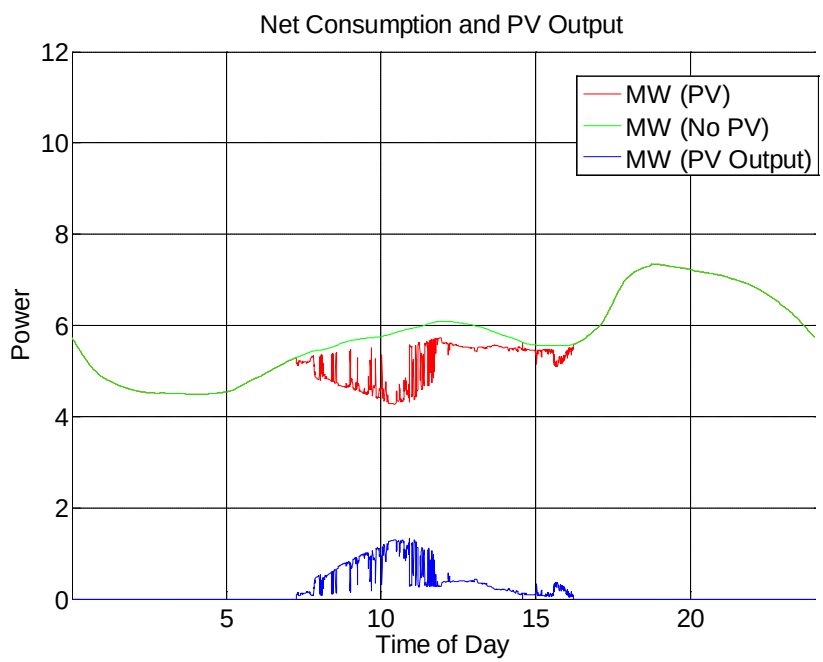

Figure A-28: MW net consumption and total PV generation for scenario 1 and case 3.

A.5 Case 4

Figure A-29 through Figure A-35 show simulation results for scenario 1 and case 4.

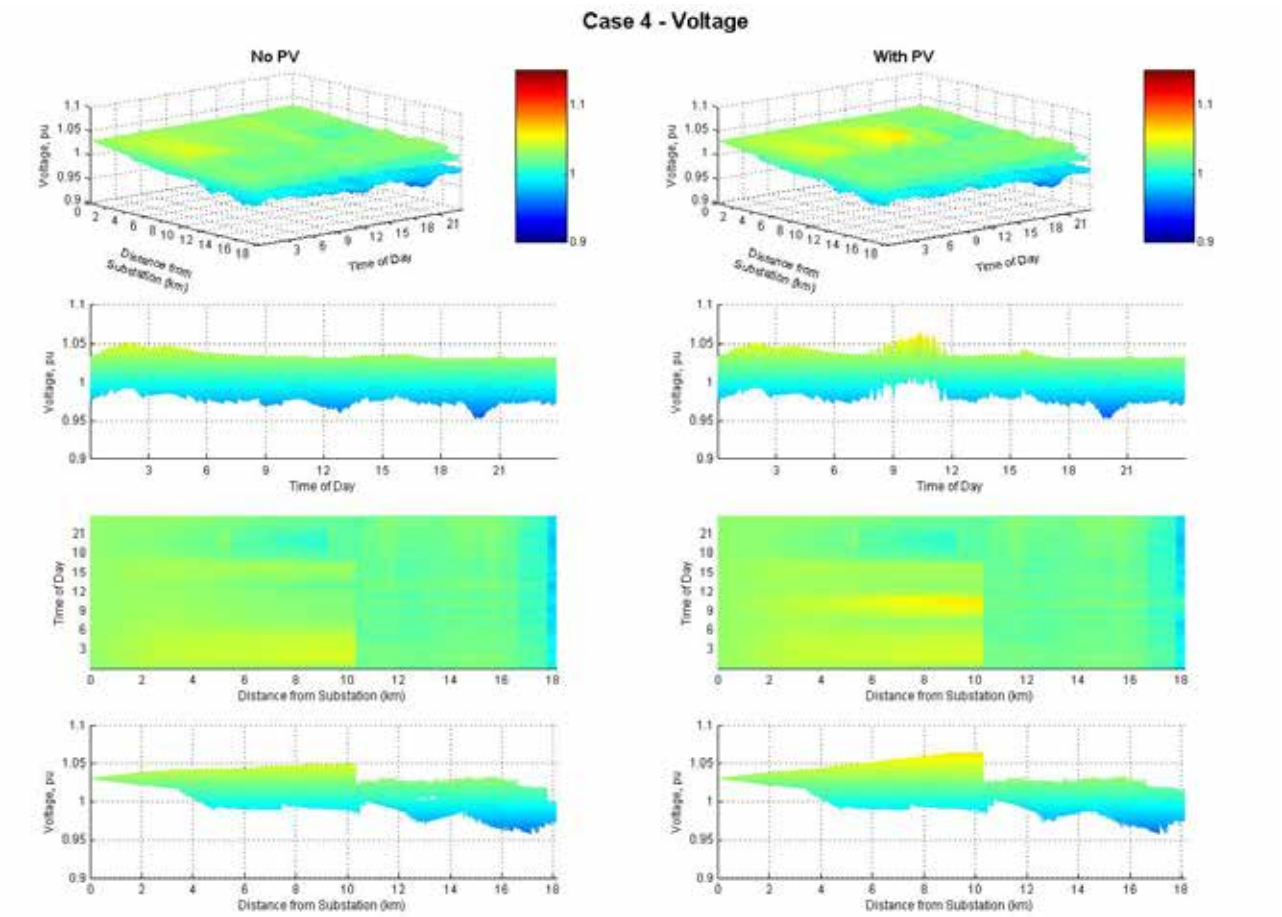

Figure A-29: Daily voltage profile for scenario 1 case 4.

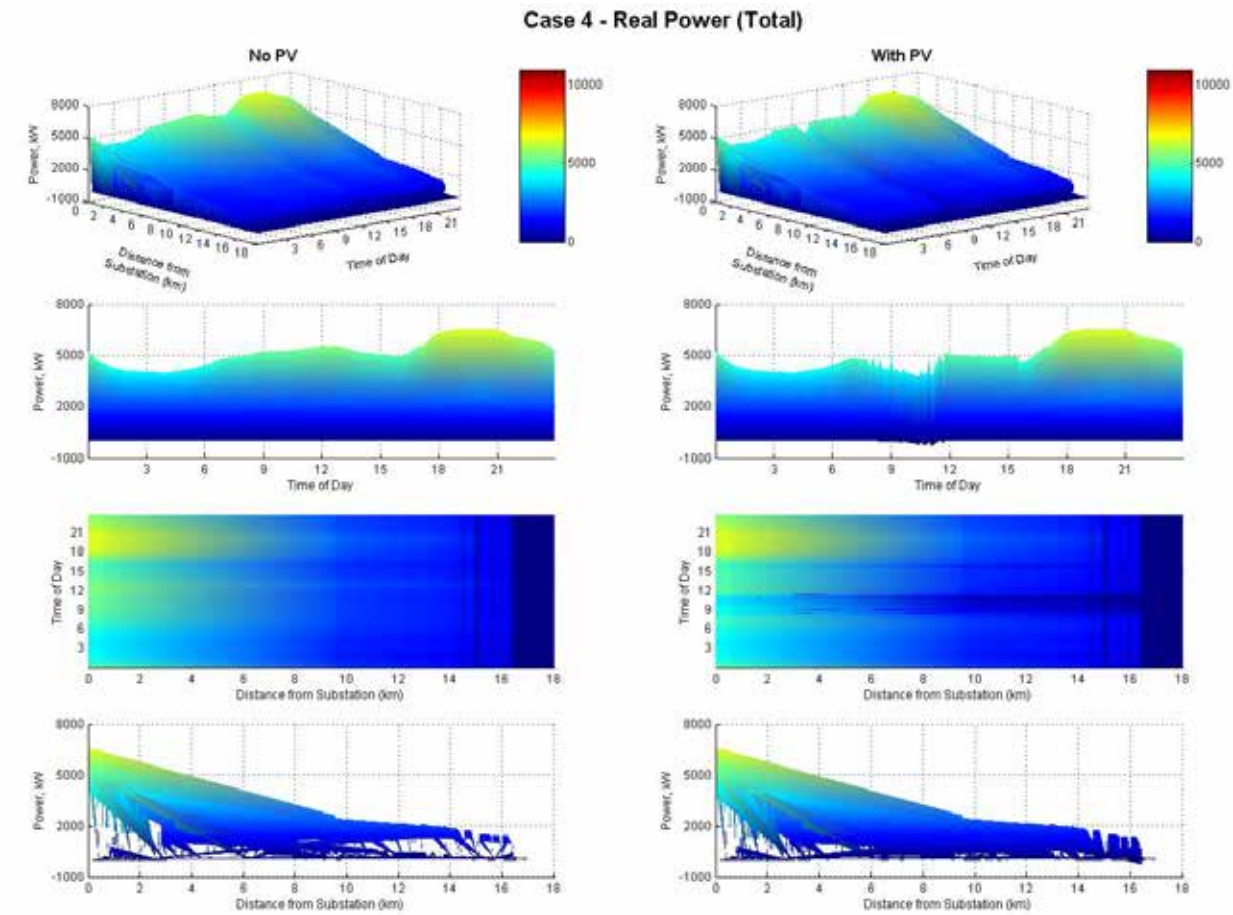

Figure A-30: Daily total real power profile for scenario 1 and case 4.

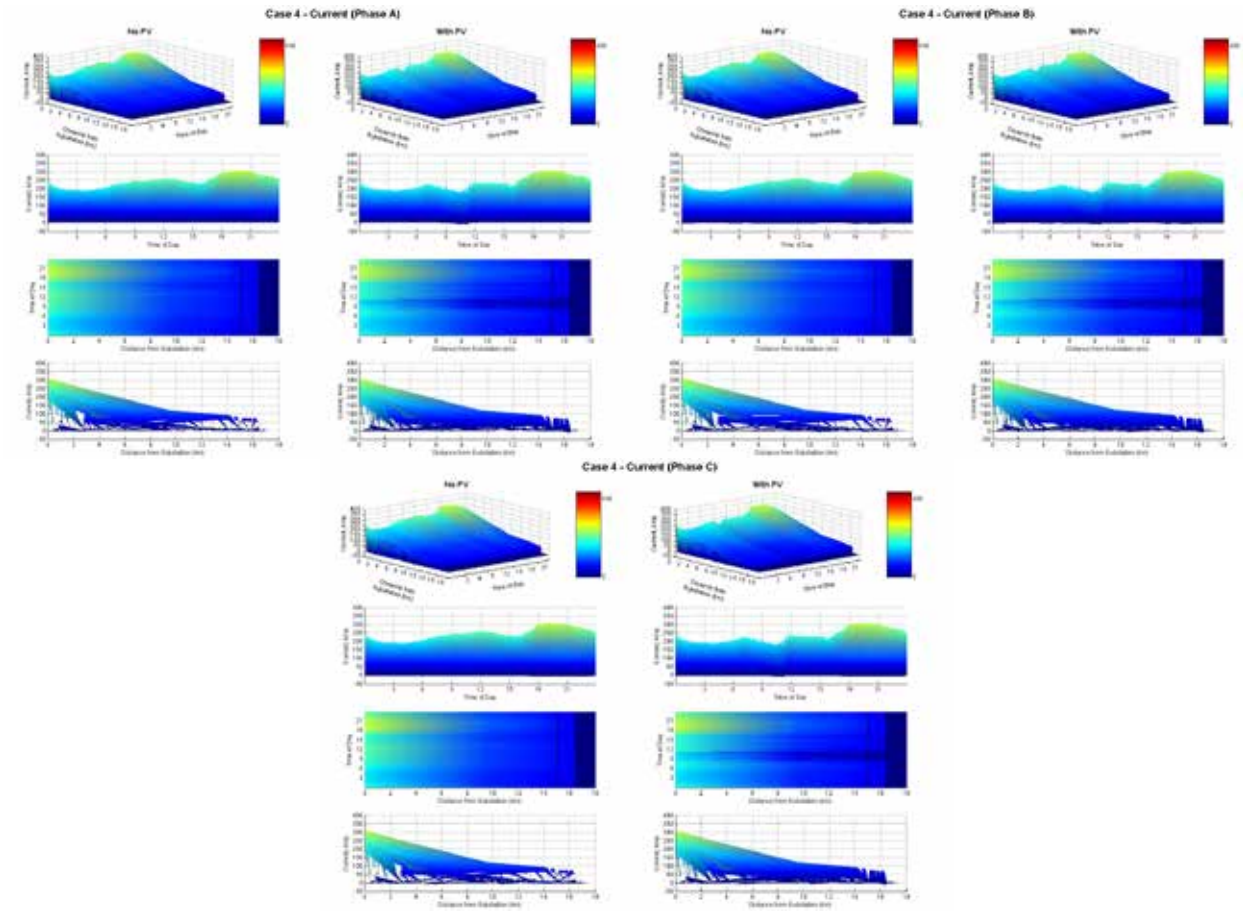

Figure A-31: Daily current profiles for scenario 1 and case 4.

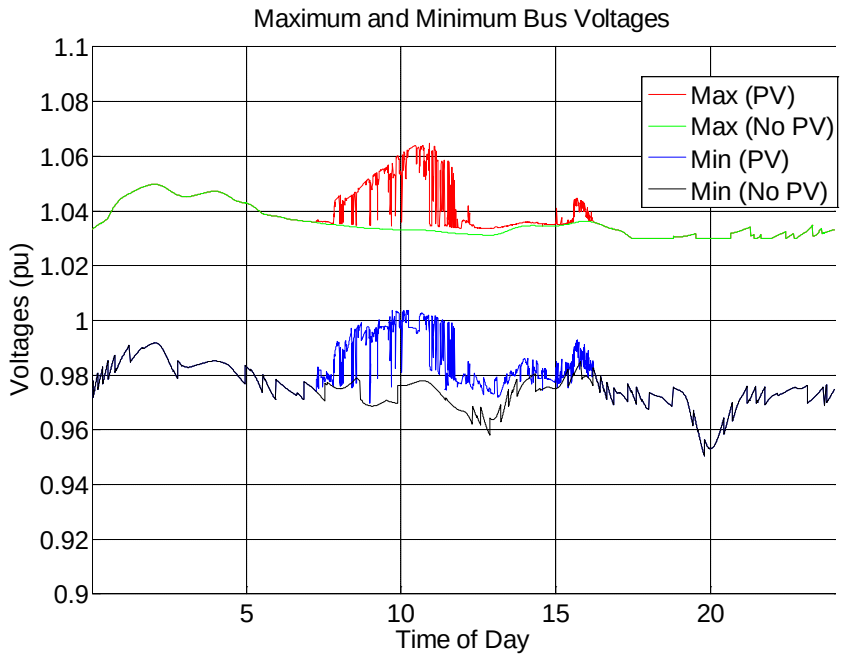

Figure A-32: Maximum and minimum voltages for scenario 1 and case 4.

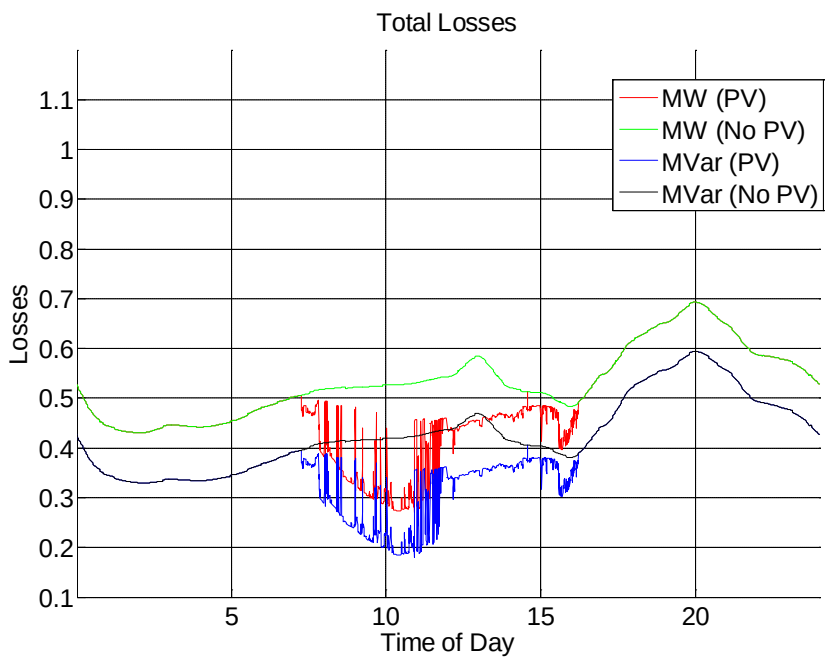

Figure A-33: MW and MVAr losses for scenario 1 and case 4.

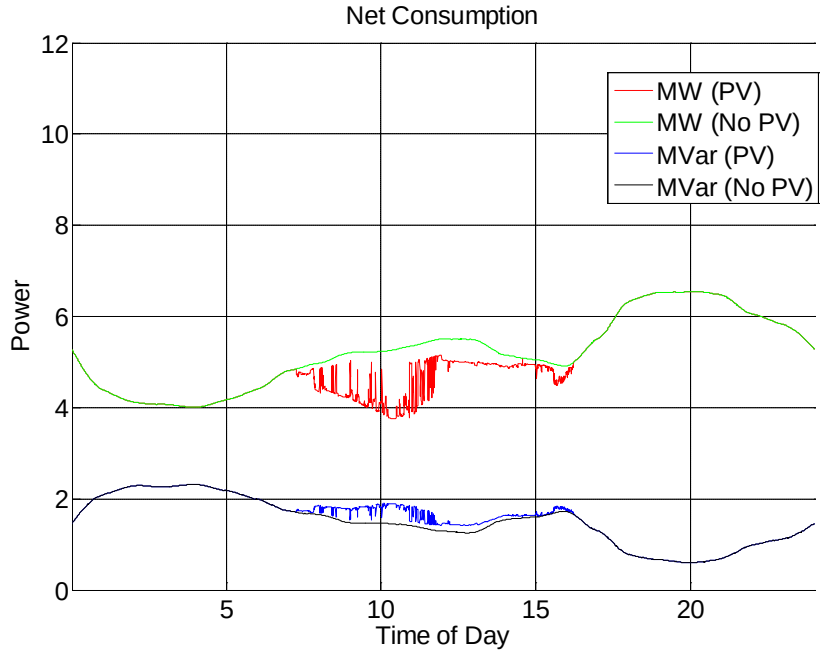

Figure A-34: MW and MVAr net consumption for scenario 1 and case 4.

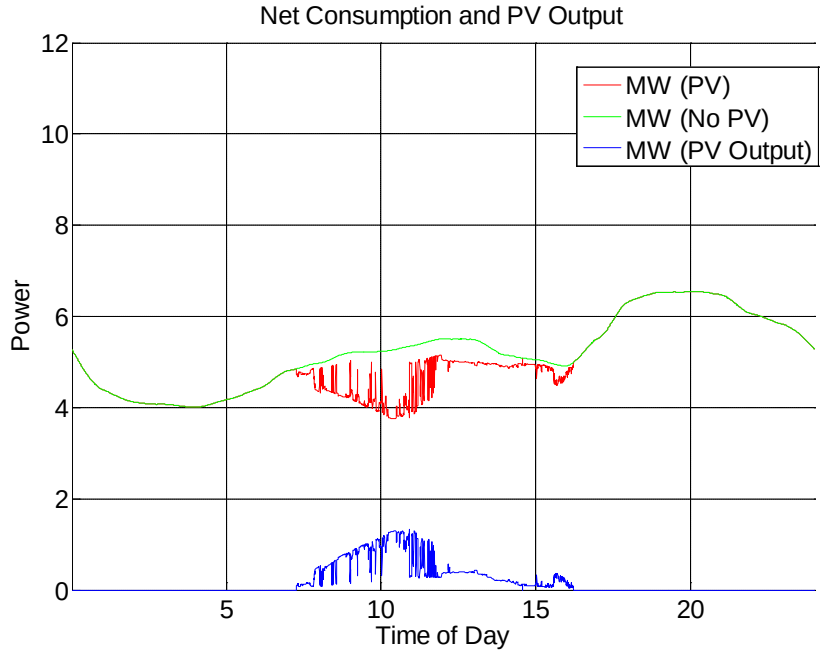

Figure A-35: MW net consumption and total PV generation for scenario 1 and case 4.

A.6 Case 5

Figure A-36 through Figure A-42 show simulation results for scenario 1 and case 5.

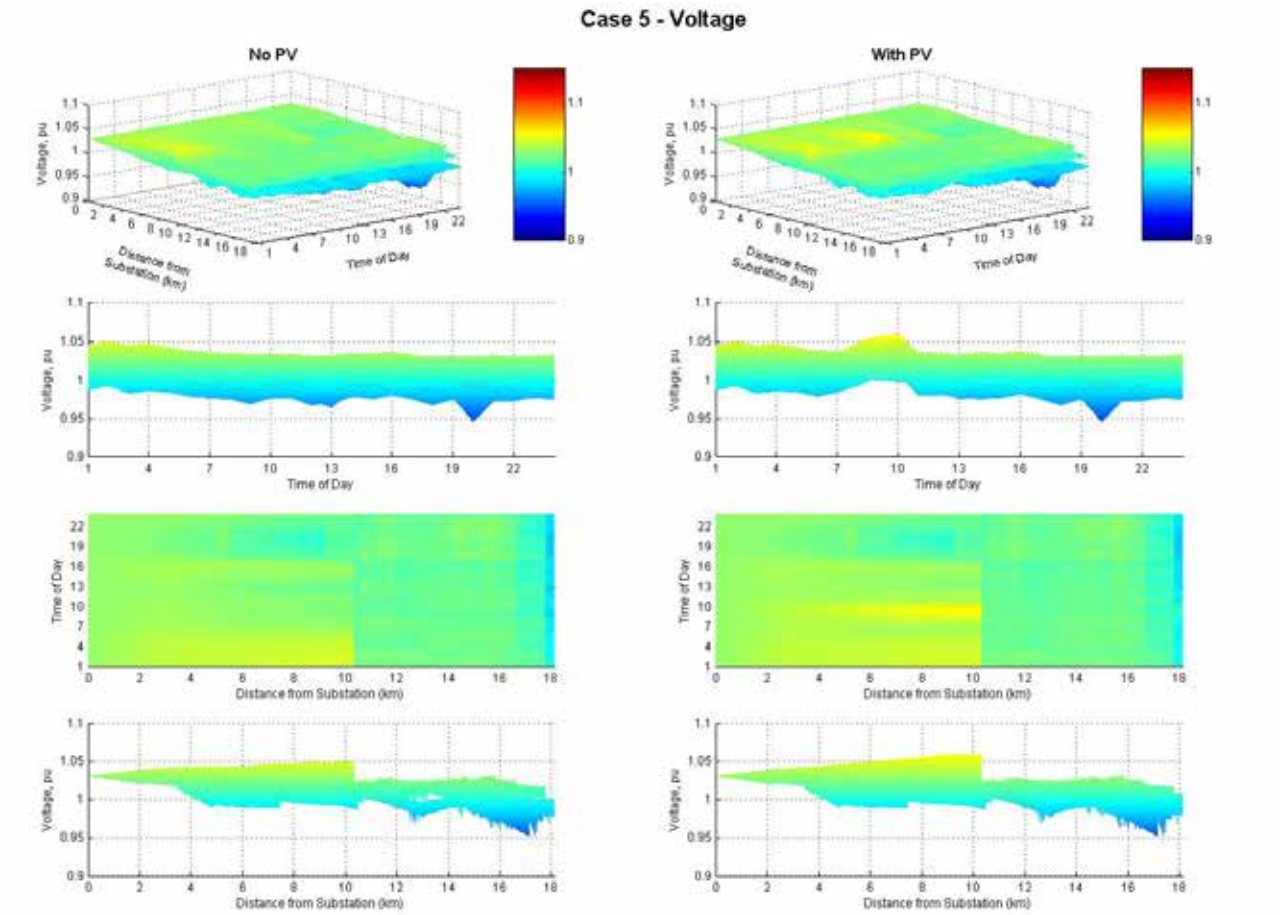

Figure A-36: Daily voltage profile for scenario 1 case 5.

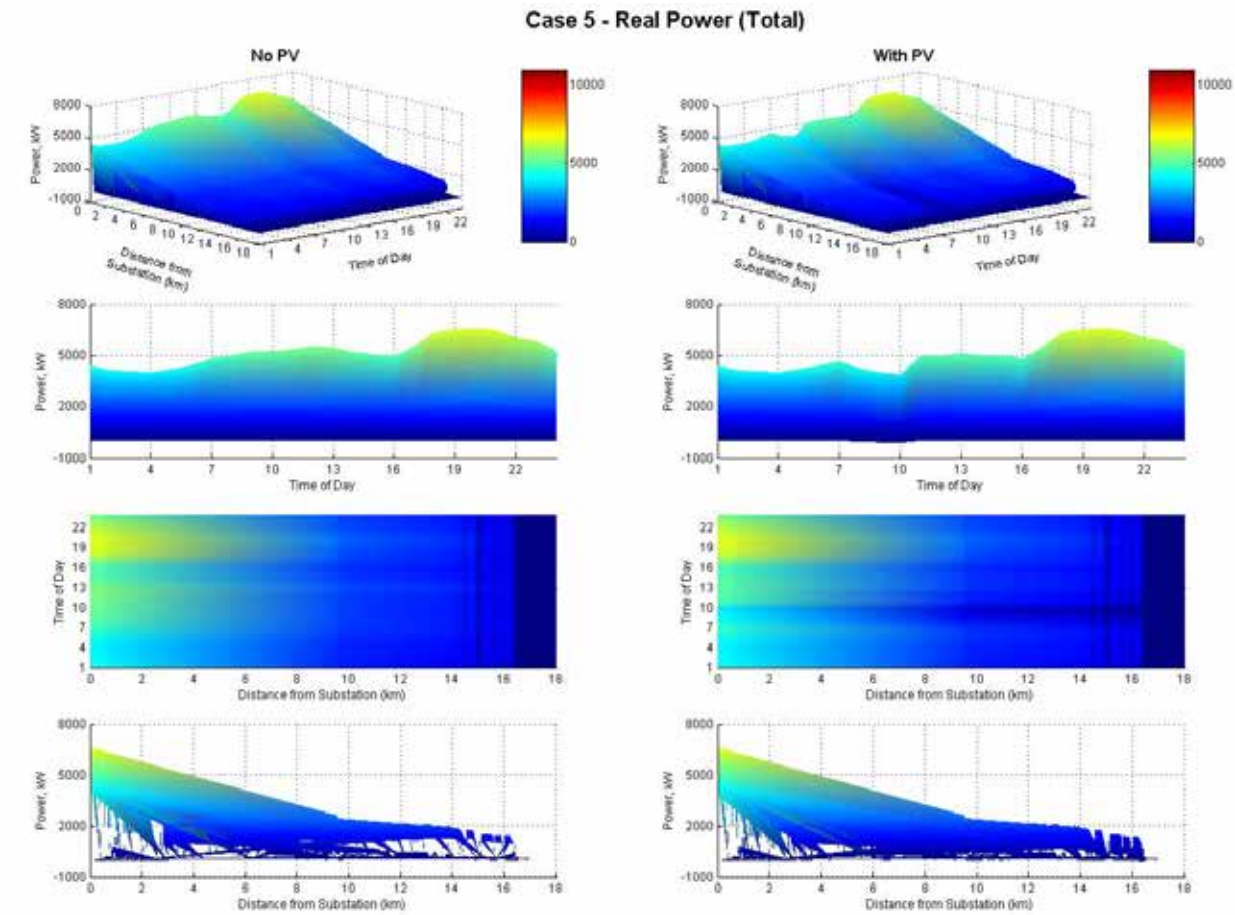

Figure A-37: Daily total real power profile for scenario 1 and case 5.

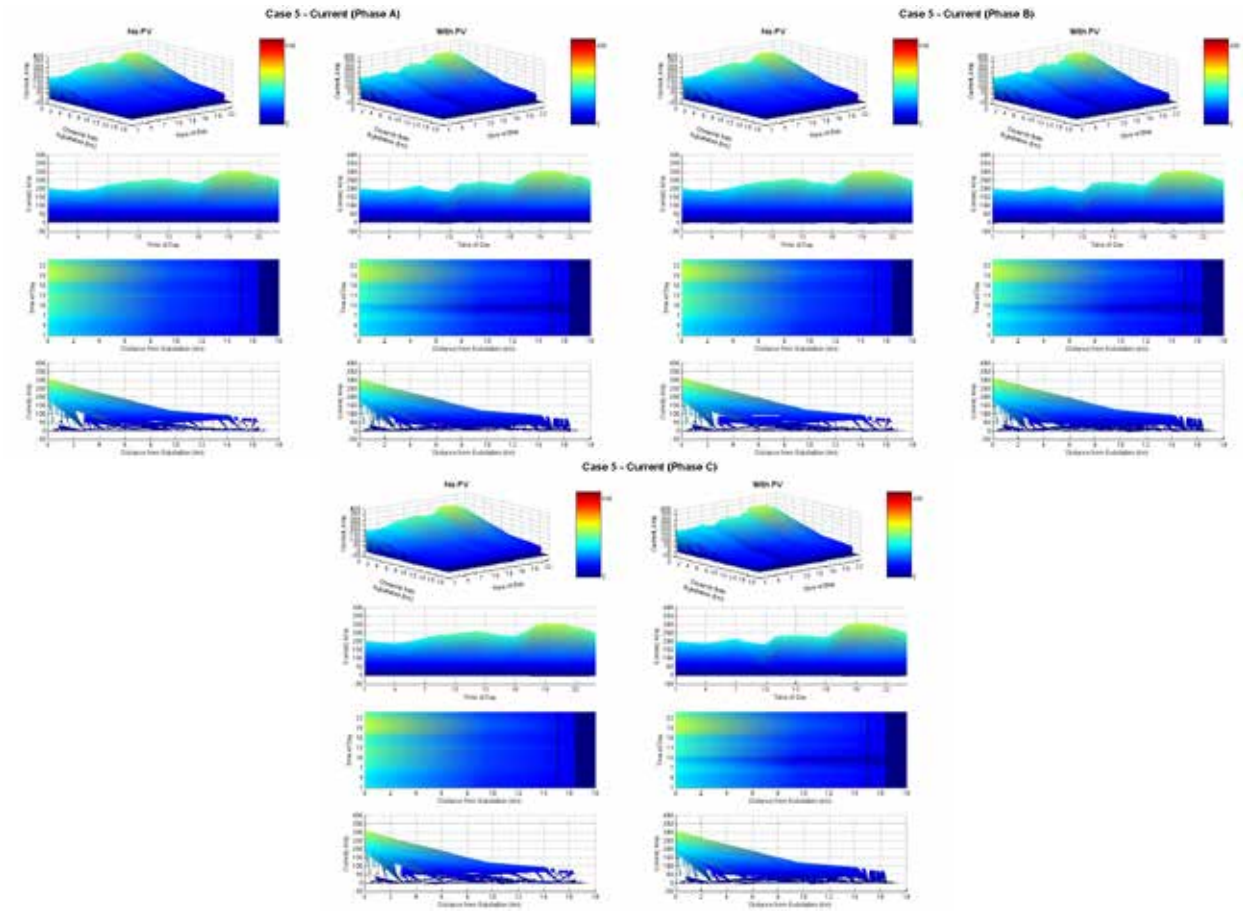

Figure A-38: Daily current profiles for scenario 1 and case 5.

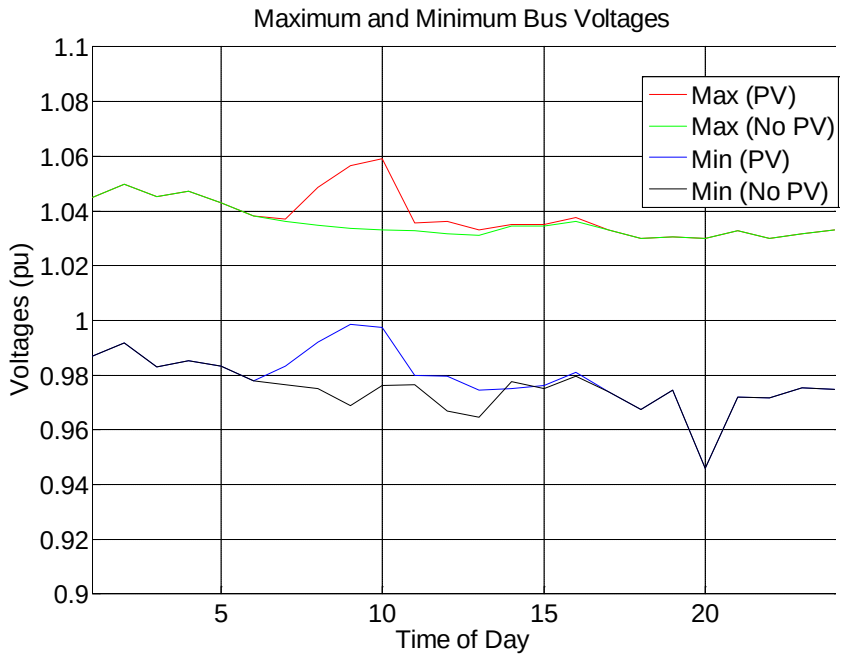

Figure A-39: Maximum and minimum voltages for scenario 1 and case 5.

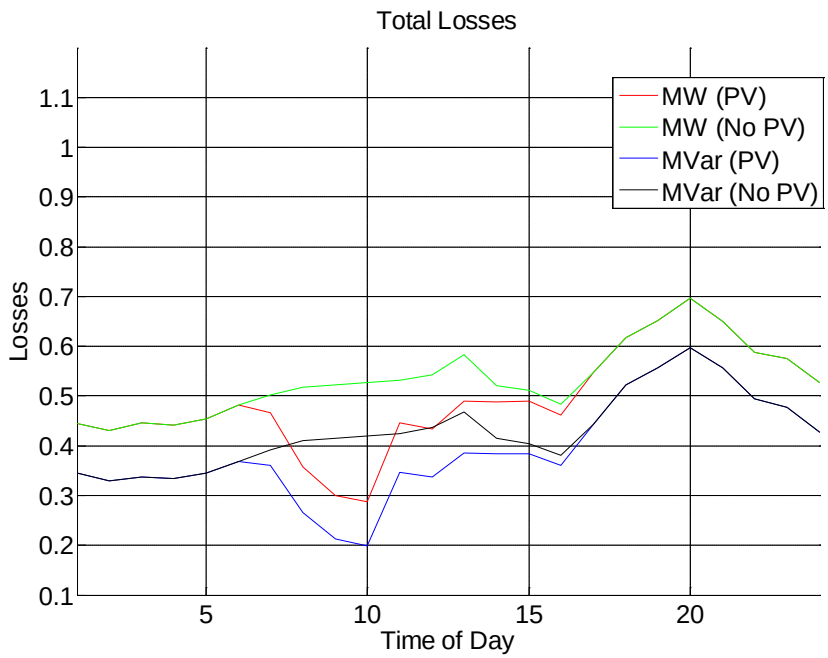

Figure A-40: MW and MVAr losses for scenario 1 and case 5.

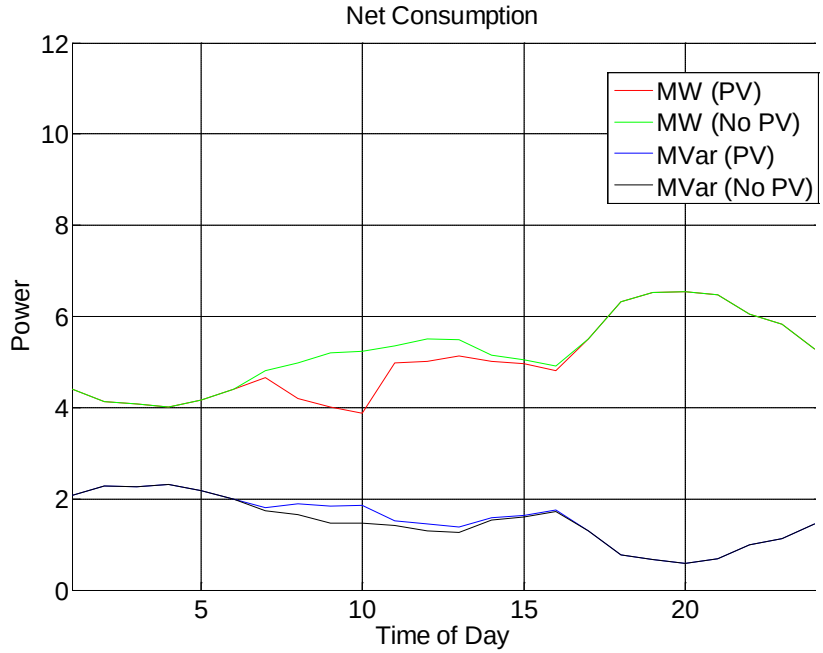

Figure A-41: MW and MVAr net consumption for scenario 1 and case 5.

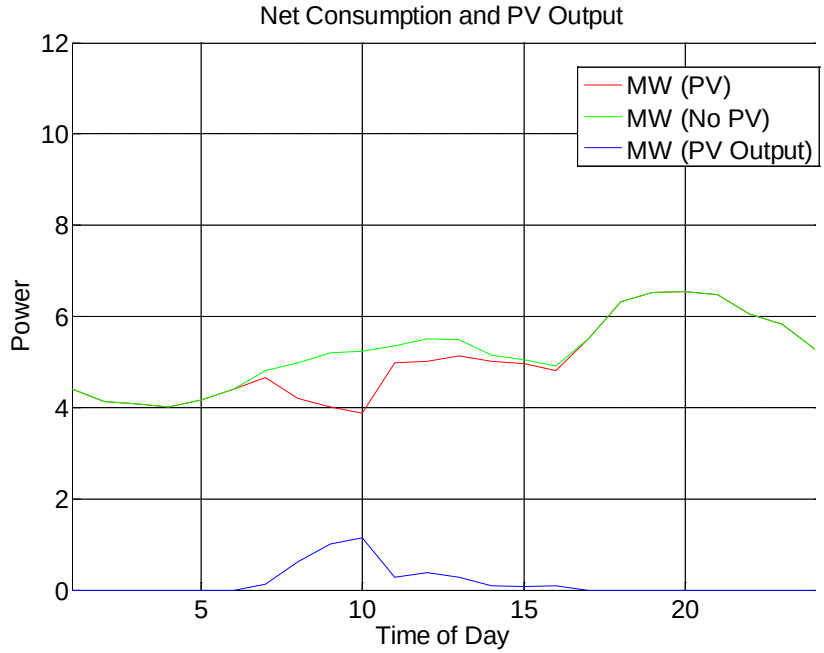

Figure A-42: MW net consumption and total PV generation for scenario 1 and case 5.

A.7 Case 6

Figure A-43 through Figure A-49 show simulation results for scenario 1 and case 6.

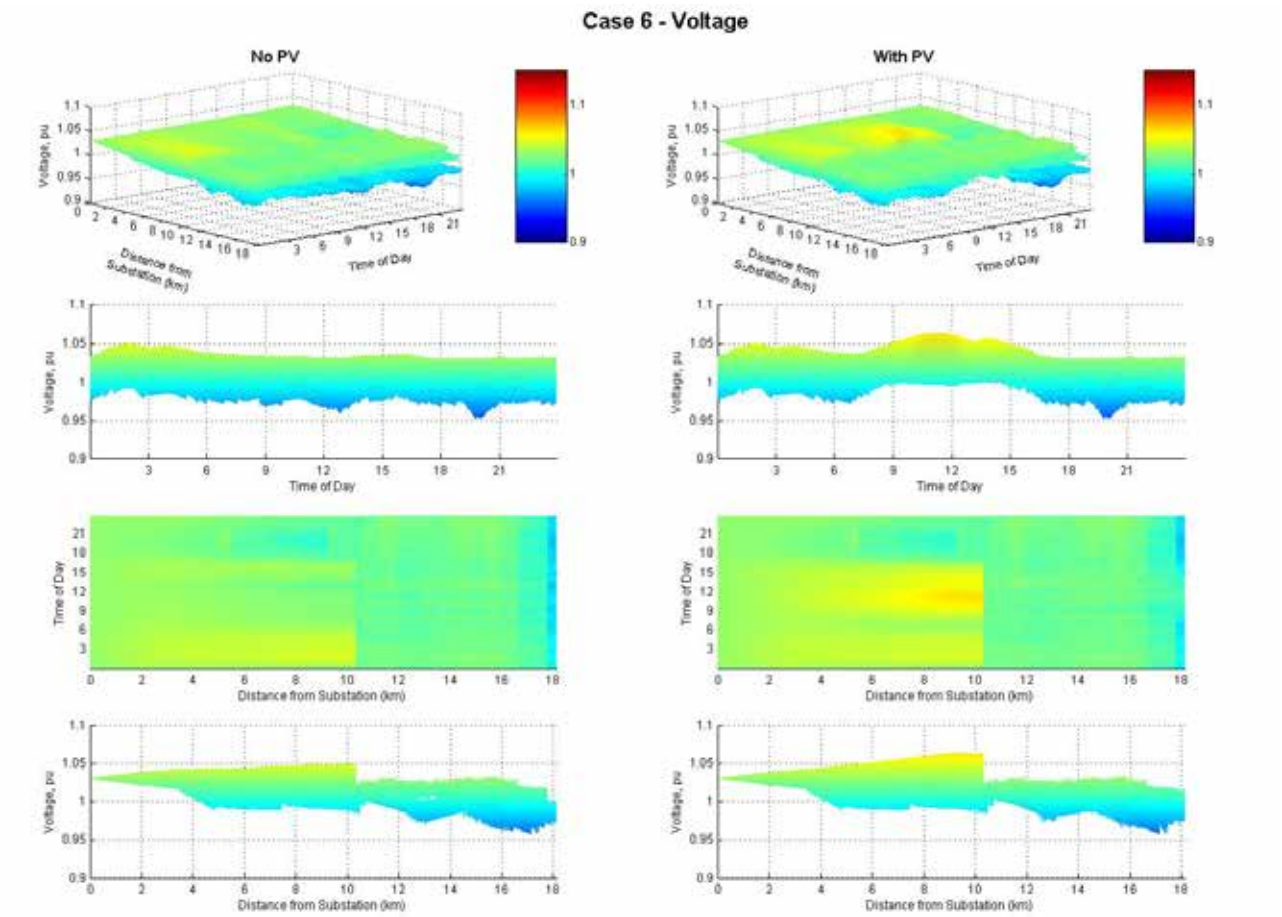

Figure A-43: Daily voltage profile for scenario 1 case 6.

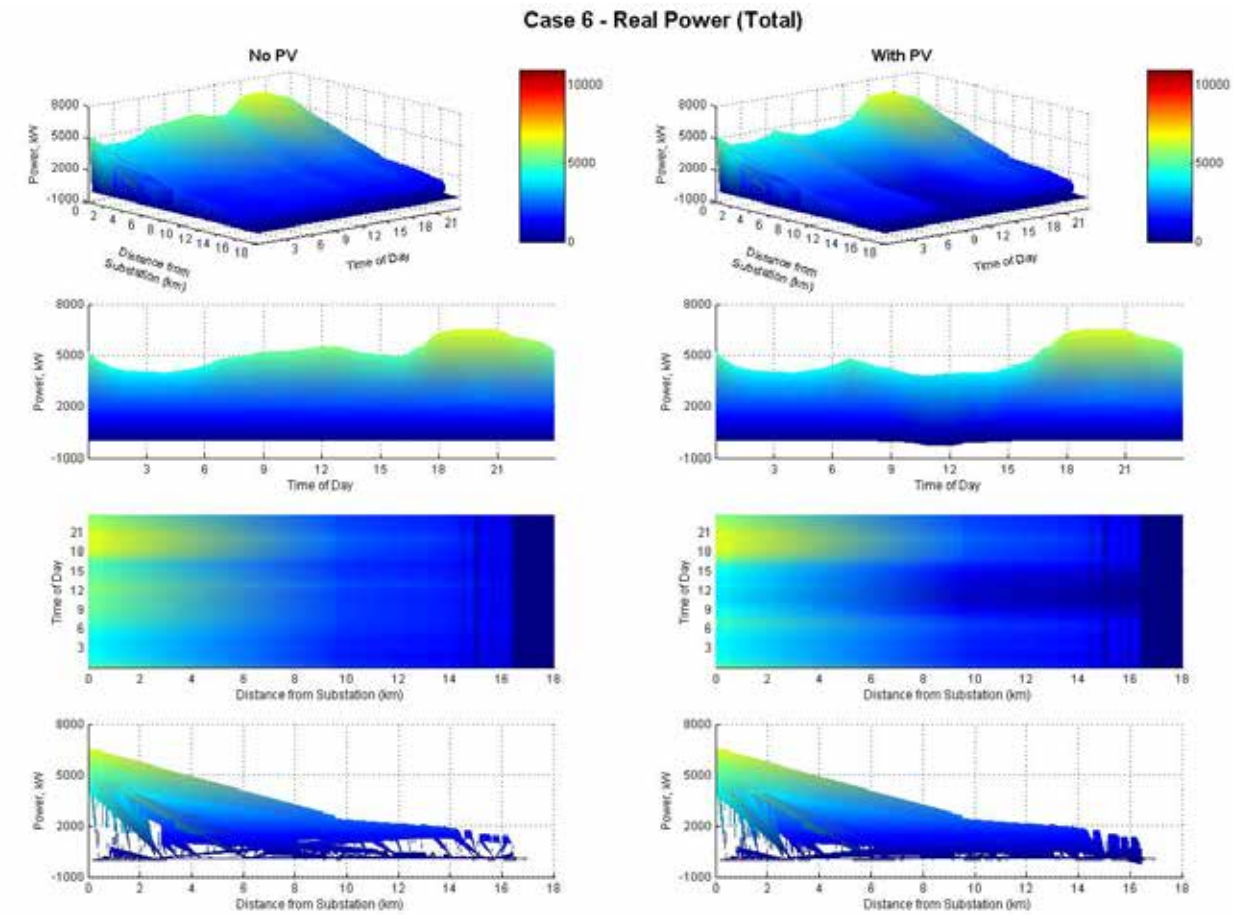

Figure A-44: Daily total real power profile for scenario 1 and case 6.

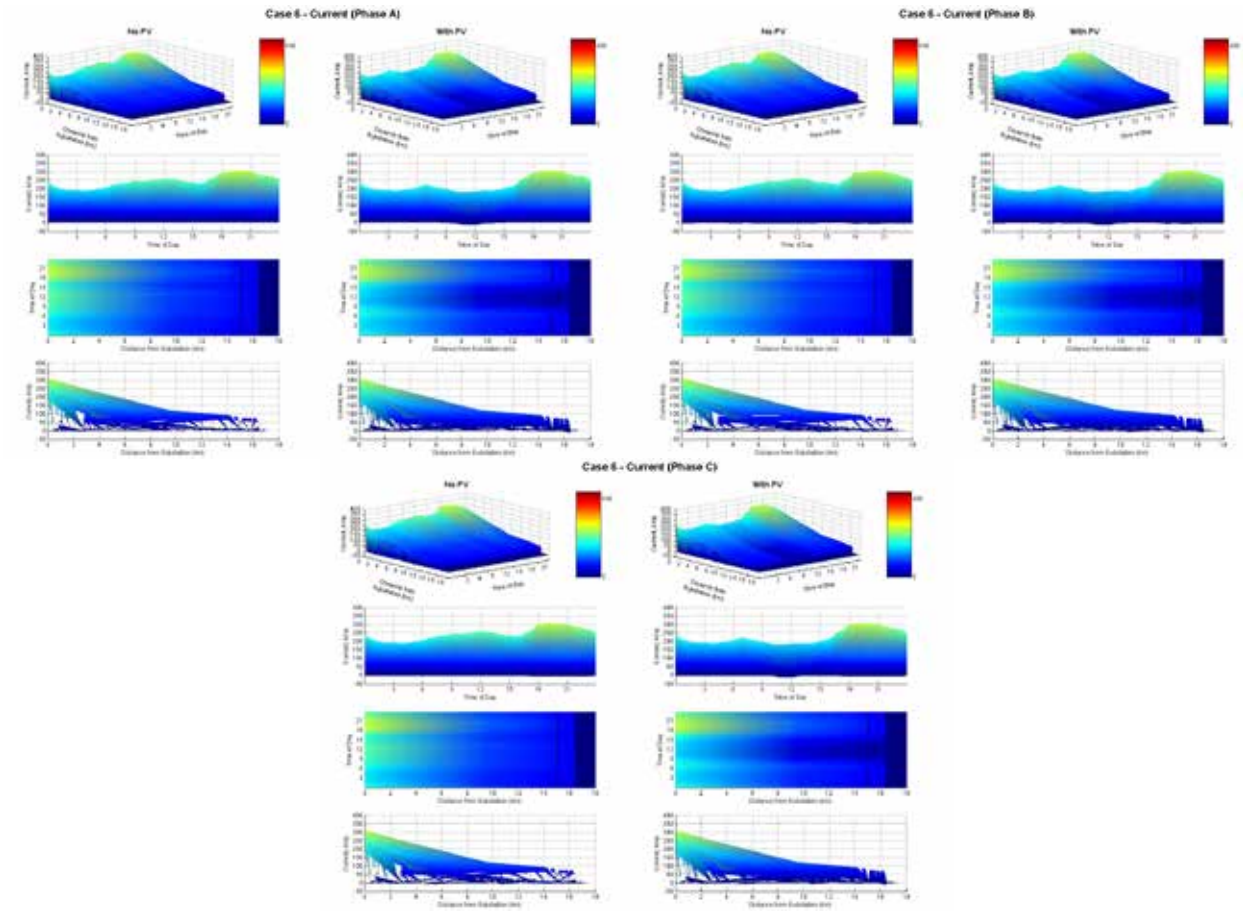

Figure A-45: Daily current profiles for scenario 1 and case 6.

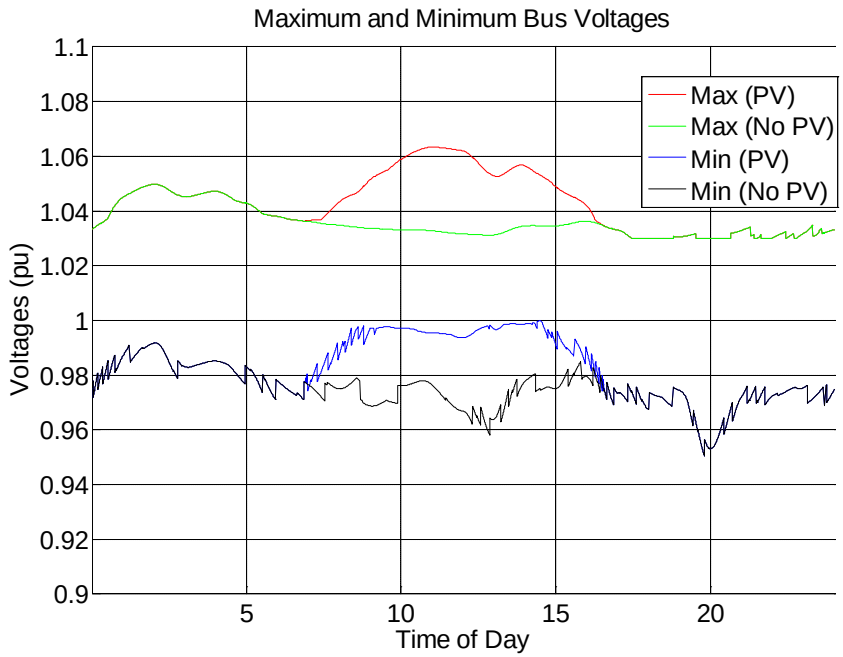

Figure A-46: Maximum and minimum voltages for scenario 1 and case 6.

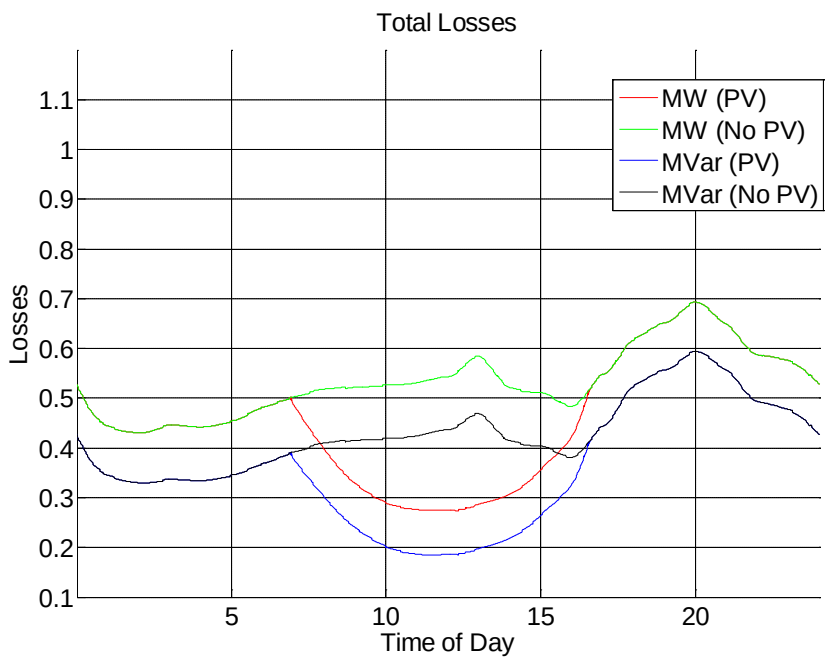

Figure A-47: MW and MVAr losses for scenario 1 and case 6.

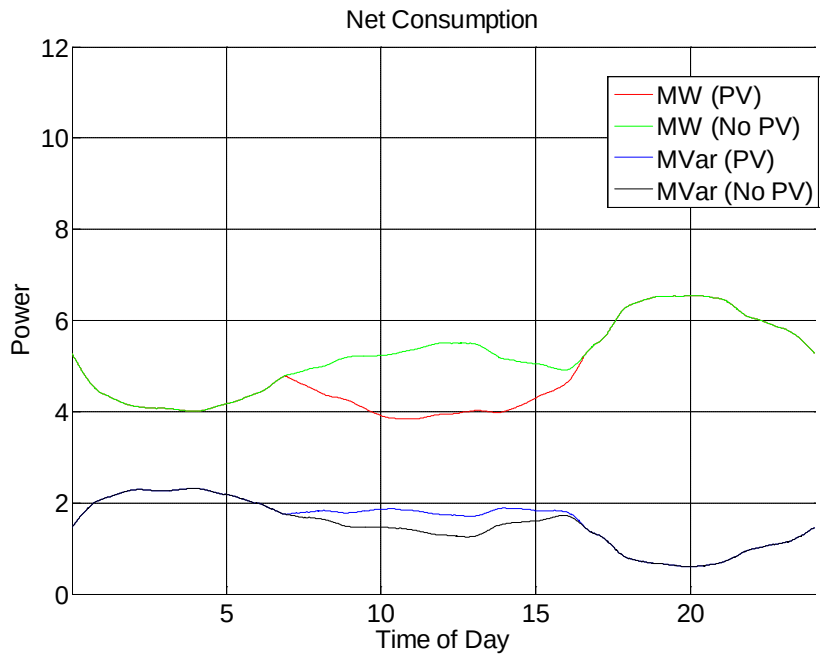

Figure A-48: MW and MVAr net consumption for scenario 1 and case 6.

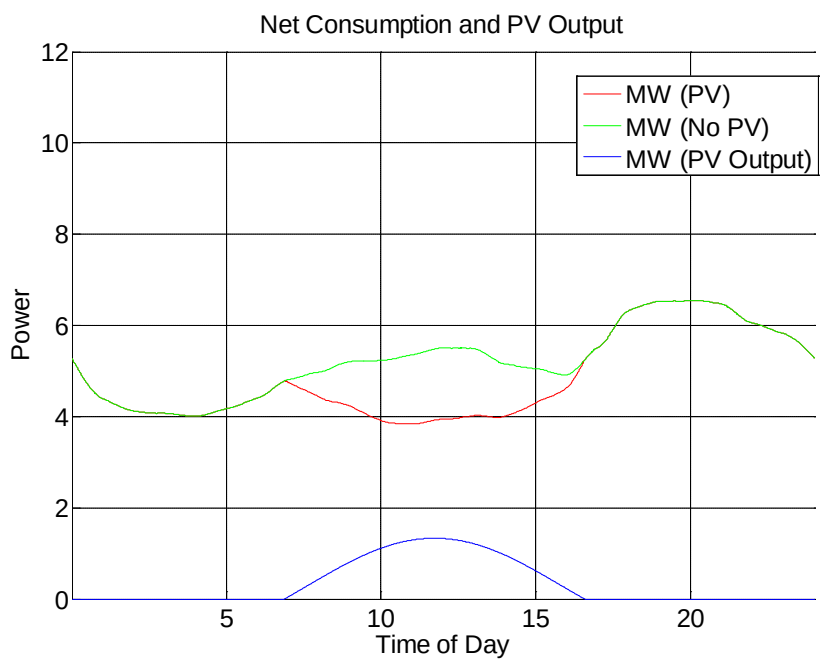

Figure A-49: MW net consumption and total PV generation for scenario 1 and case 6.

Appendix B - Scenario 2

In this Section we present the simulation results obtained for scenario 2 (the PV rating for this scenario totals in 0.298 MW (about 2.47% of the total load MW rating)).

B.1 Case 0

Figure B-1 through Figure B-7 show simulation results for scenario 2 and case 0.

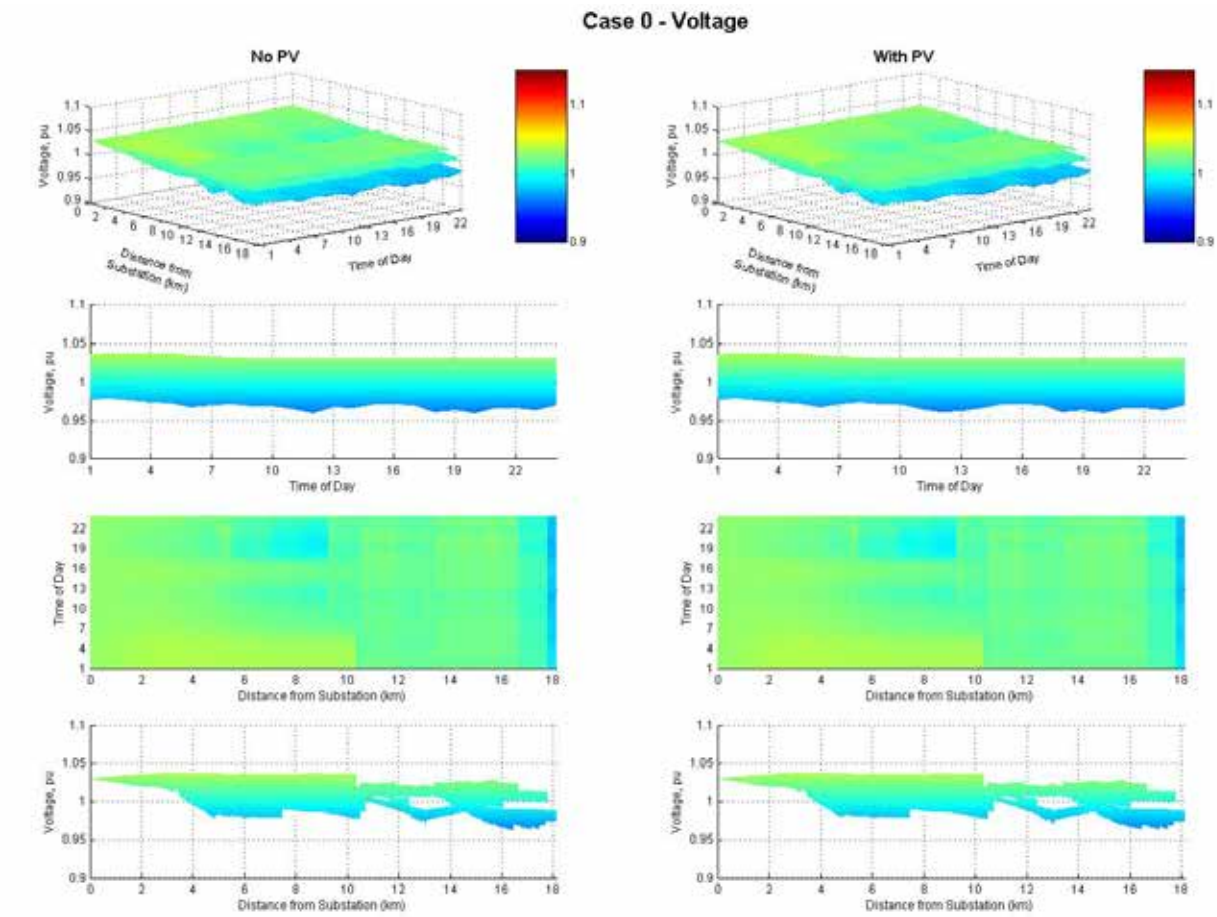

Figure B-1: Daily voltage profile for scenario 2 case 0.

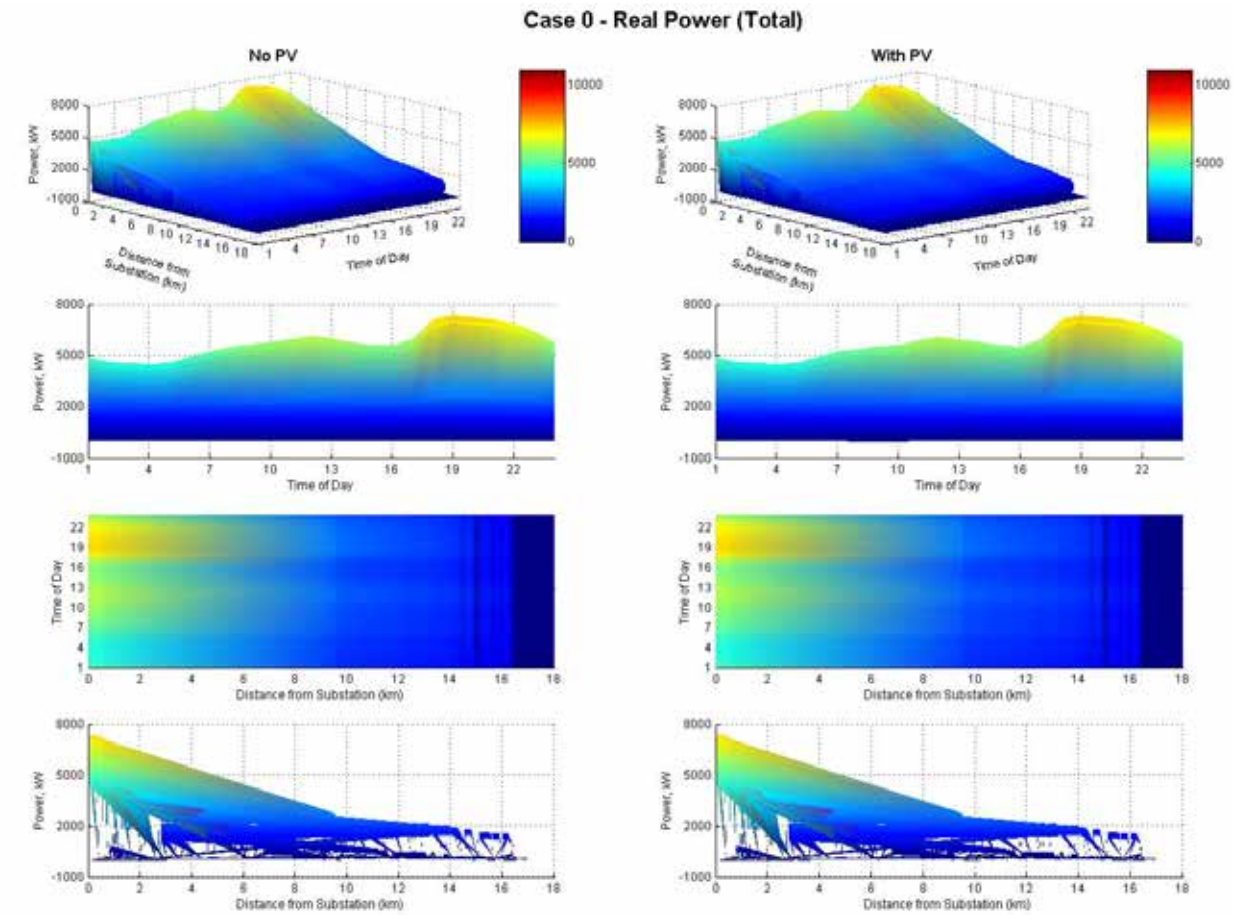

Figure B-2: Daily total real power profile for scenario 2 and case 0.

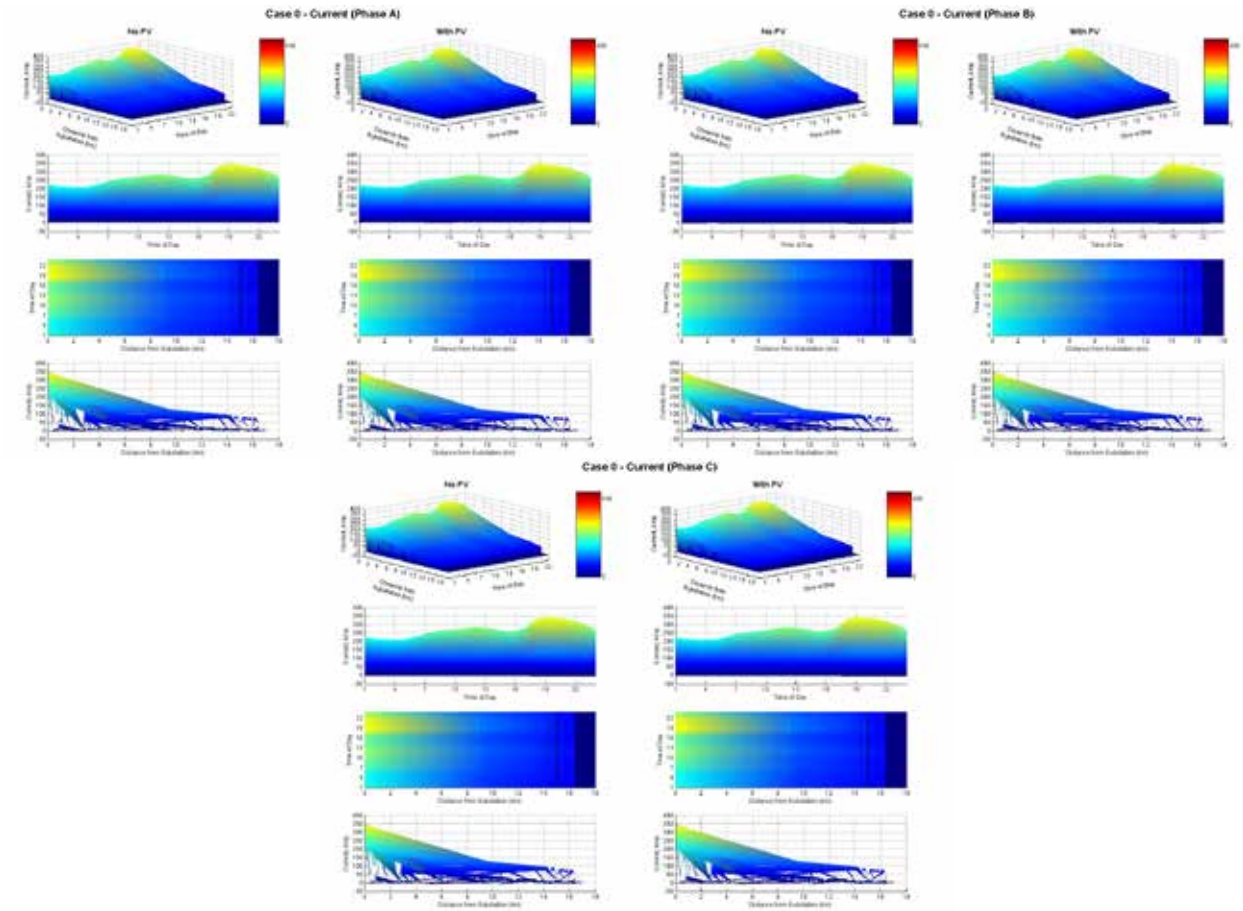

Figure B-3: Daily current profiles for scenario 2 and case 0.

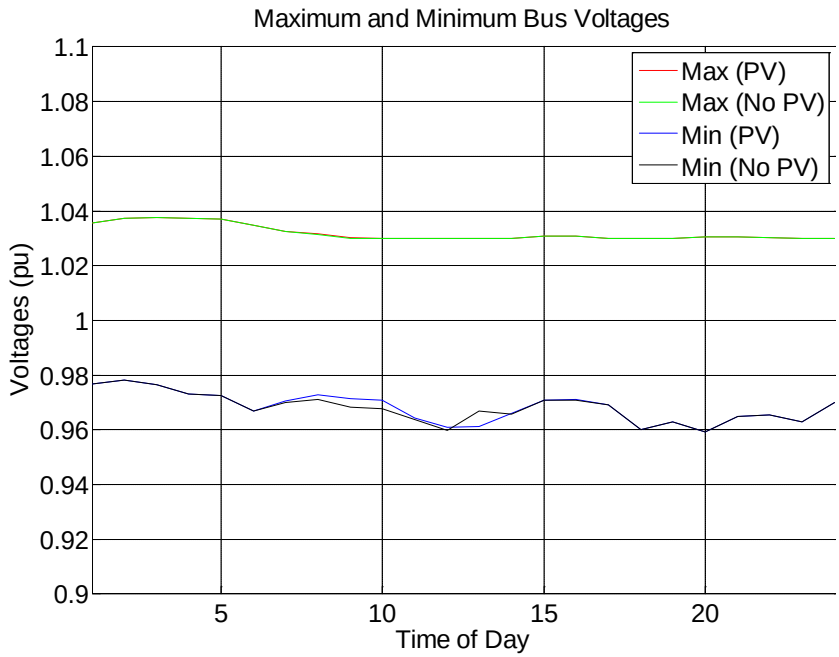

Figure B-4: Maximum and minimum voltages for scenario 2 and case 0.

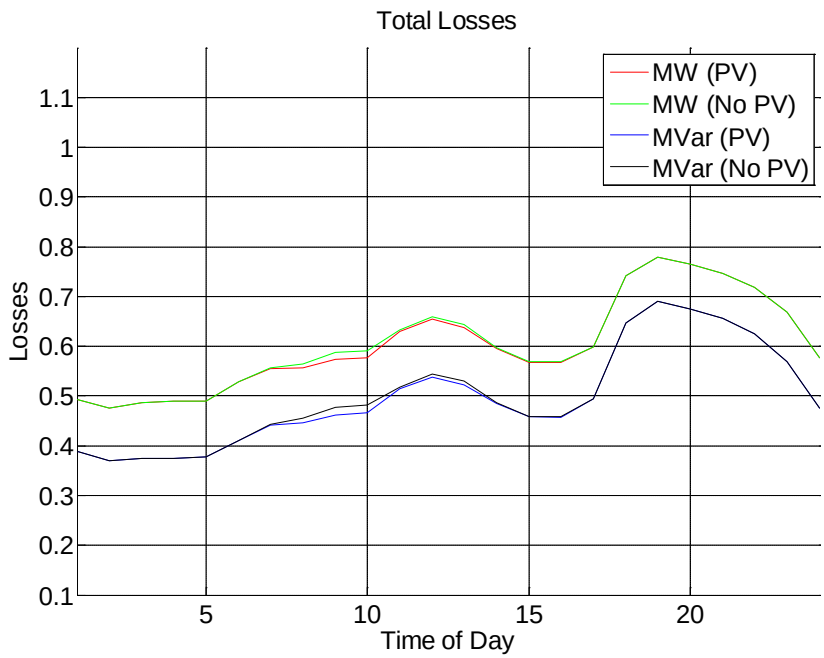

Figure B-5: MW and MVAr losses for scenario 2 and case 0.

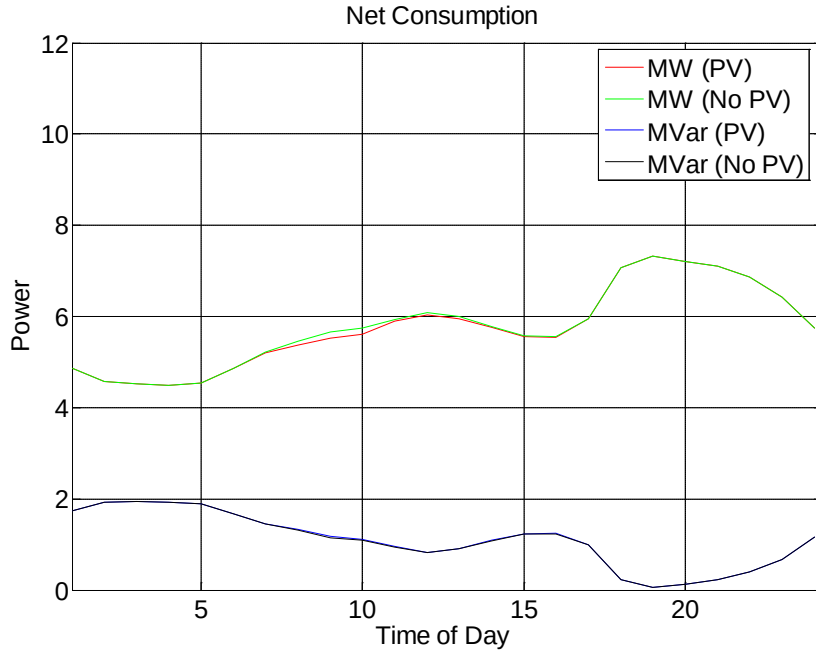

Figure B-6: MW and MVAr net consumption for scenario 2 and case 0.

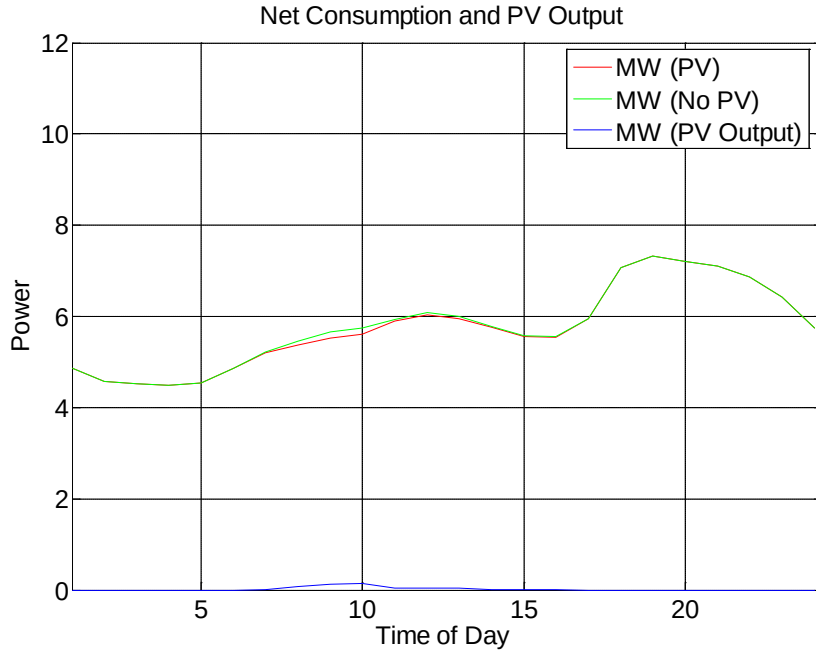

Figure B-7: MW net consumption and total PV generation for scenario 2 and case 0.

B.2 Case 1

Figure B-8 through Figure B-14 show simulation results for scenario 2 and case 1.

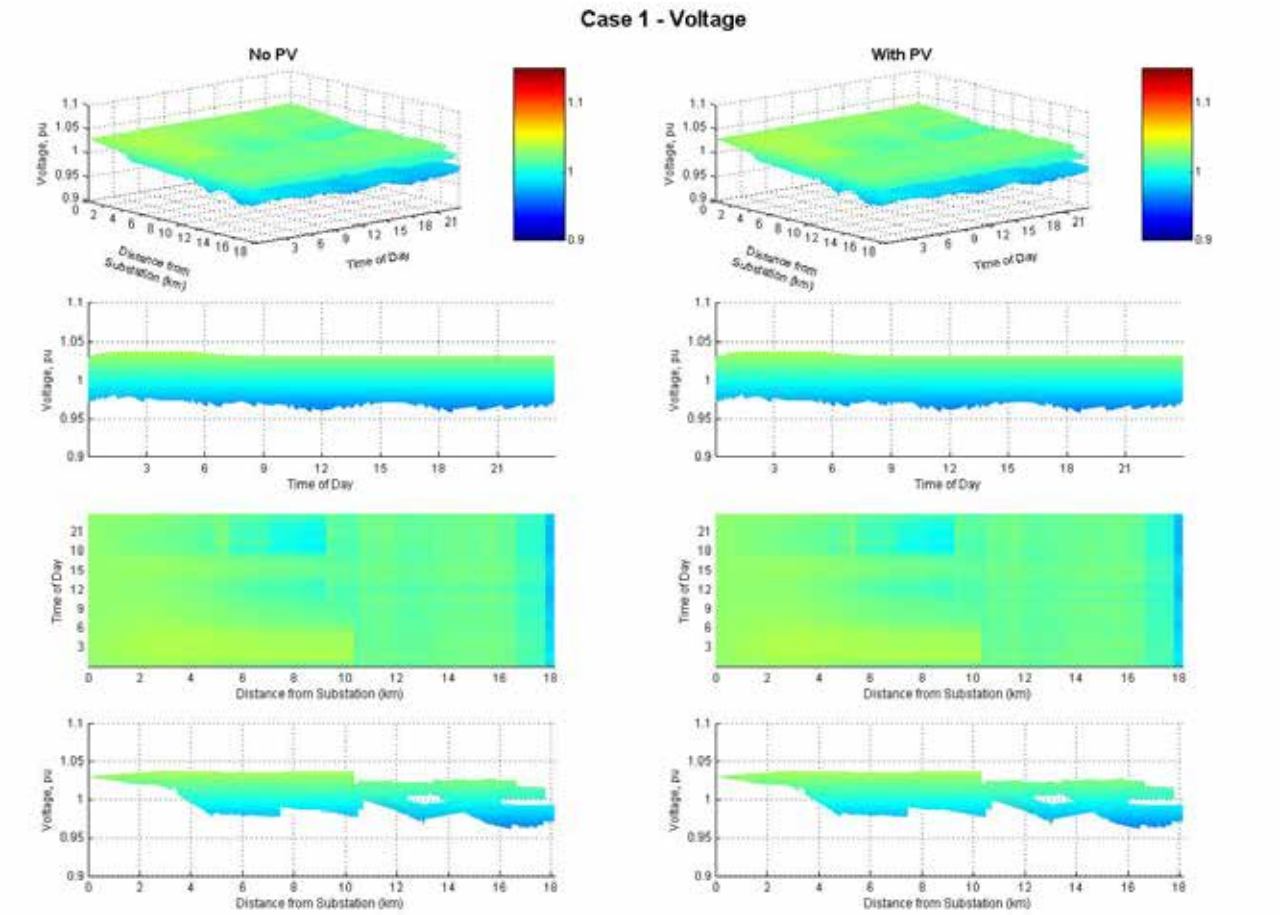

Figure B-8: Daily voltage profile for scenario 2 case 1.

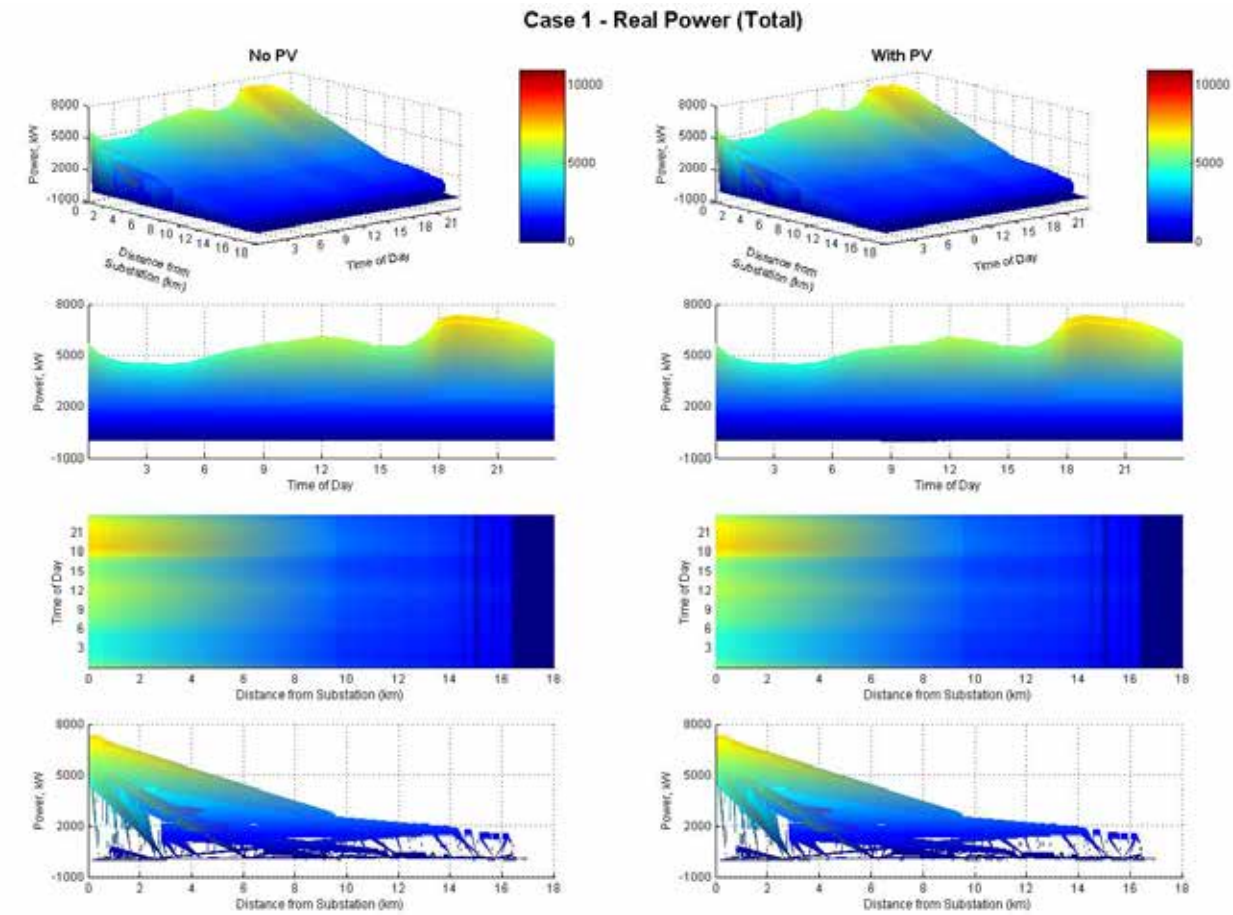

Figure B-9: Daily total real power profile for scenario 2 and case 1.

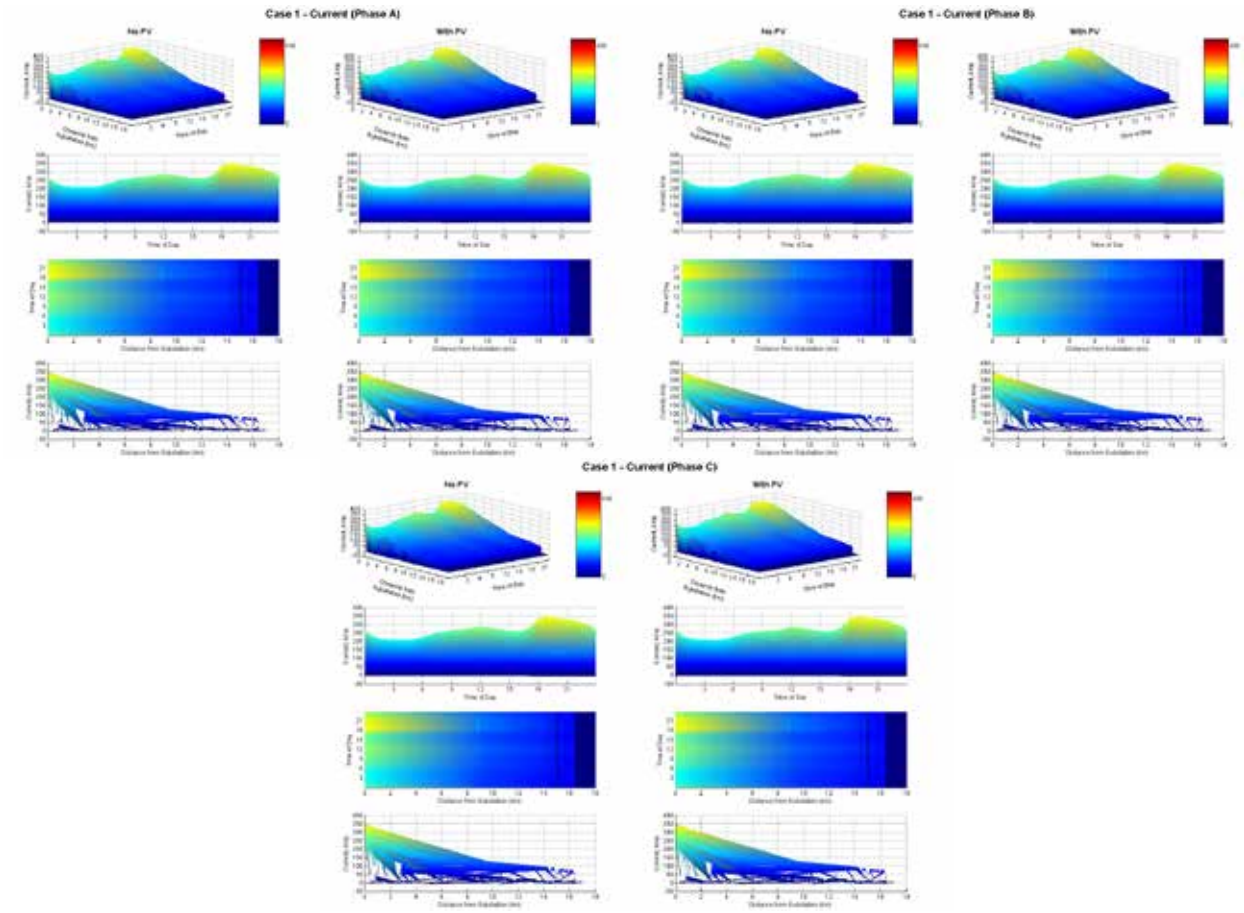

Figure B-10: Daily current profiles for scenario 2 and case 1.

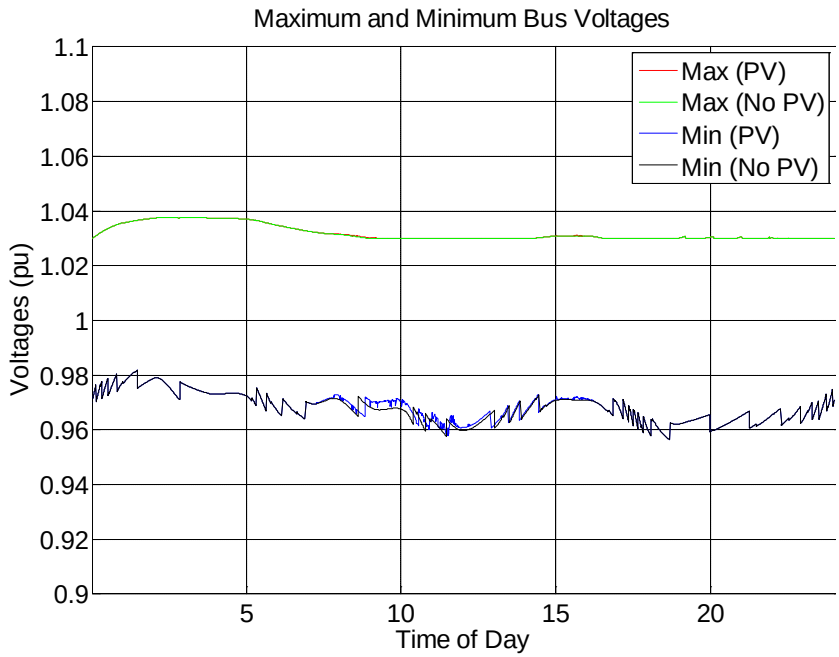

Figure B-11: Maximum and minimum voltages for scenario 2 and case 1.

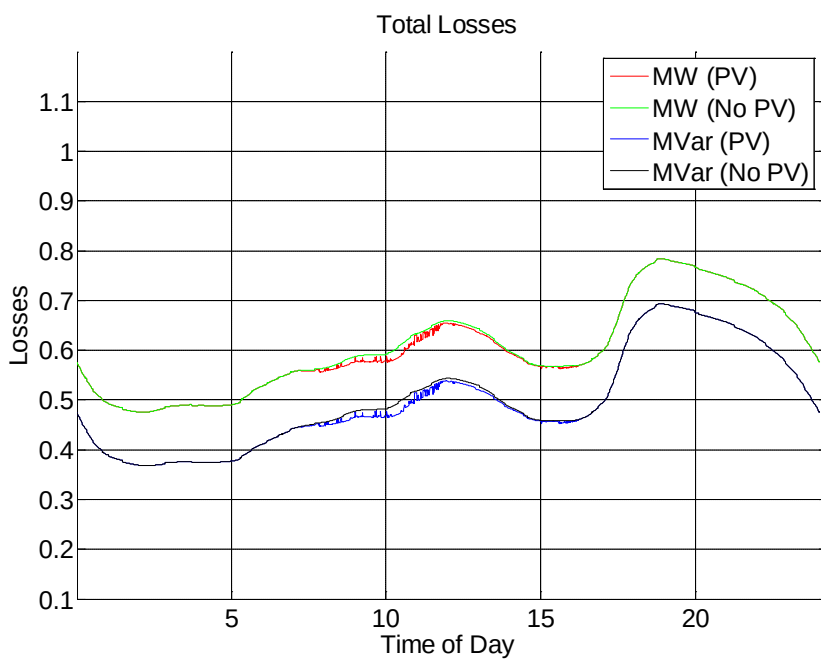

Figure B-12: MW and MVAr losses for scenario 2 and case 1.

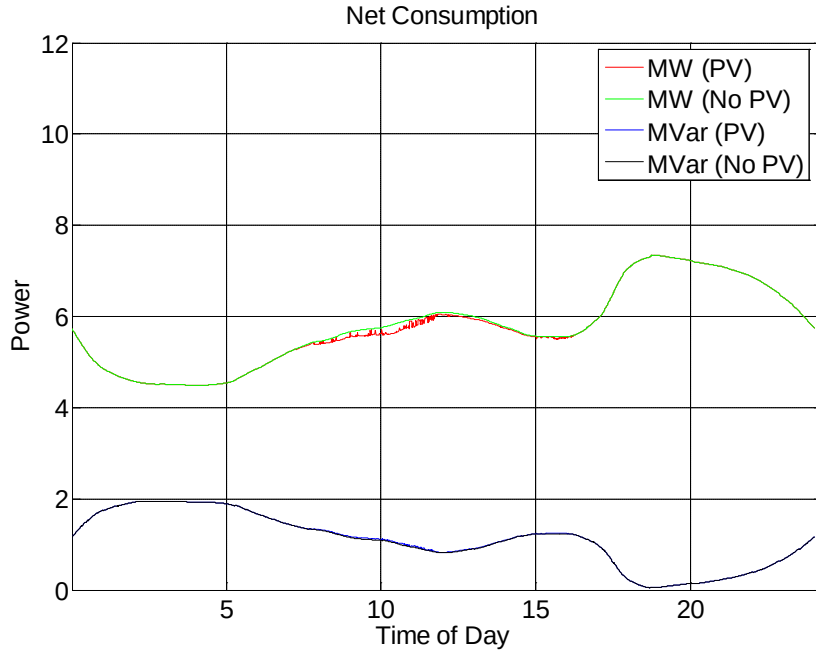

Figure B-13: MW and MVAr net consumption for scenario 2 and case 1.

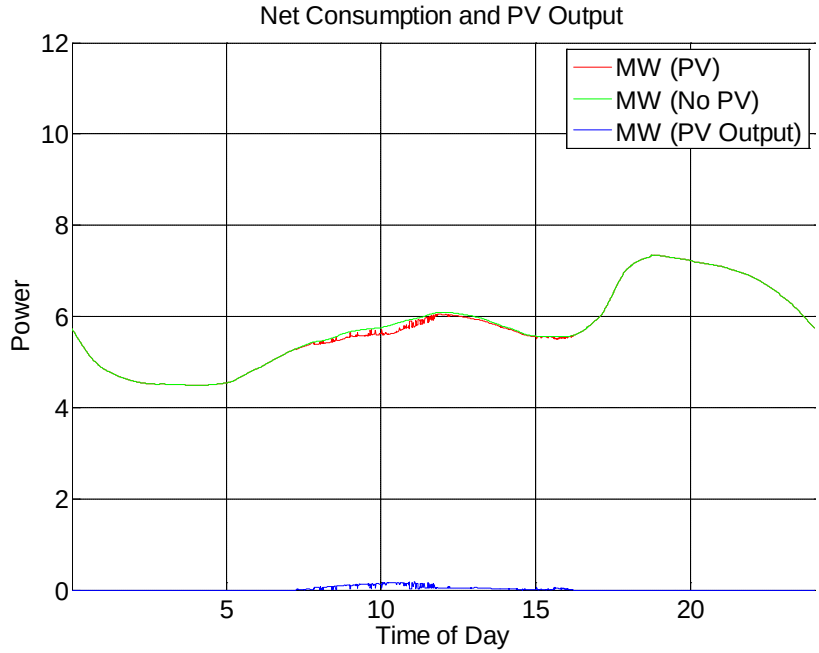

Figure B-14: MW net consumption and total PV generation for scenario 2 and case 1.

B.3 Case 2

Figure B-15 through Figure B-21 show simulation results for scenario 2 and case 2.

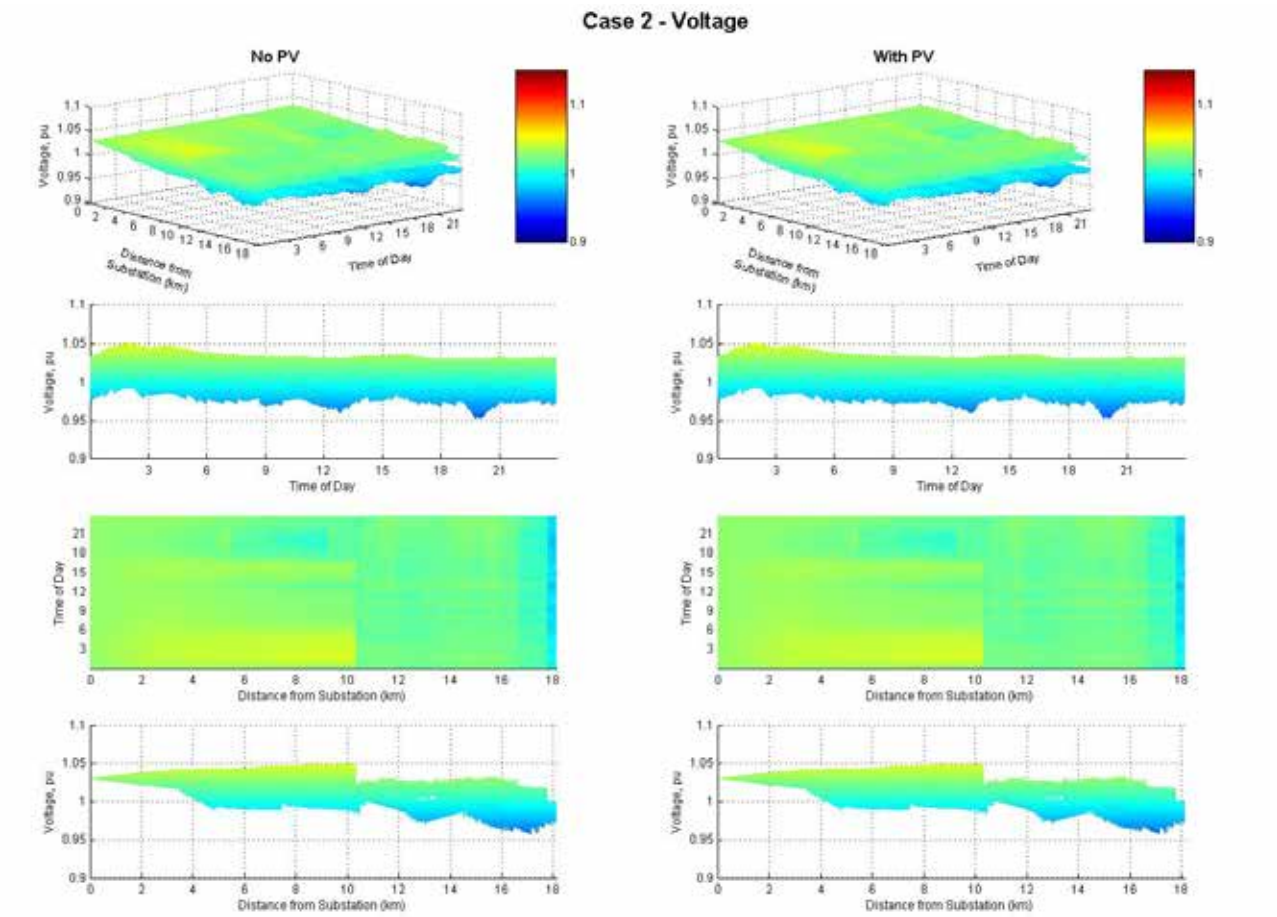

Figure B-15: Daily voltage profile for scenario 2 case 2.

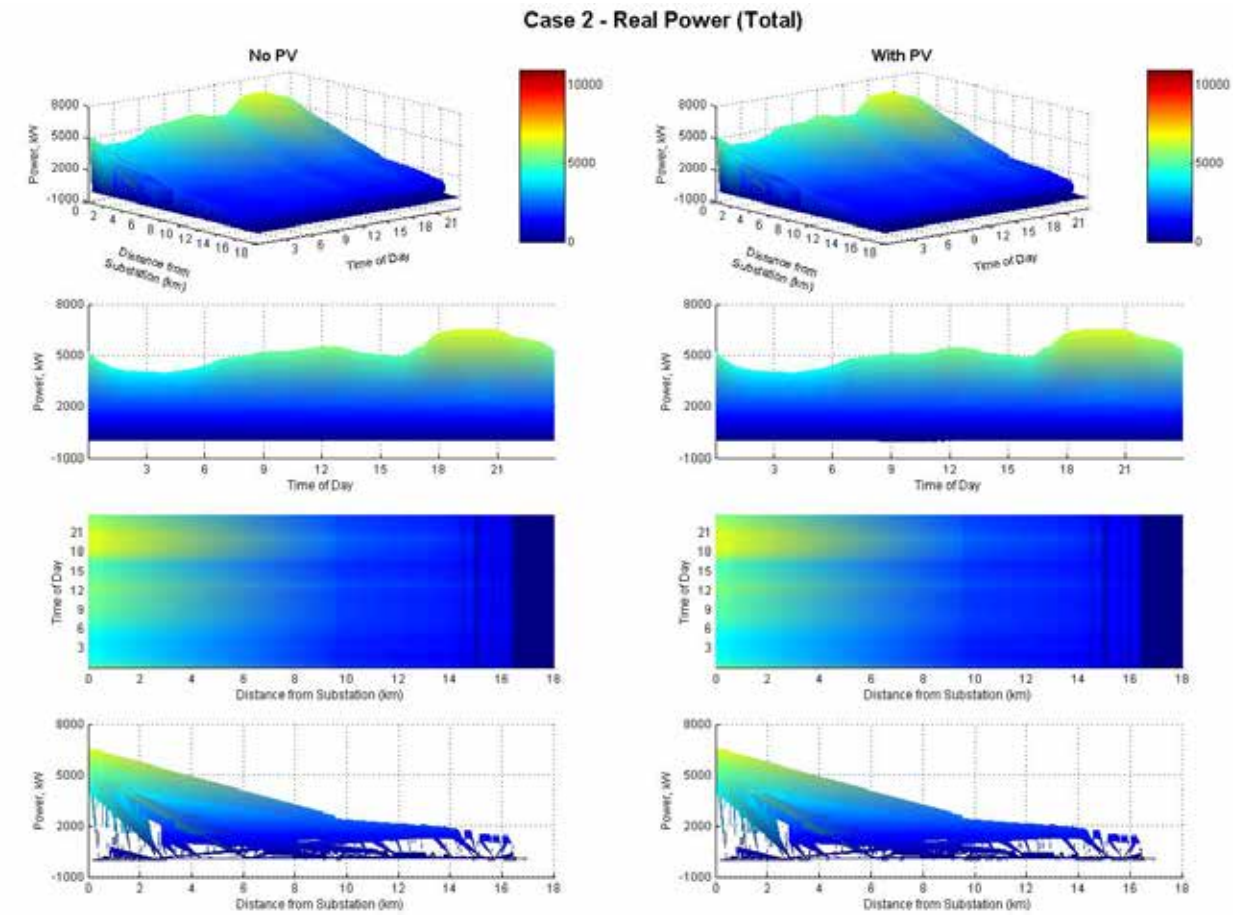

Figure B-16: Daily total real power profile for scenario 2 and case 2.

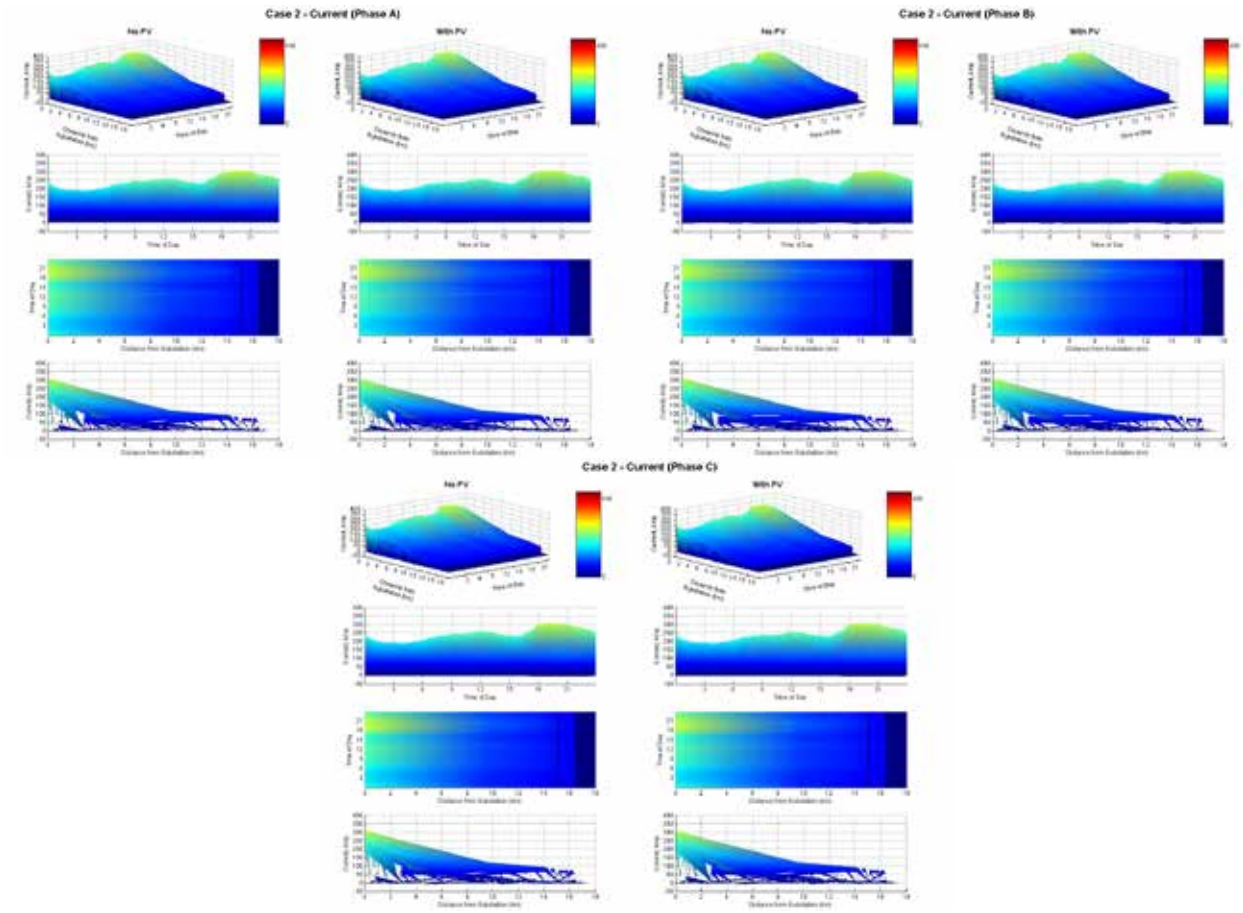

Figure B-17: Daily current profiles for scenario 2 and case 2.

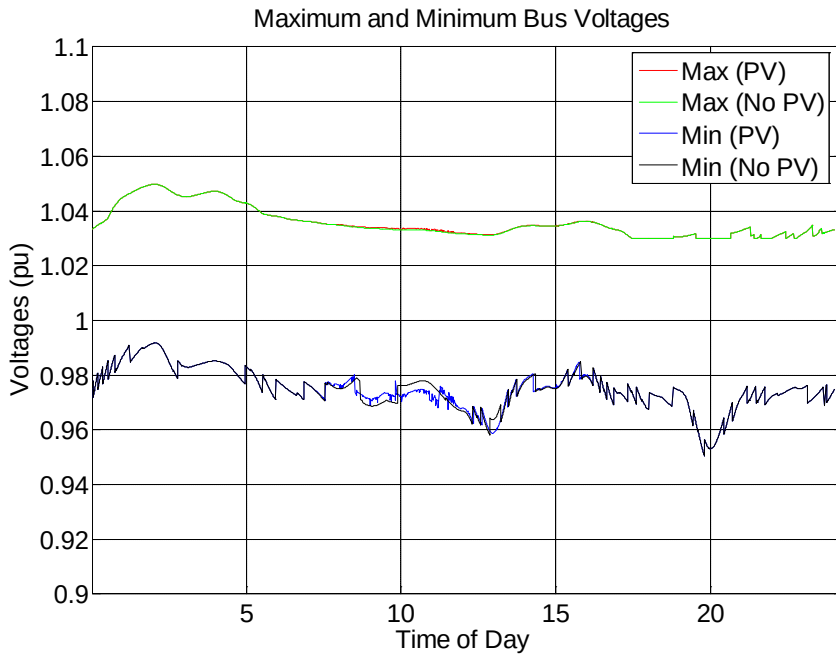

Figure B-18: Maximum and minimum voltages for scenario 2 and case 2.

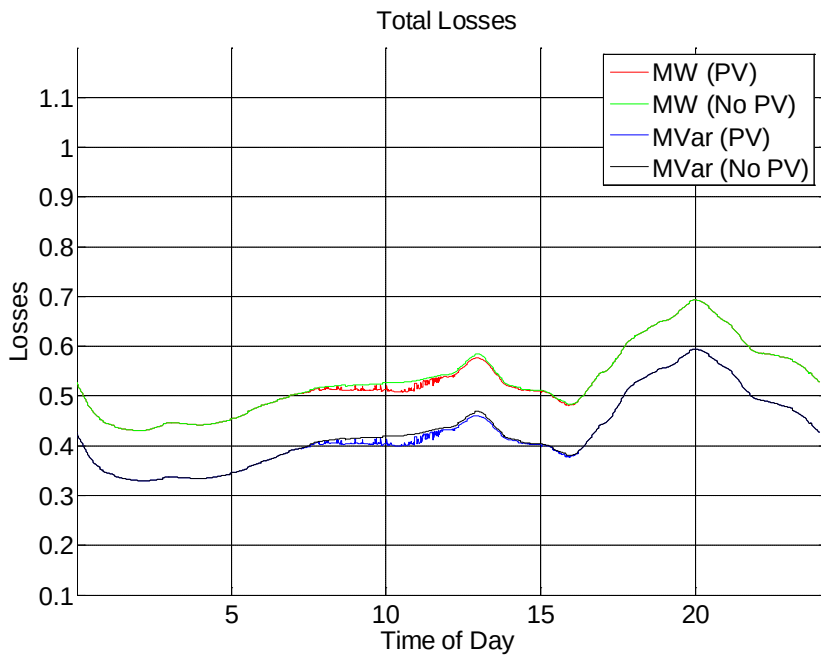

Figure B-19: MW and MVAr losses for scenario 2 and case 2.

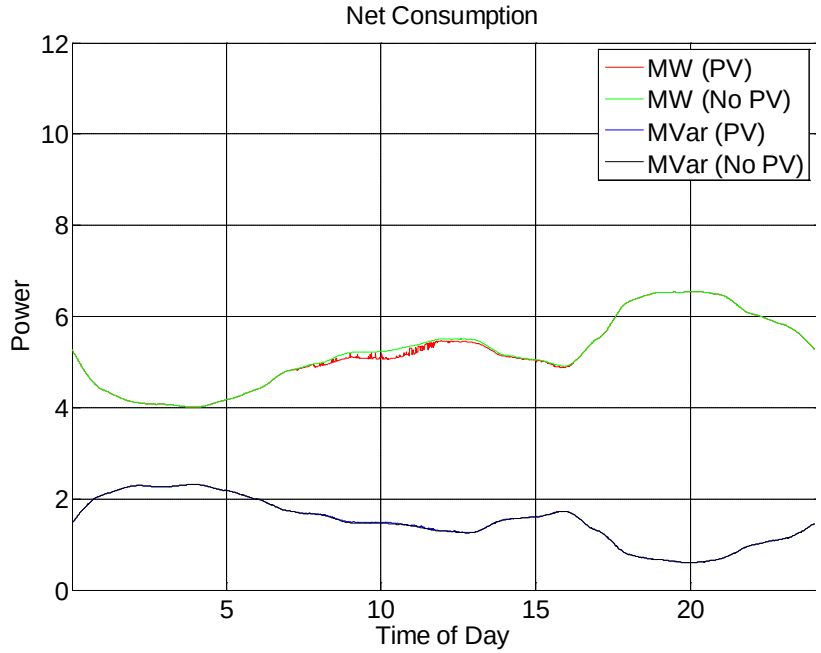

Figure B-20: MW and MVAr net consumption for scenario 2 and case 2.

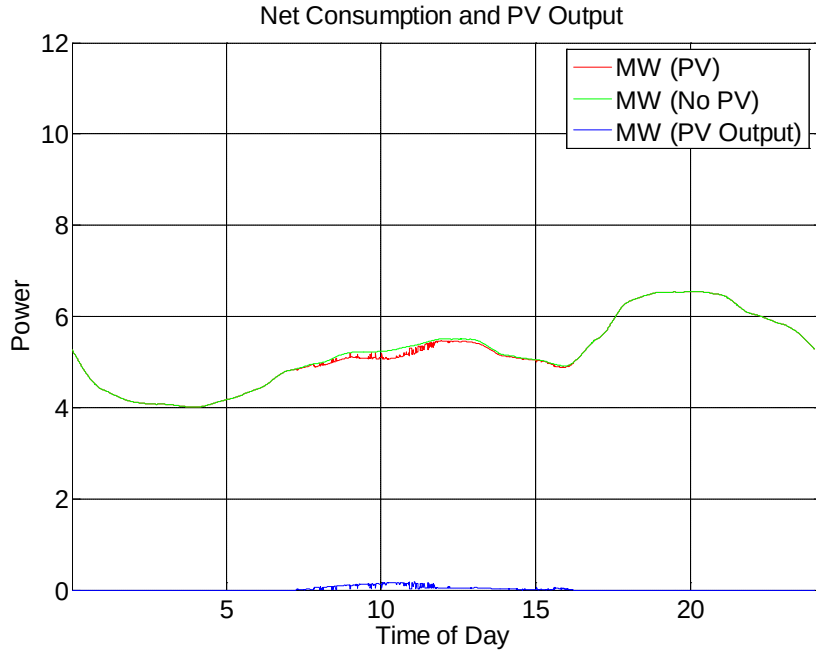

Figure B-21: MW net consumption and total PV generation for scenario 2 and case 2.

B.4 Case 3

Figure B-22through Figure B-28 show simulation results for scenario 2 and case 3.

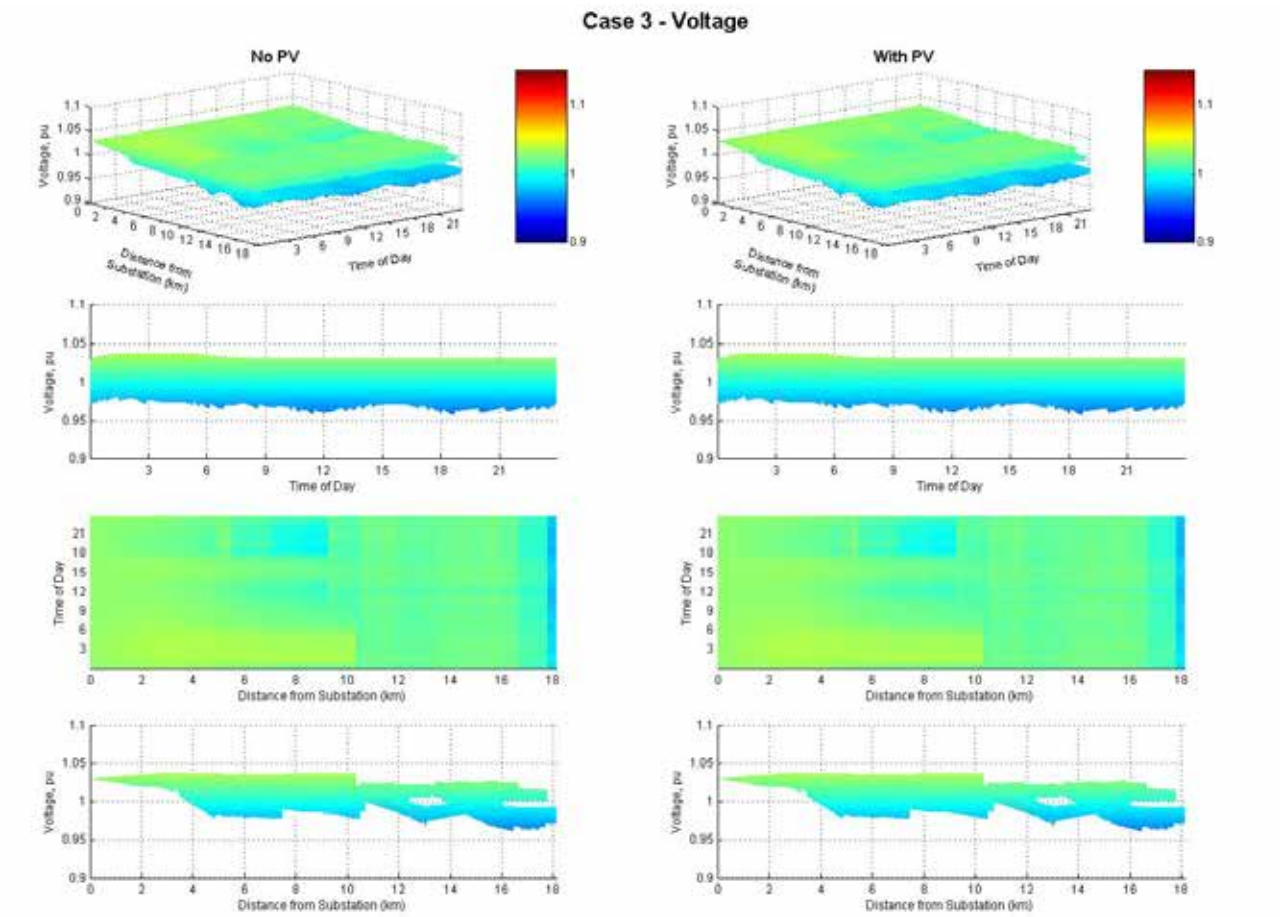

Figure B-22: Daily voltage profile for scenario 2 case 3.

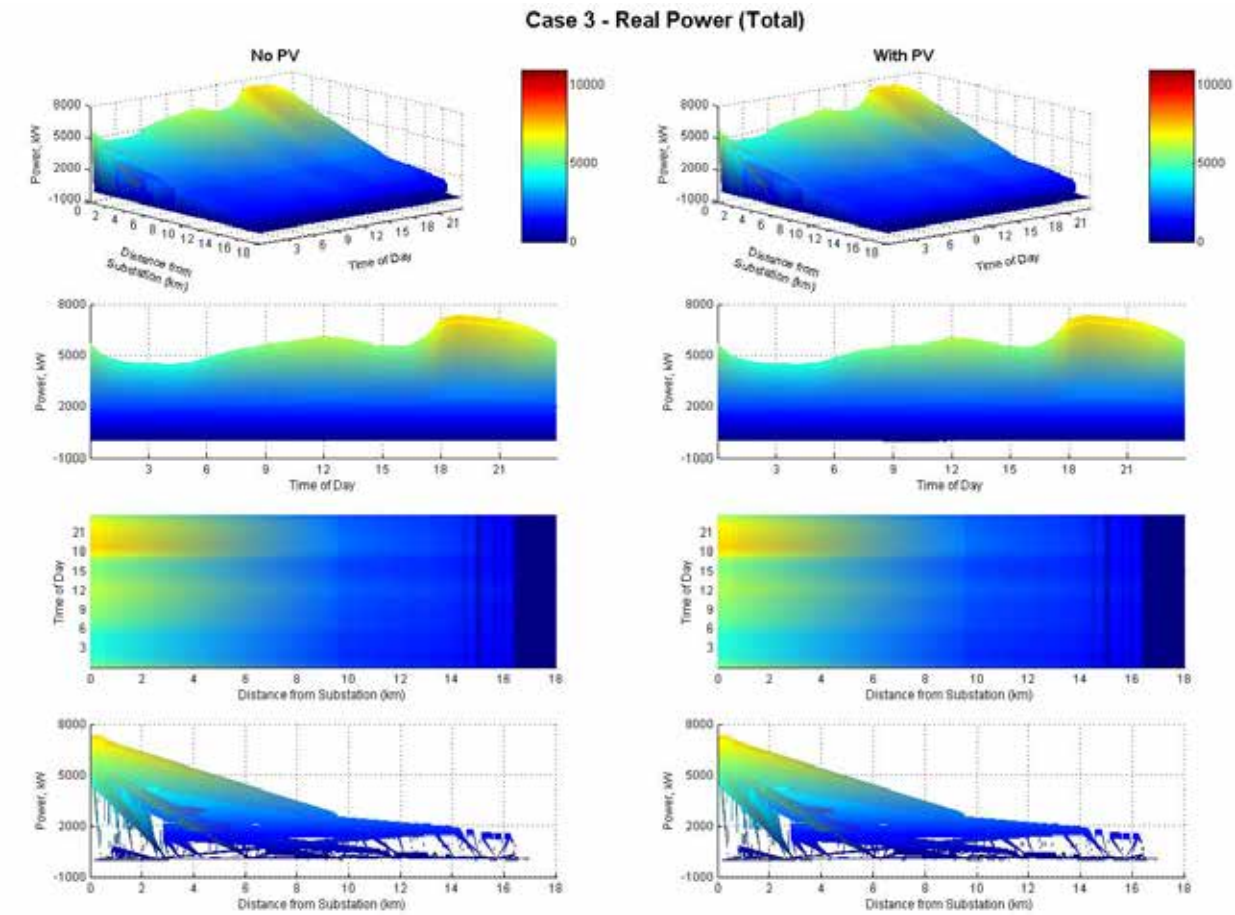

Figure B-23: Daily total real power profile for scenario 2 and case 3.

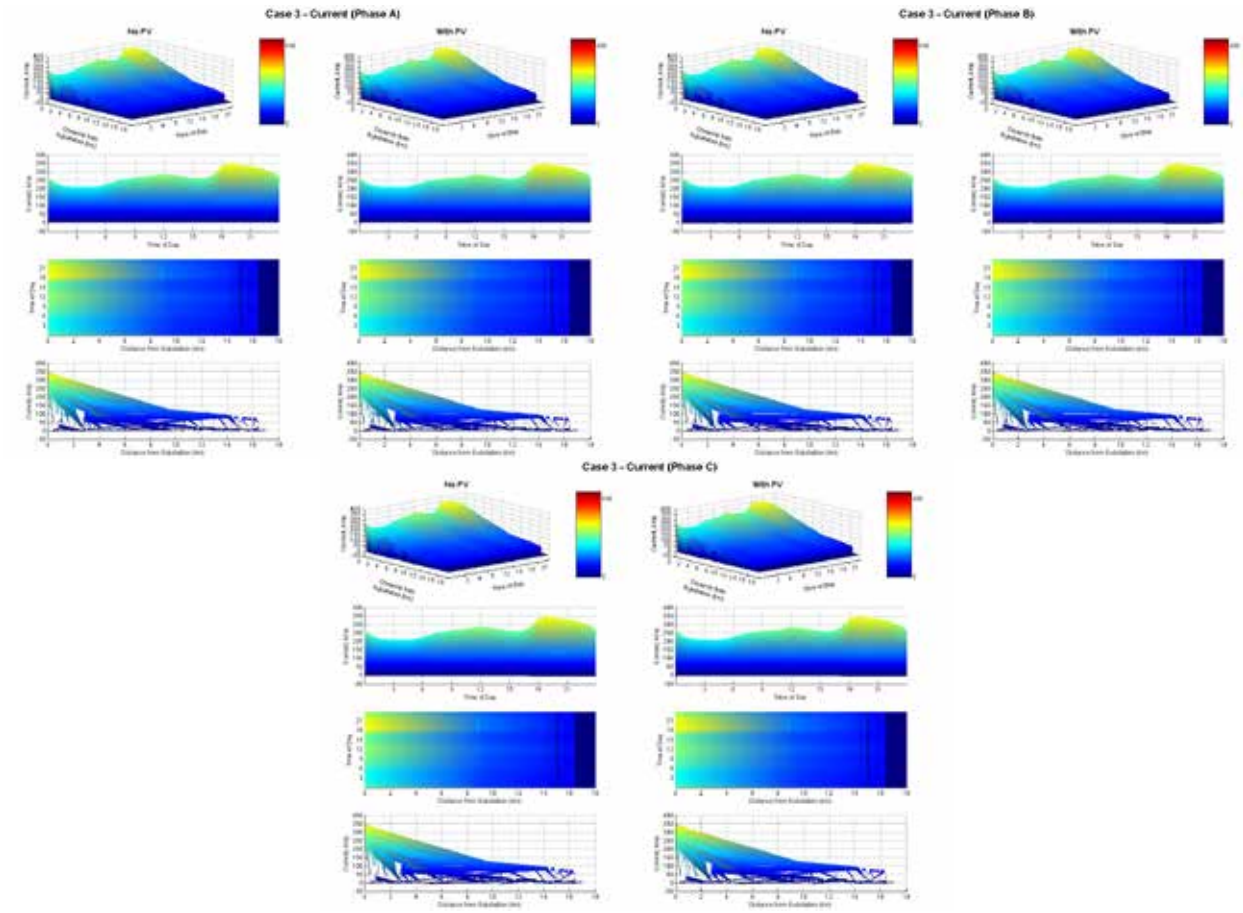

Figure B-24: Daily current profiles for scenario 2 and case 3.

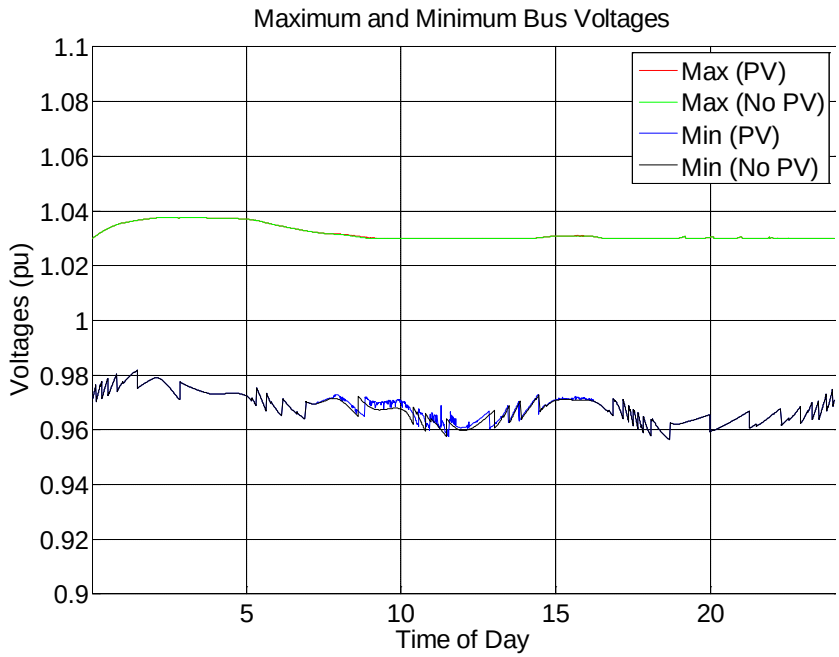

Figure B-25: Maximum and minimum voltages for scenario 2 and case 3.

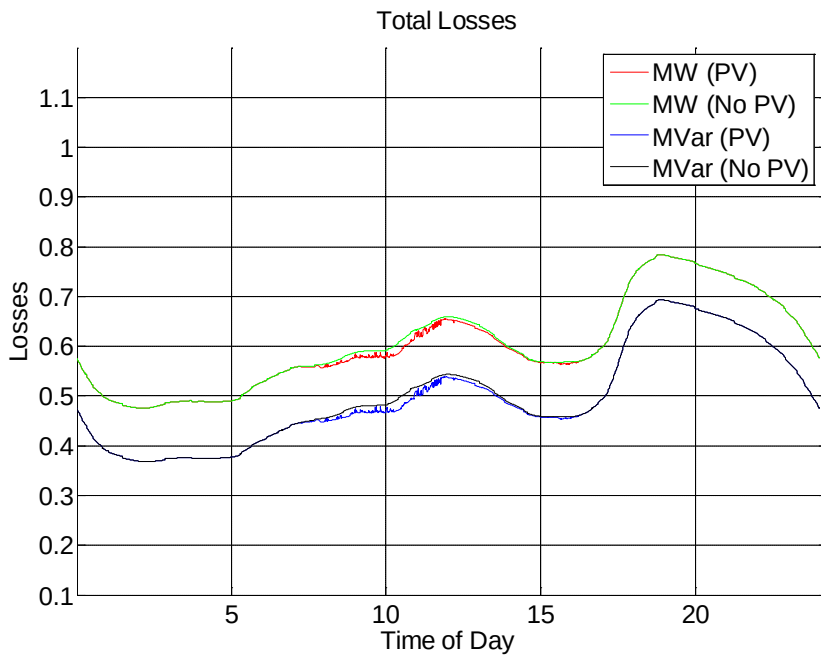

Figure B-26: MW and MVAr losses for scenario 2 and case 3.

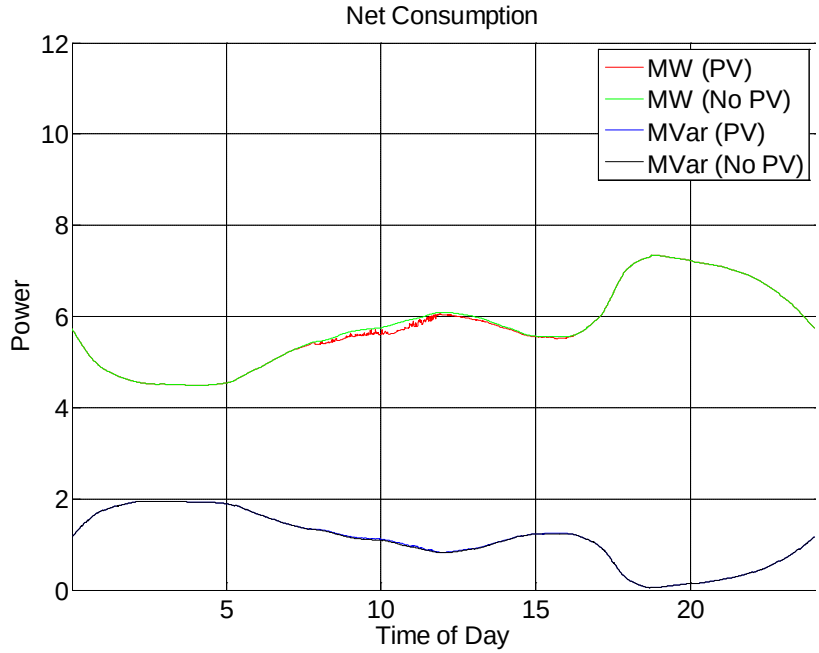

Figure B-27: MW and MVAr net consumption for scenario 2 and case 3.

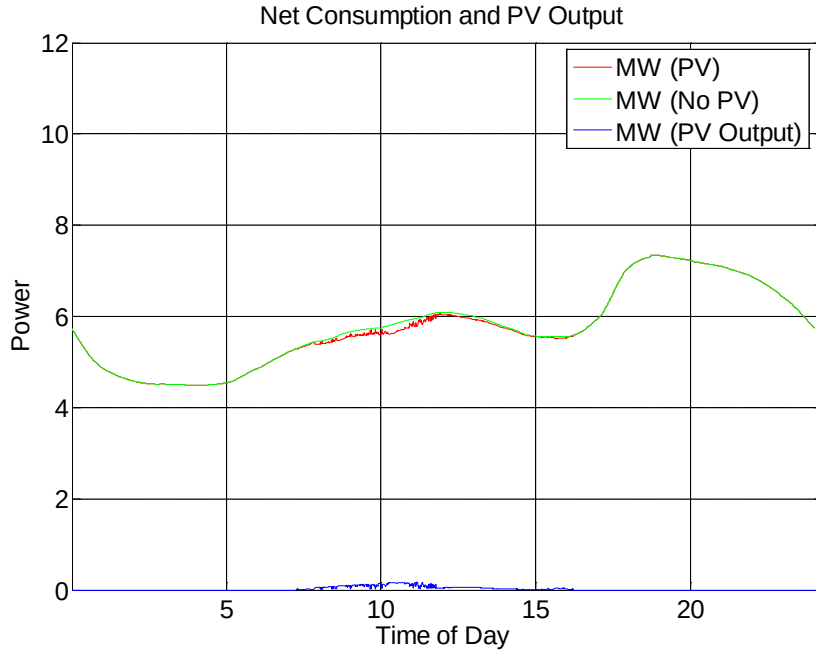

Figure B-28: MW net consumption and total PV generation for scenario 2 and case 3.

B.5 Case 4

Figure B-29 through Figure B-35 show simulation results for scenario 2 and case 4.

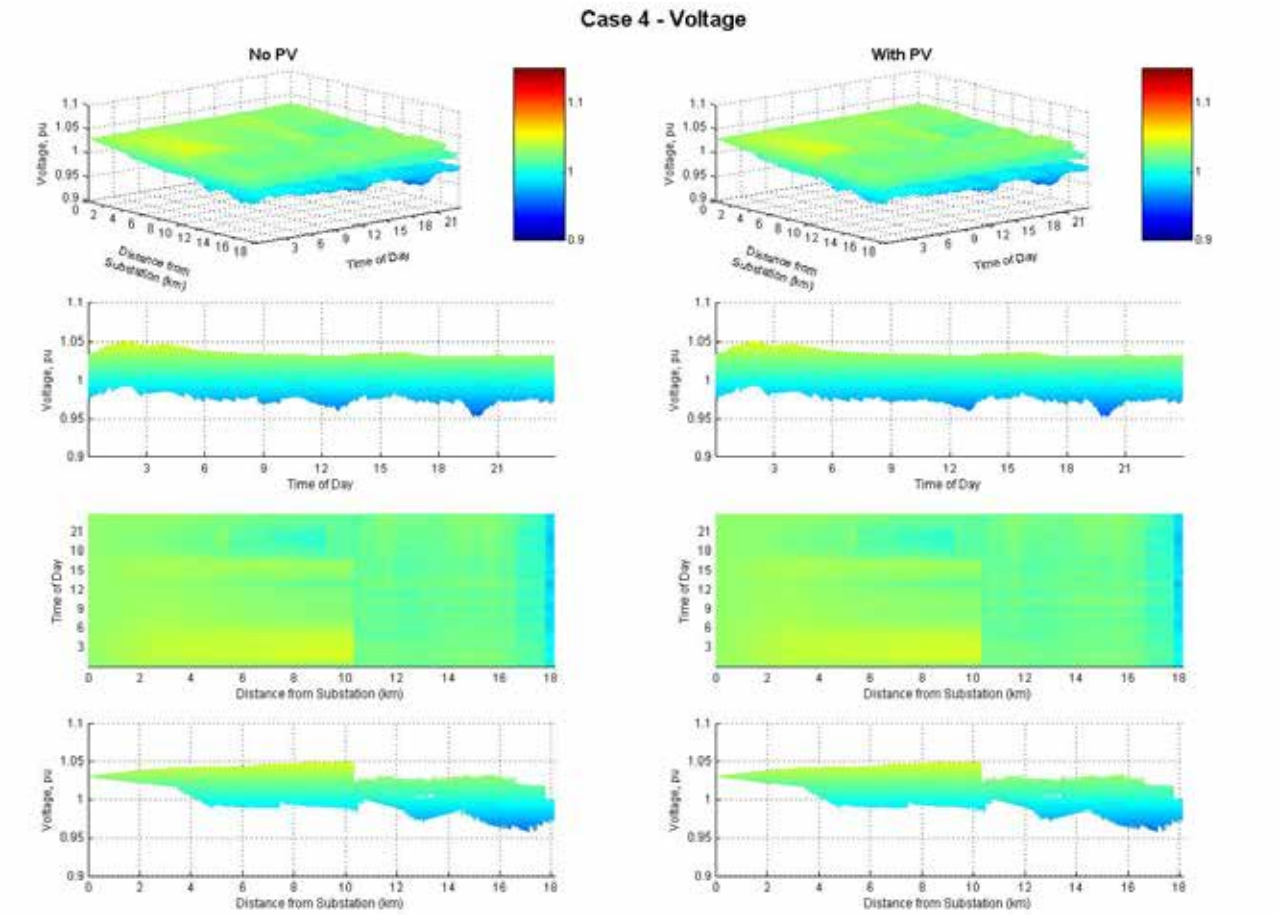

Figure B-29: Daily voltage profile for scenario 2 case 4.

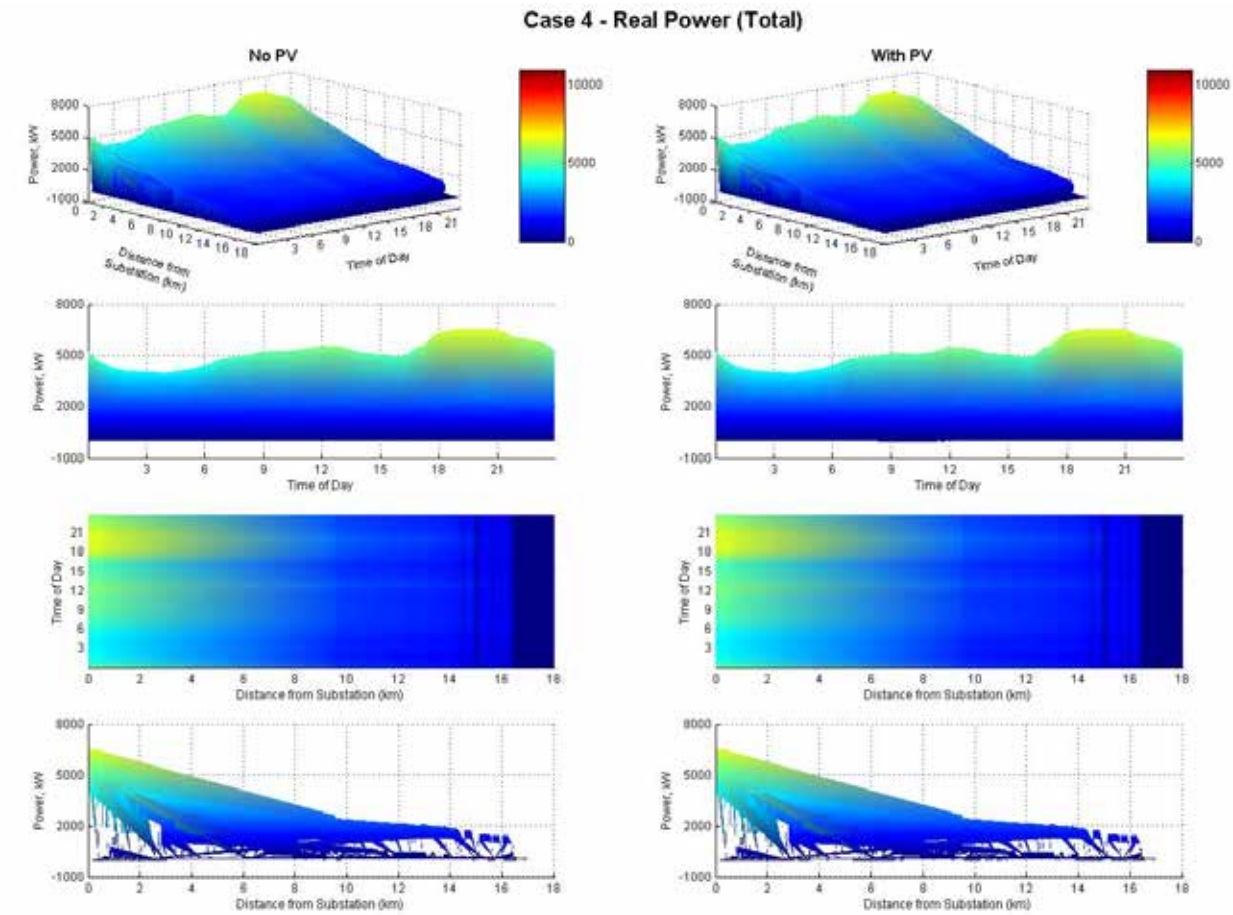

Figure B-30: Daily total real power profile for scenario 2 and case 4.

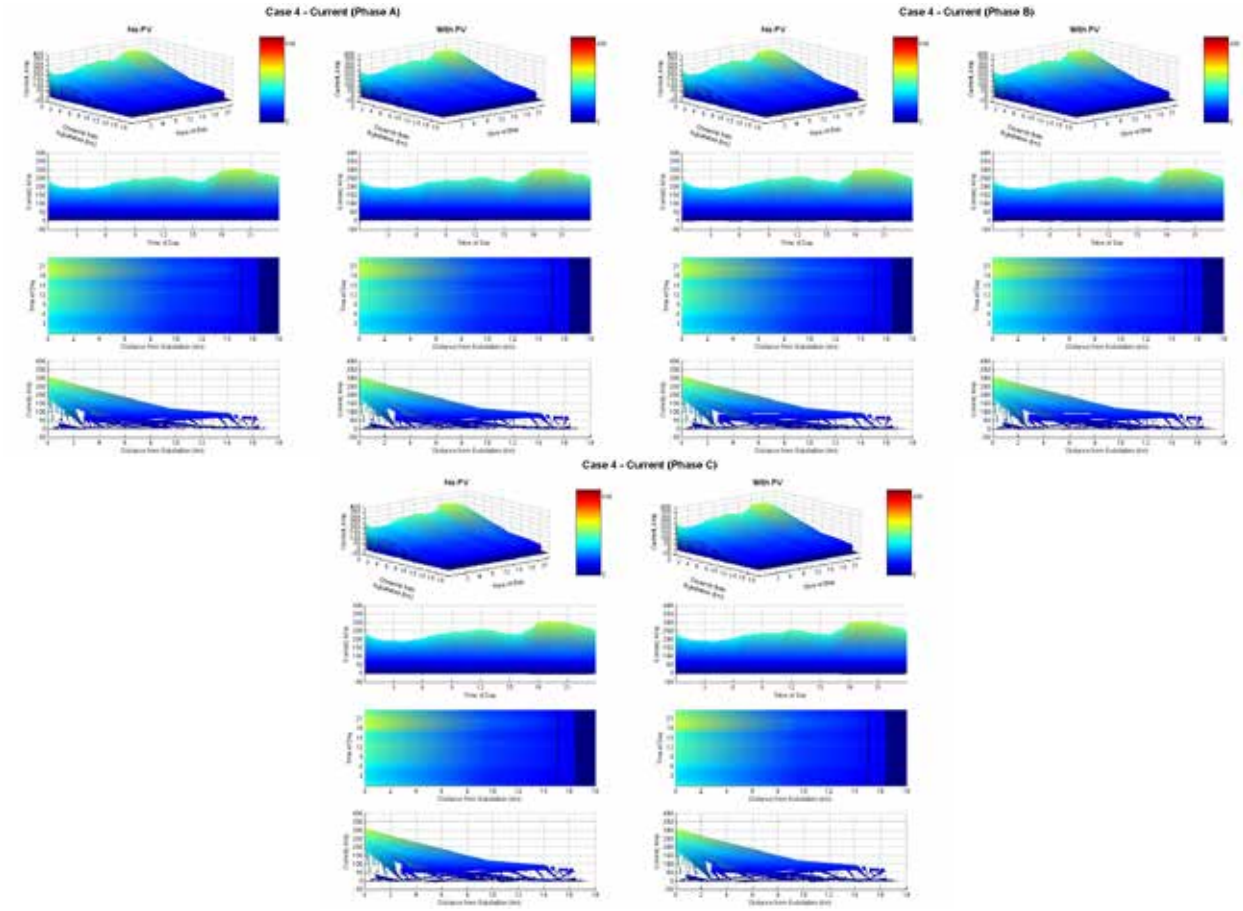

Figure B-31: Daily current profiles for scenario 2 and case 4.

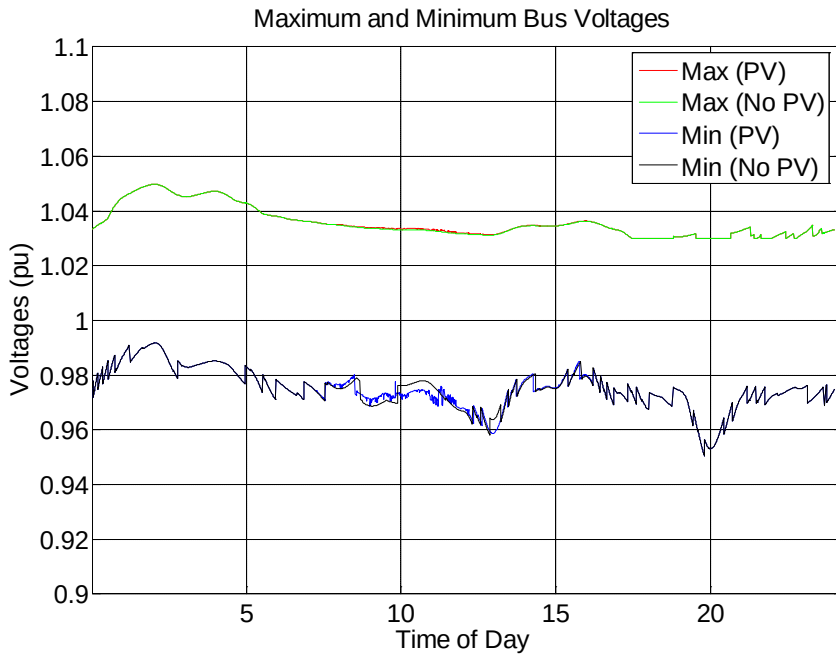

Figure B-32: Maximum and minimum voltages for scenario 2 and case 4.

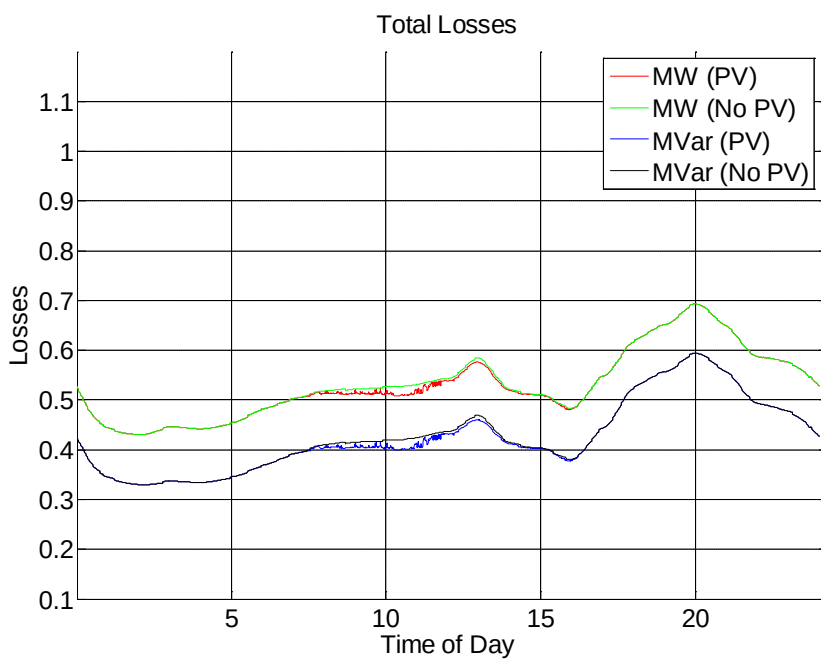

Figure B-33: MW and MVAr losses for scenario 2 and case 4.

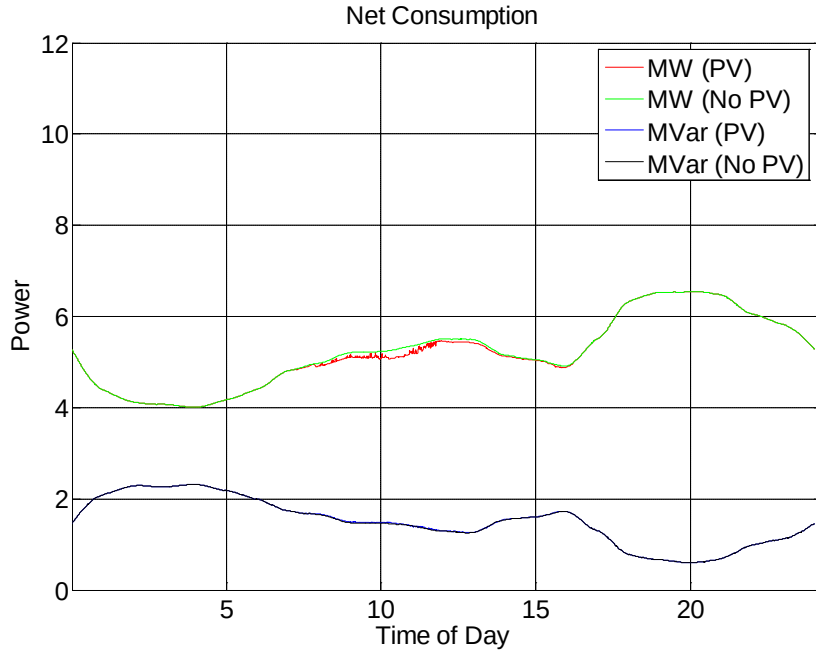

Figure B-34: MW and MVAr net consumption for scenario 2 and case 4.

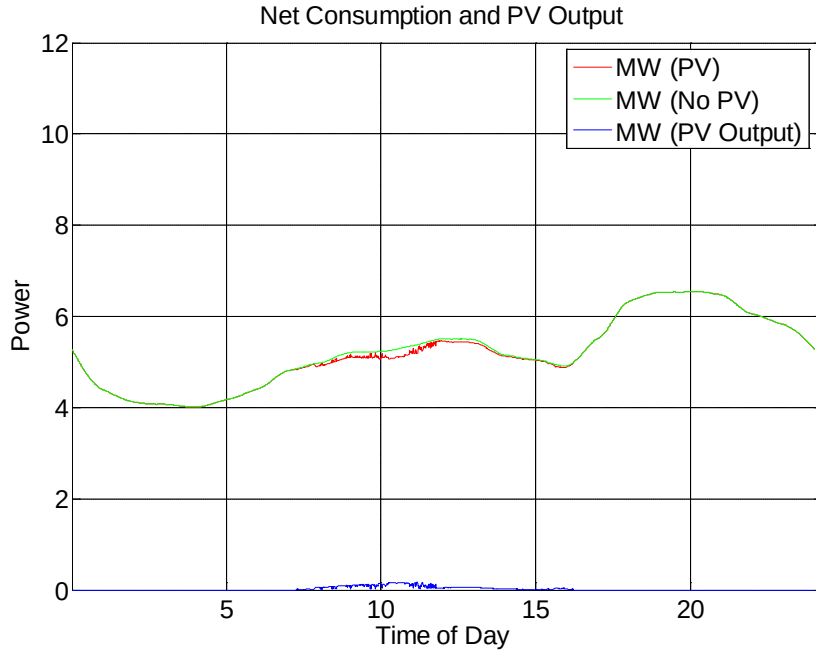

Figure B-35: MW net consumption and total PV generation for scenario 2 and case 4.

B.6 Case 5

Figure B-36 through Figure B-42 show simulation results for scenario 2 and case 5.

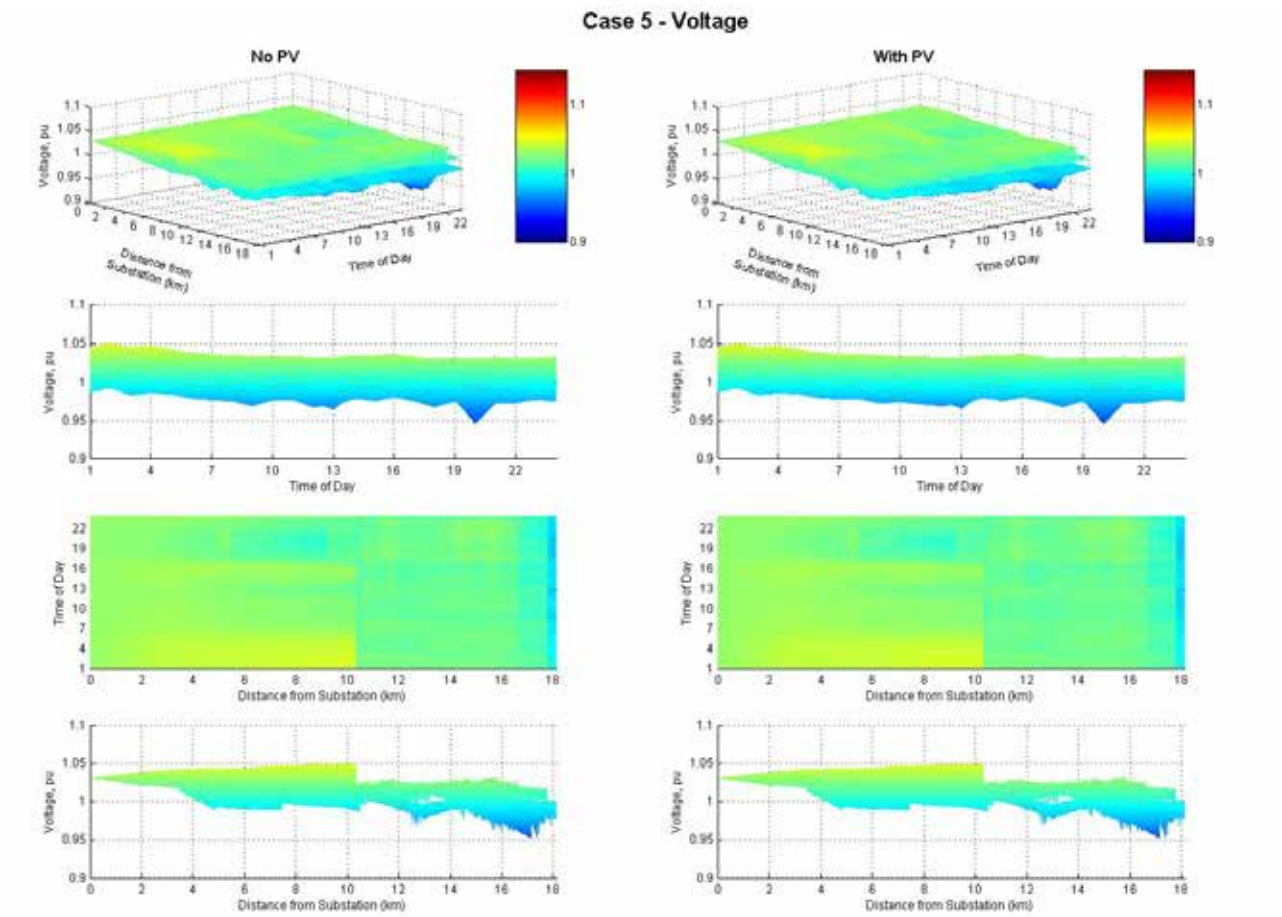

Figure B-36: Daily voltage profile for scenario 2 case 5.

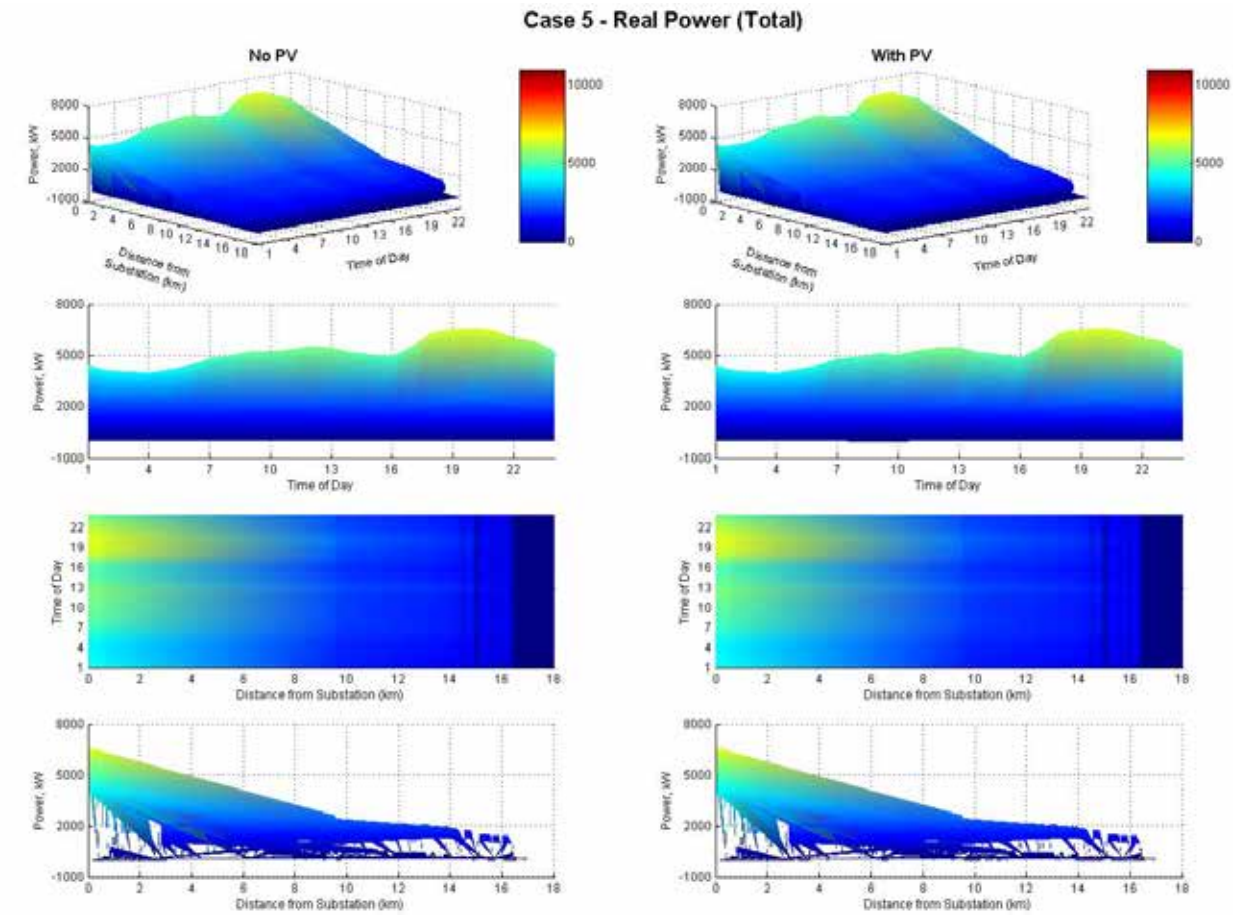

Figure B-37: Daily total real power profile for scenario 2 and case 5.

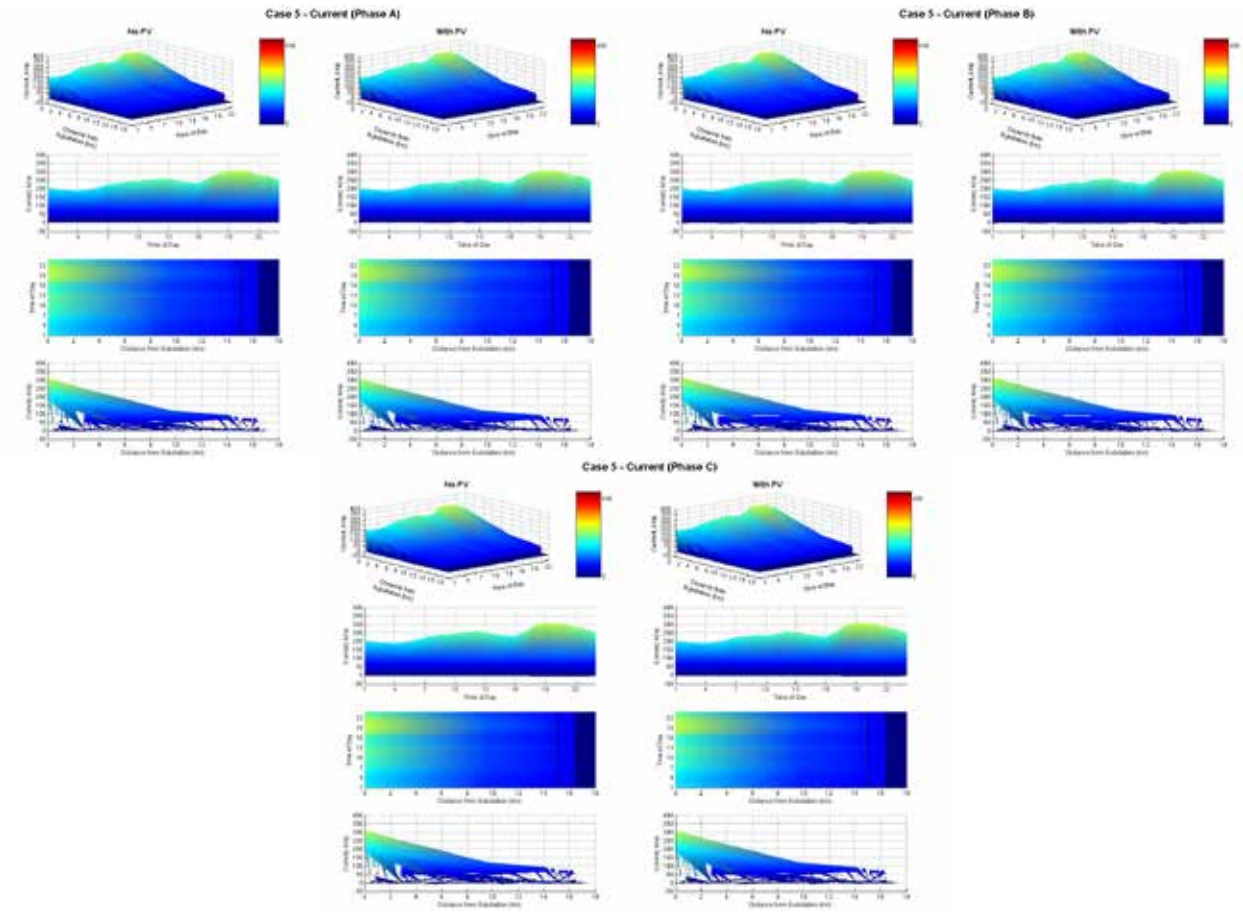

Figure B-38: Daily current profiles for scenario 2 and case 5.

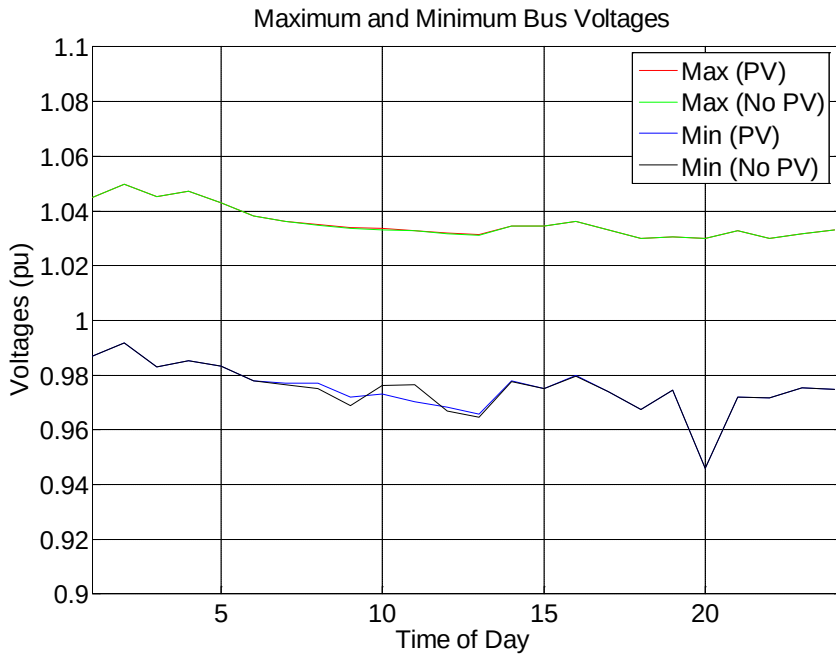

Figure B-39: Maximum and minimum voltages for scenario 2 and case 5.

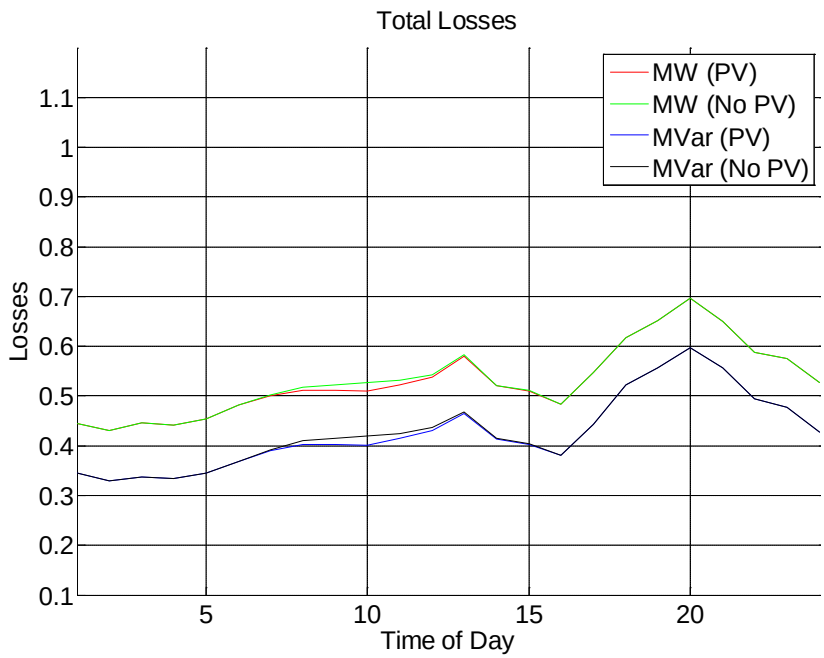

Figure B-40: MW and MVAr losses for scenario 2 and case 5.

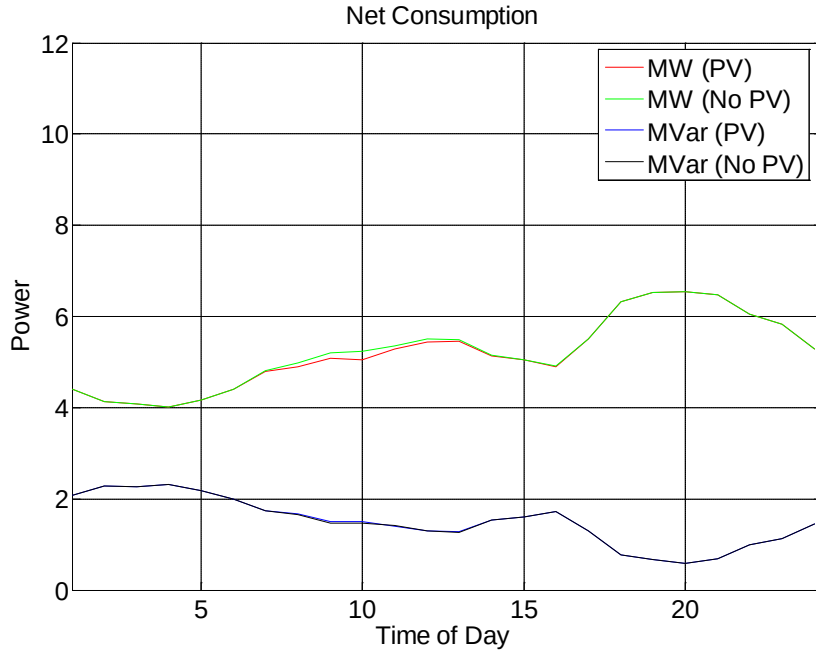

Figure B-41: MW and MVAr net consumption for scenario 2 and case 5.

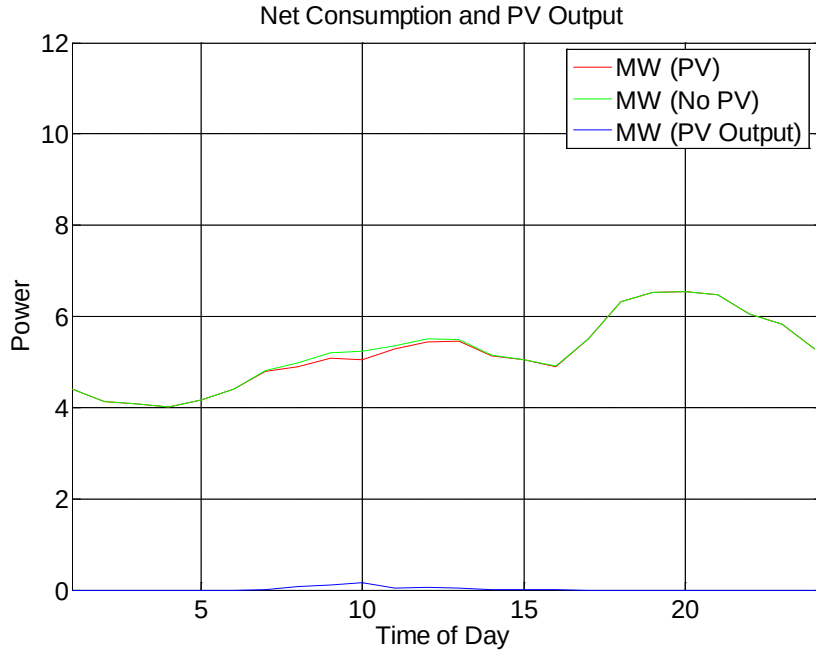

Figure B-42: MW net consumption and total PV generation for scenario 2 and case 5.

B.7 Case 6

Figure B-43 through Figure B-49 show simulation results for scenario 2 and case 5.

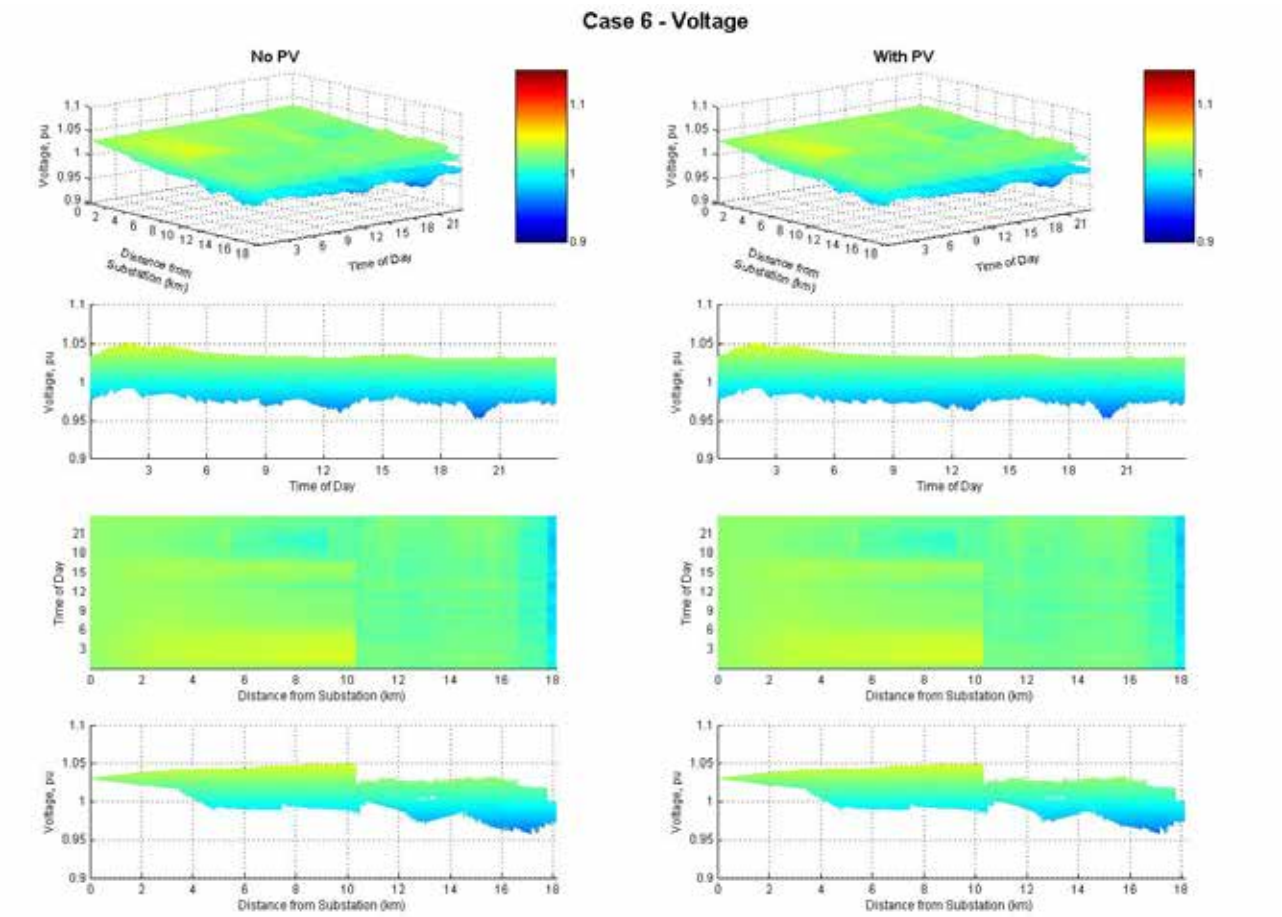

Figure B-43: Daily voltage profile for scenario 2 case 6.

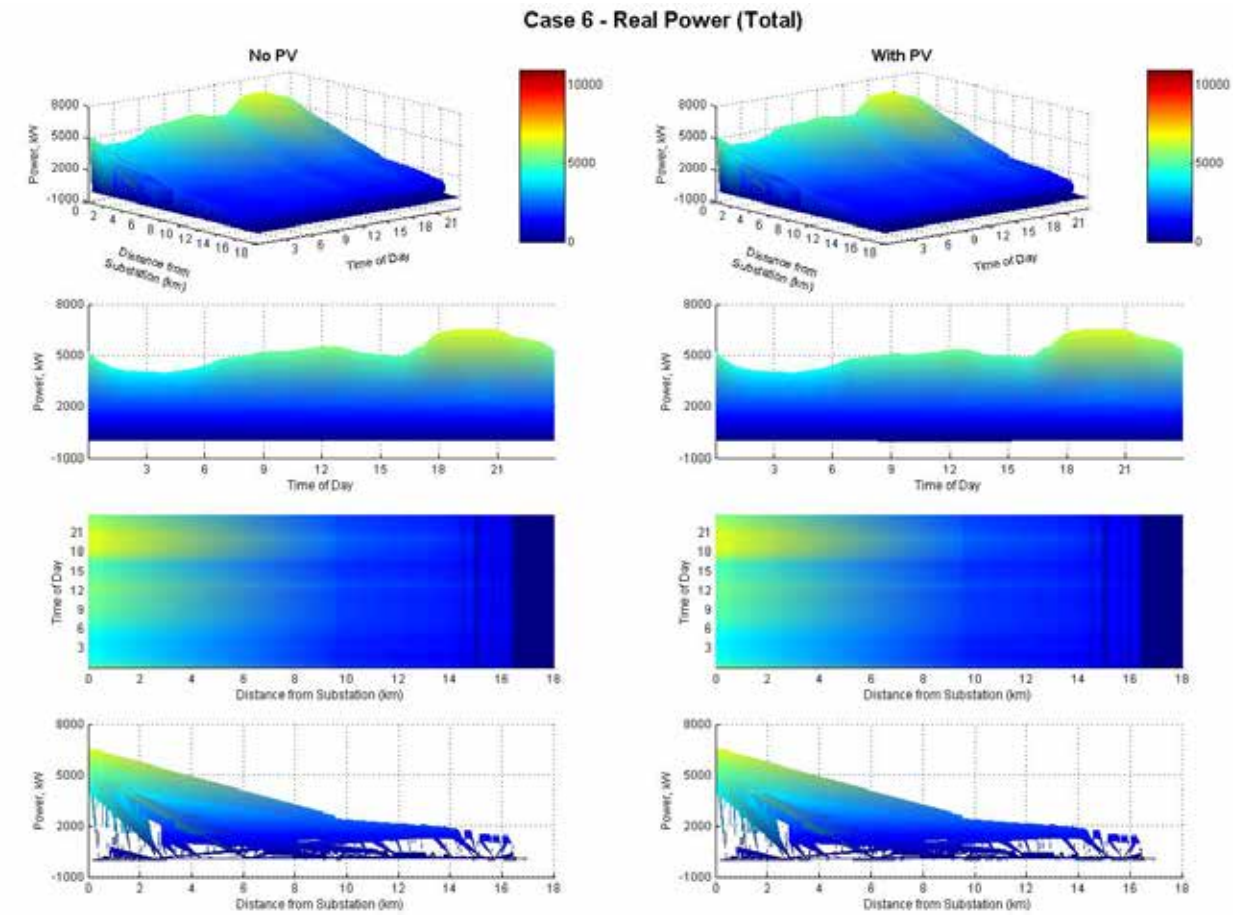

Figure B-44: Daily total real power profile for scenario 2 and case 6.

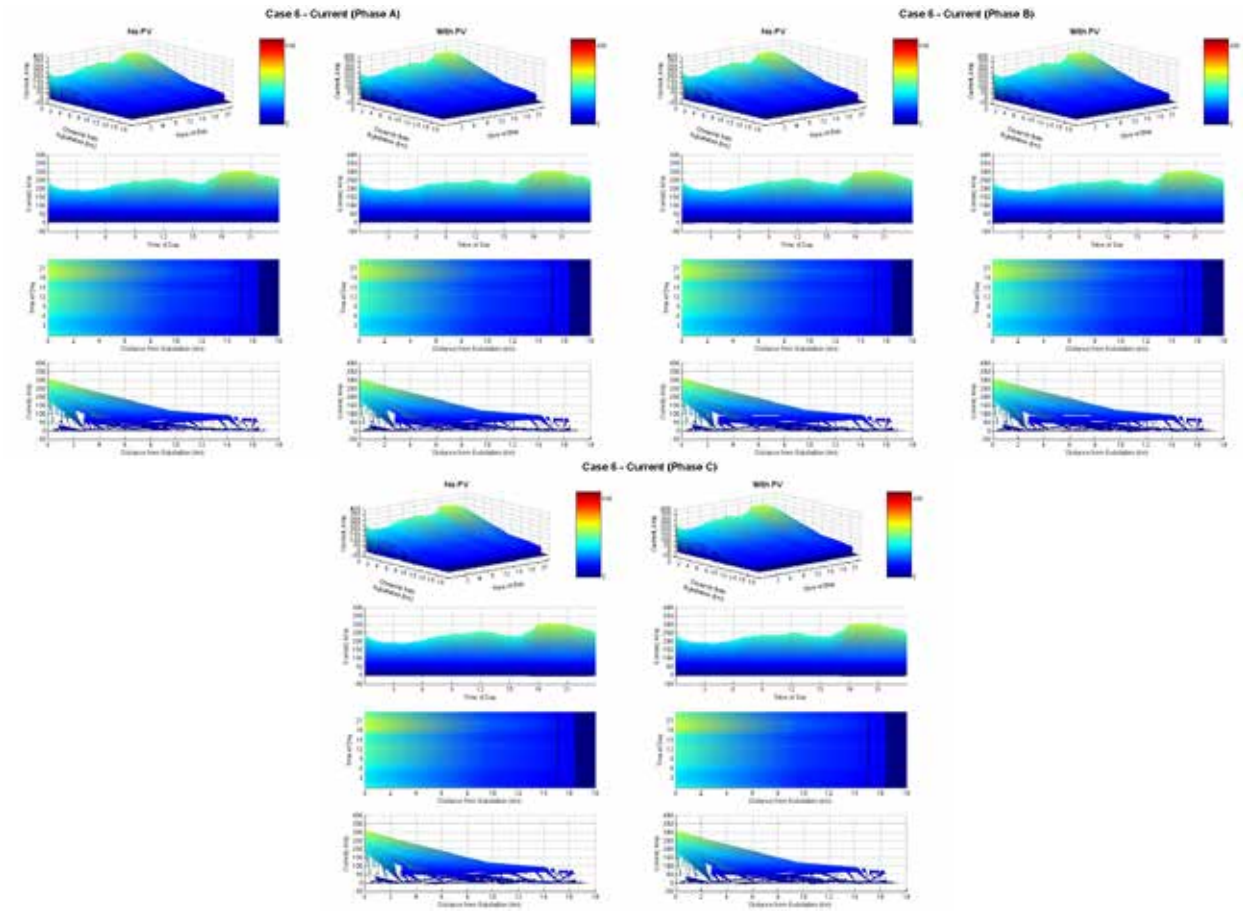

Figure B-45: Daily current profiles for scenario 2 and case 6.

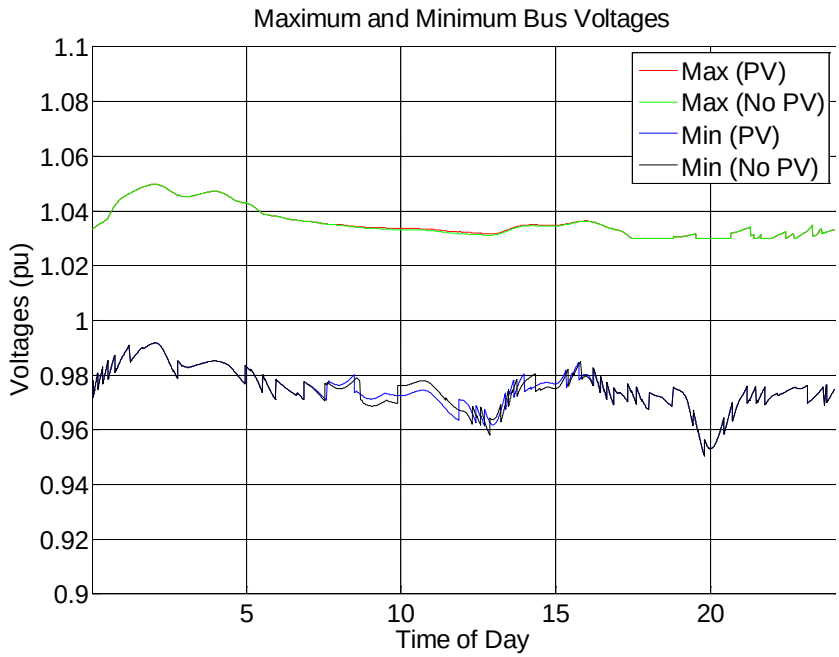

Figure B-46: Maximum and minimum voltages for scenario 2 and case 6.

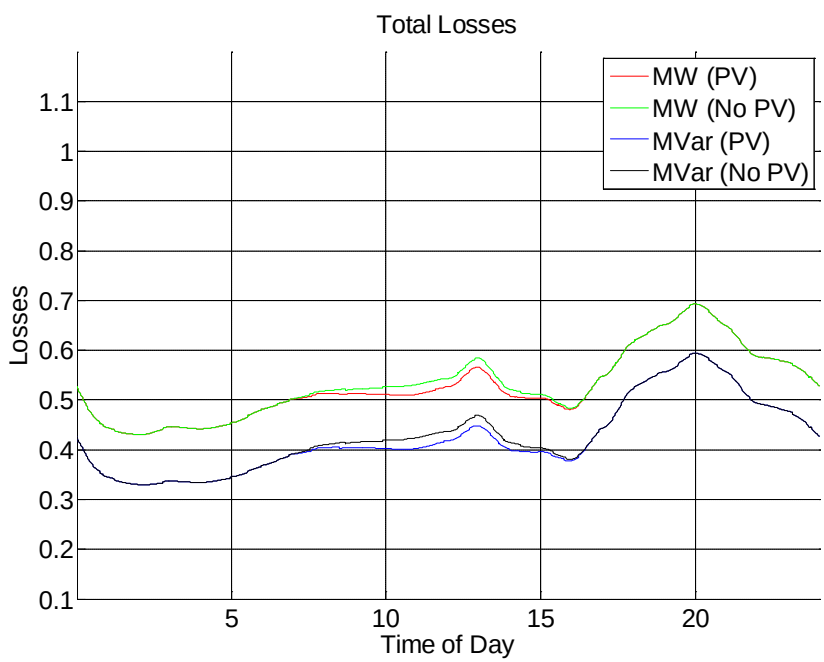

Figure B-47: MW and MVAr losses for scenario 2 and case 6.

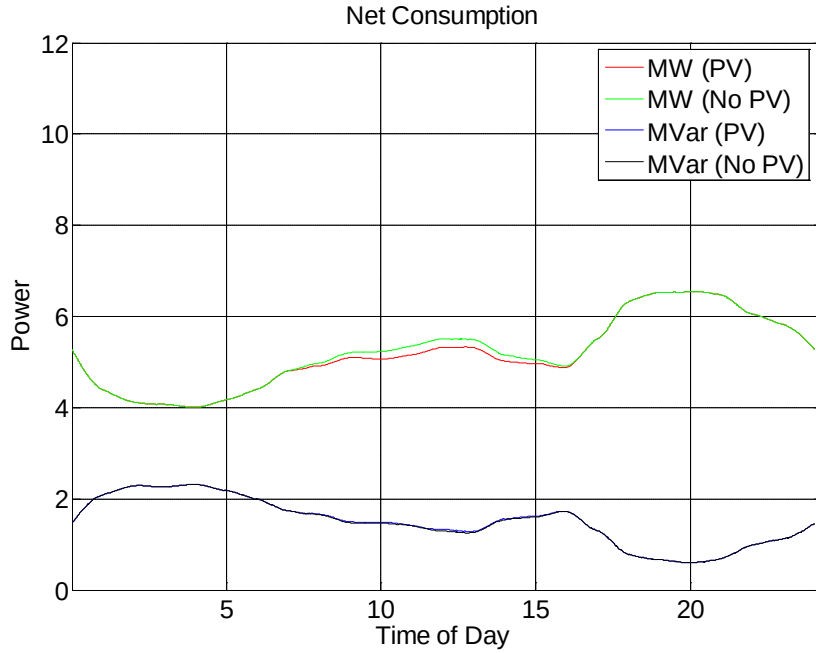

Figure B-48: MW and MVAr net consumption for scenario 2 and case 6.

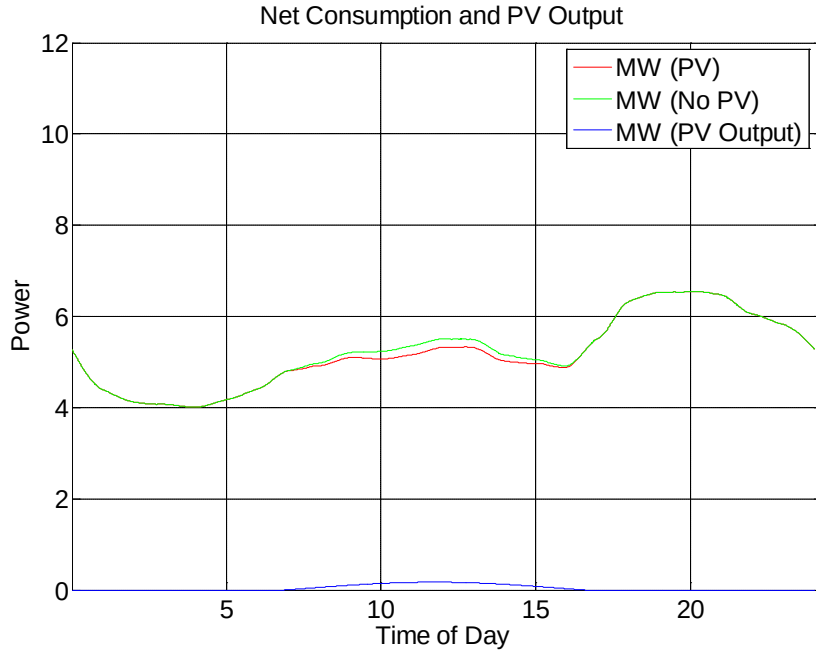

Figure B-49: MW net consumption and total PV generation for scenario 2 and case 6.

Appendix C - Scenario 3

In this Section we present the simulation results obtained for scenario 2 (the pv rating for this scenario totals in 4.973 MW (~ 41 % of the total load MW rating)).

C.1 Case 0

Figure C-1 through Figure C-7 show simulation results for scenario 3 and case 0.

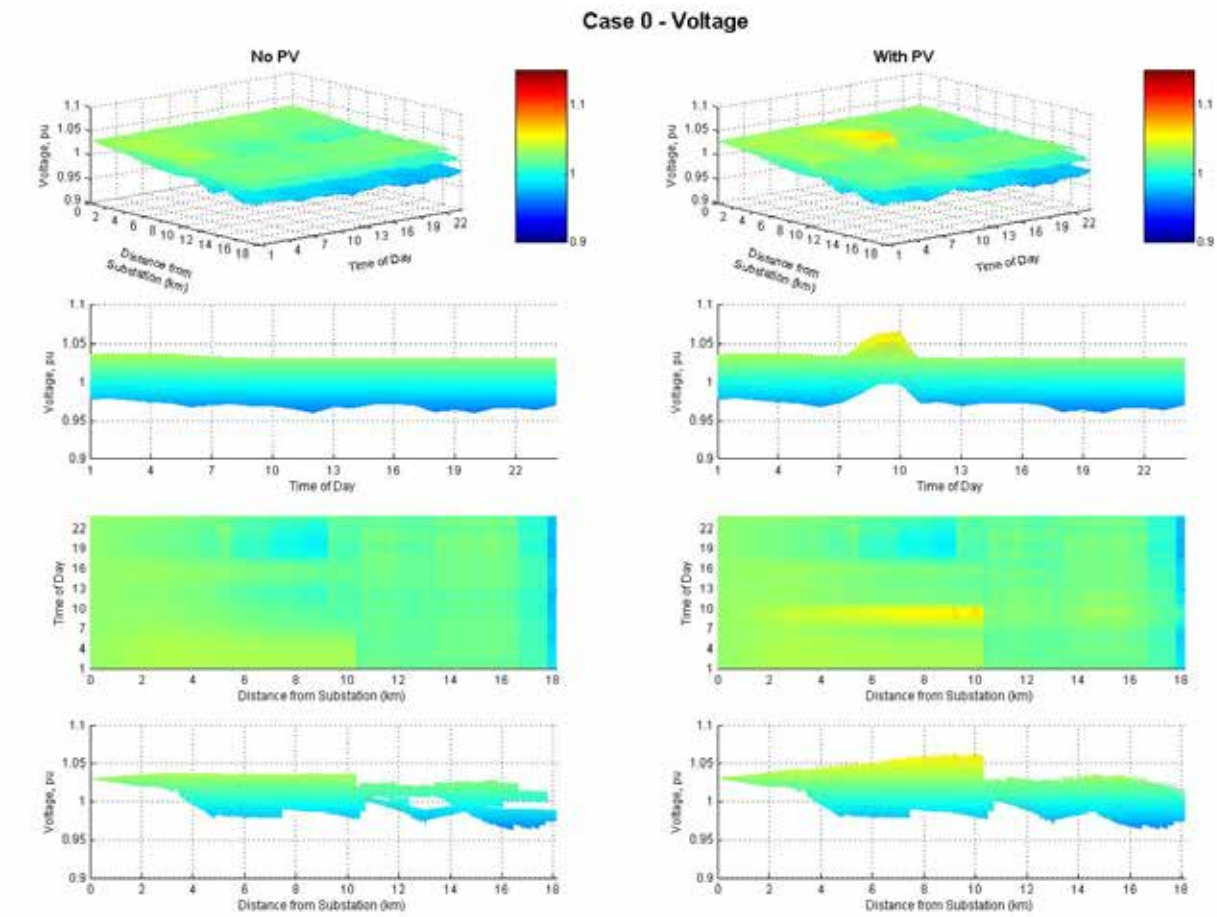

Figure C-1: Daily voltage profile for scenario 3 case 0.

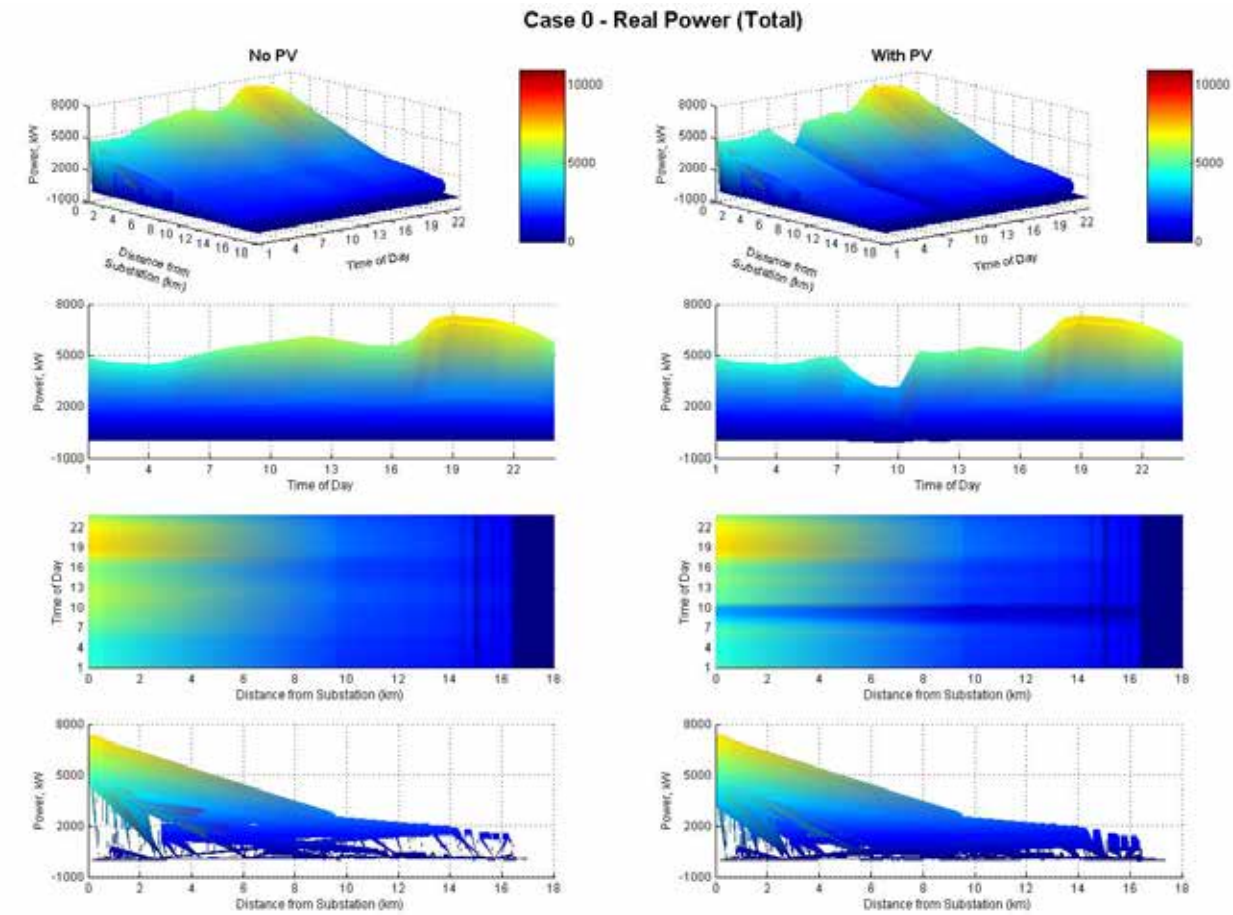

Figure C-2: Daily total real power profile for scenario 3 and case 0.

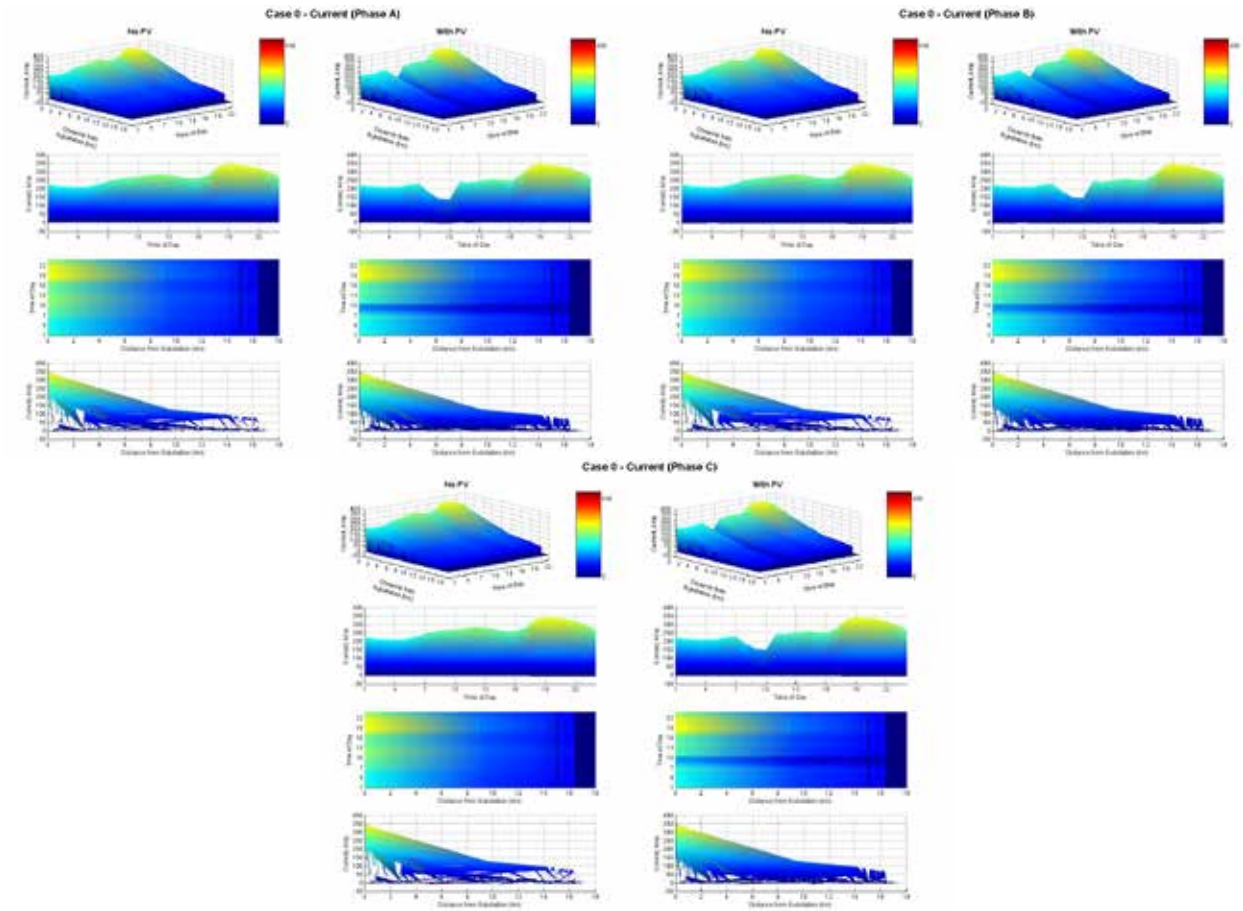

Figure C-3: Daily current profiles for scenario 3 and case 0.

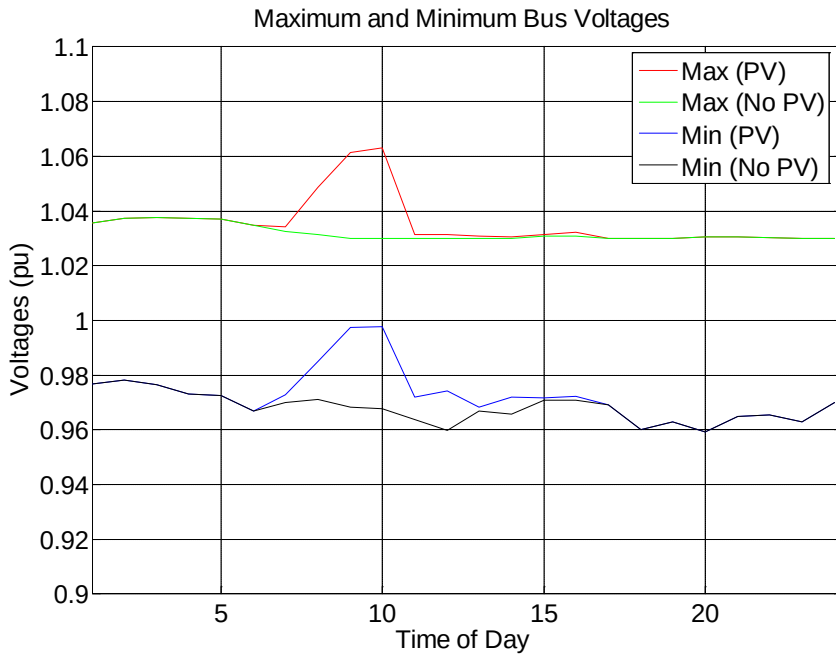

Figure C-4: Maximum and minimum voltages for scenario 3 and case 0.

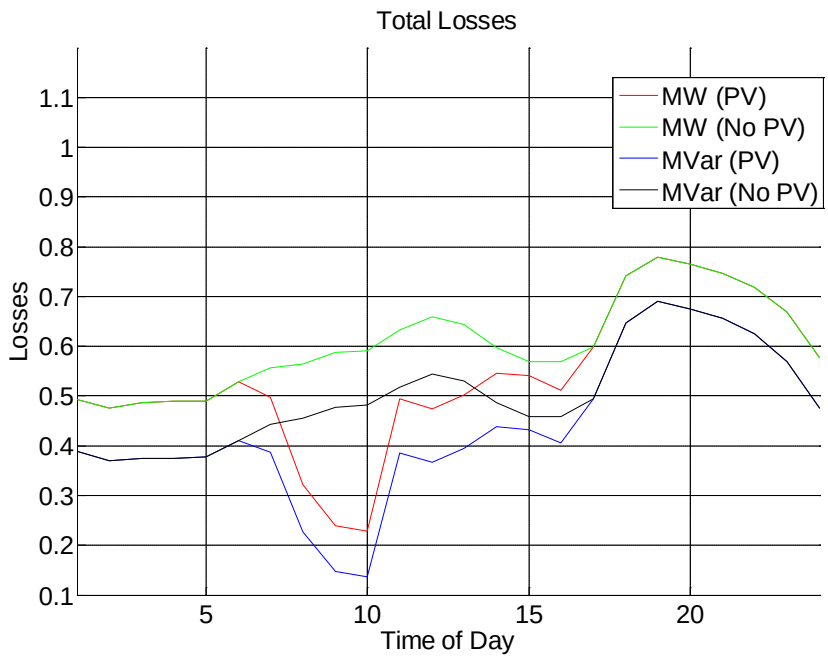

Figure C-5: MW and MVAr losses for scenario 3 and case 0.

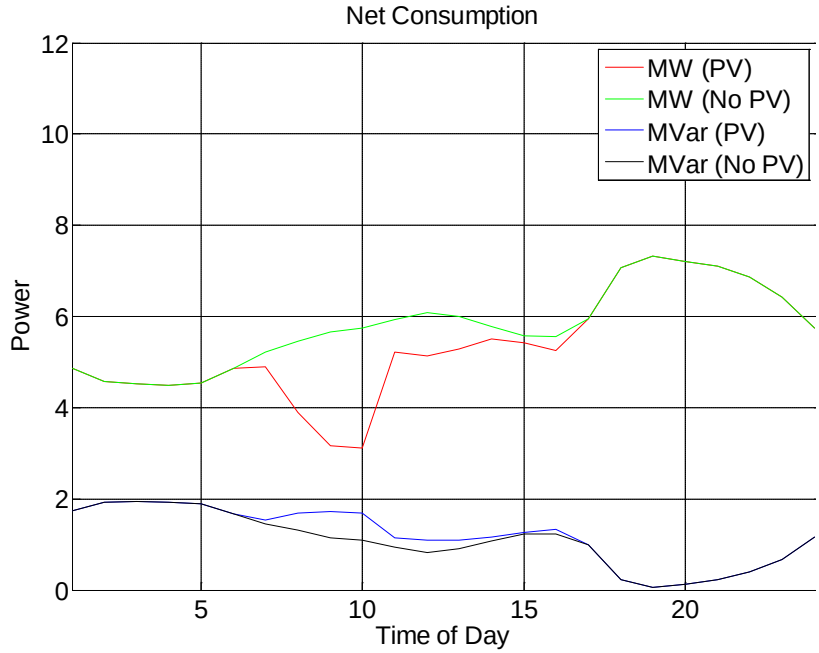

Figure C-6: MW and MVAr net consumption for scenario 3 and case 0.

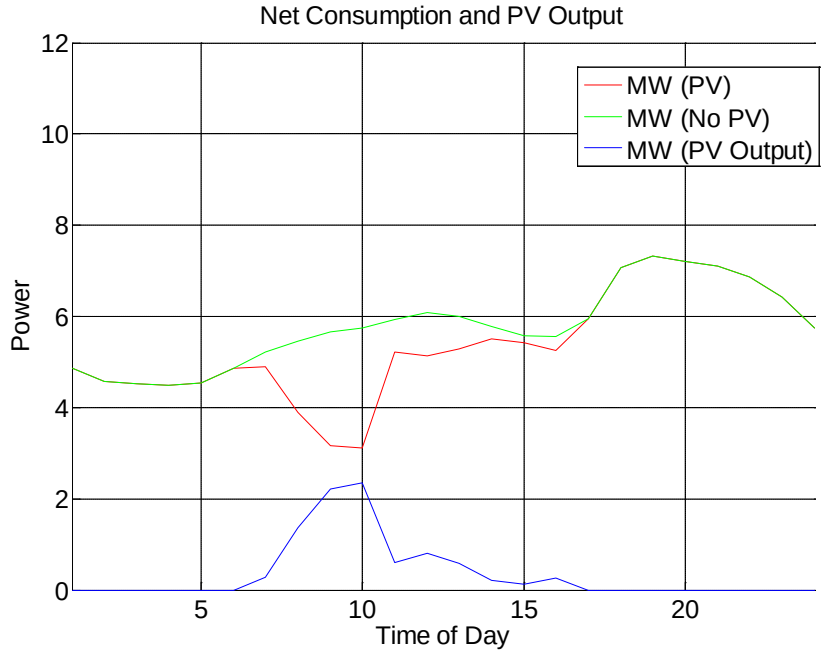

Figure C-7: MW net consumption and total PV generation for scenario 3 and case 0.

C.2 Case 1

Figure C-8 through Figure C-14 show simulation results for scenario 3 and case 1.

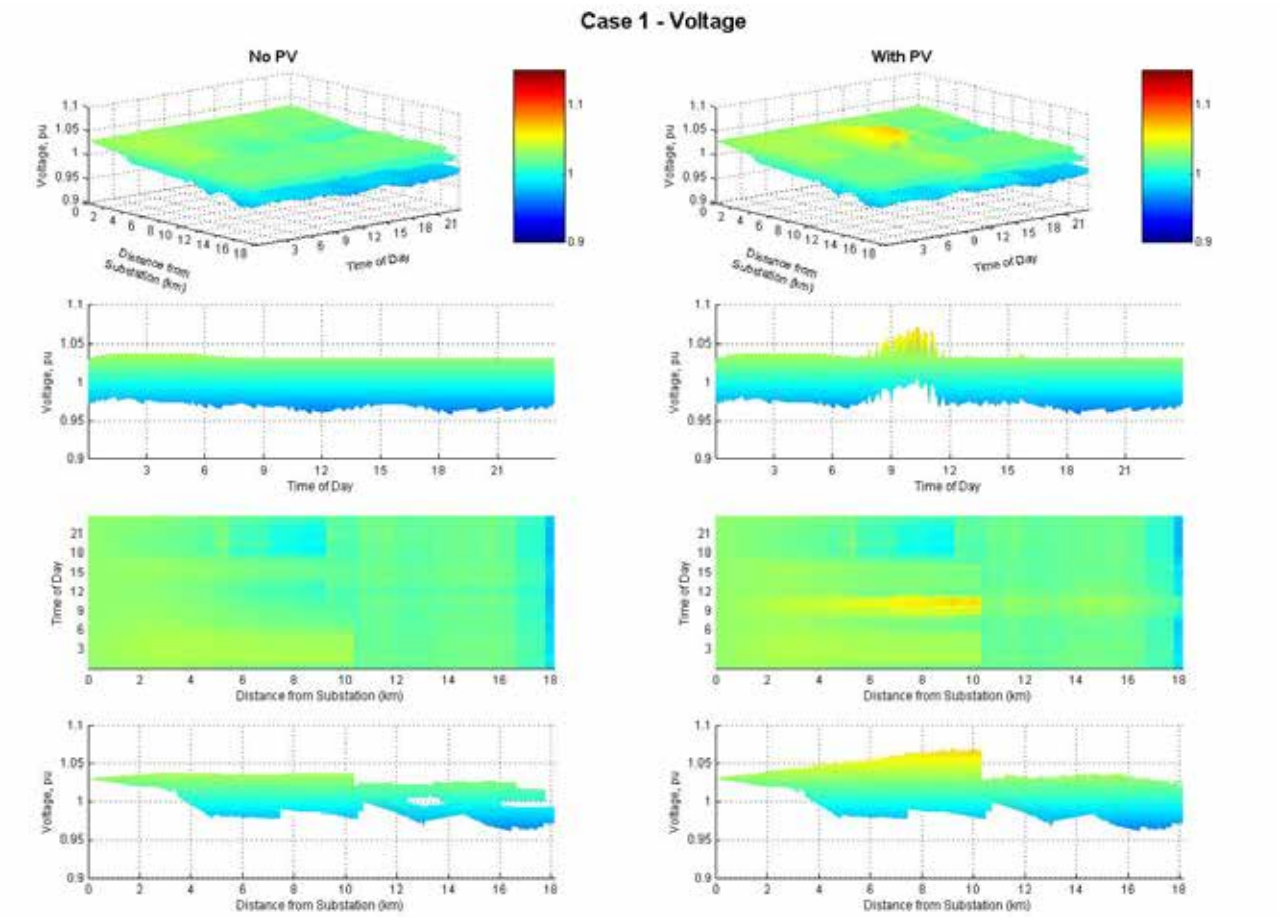

Figure C-8: Daily voltage profile for scenario 3 case 1.

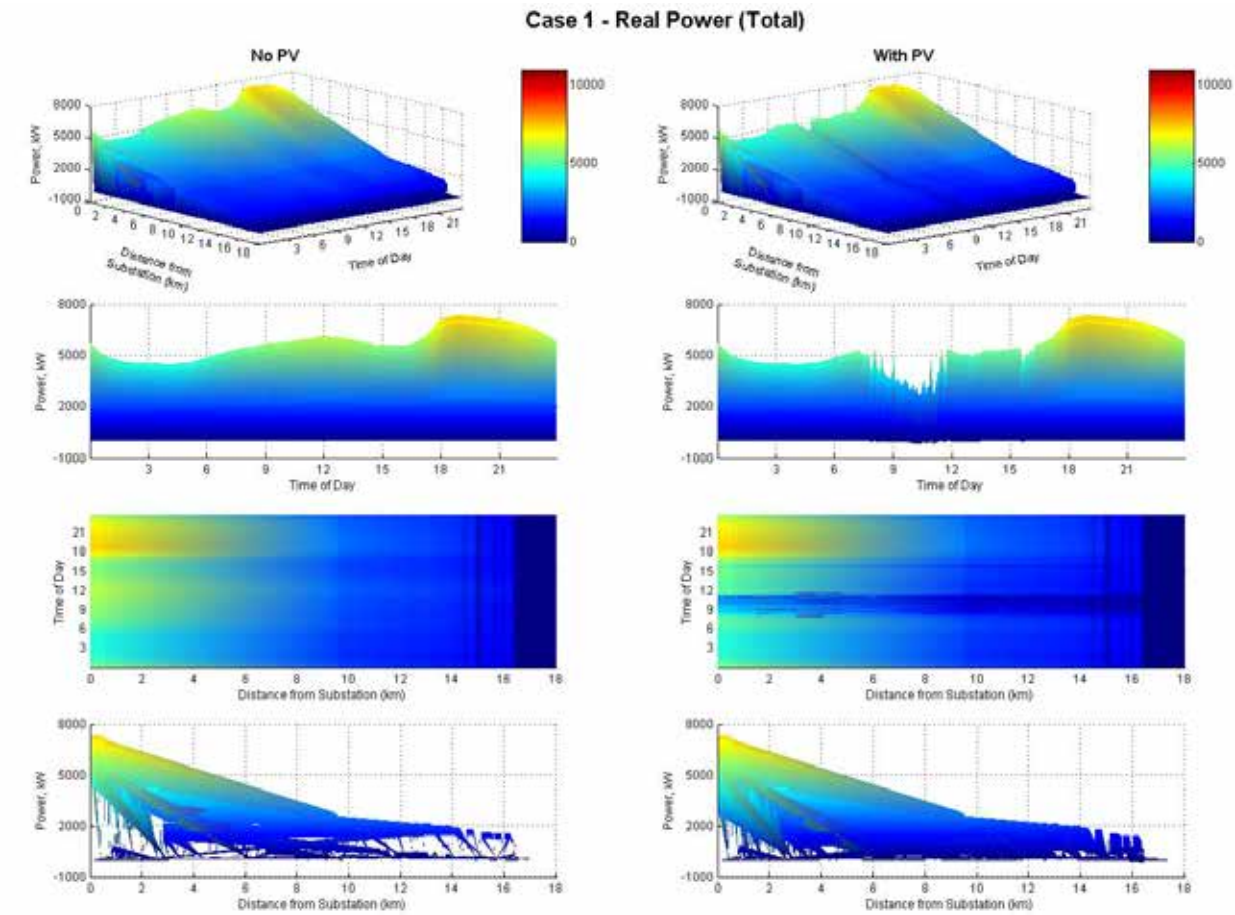

Figure C-9: Daily total real power profile for scenario 3 and case 1.

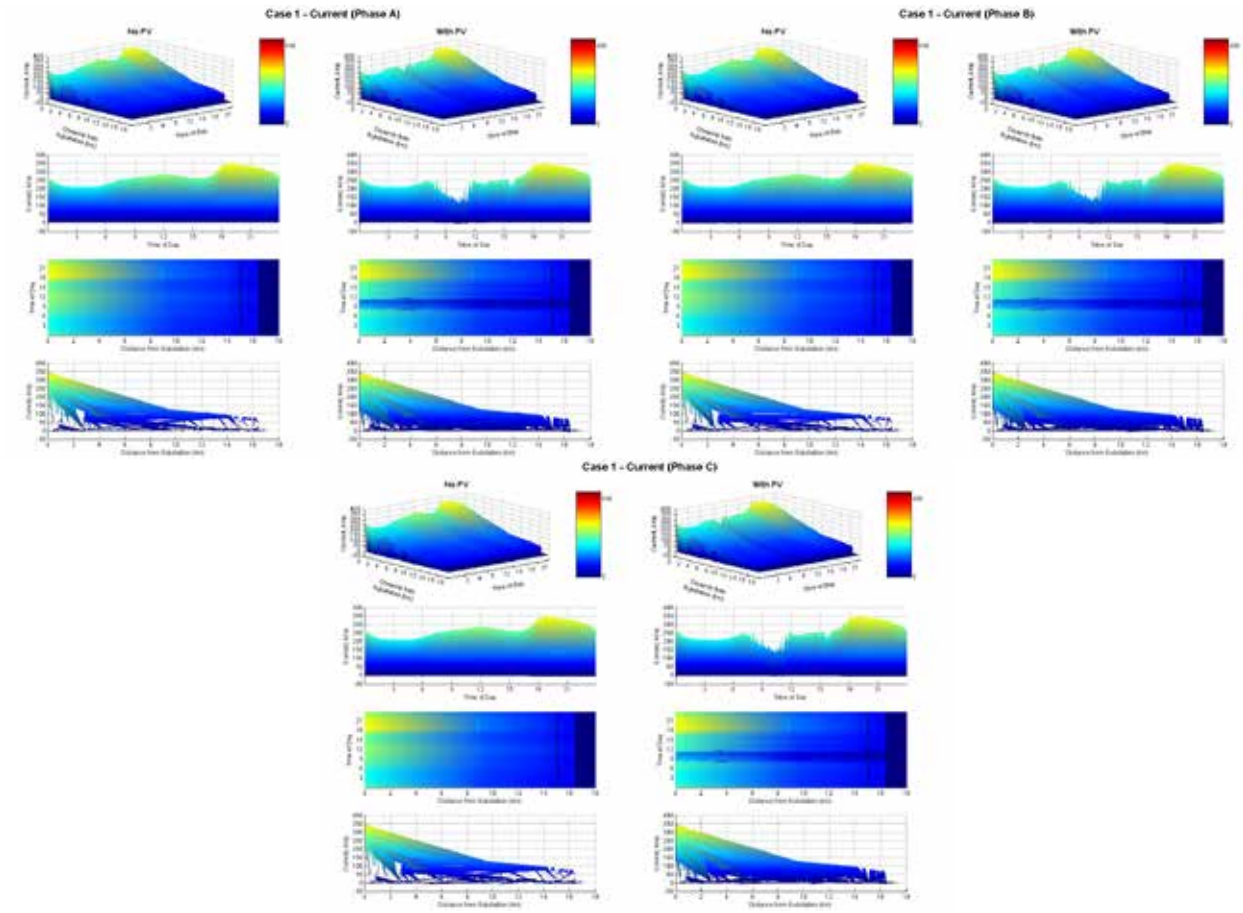

Figure C-10: Daily current profiles for scenario 3 and case 1.

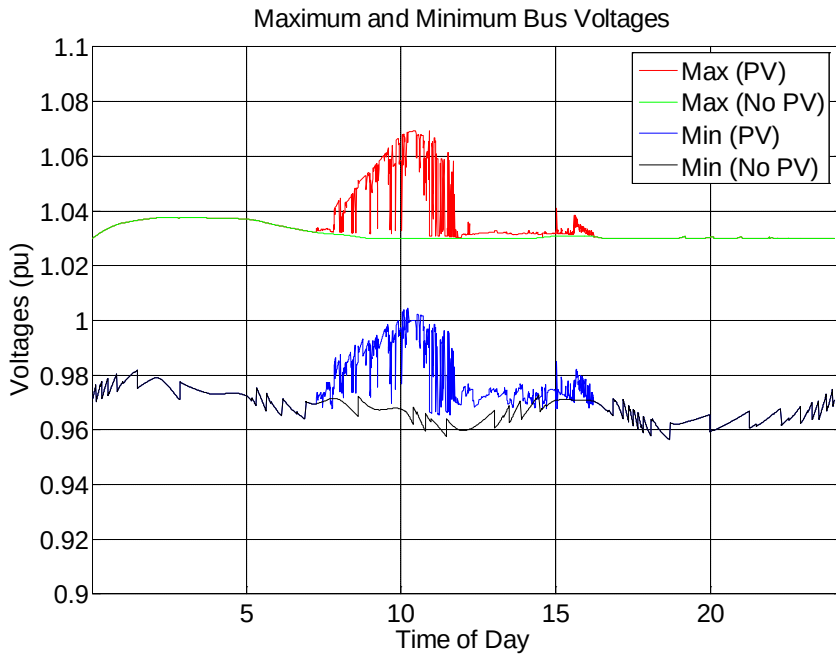

Figure C-11: Maximum and minimum voltages for scenario 3 and case 1.

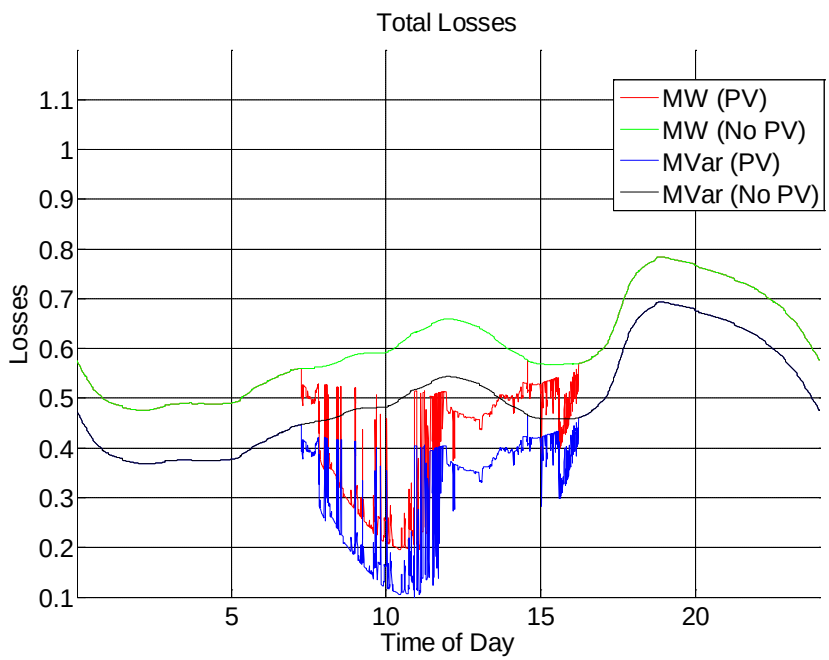

Figure C-12: MW and MVAr losses for scenario 3 and case 1.

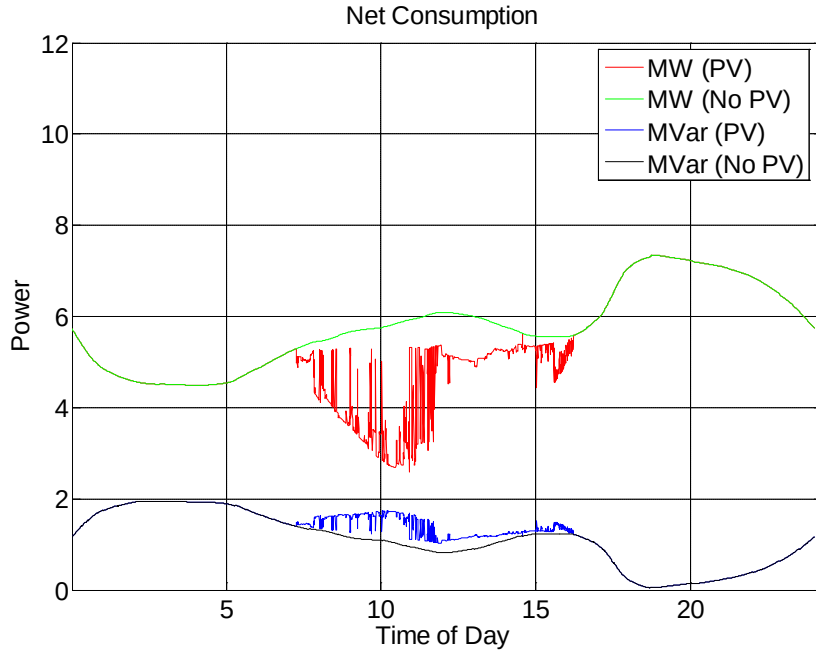

Figure C-13: MW and MVAr net consumption for scenario 3 and case 1.

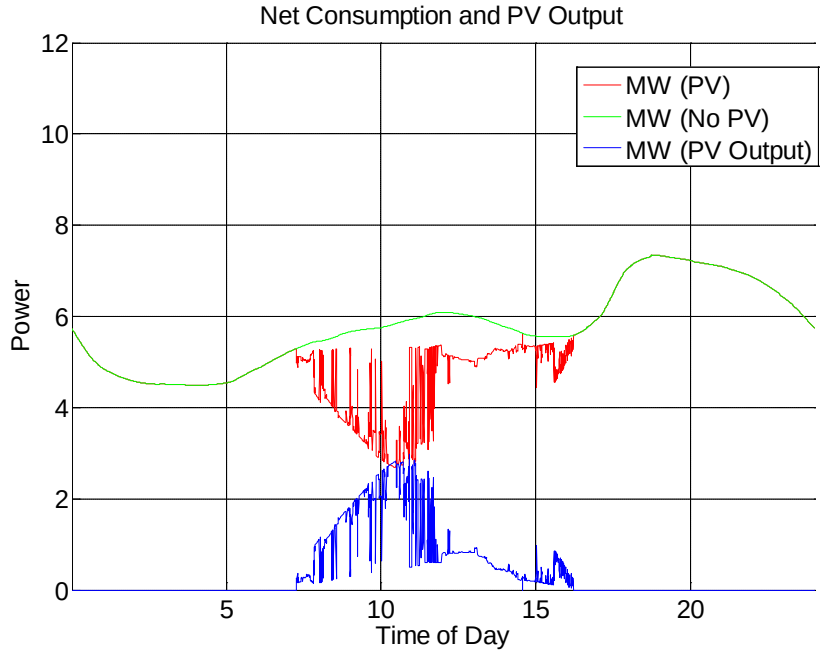

Figure C-14: MW net consumption and total PV generation for scenario 3 and case 1.

C.3 Case 2

Figure C-15 through Figure C-22 show simulation results for scenario 3 and case 2.

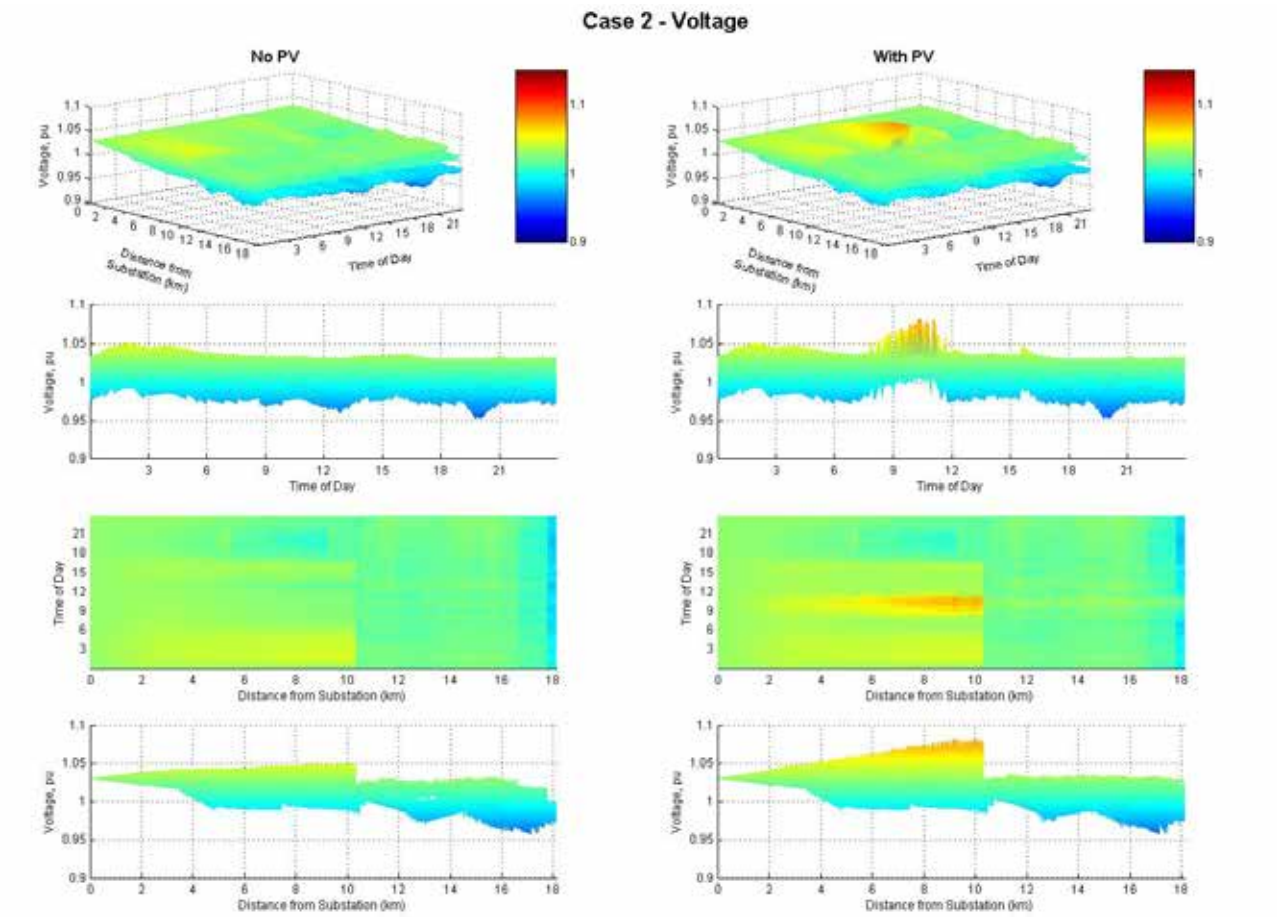

Figure C-15: Daily voltage profile for scenario 3 case 2.

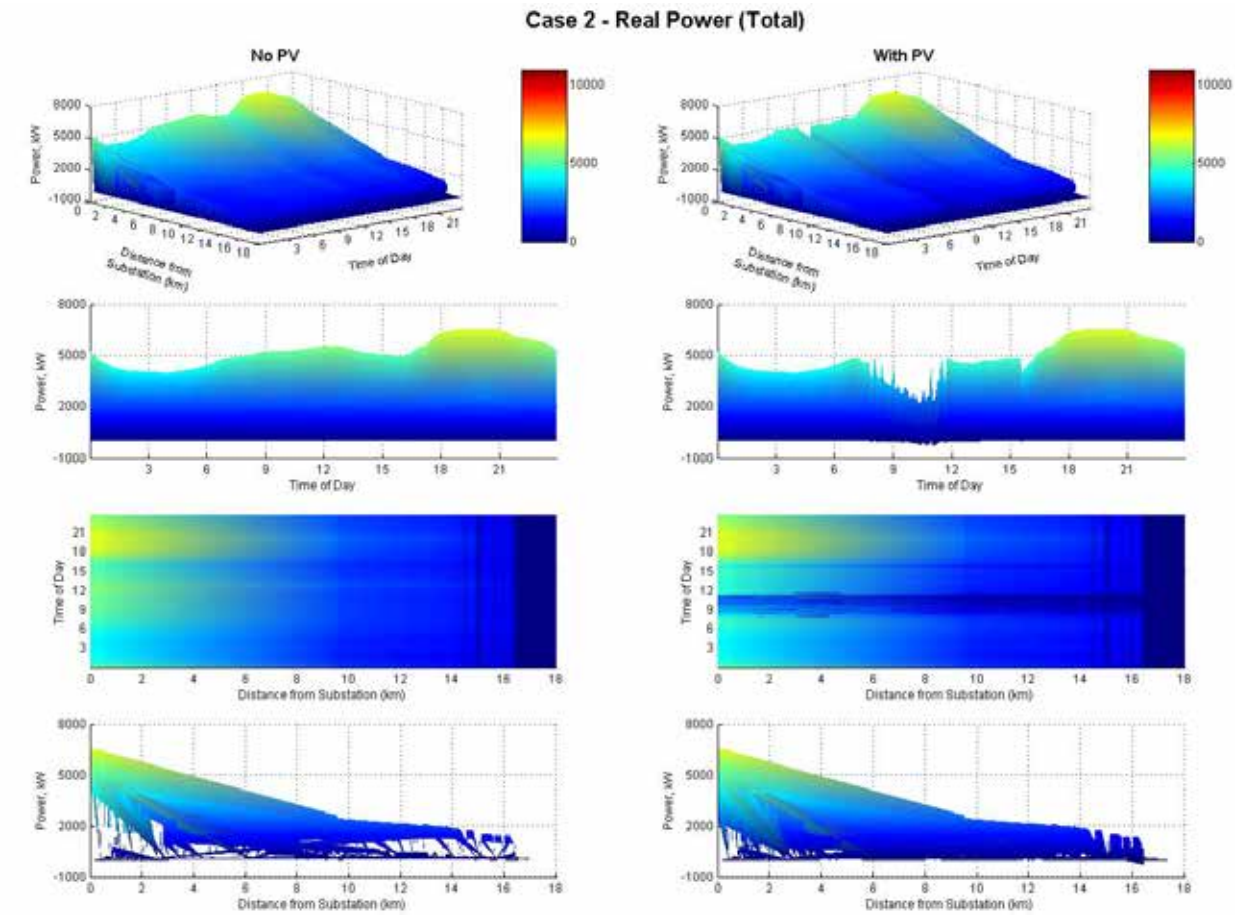

Figure C-16: Daily total real power profile for scenario 3 and case 2.

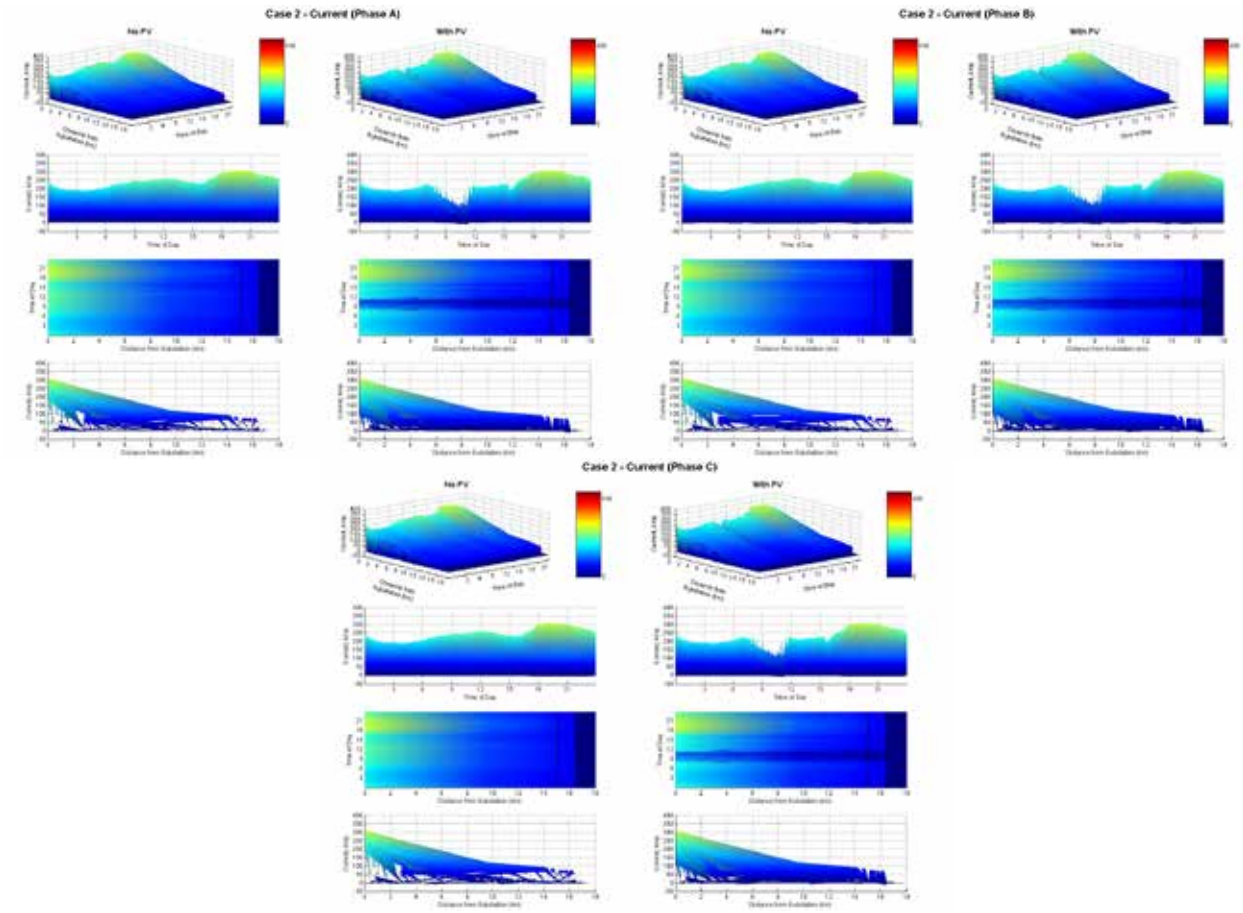

Figure C-17: Daily current profiles for scenario 3 and case 2.

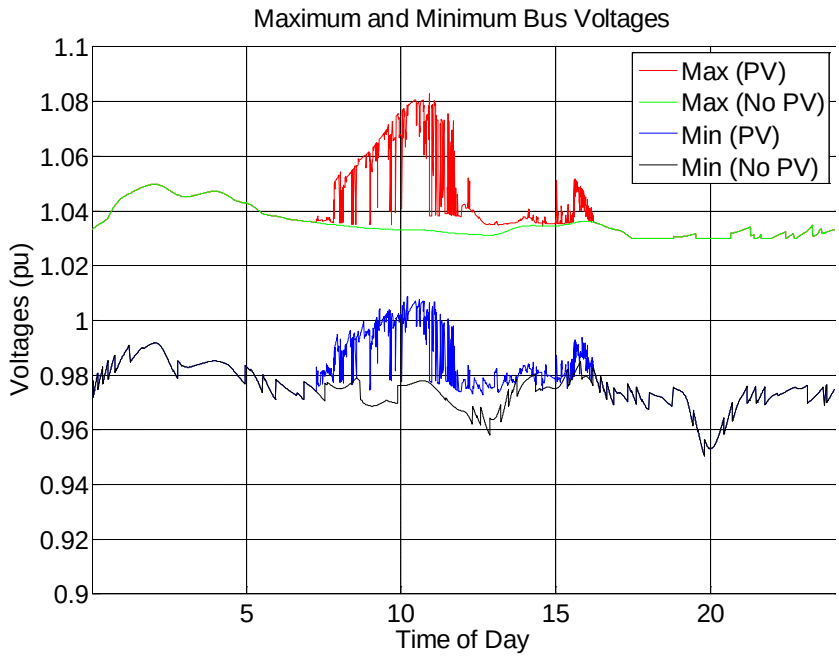

Figure C-18: Maximum and minimum voltages for scenario 3 and case 2.

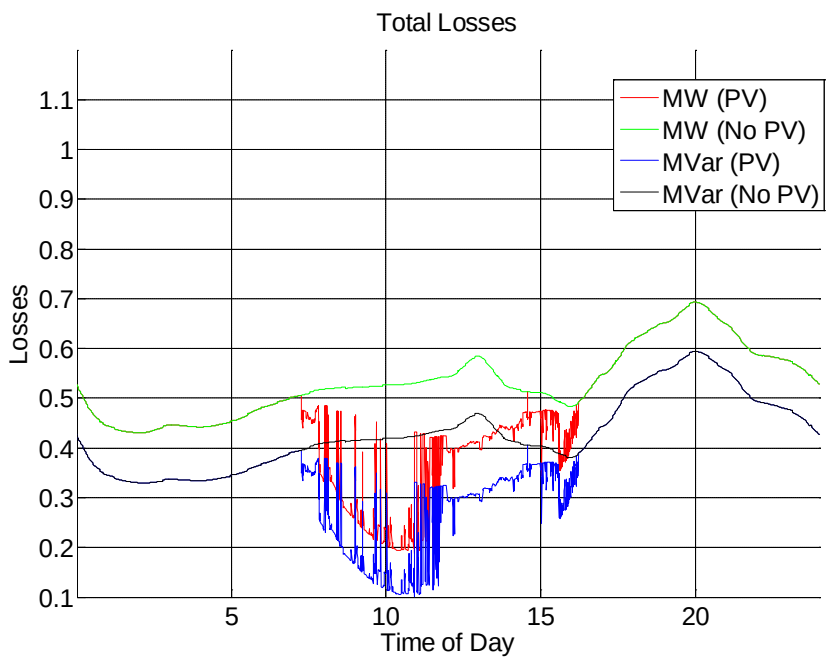

Figure C-19: MW and MVAr losses for scenario 3 and case 2.

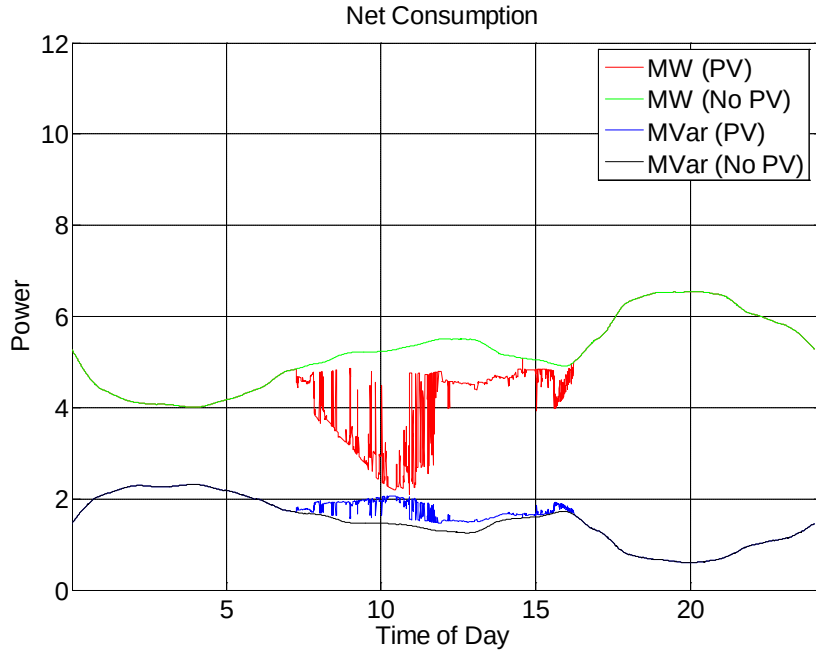

Figure C-20: MW and MVAr net consumption for scenario 3 and case 2.

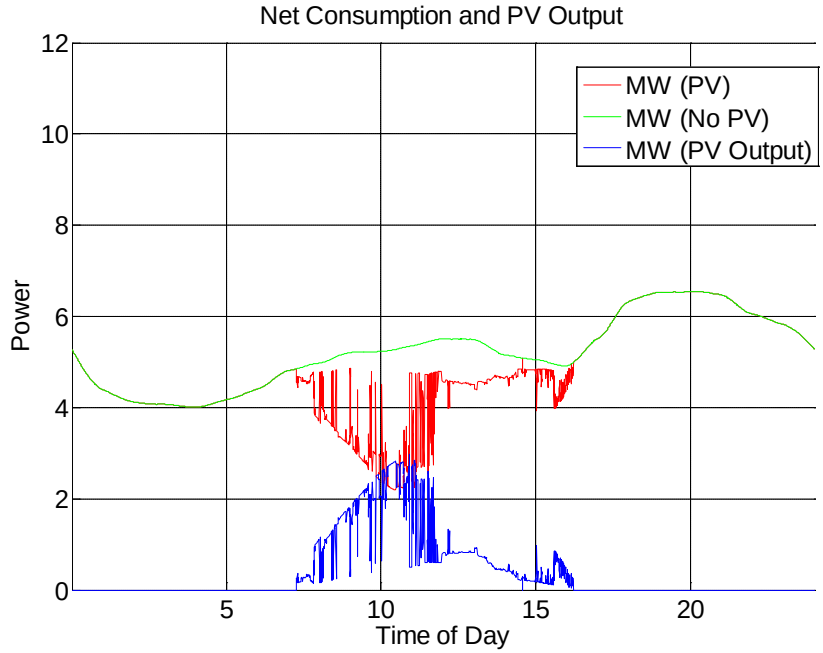

Figure C-21: MW net consumption and total PV generation for scenario 3 and case 2.

C.4 Case 3

Figure C-22 through Figure C-28 show simulation results for scenario 3 and case 3.

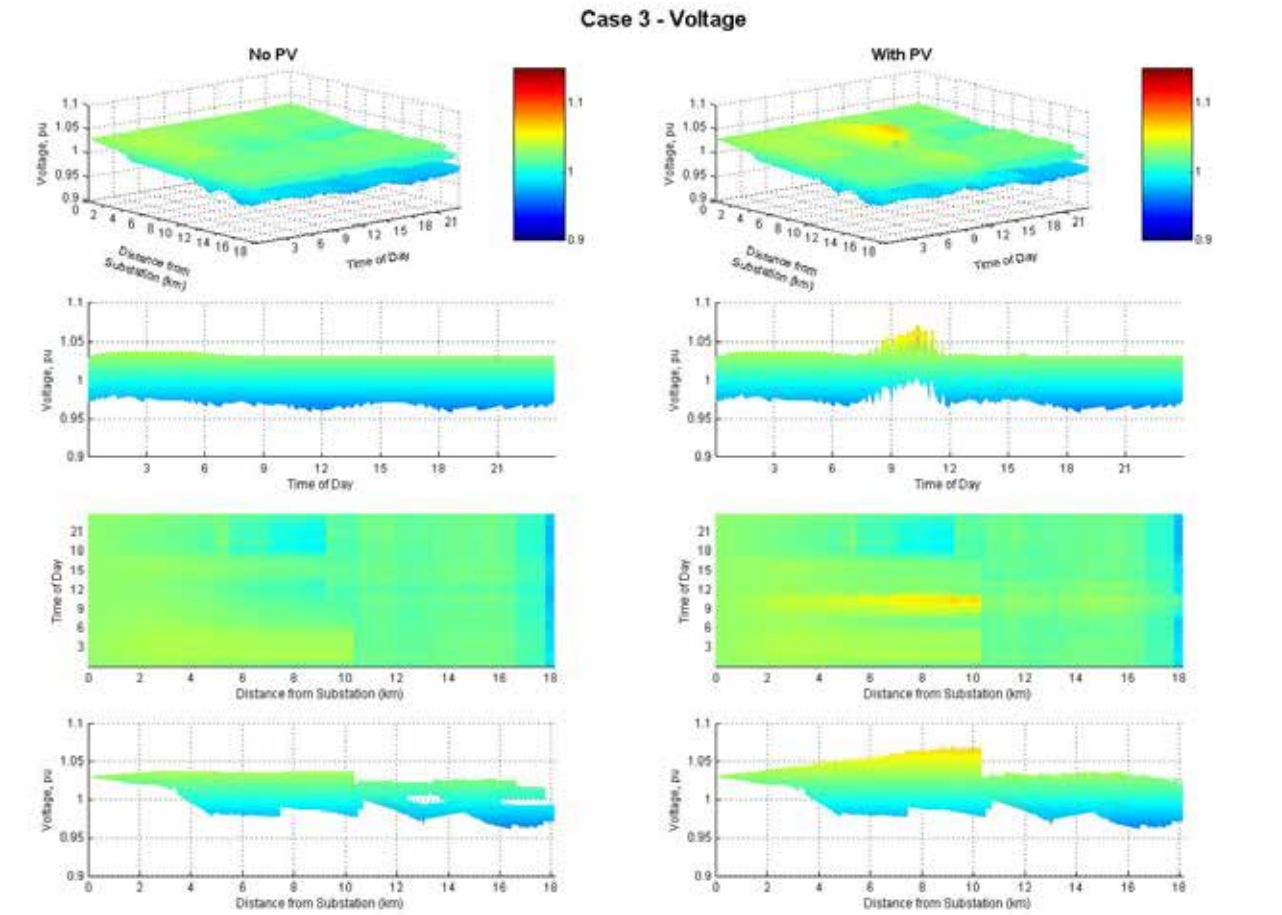

Figure C-22: Daily voltage profile for scenario 3 case 3.

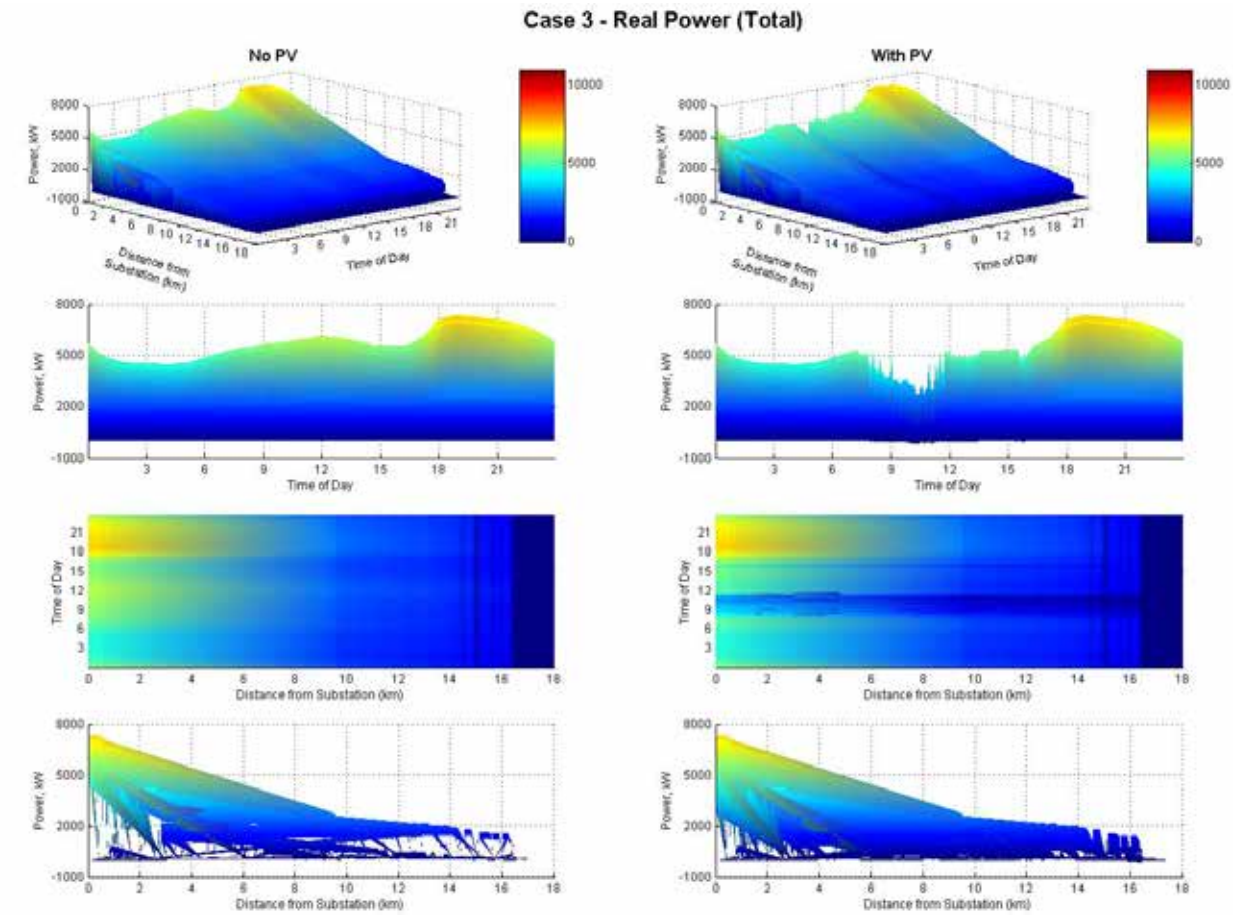

Figure C-23: Daily total real power profile for scenario 3 and case 3.

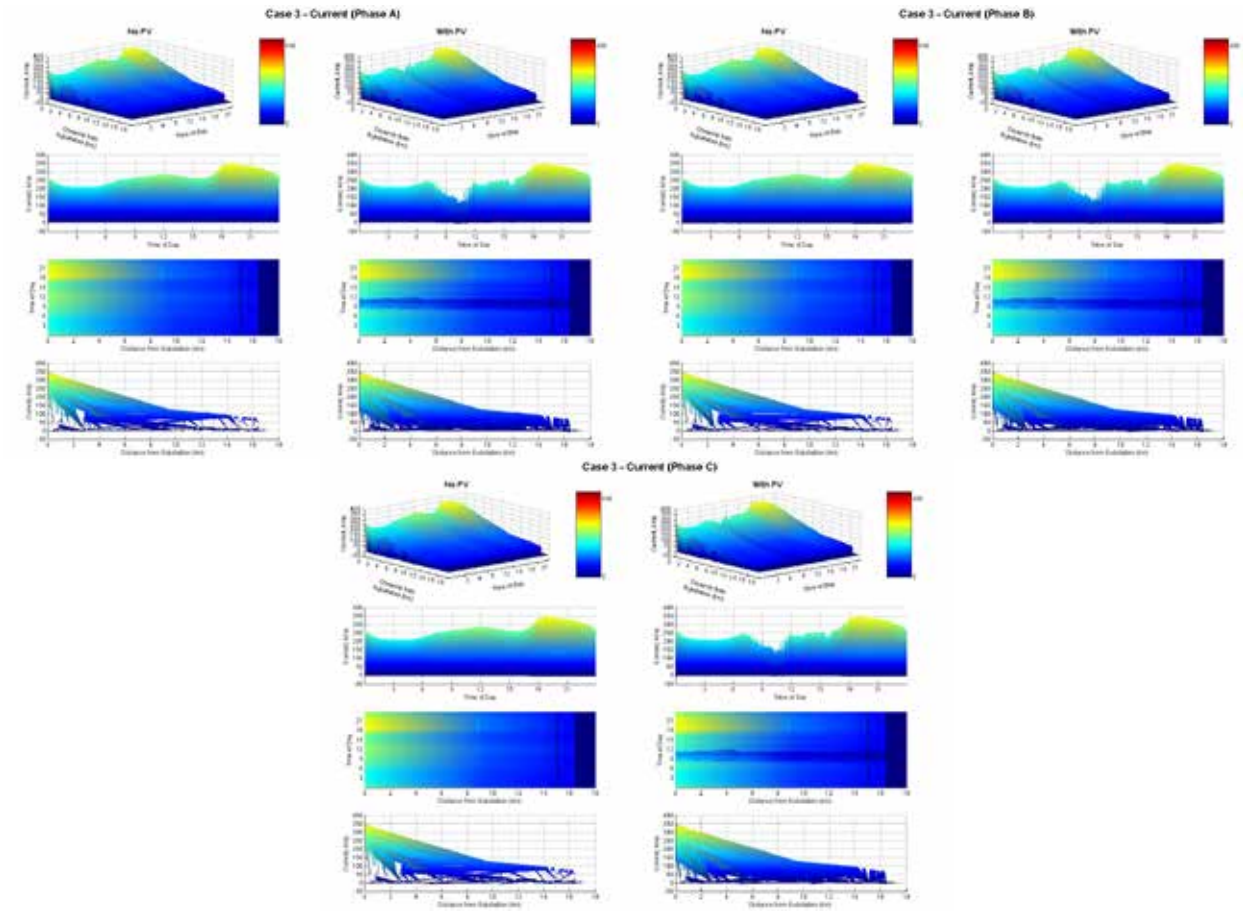

Figure C-24: Daily current profiles for scenario 3 and case 3.

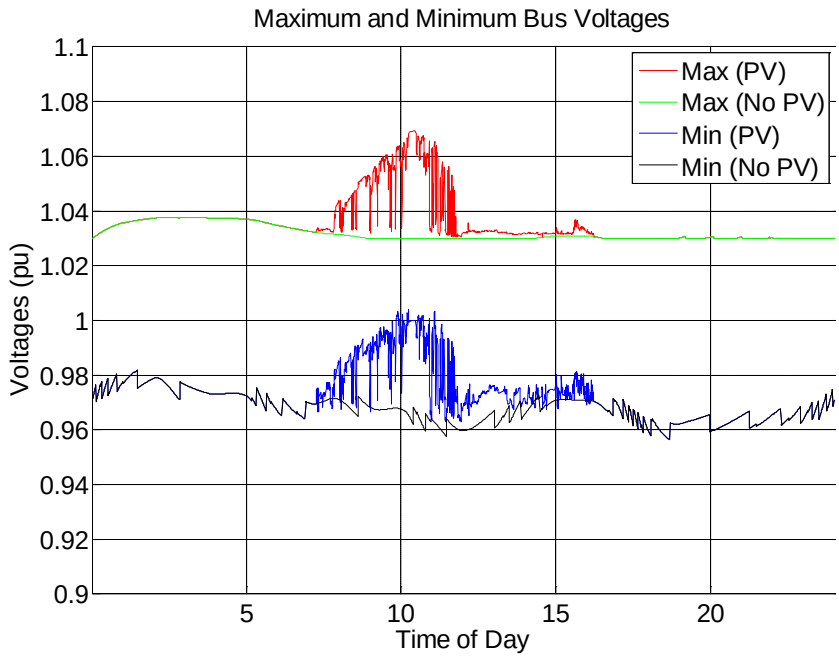

Figure C-25: Maximum and minimum voltages for scenario 3 and case 3.

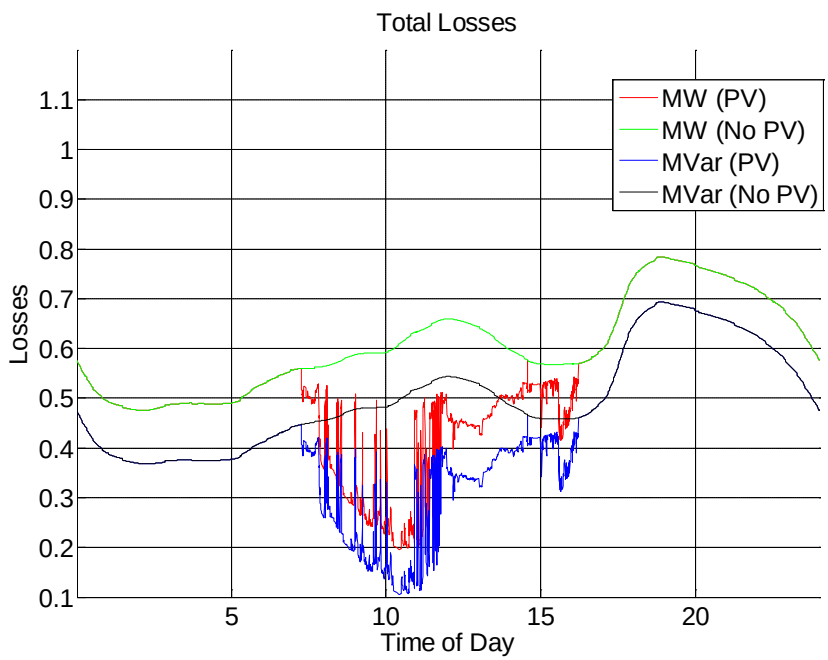

Figure C-26: MW and MVAr losses for scenario 3 and case 3.

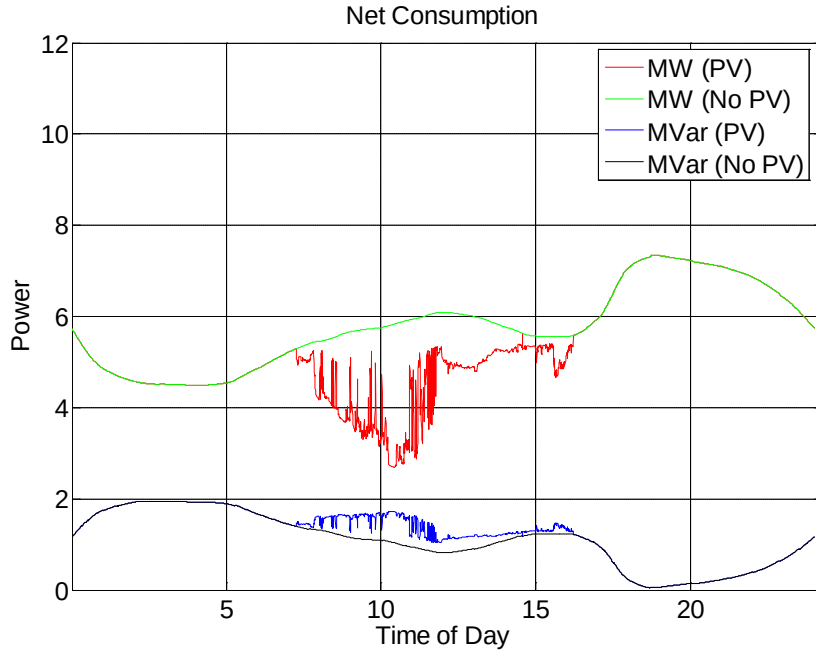

Figure C-27: MW and MVAr net consumption for scenario 3 and case 3.

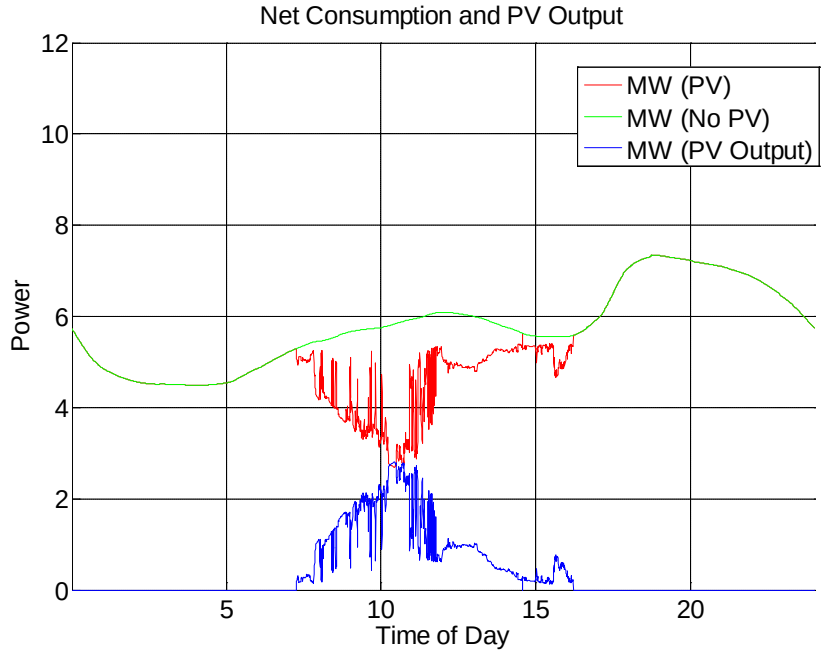

Figure C-28: MW net consumption and total PV generation for scenario 3 and case 3.

C.5 Case 4

Figure C-29 through Figure C-35 show simulation results for scenario 3 and case 4.

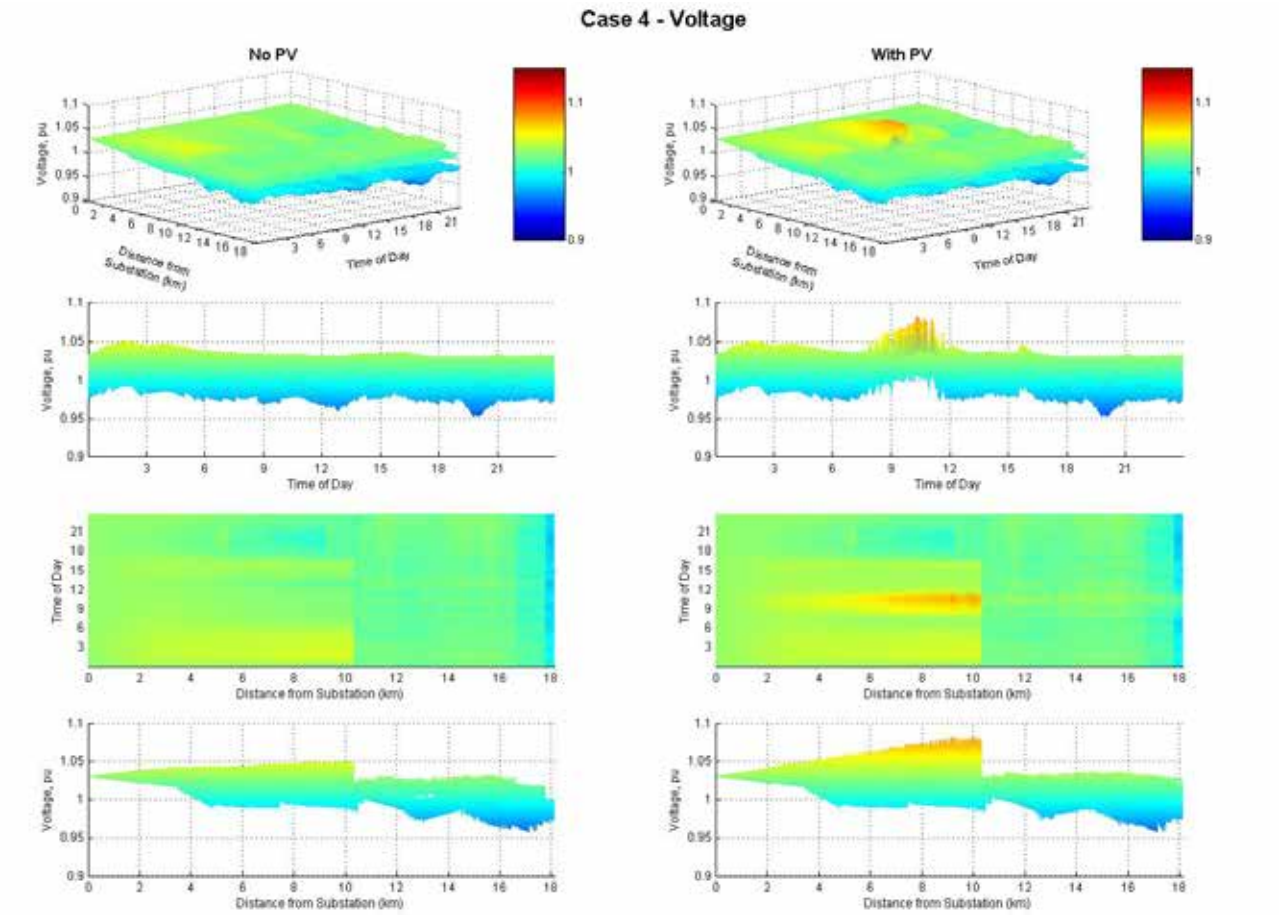

Figure C-29: Daily voltage profile for scenario 3 case 4.

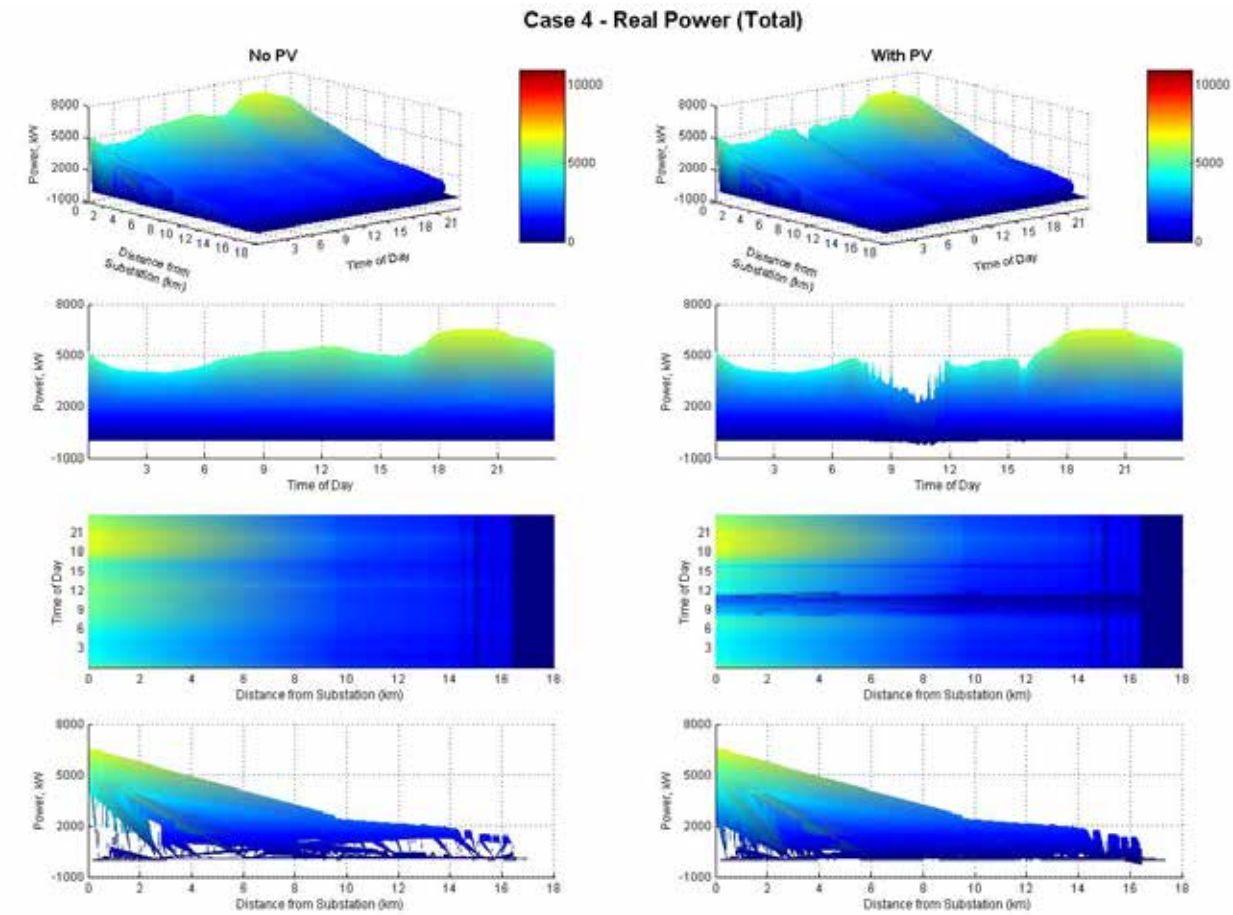

Figure C-30: Daily total real power profile for scenario 3 and case 4.

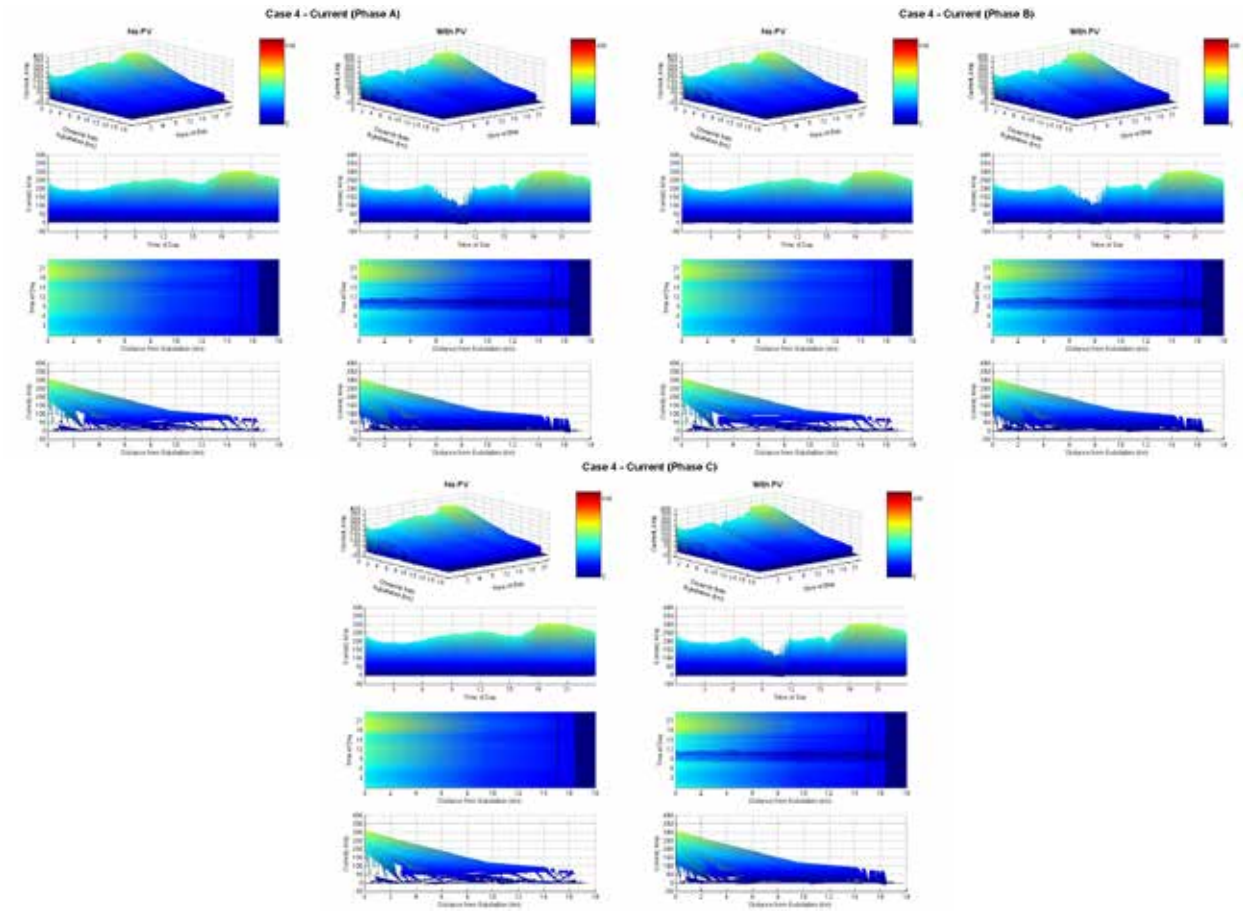

Figure C-31: Daily current profiles for scenario 3 and case 4.

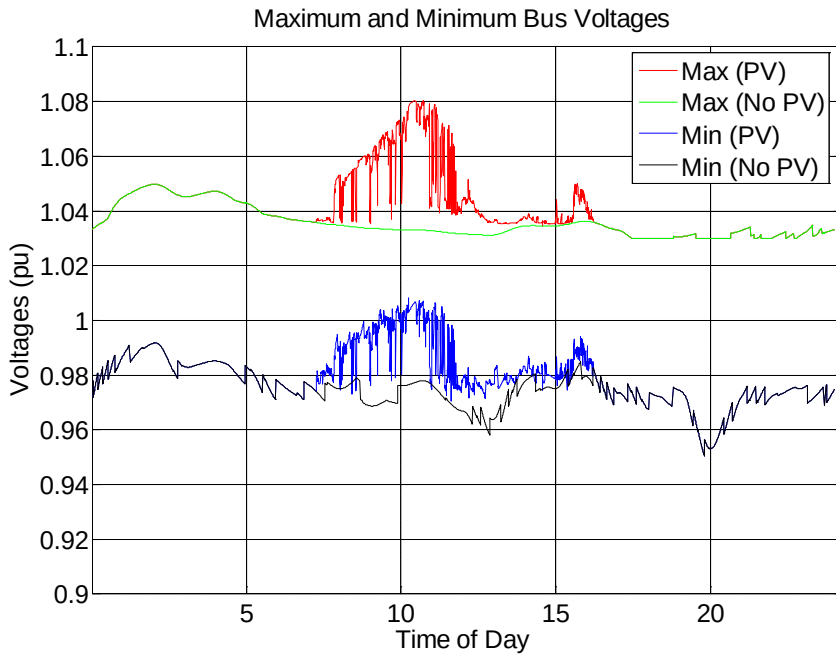

Figure C-32: Maximum and minimum voltages for scenario 3 and case 4.

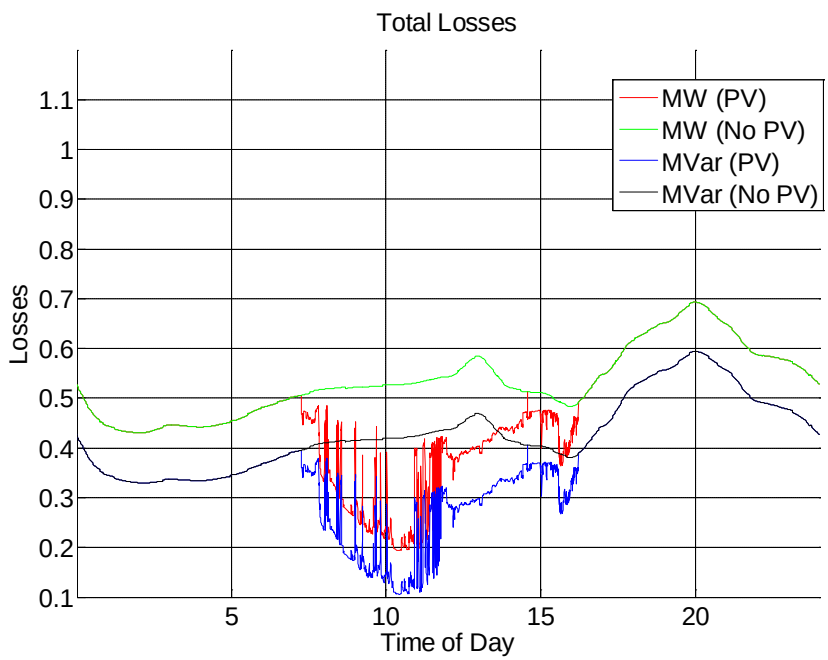

Figure C-33: MW and MVAr losses for scenario 3 and case 4.

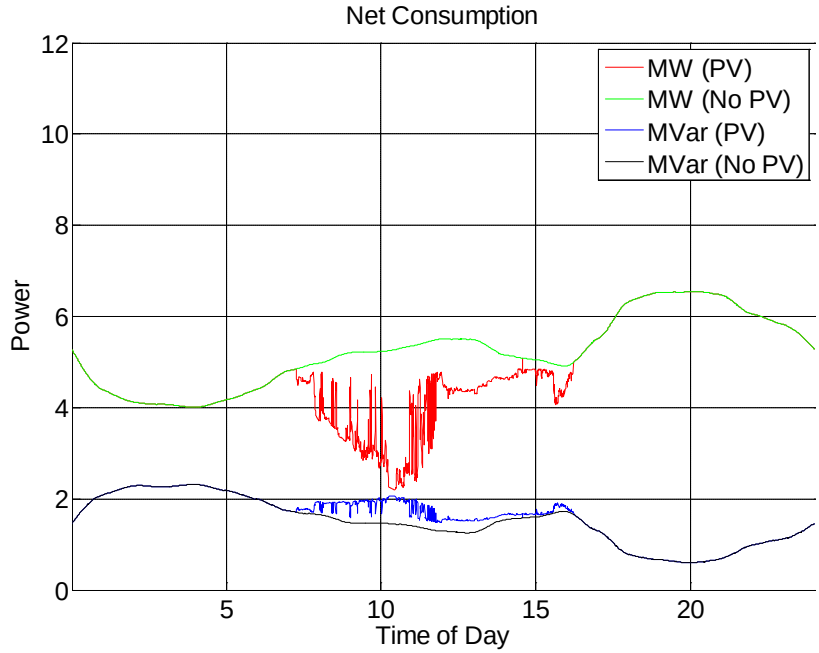

Figure C-34: MW and MVAr net consumption for scenario 3 and case 4.

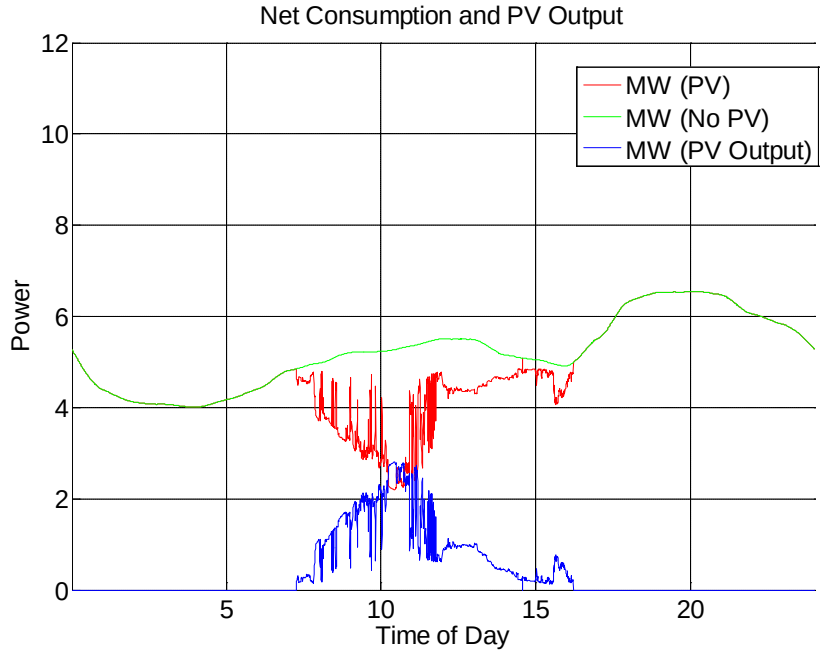

Figure C-35: MW net consumption and total PV generation for scenario 3 and case 4.

C.6 Case 5

Figure C-36 through Figure C-42 show simulation results for scenario 3 and case 5.

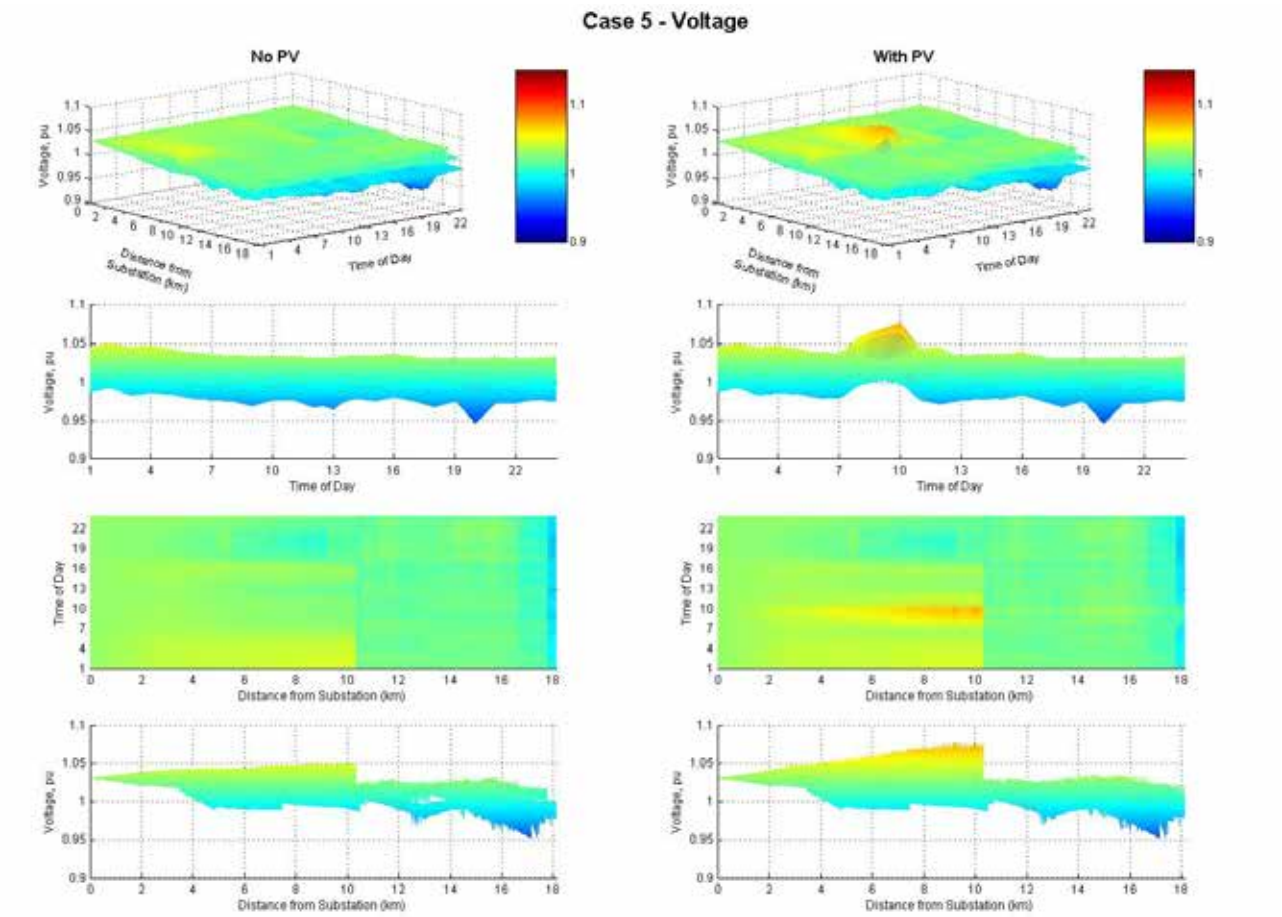

Figure C-36: Daily voltage profile for scenario 3 case 5.

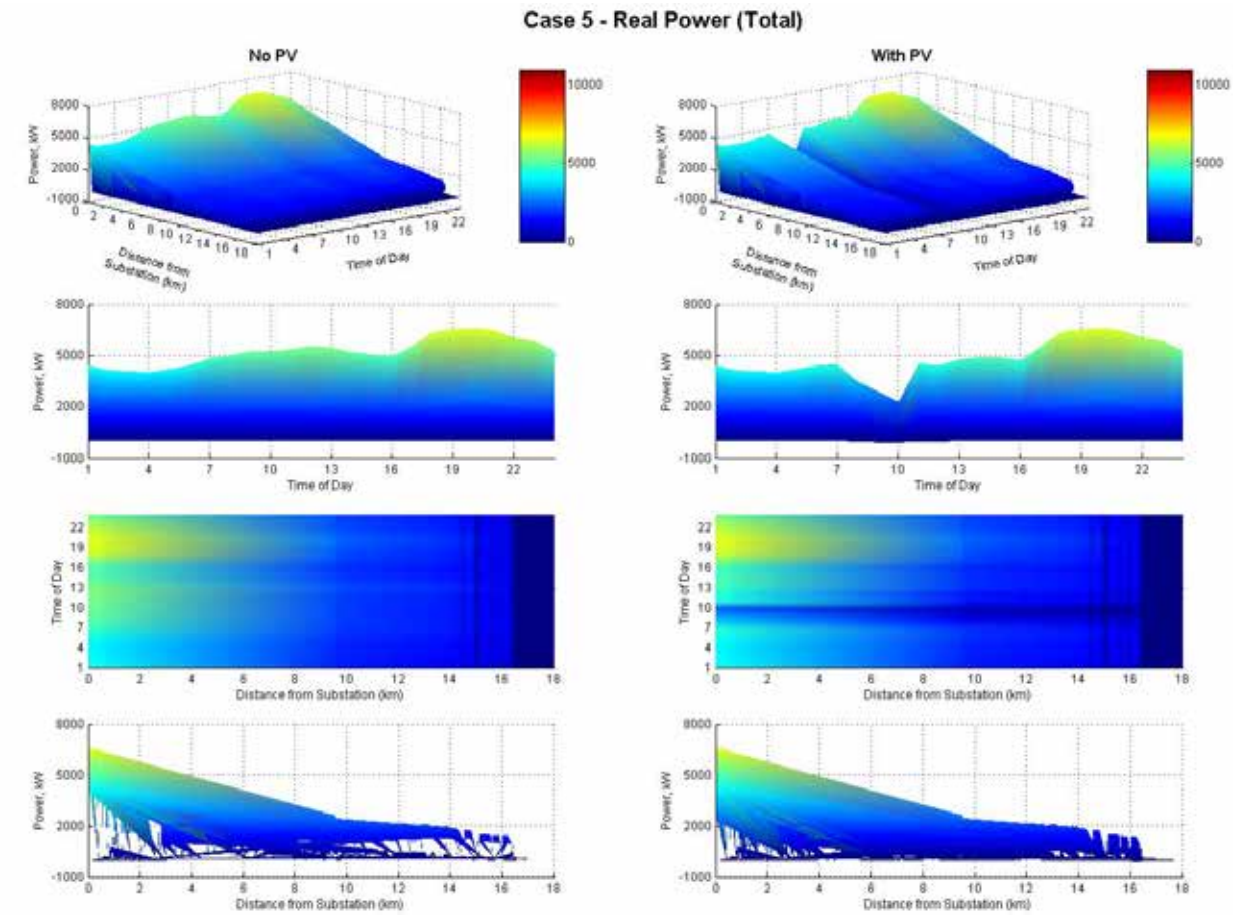

Figure C-37: Daily total real power profile for scenario 3 and case 5.

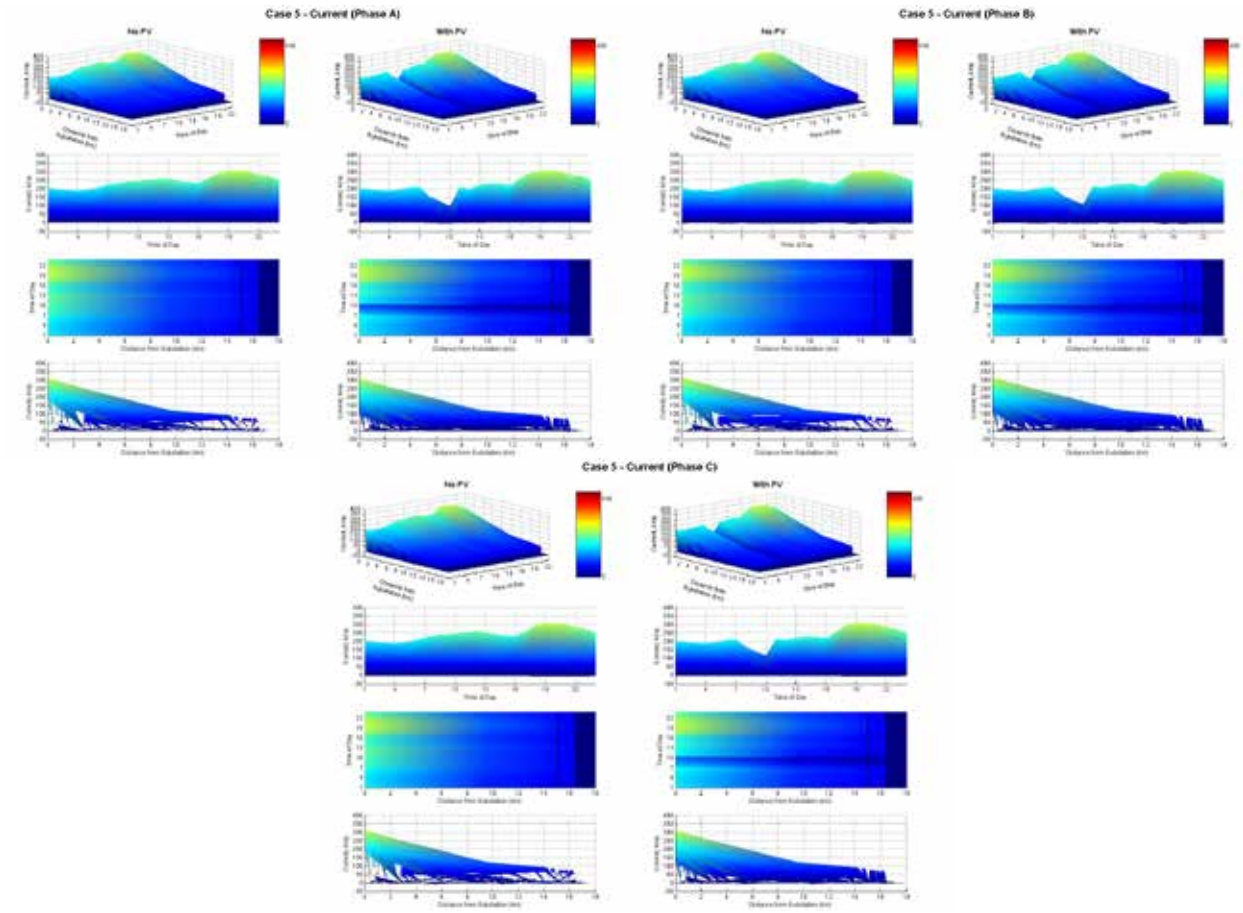

Figure C-38: Daily current profiles for scenario 3 and case 5.

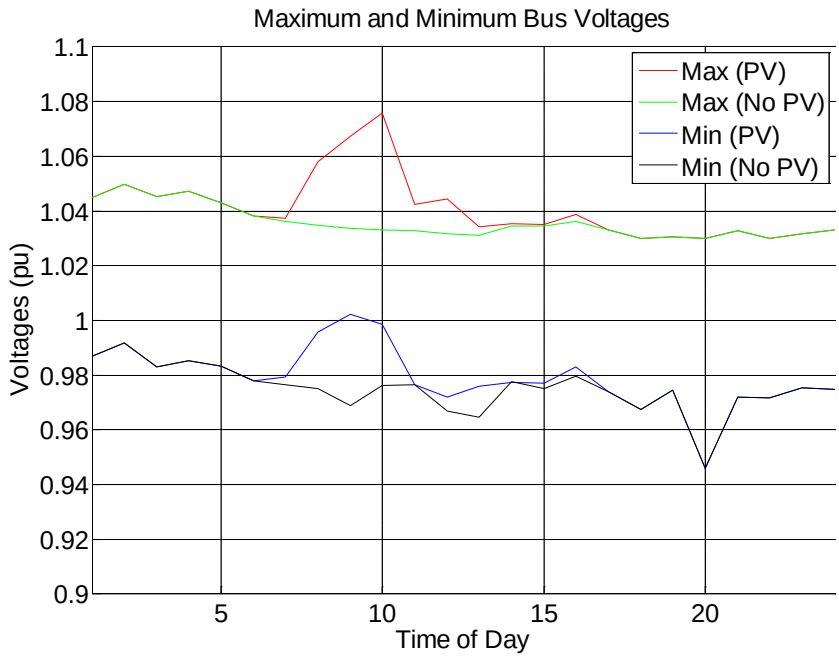

Figure C-39: Maximum and minimum voltages for scenario 3 and case 5.

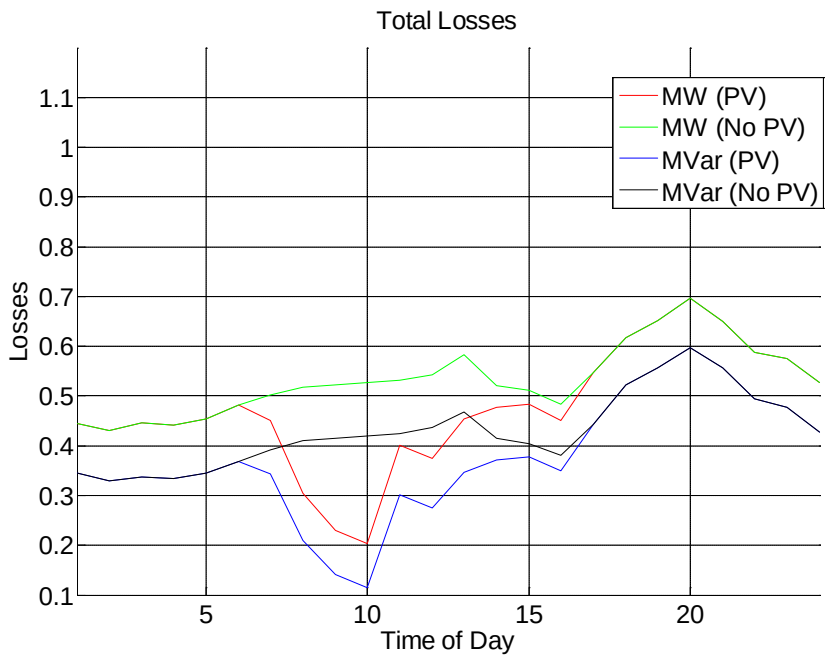

Figure C-40: MW and MVAr losses for scenario 3 and case 5.

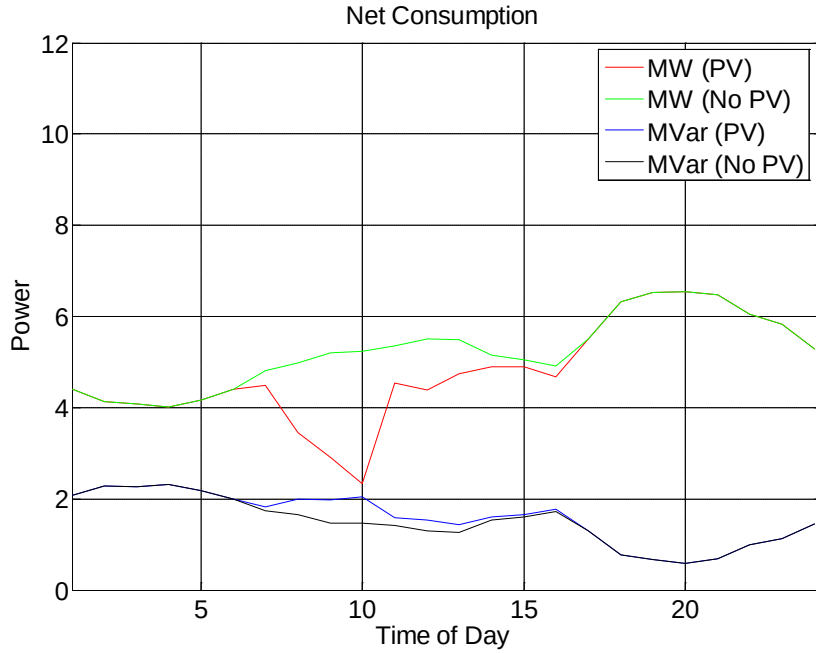

Figure C-41: MW and MVAr net consumption for scenario 3 and case 5.

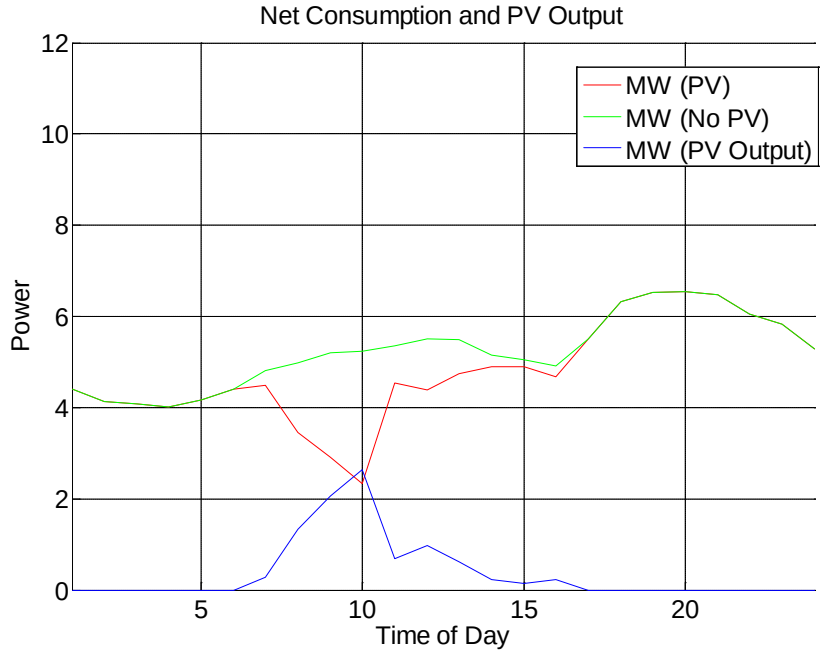

Figure C-42: MW net consumption and total PV generation for scenario 3 and case 5.

C.7 Case 6

Figure C-43 through Figure C-49 show simulation results for scenario 3 and case 5.

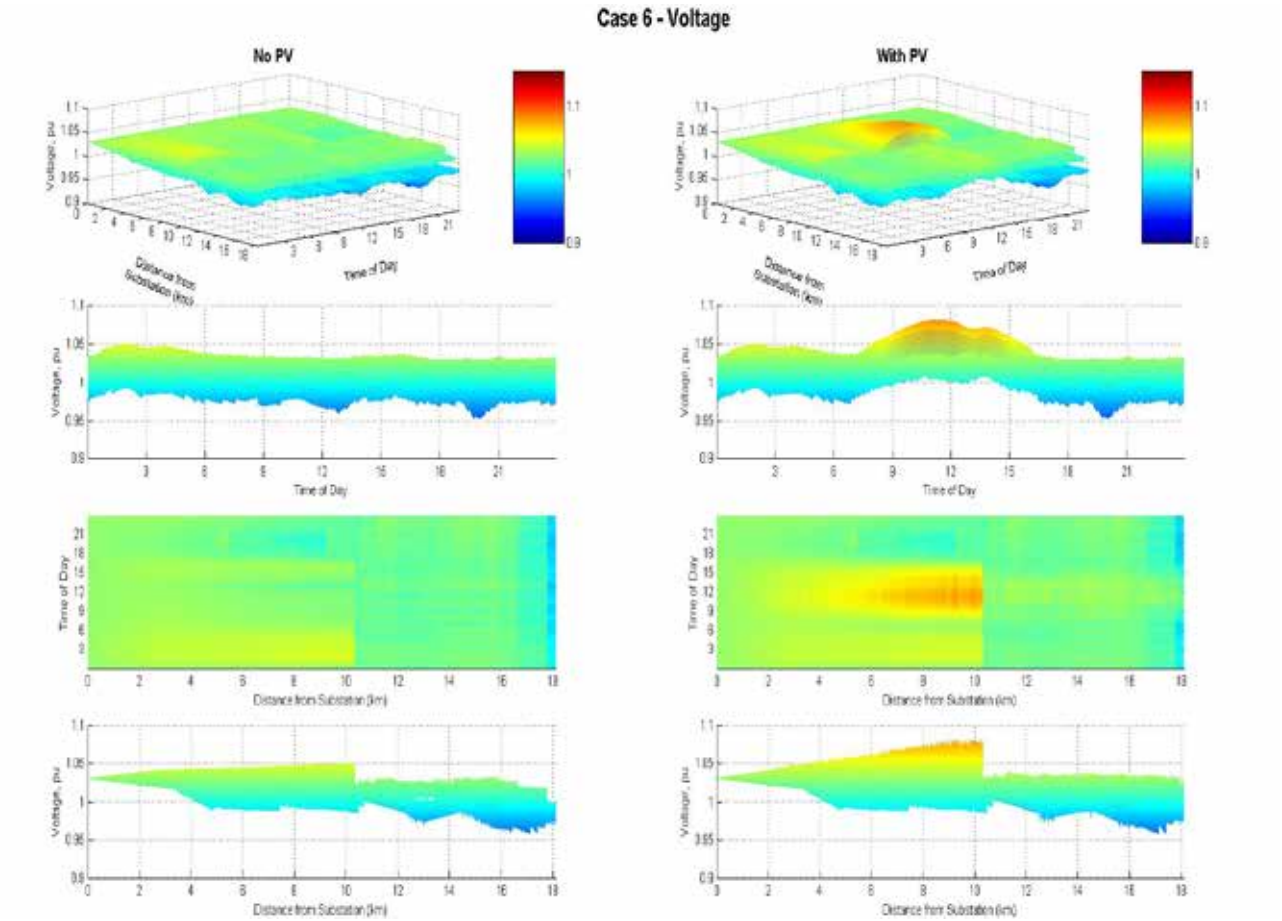

Figure C-43: Daily voltage profile for scenario 3 case 6.

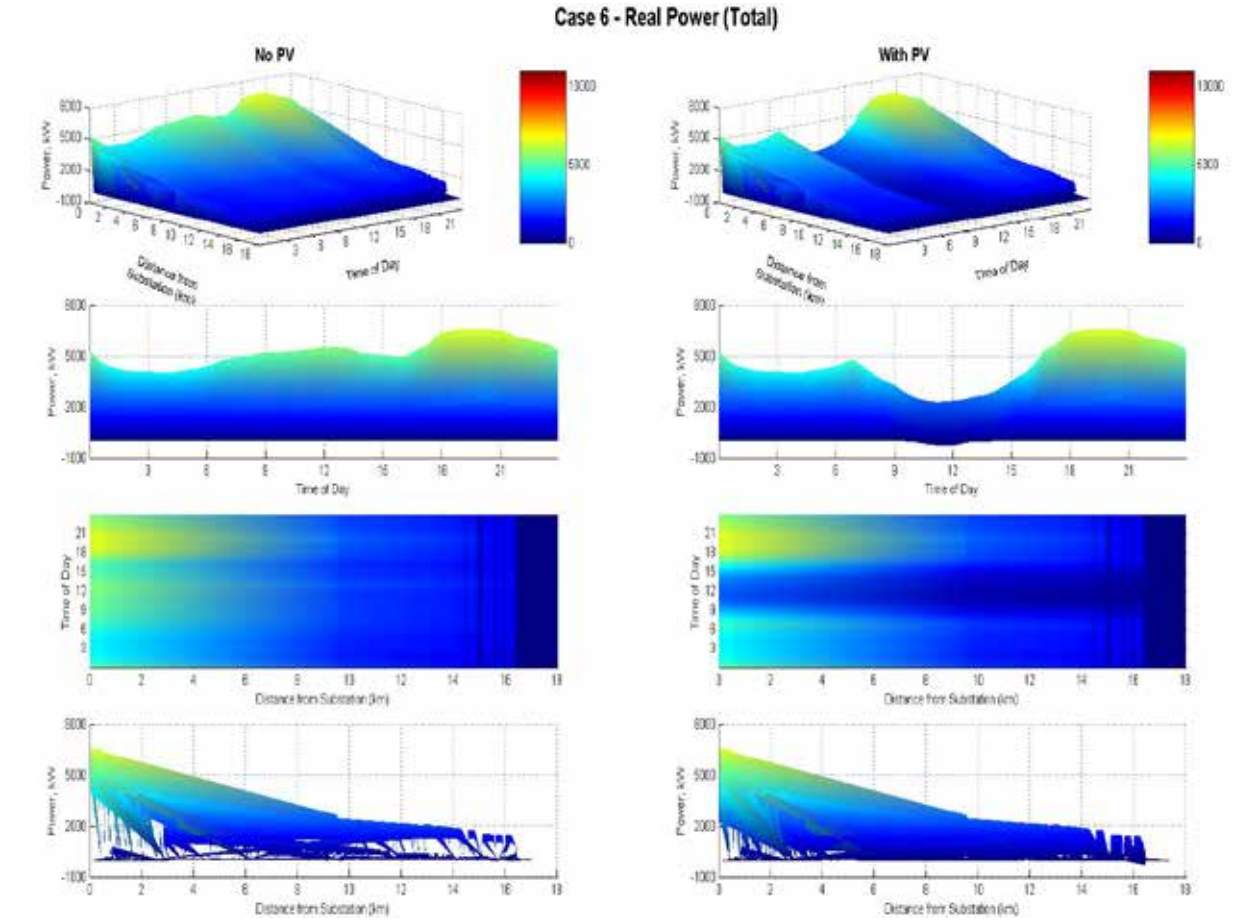

Figure C-44: Daily total real power profile for scenario 3 and case 6.

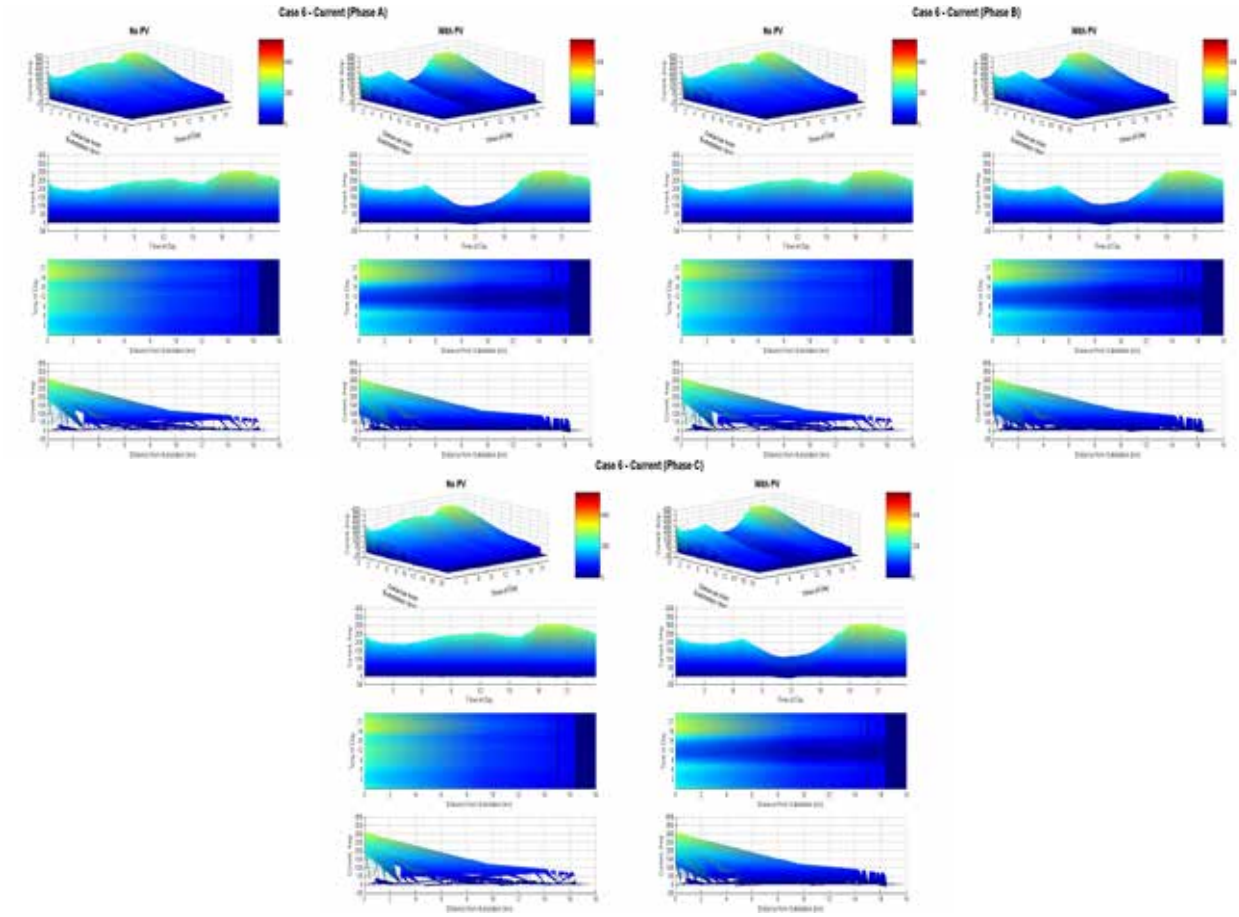

Figure C-45: Daily current profiles for scenario 3 and case 6.

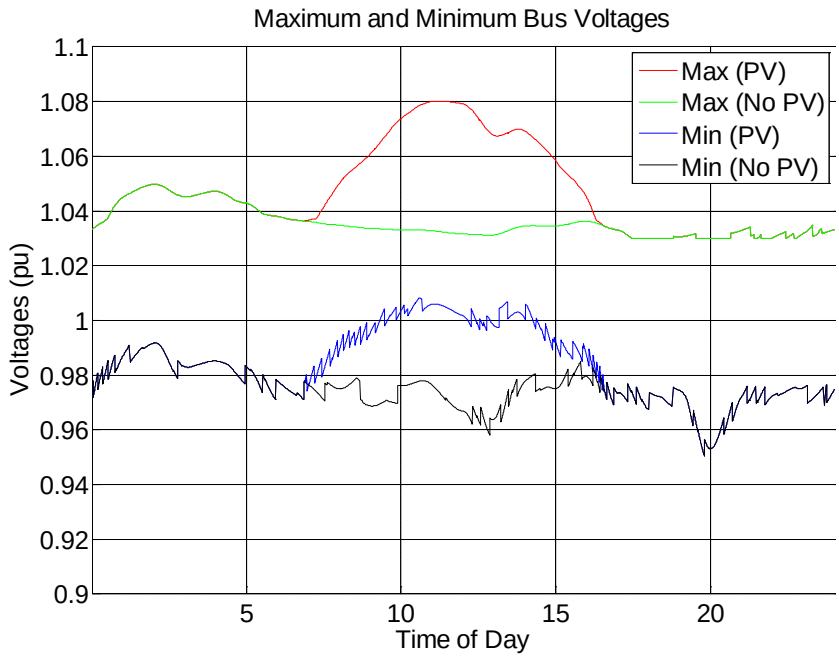

Figure C-46: Maximum and minimum voltages for scenario 3 and case 6.

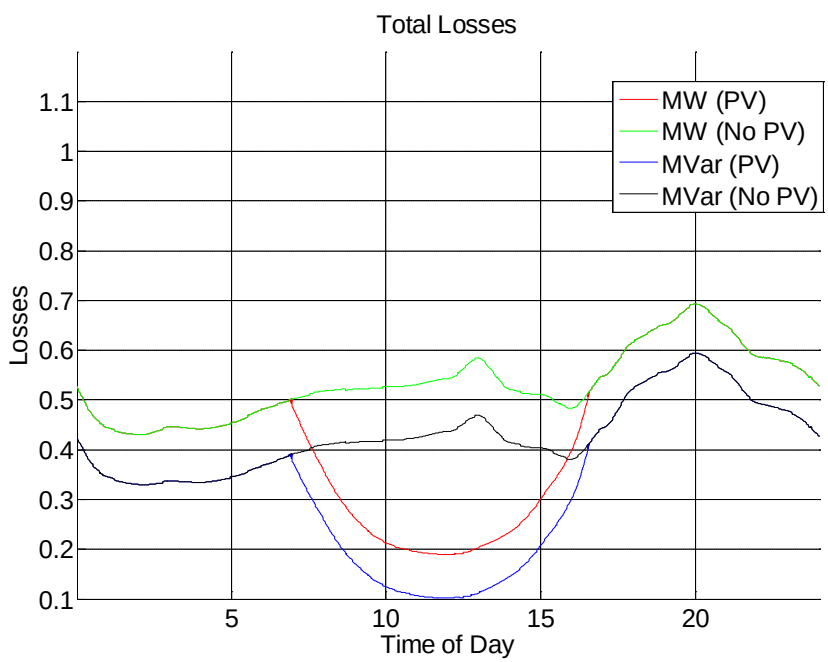

Figure C-47: MW and MVAr losses for scenario 3 and case 6.

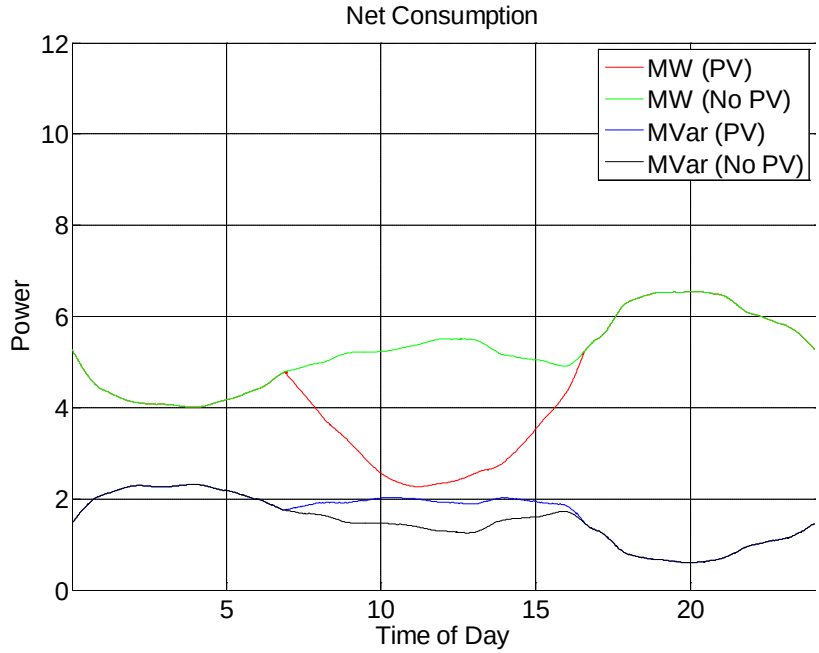

Figure C-48: MW and MVAr net consumption for scenario 3 and case 6.

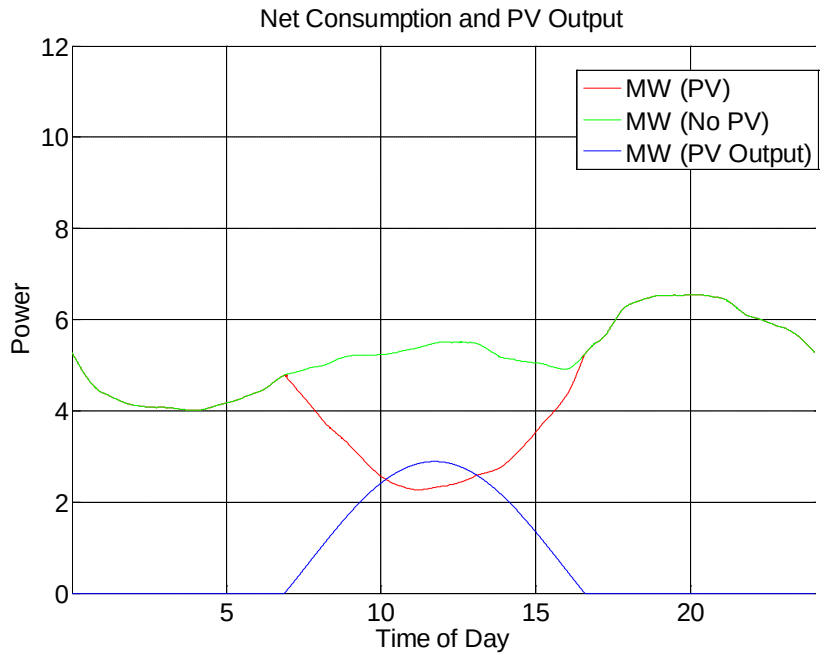

Figure C-49: MW net consumption and total PV generation for scenario 3 and case 6.

Appendix D - Scenario 4

In this Section we present the simulation results obtained for scenario 4 (the PV rating for this scenario totals in 2.975 MW (~ 25 % of the total load MW rating)).

D.1 Case 0

Figure D-1 through Figure D-7 show simulation results for scenario 4 and case 0.

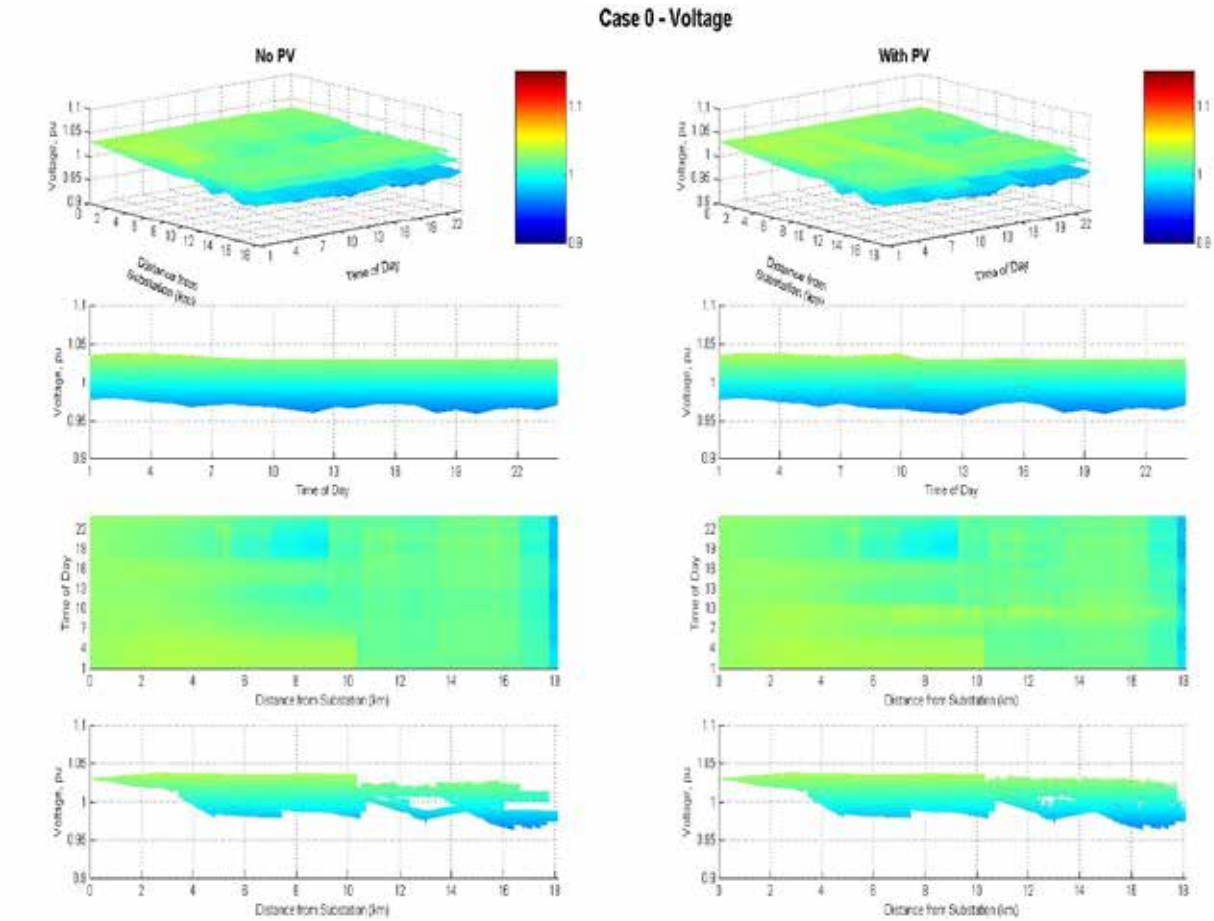

Figure D-1: Daily voltage profile for scenario 4 case 0.

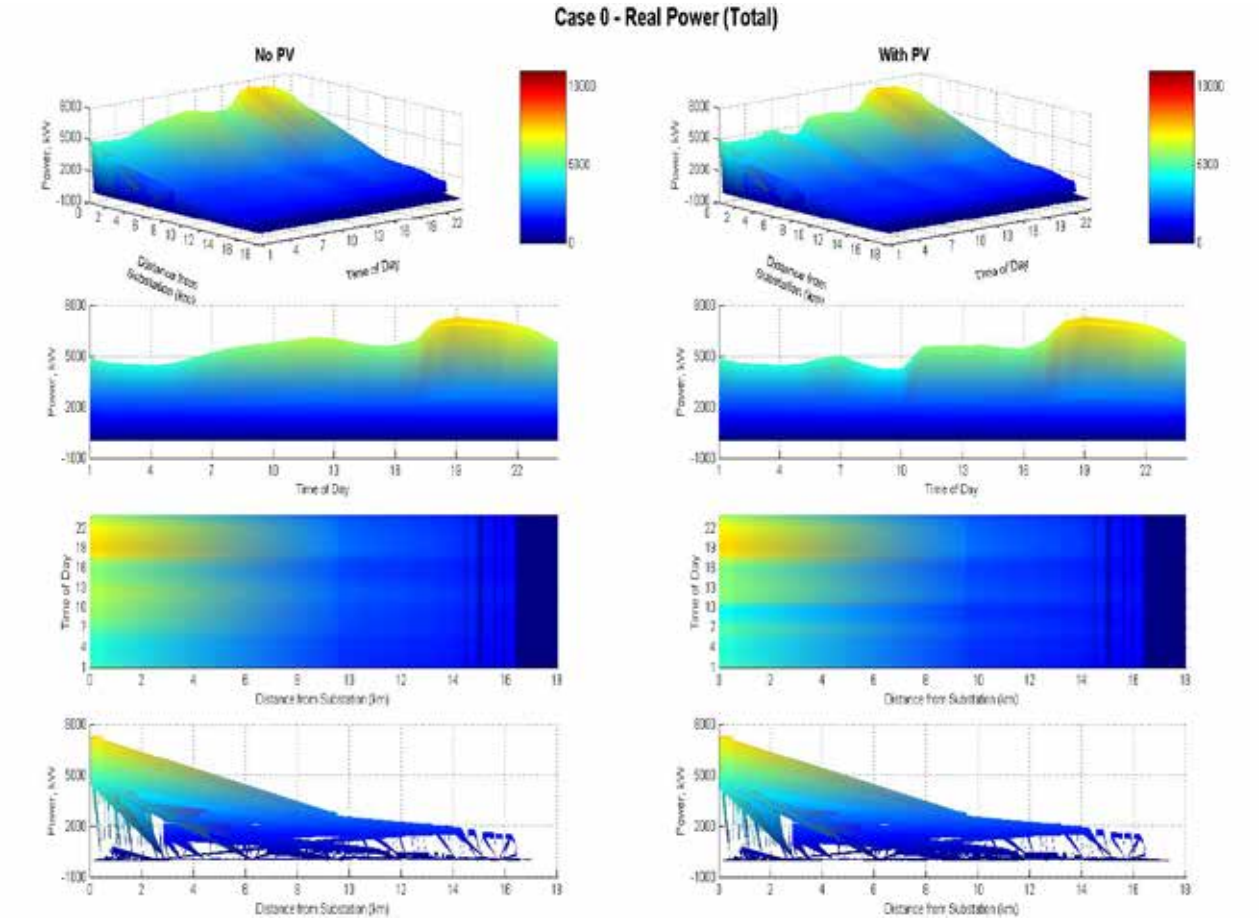

Figure D-2: Daily total real power profile for scenario 4 and case 0.

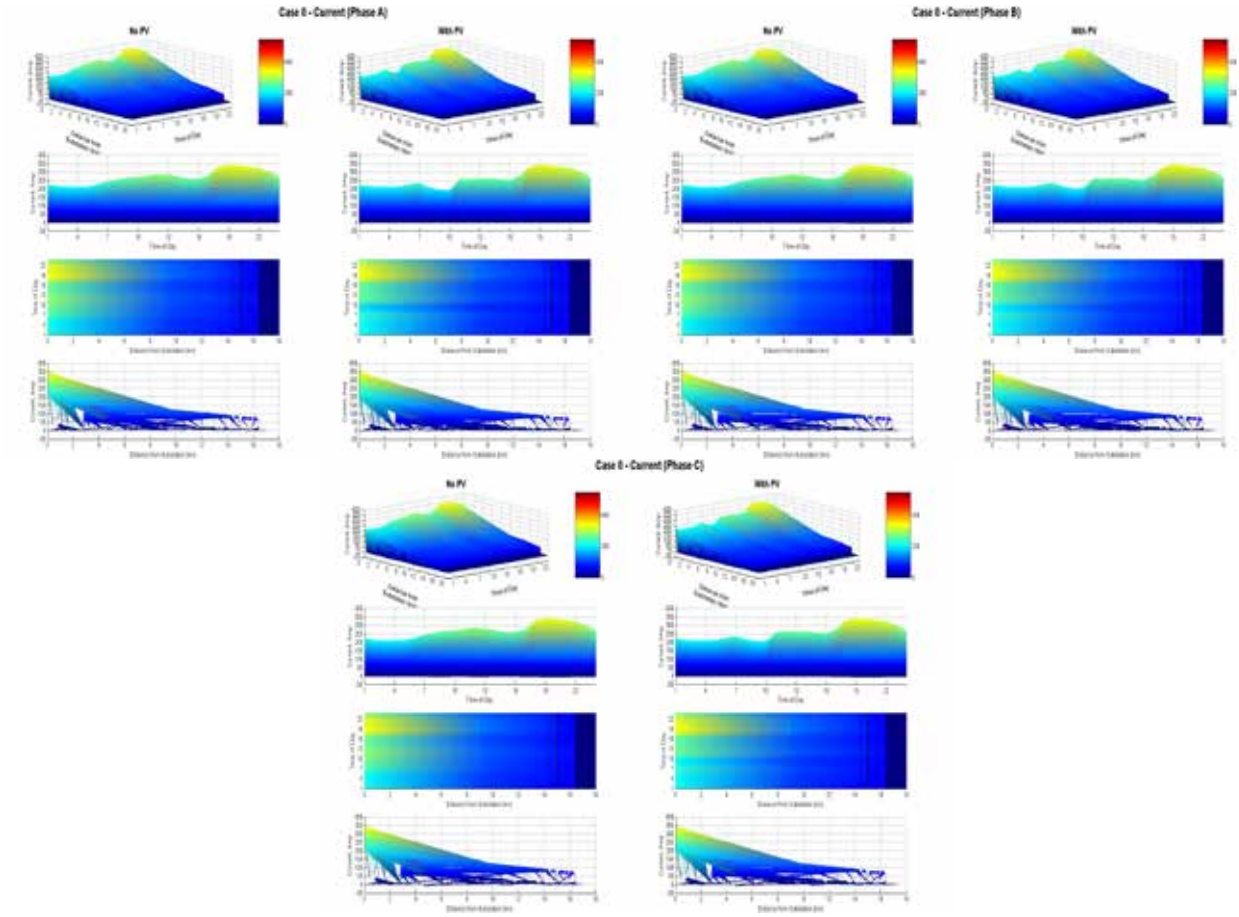

Figure D-3: Daily current profiles for scenario 4 and case 0.

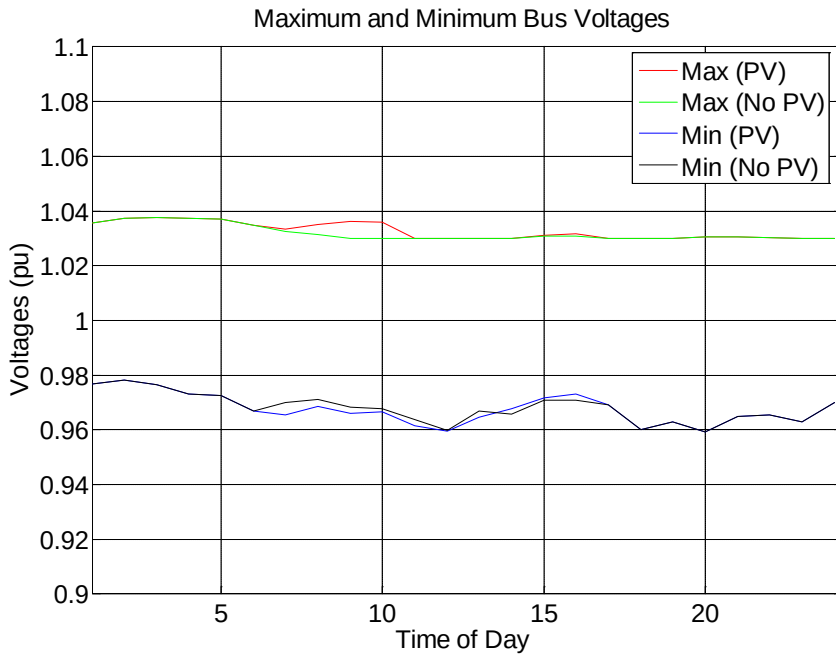

Figure D-4: Maximum and minimum voltages for scenario 4 and case 0.

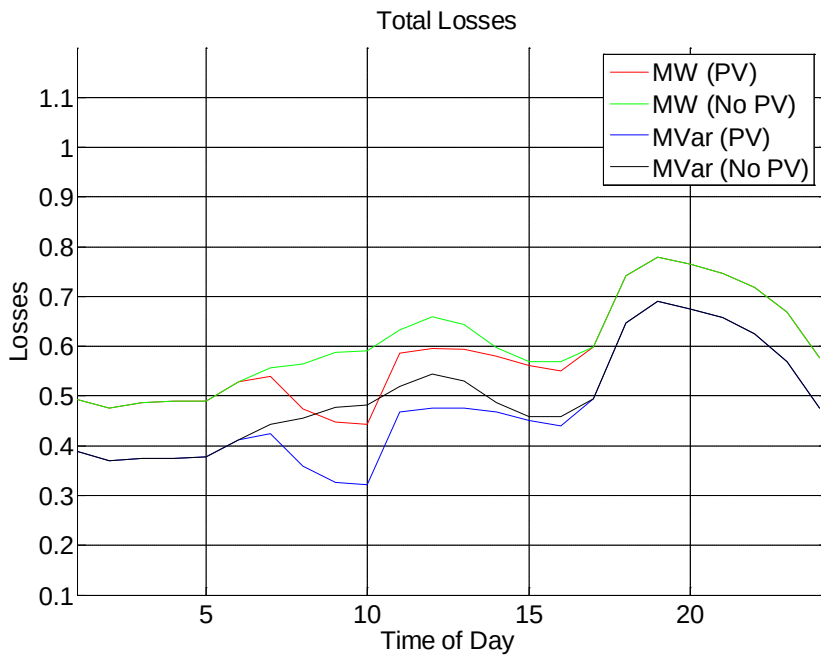

Figure D-5: MW and MVAr losses for scenario 4 and case 0.

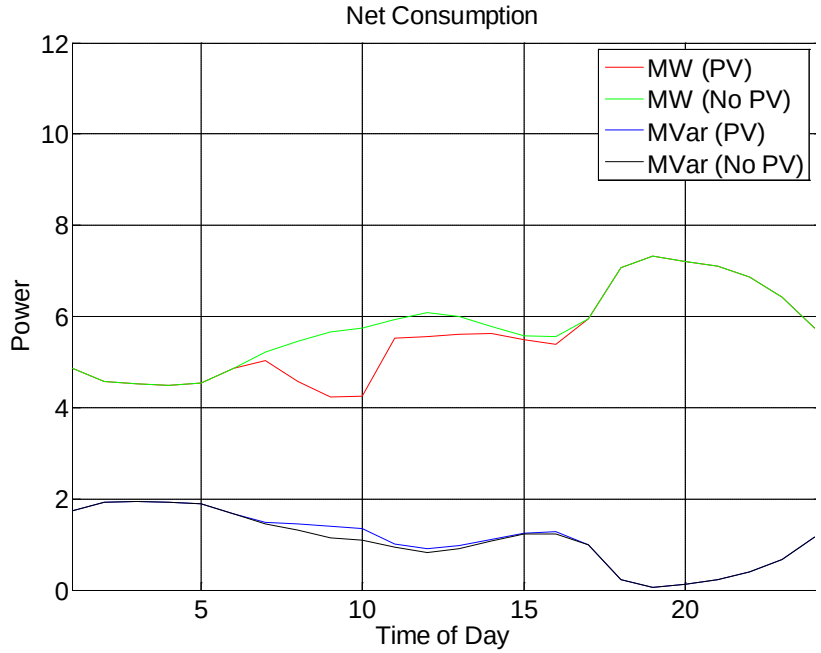

Figure D-6: MW and MVAr net consumption for scenario 4 and case 0.

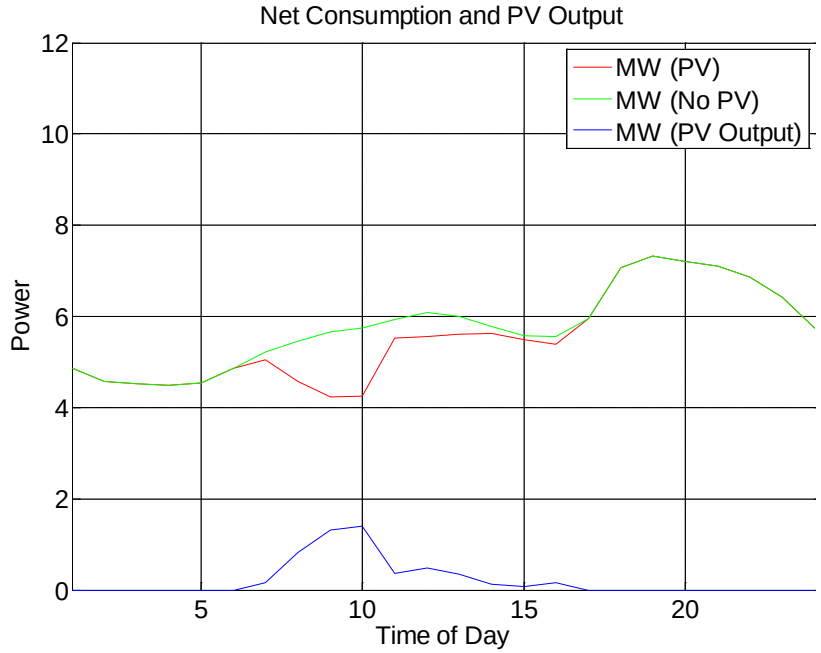

Figure D-7: MW net consumption and total PV generation for scenario 4 and case 0.

D.2 Case 1

Figure D-8 through Figure D-14 show simulation results for scenario 4 and case 1.

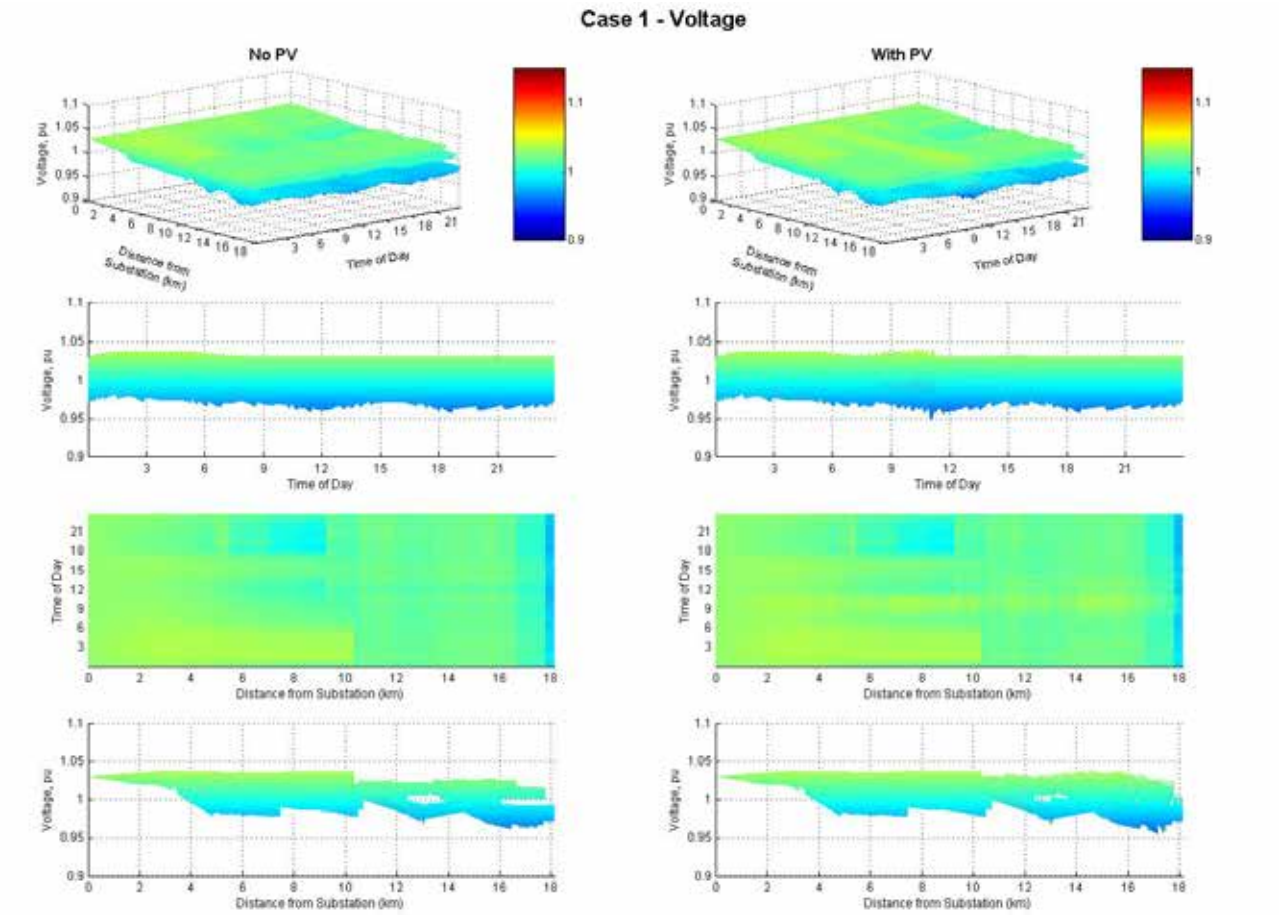

Figure D-8: Daily voltage profile for scenario 4 case 1.

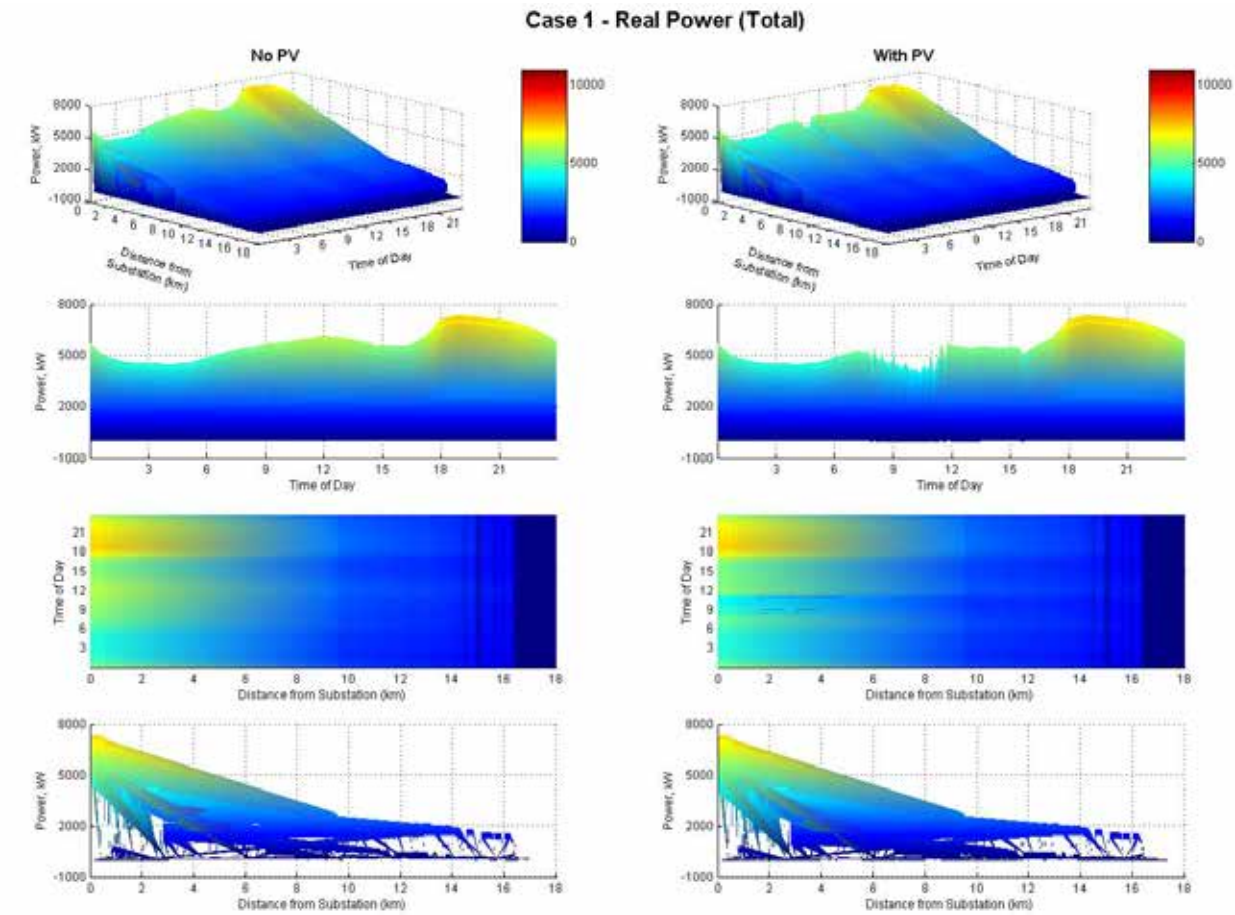

Figure D-9: Daily total real power profile for scenario 4 and case 1.

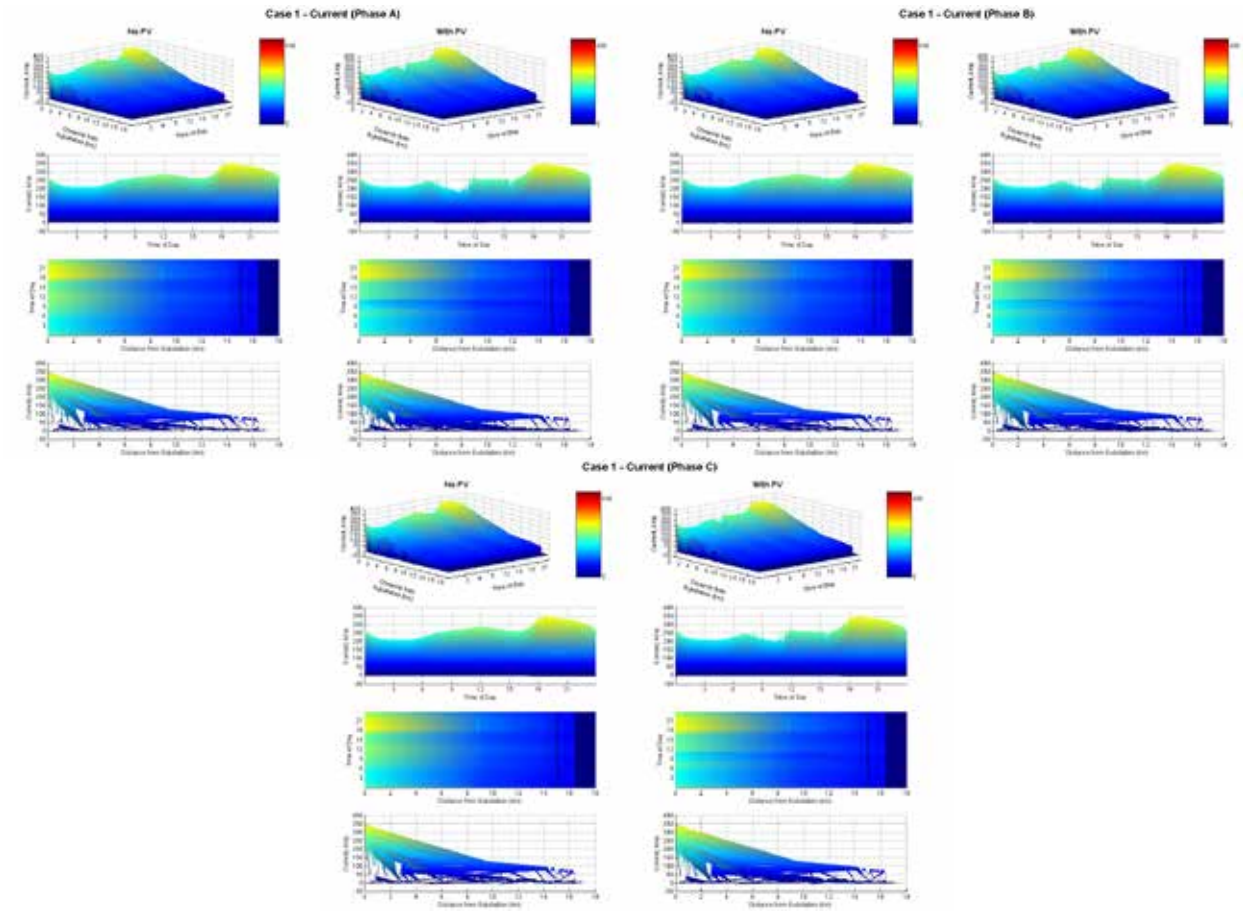

Figure D-10: Daily current profiles for scenario 4 and case 1.

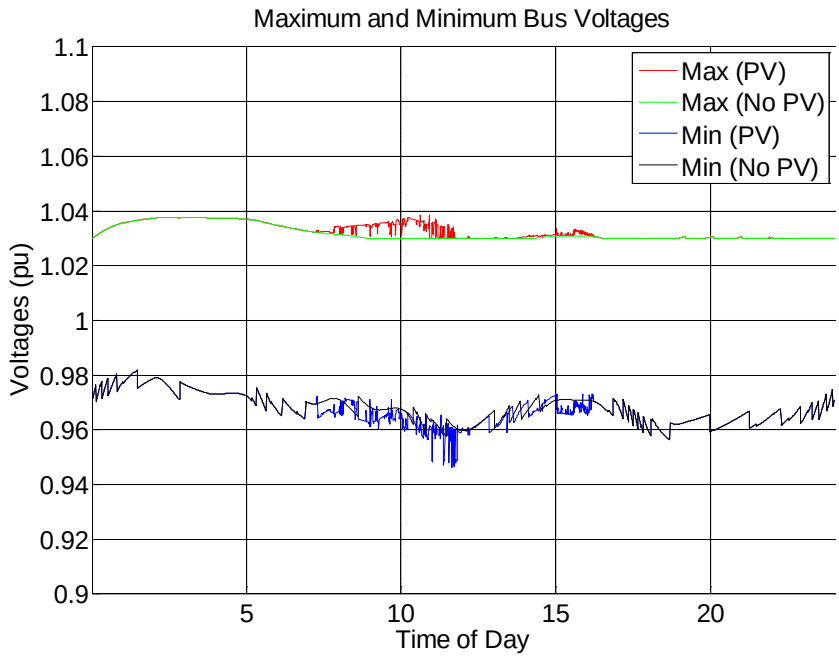

Figure D-11: Maximum and minimum voltages for scenario 4 and case 1.

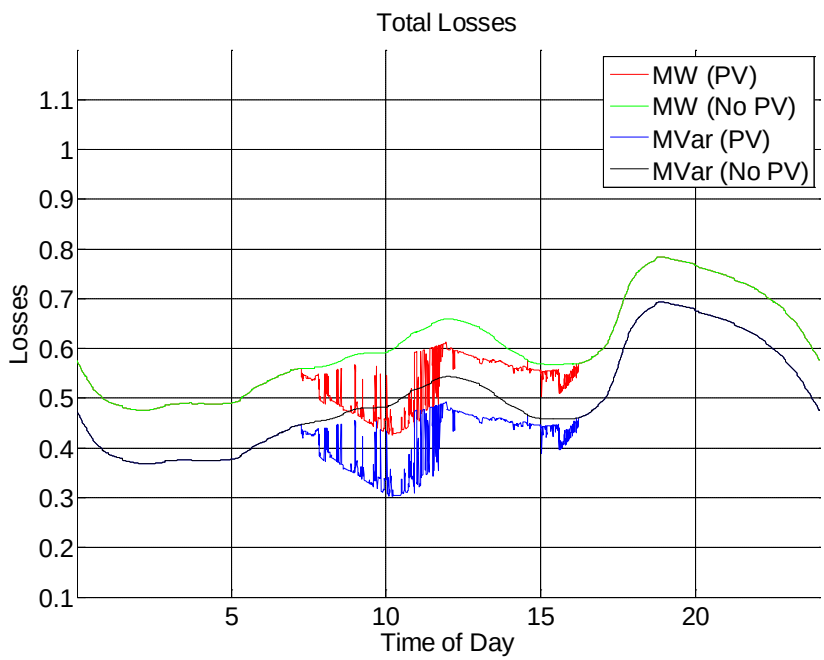

Figure D-12: MW and MVAr losses for scenario 4 and case 1.

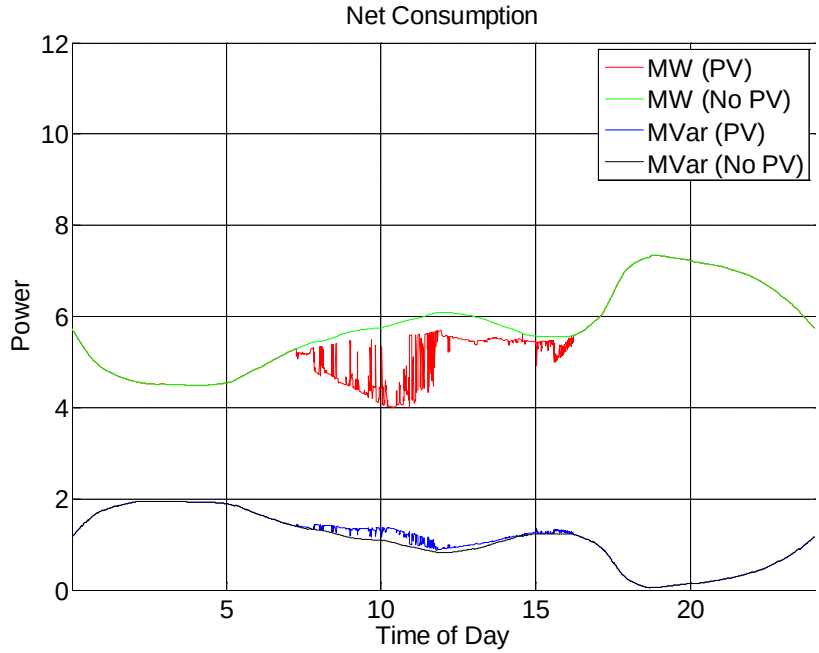

Figure D-13: MW and MVAr net consumption for scenario 4 and case 1.

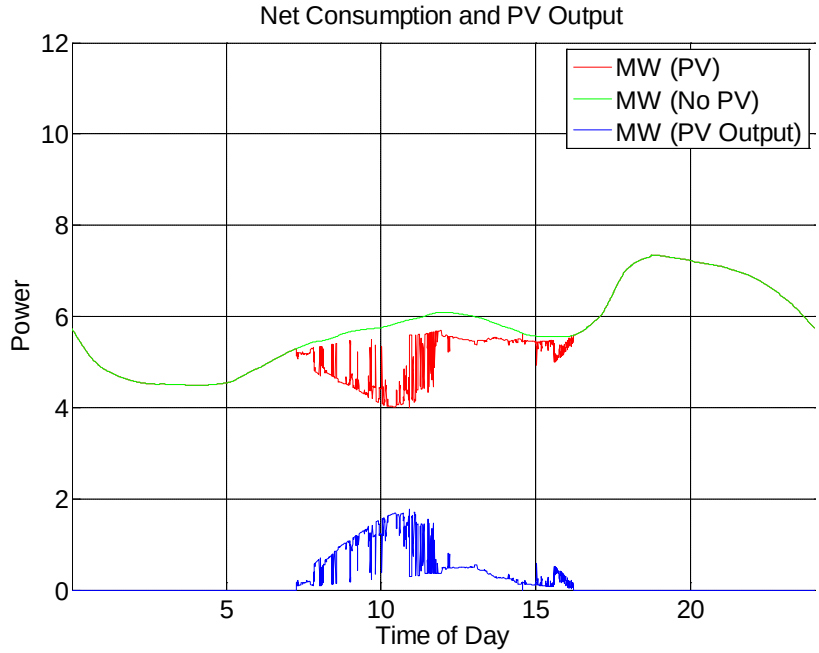

Figure D-14: MW net consumption and total PV generation for scenario 4 and case 1.

D.3 Case 2

Figure D-15 through Figure D-21 show simulation results for scenario 4 and case 2.

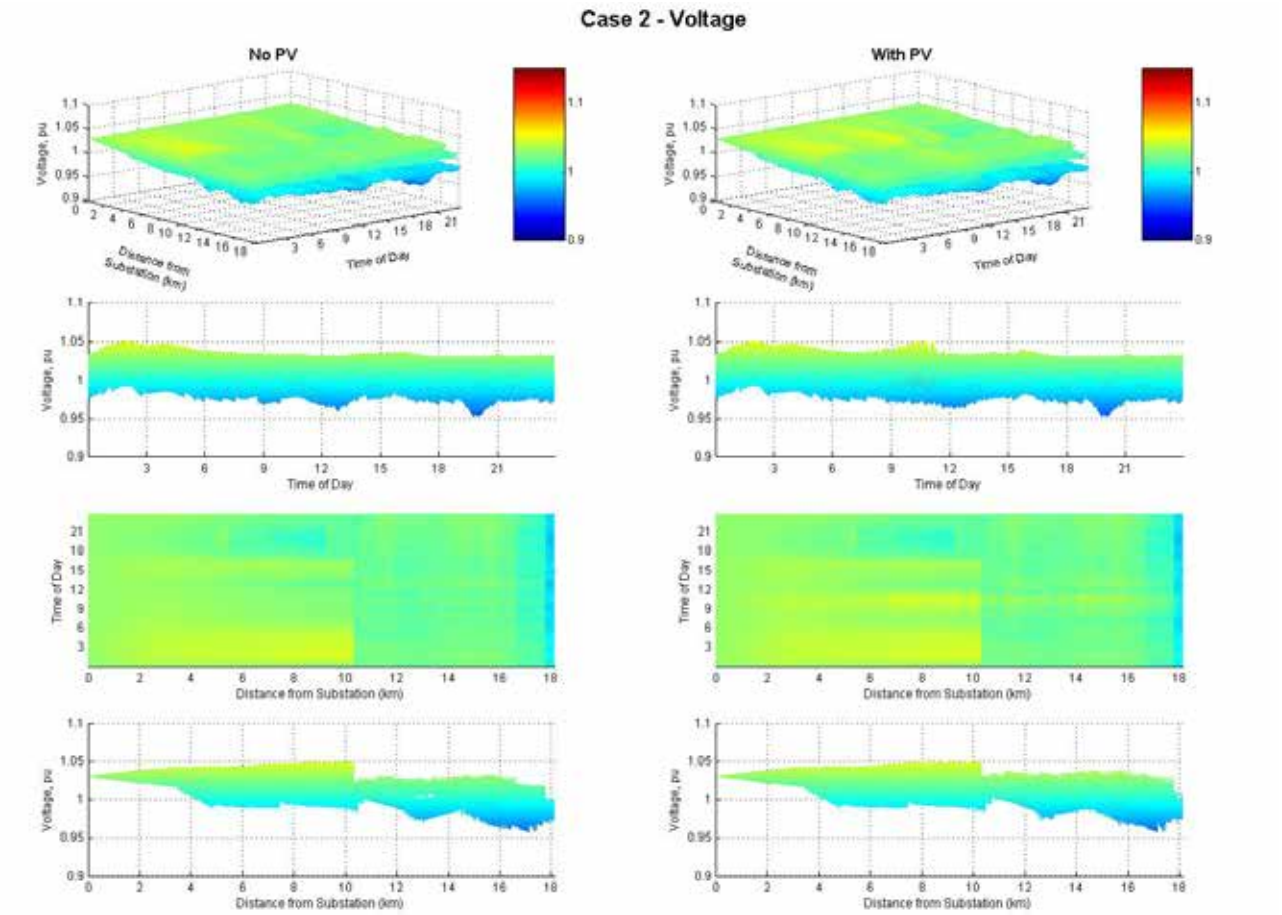

Figure D-15: Daily voltage profile for scenario 4 case 2.

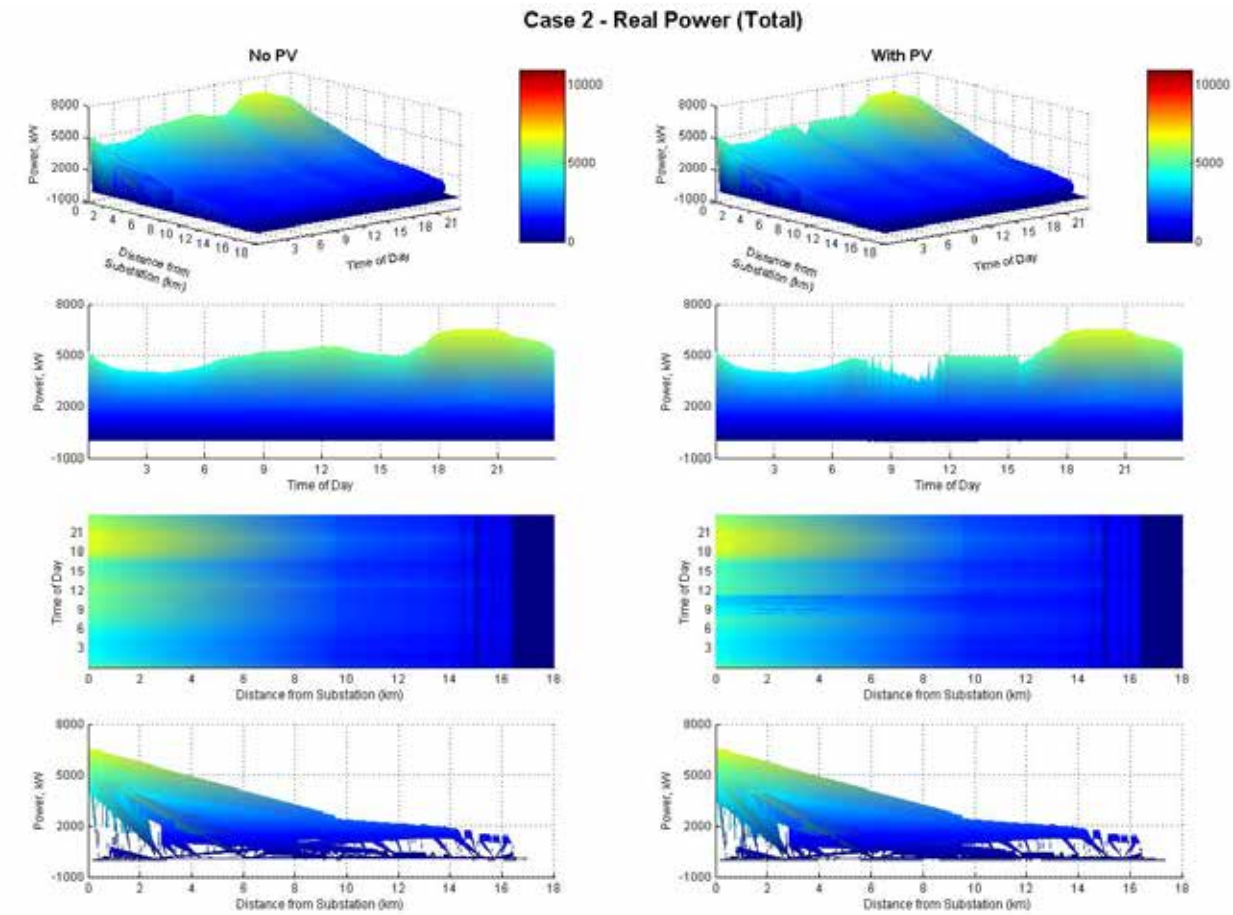

Figure D-16: Daily total real power profile for scenario 4 and case 2.

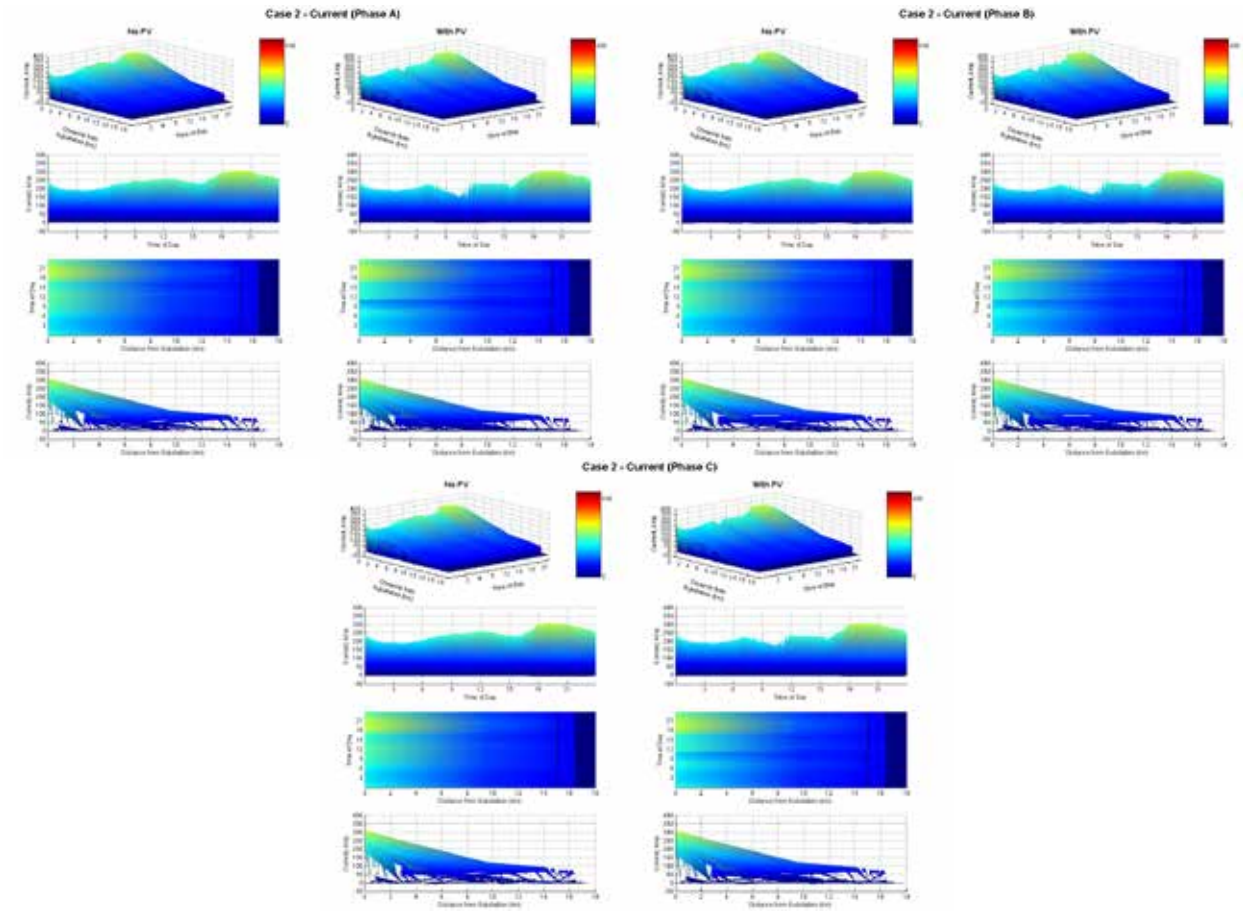

Figure D-17: Daily current profiles for scenario 4 and case 2.

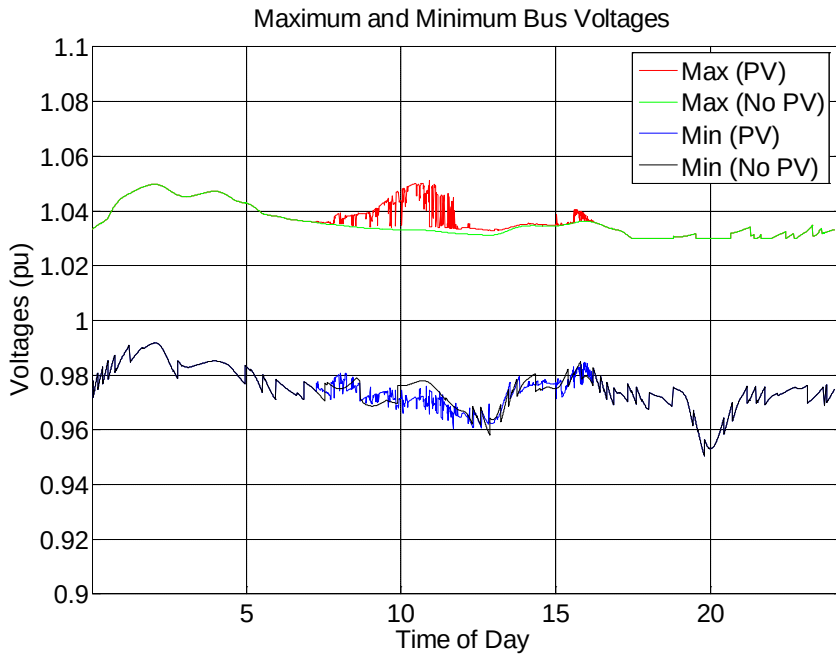

Figure D-18: Maximum and minimum voltages for scenario 4 and case 2.

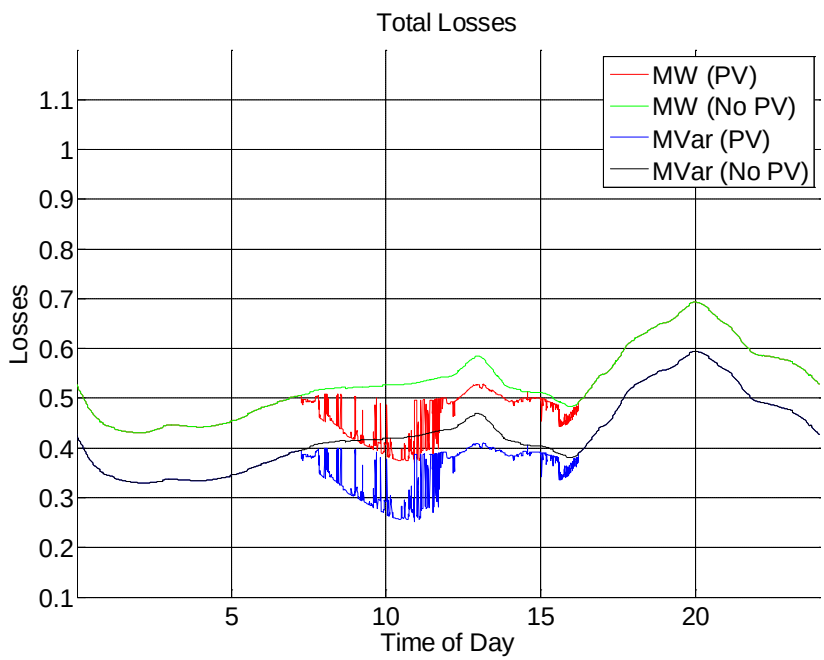

Figure D-19: MW and MVAr losses for scenario 4 and case 2.

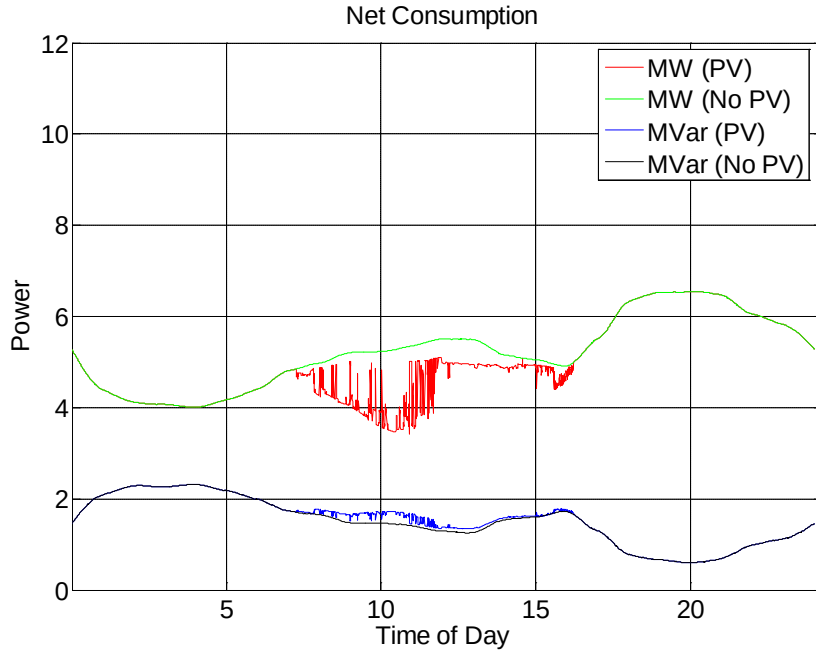

Figure D-20: MW and MVAr net consumption for scenario 4 and case 2.

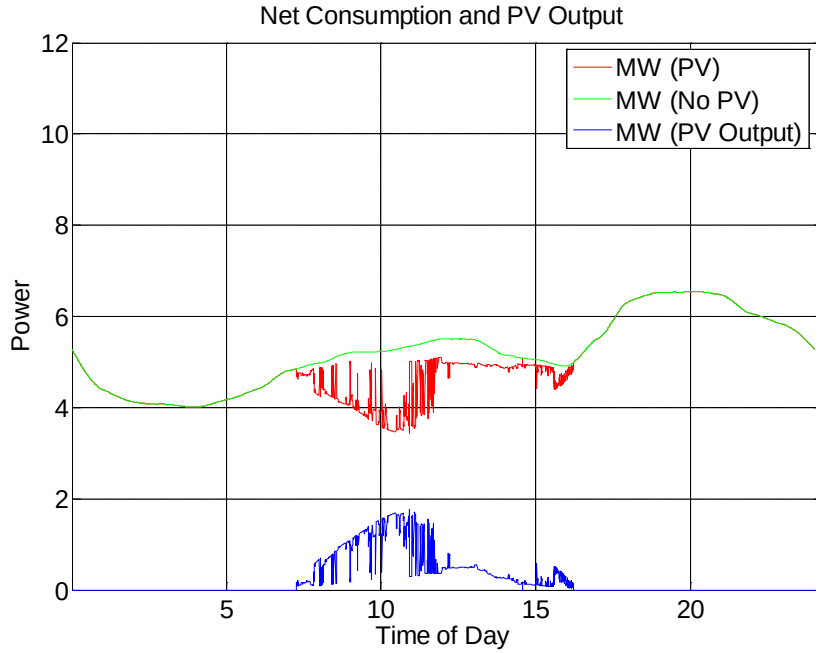

Figure D-21: MW net consumption and total PV generation for scenario 4 and case 2.

D.4 Case 3

Figure D-22 through Figure D-28 show simulation results for scenario 4 and case 3.

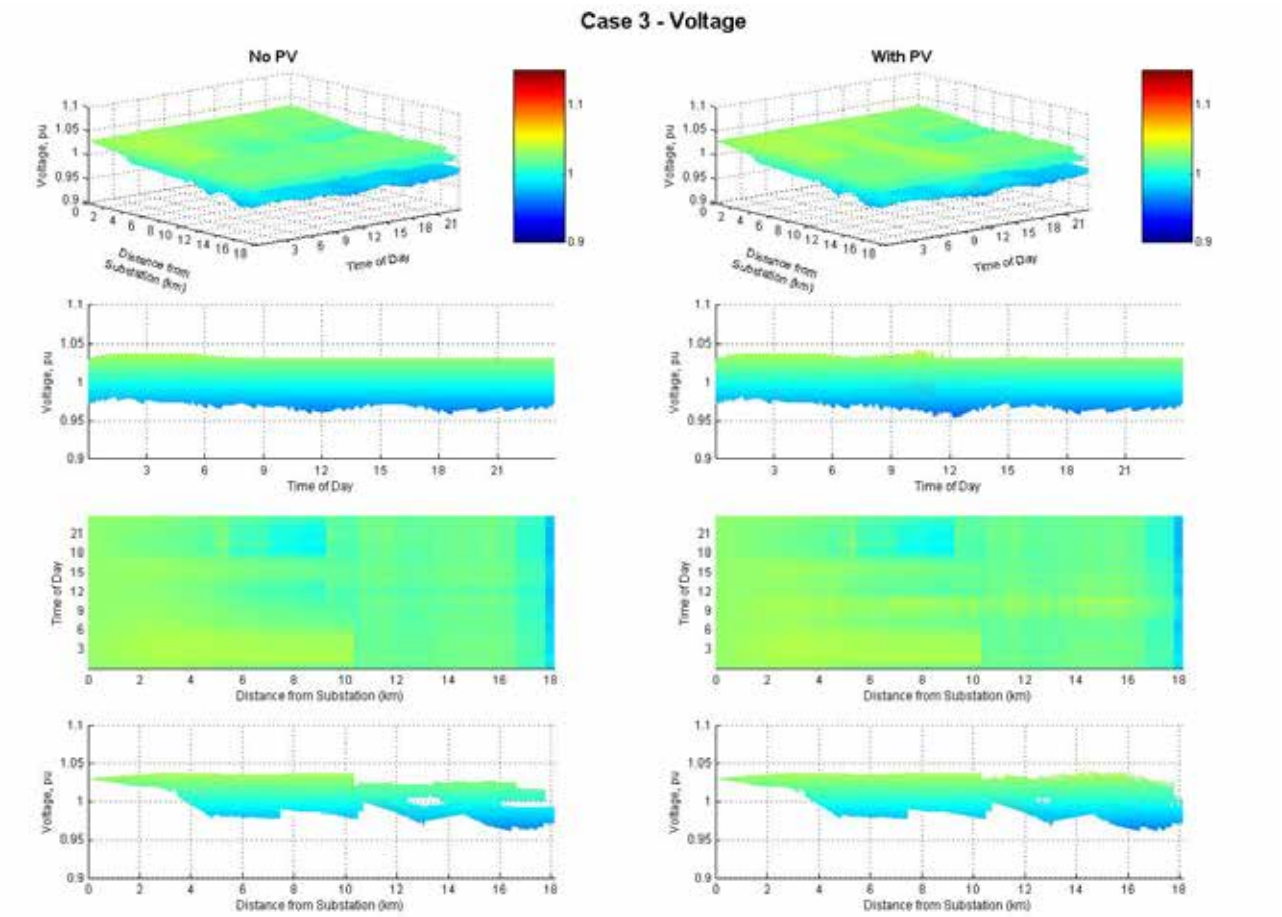

Figure D-22: Daily voltage profile for scenario 4 case 3.

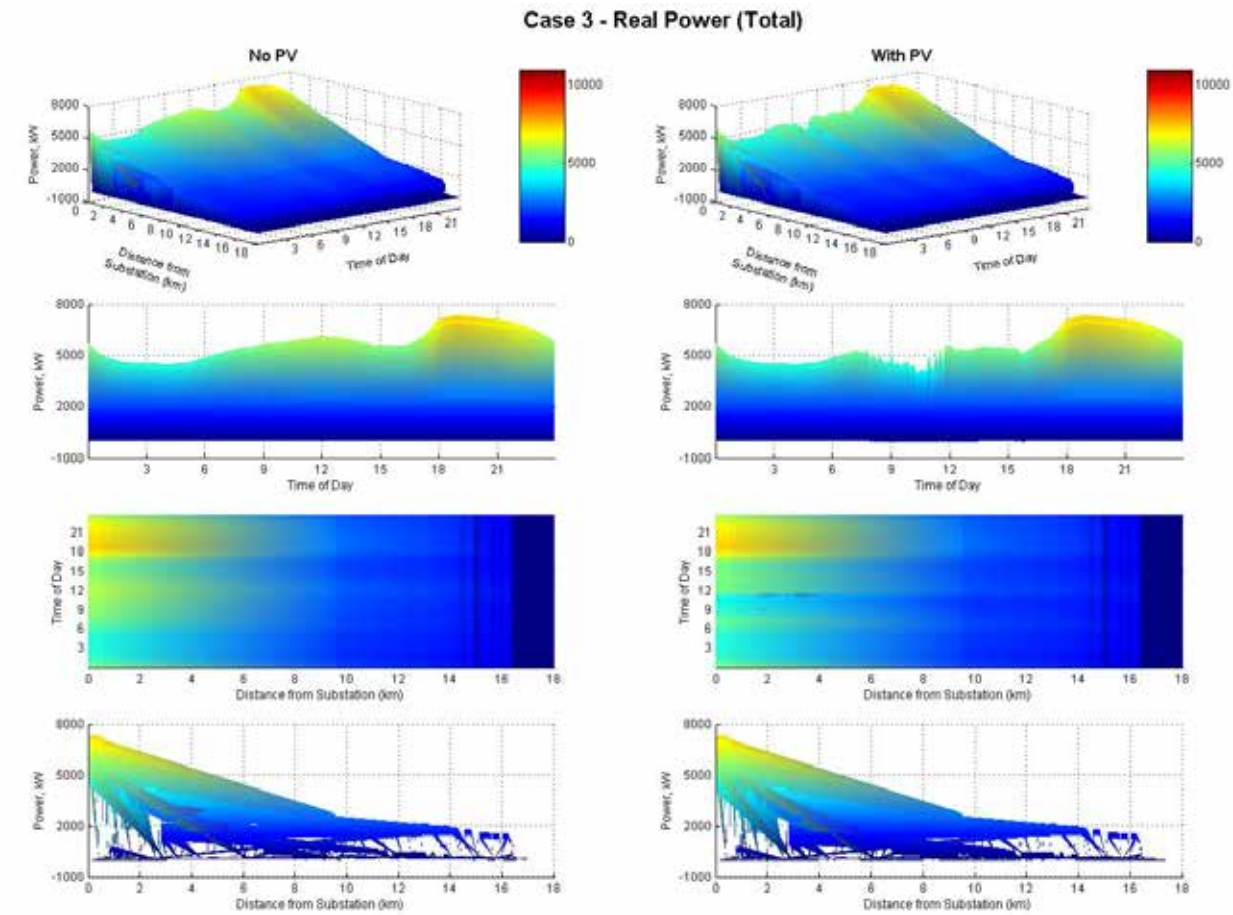

Figure D-23: Daily total real power profile for scenario 4 and case 3.

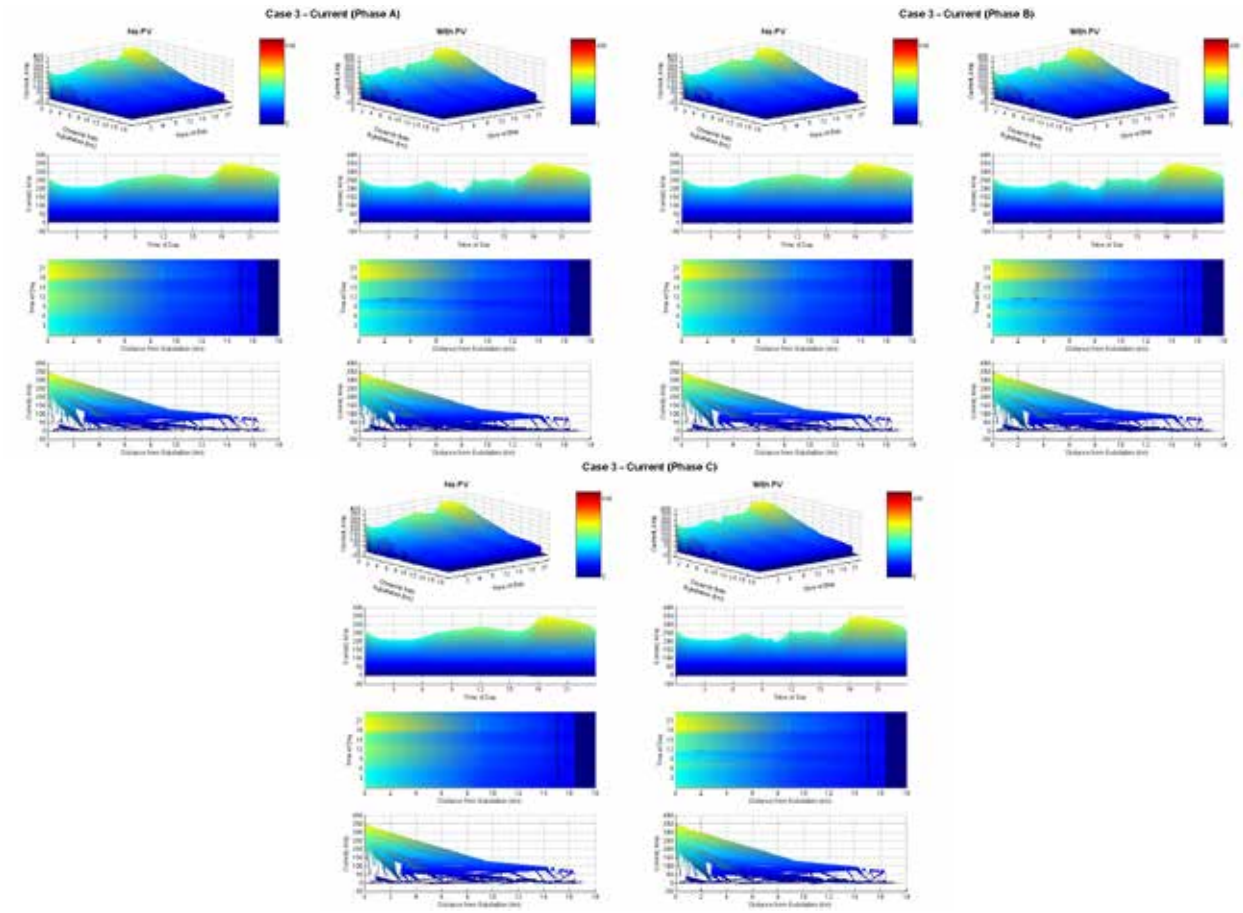

Figure D-24: Daily current profiles for scenario 4 and case 3.

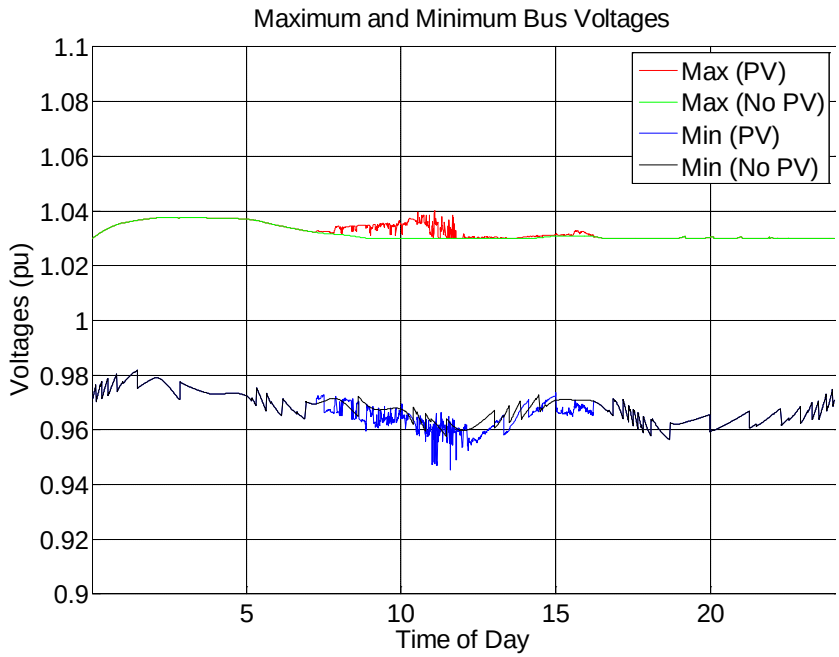

Figure D-25: Maximum and minimum voltages for scenario 4 and case 3.

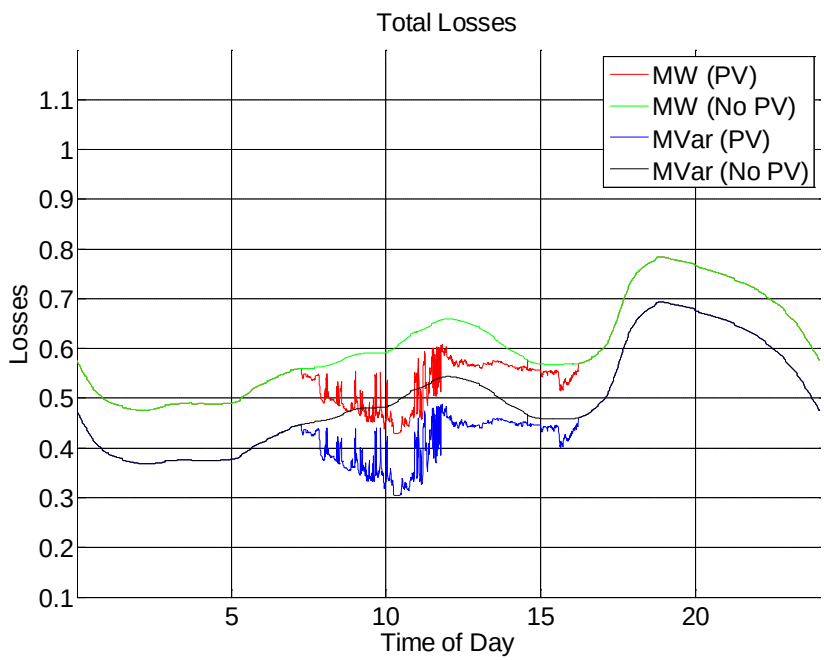

Figure D-26: MW and MVAr losses for scenario 4 and case 3.

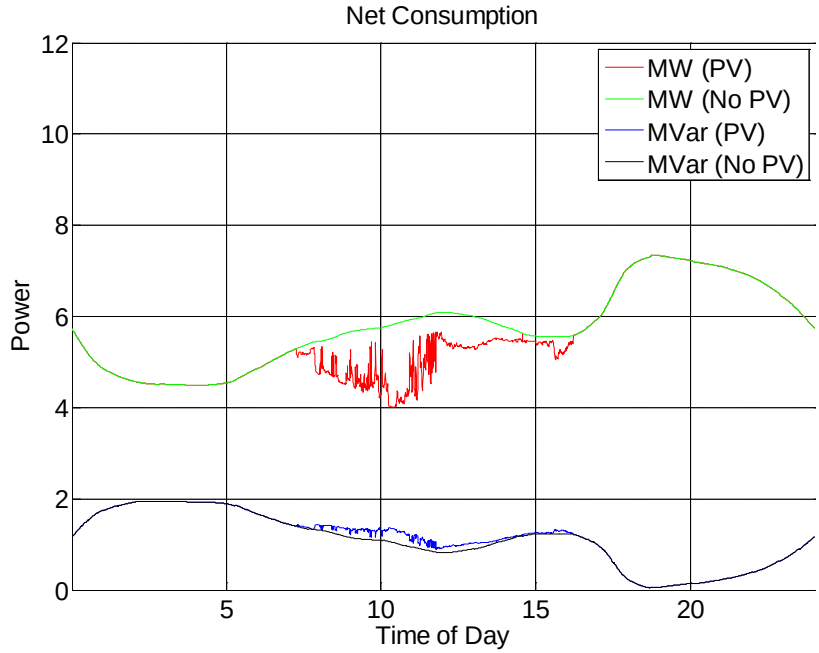

Figure D-27: MW and MVAr net consumption for scenario 4 and case 3.

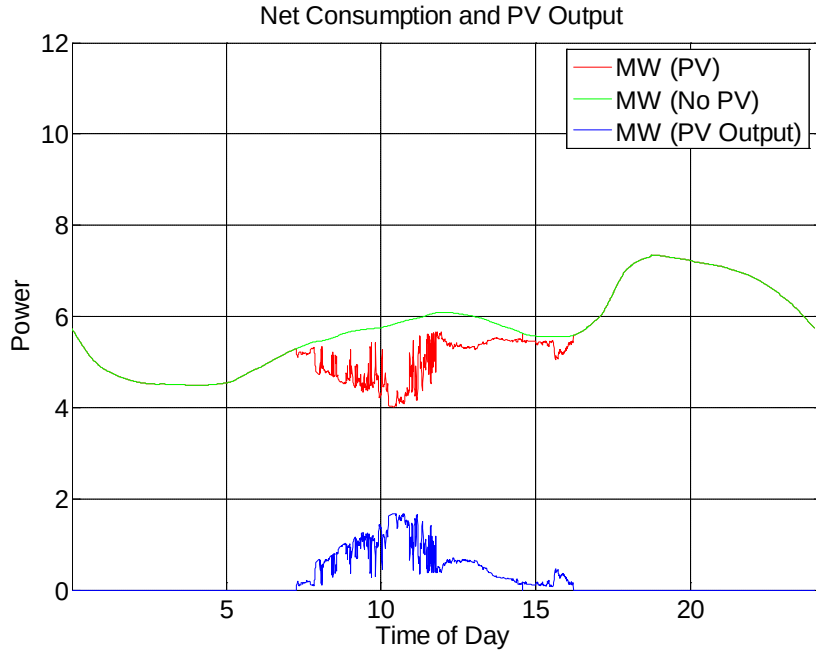

Figure D-28: MW net consumption and total PV generation for scenario 4 and case 3.

D.5 Case 4

Figure D-29 through Figure D-35 show simulation results for scenario 4 and case 4.

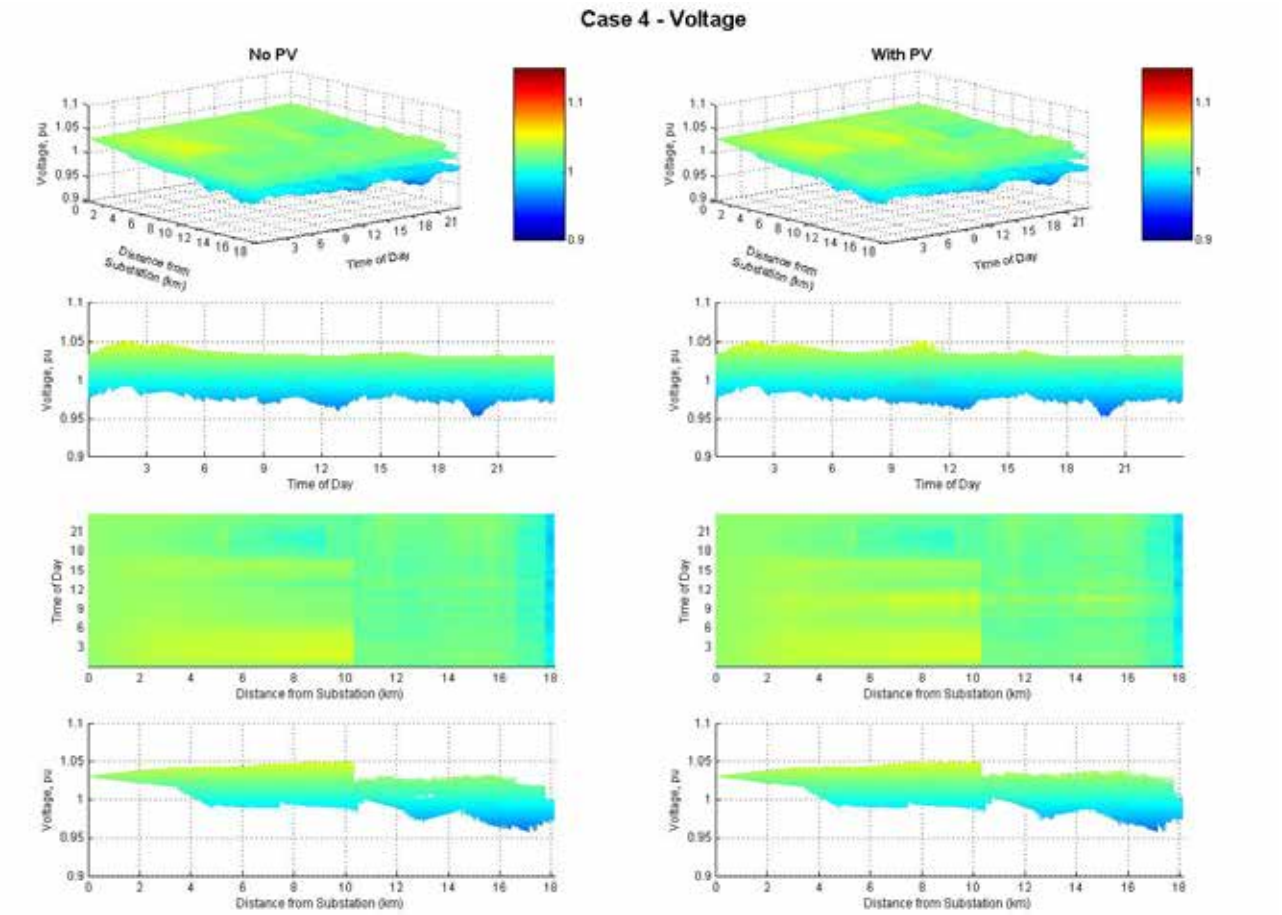

Figure D-29: Daily voltage profile for scenario 4 case 4.

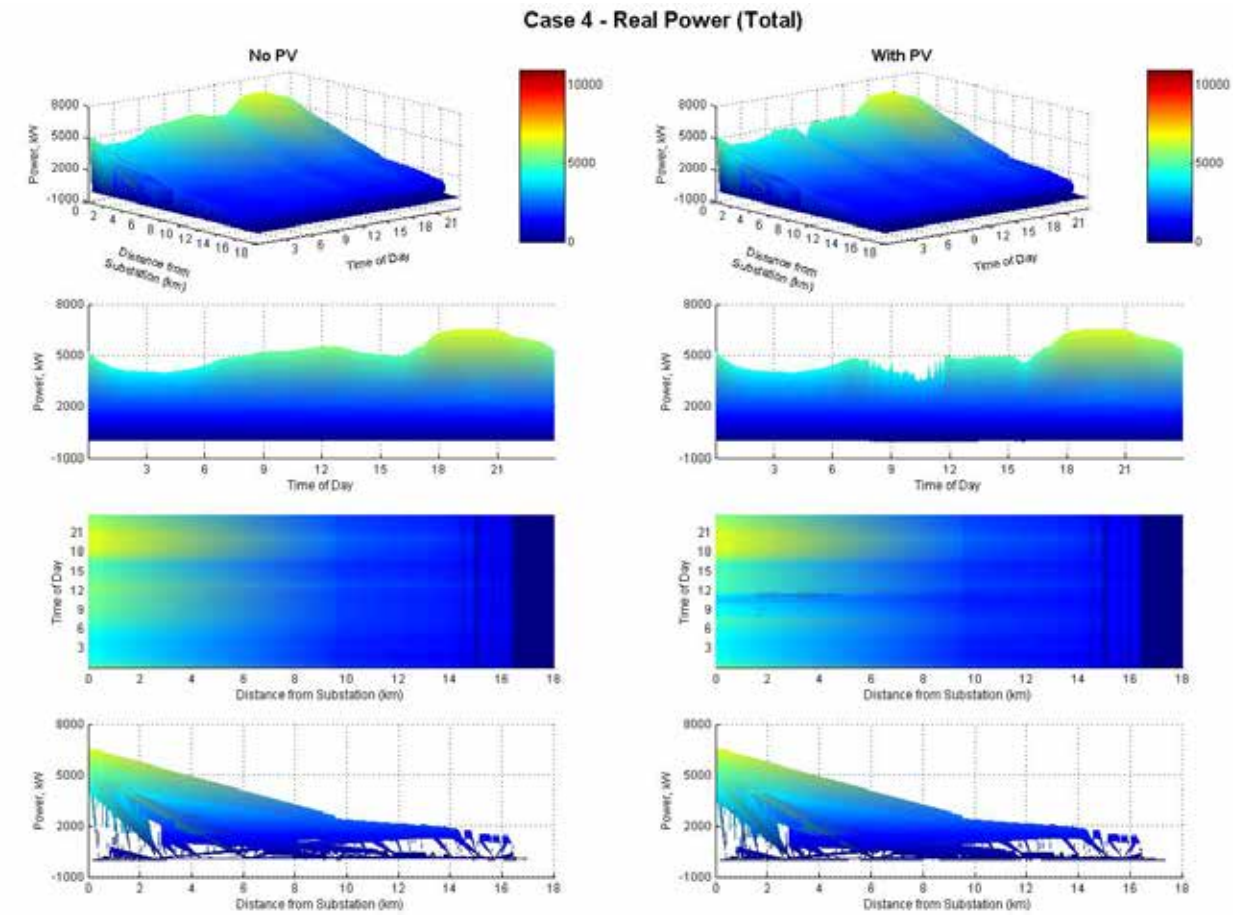

Figure D-30: Daily total real power profile for scenario 4 and case 4.

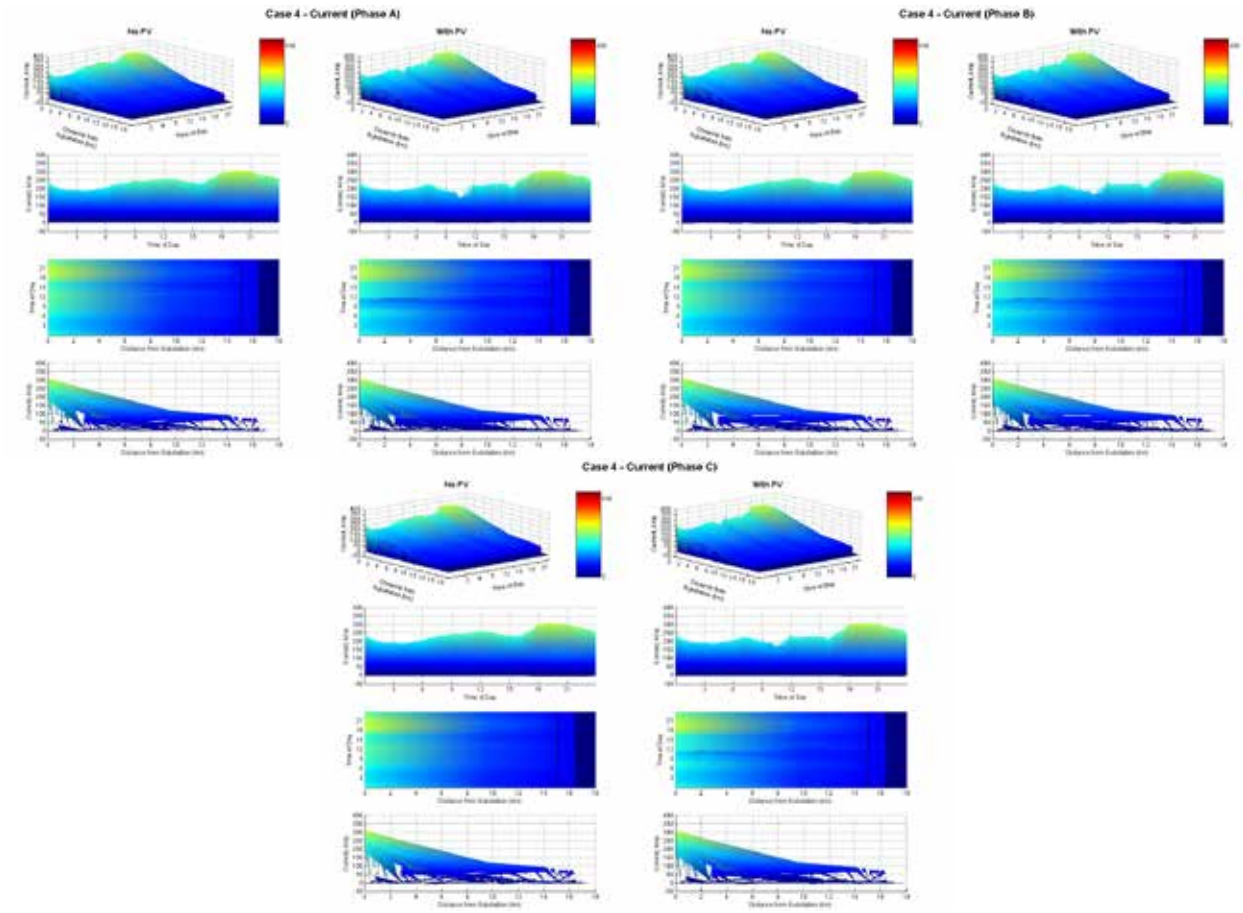

Figure D-31: Daily current profiles for scenario 4 and case 4.

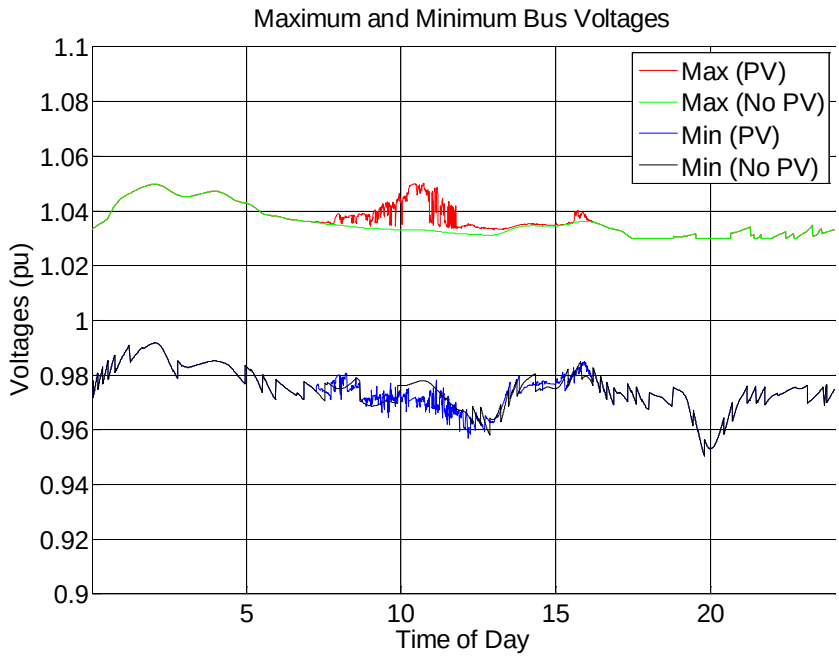

Figure D-32: Maximum and minimum voltages for scenario 4 and case 4.

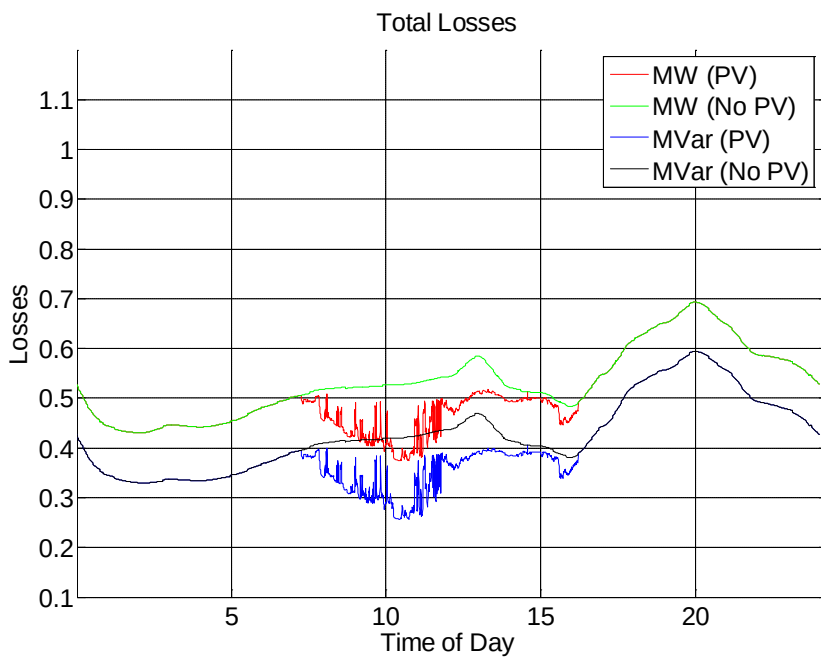

Figure D-33: MW and MVAr losses for scenario 4 and case 4.

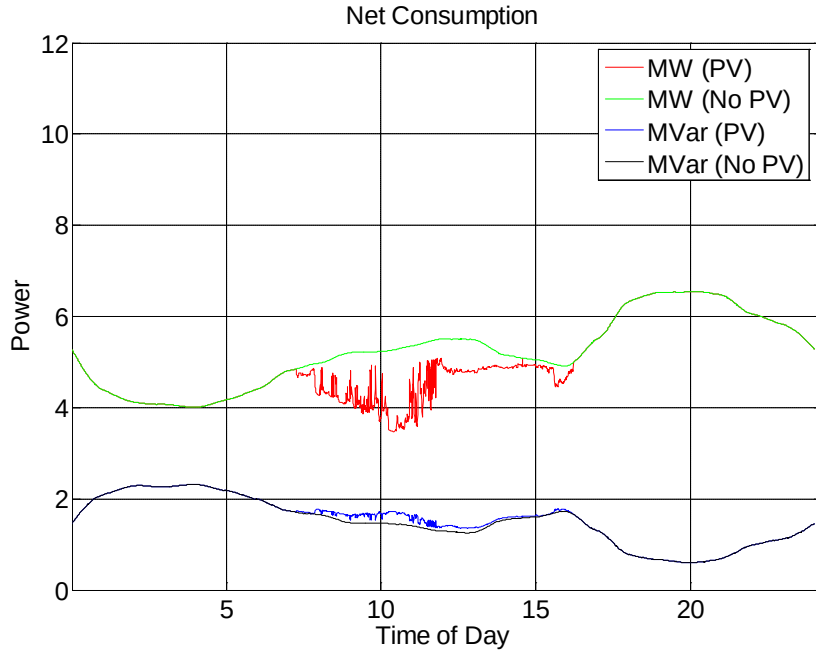

Figure D-34: MW and MVAr net consumption for scenario 4 and case 4.

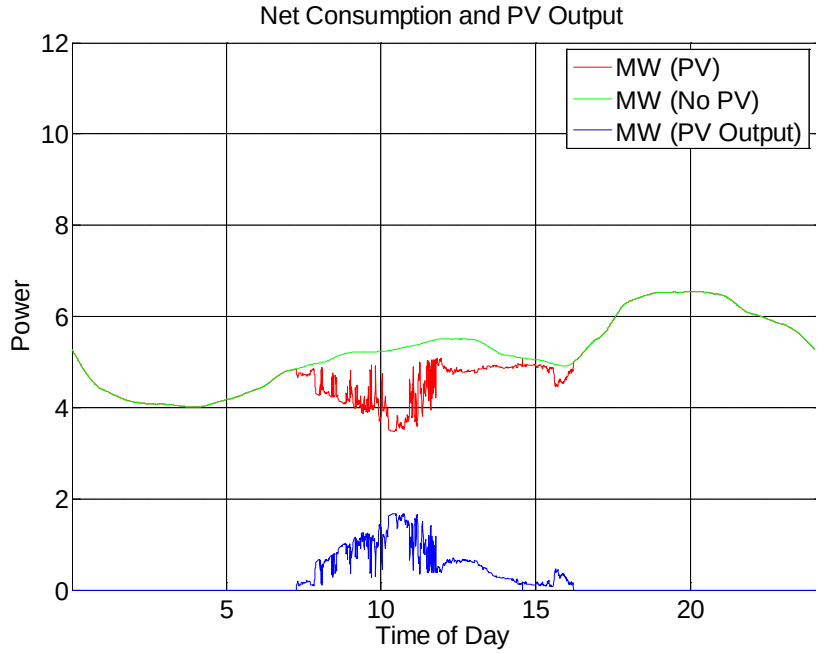

Figure D-35: MW net consumption and total PV generation for scenario 4 and case 4.

D.6 Case 5

Figure D-36 through Figure D-42 show simulation results for scenario 4 and case 5.

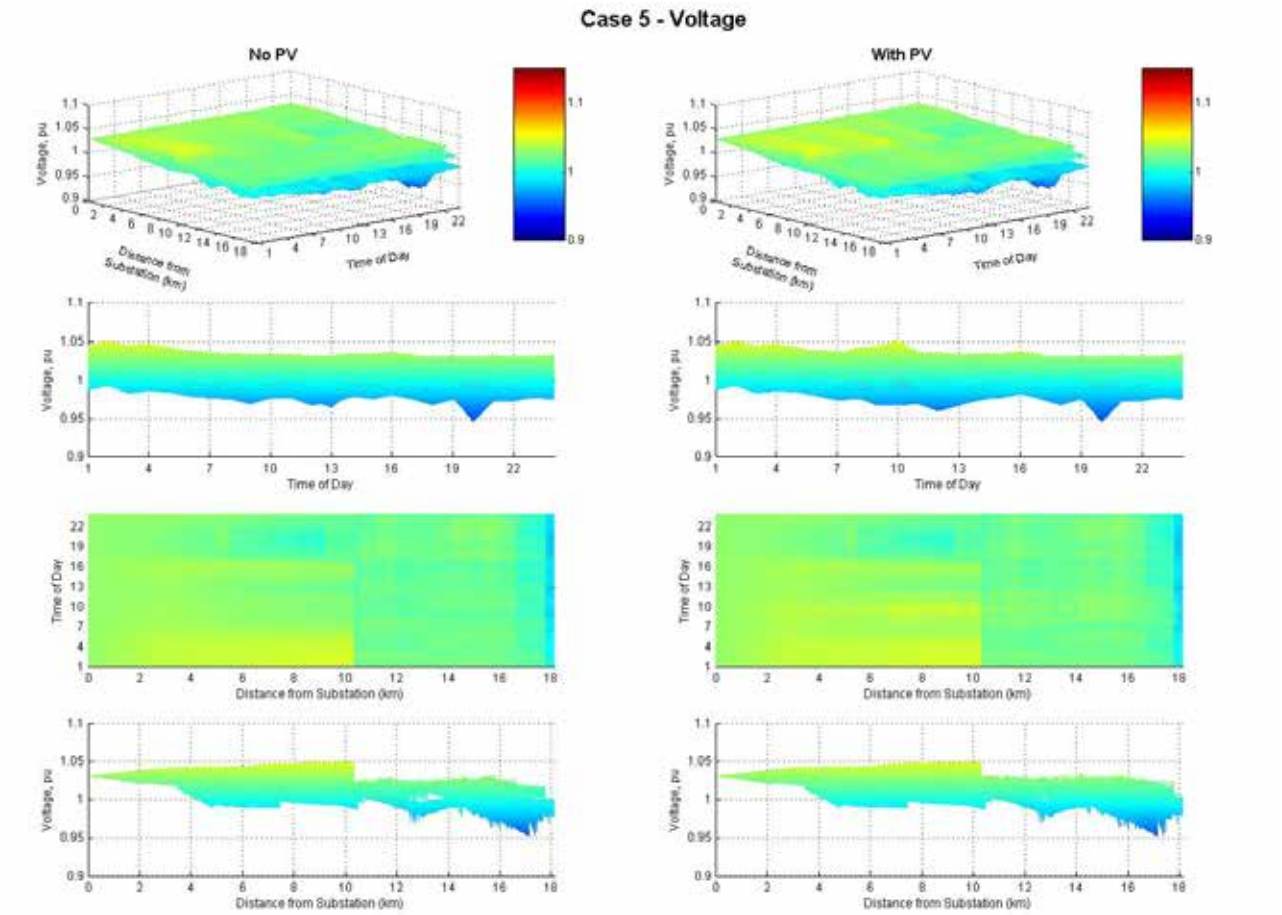

Figure D-36: Daily voltage profile for scenario 4 case 5.

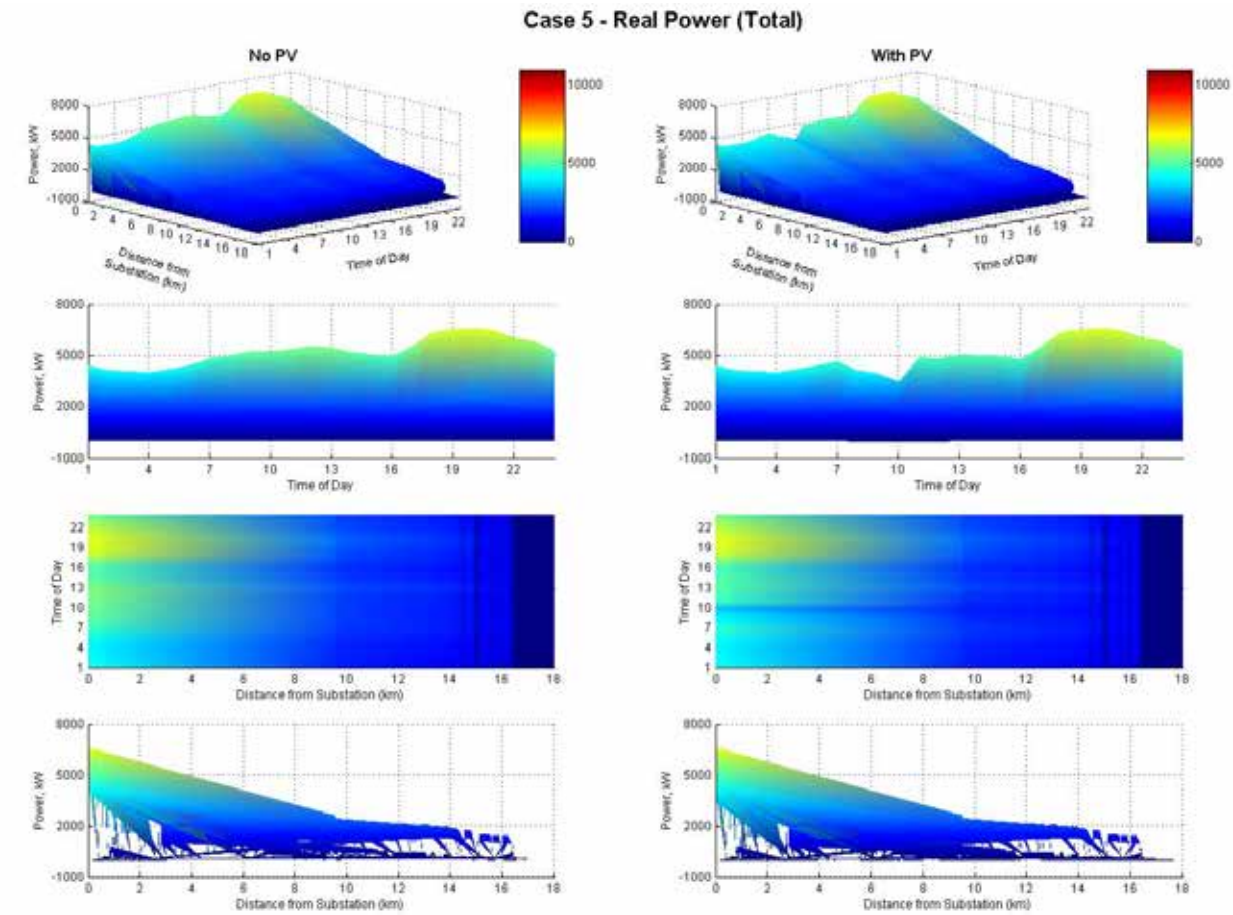

Figure D-37: Daily total real power profile for scenario 4 and case 5.

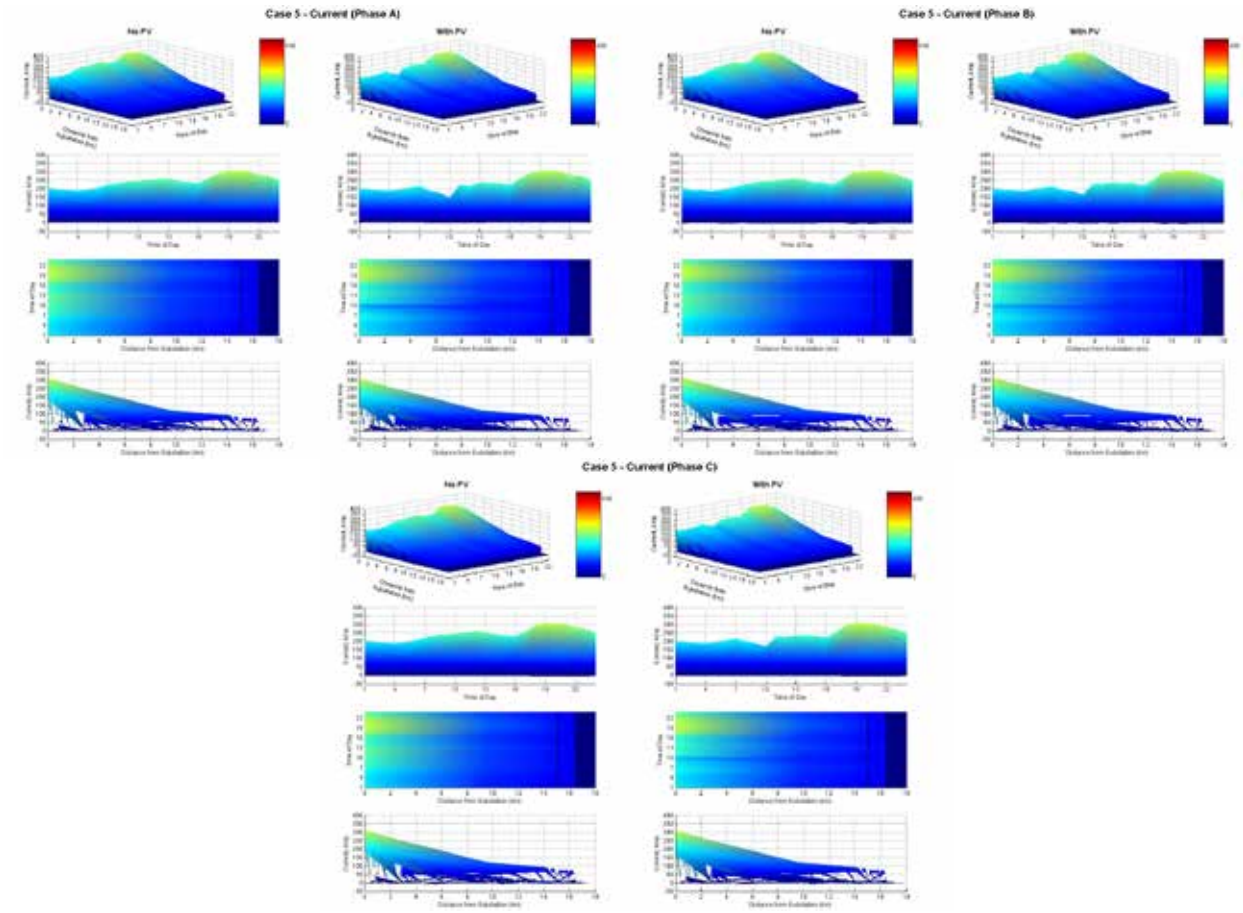

Figure D-38: Daily current profiles for scenario 4 and case 5.

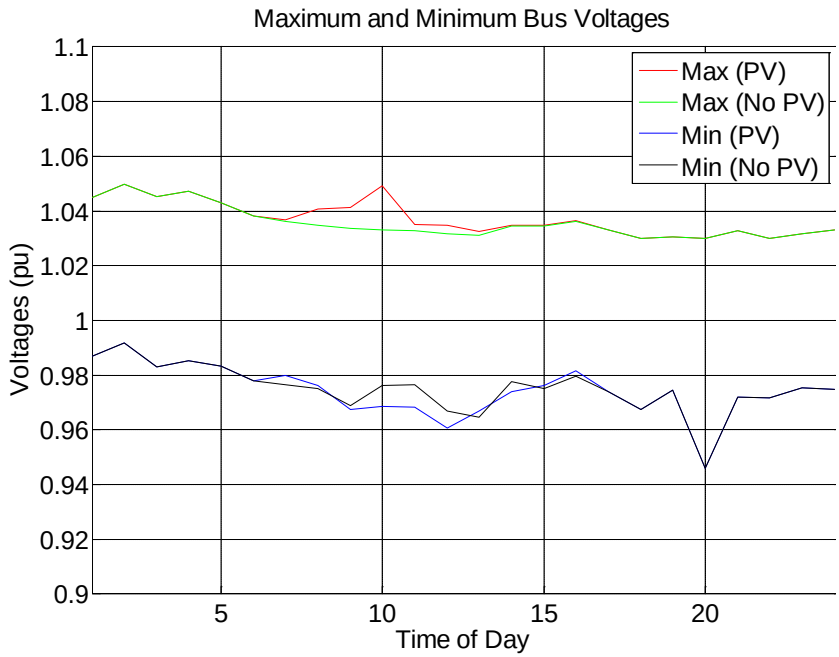

Figure D-39: Maximum and minimum voltages for scenario 4 and case 5.

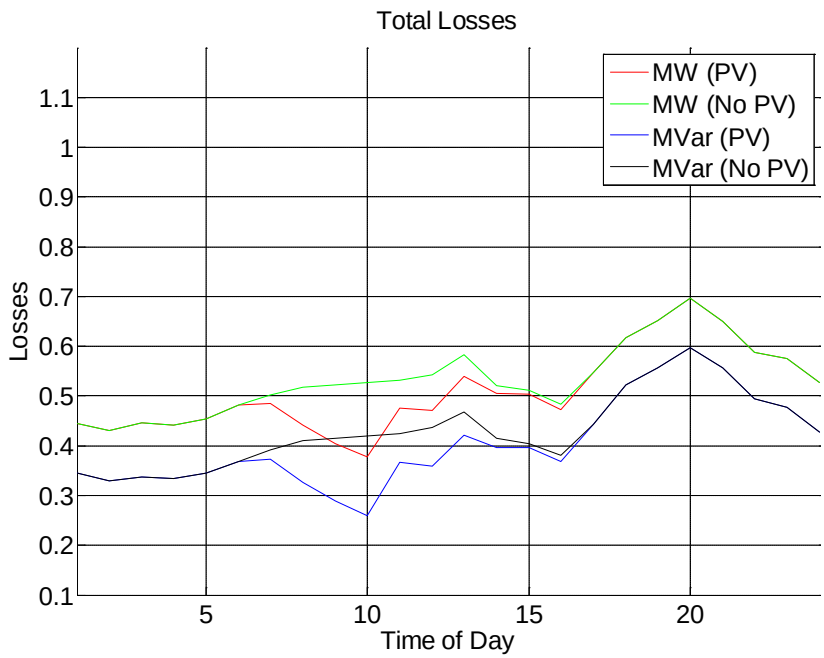

Figure D-40: MW and MVAr losses for scenario 4 and case 5.

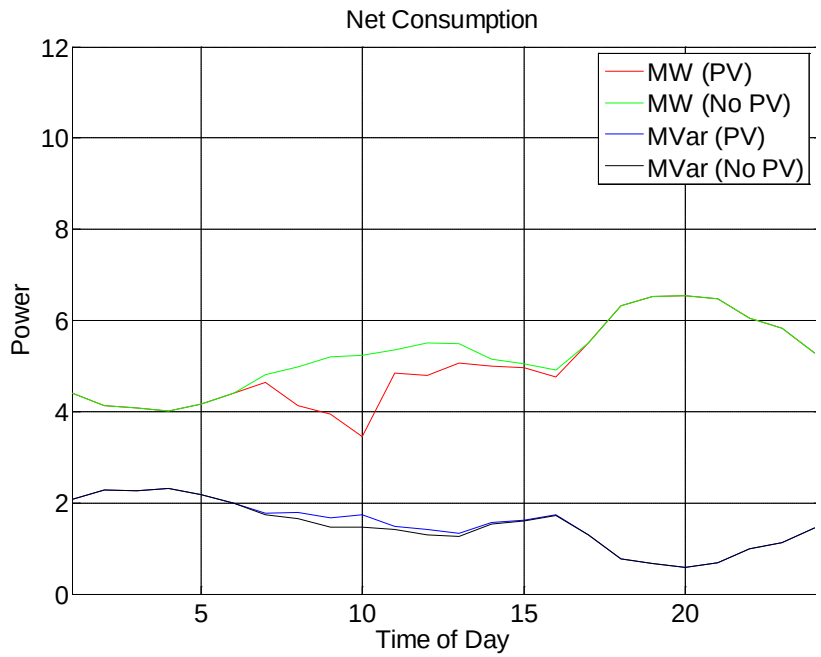

Figure D-41: MW and MVAr net consumption for scenario 4 and case 5.

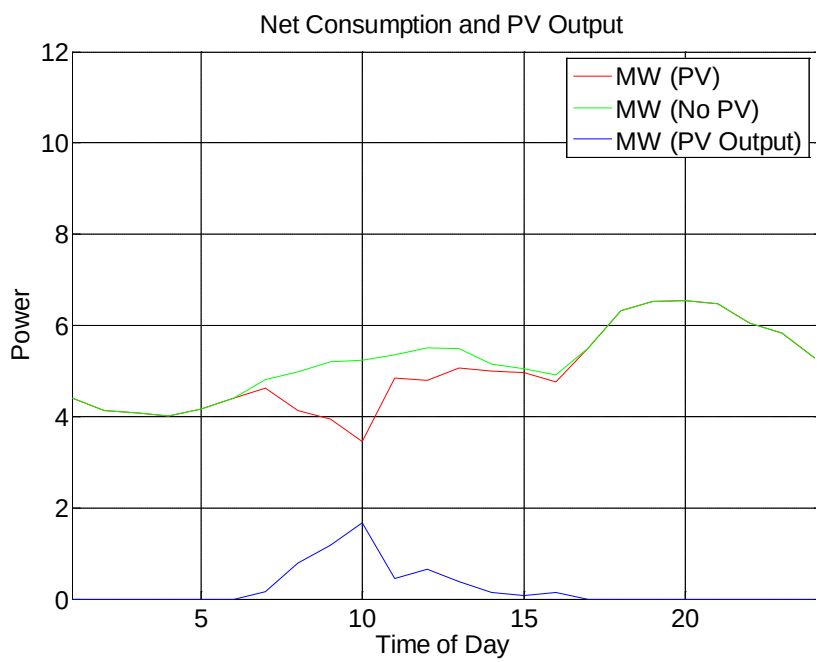

Figure D-42: MW net consumption and total PV generation for scenario 4 and case 5.

D.7 Case 6

Figure D-43 through Figure D-49 show simulation results for scenario 4 and case 5.

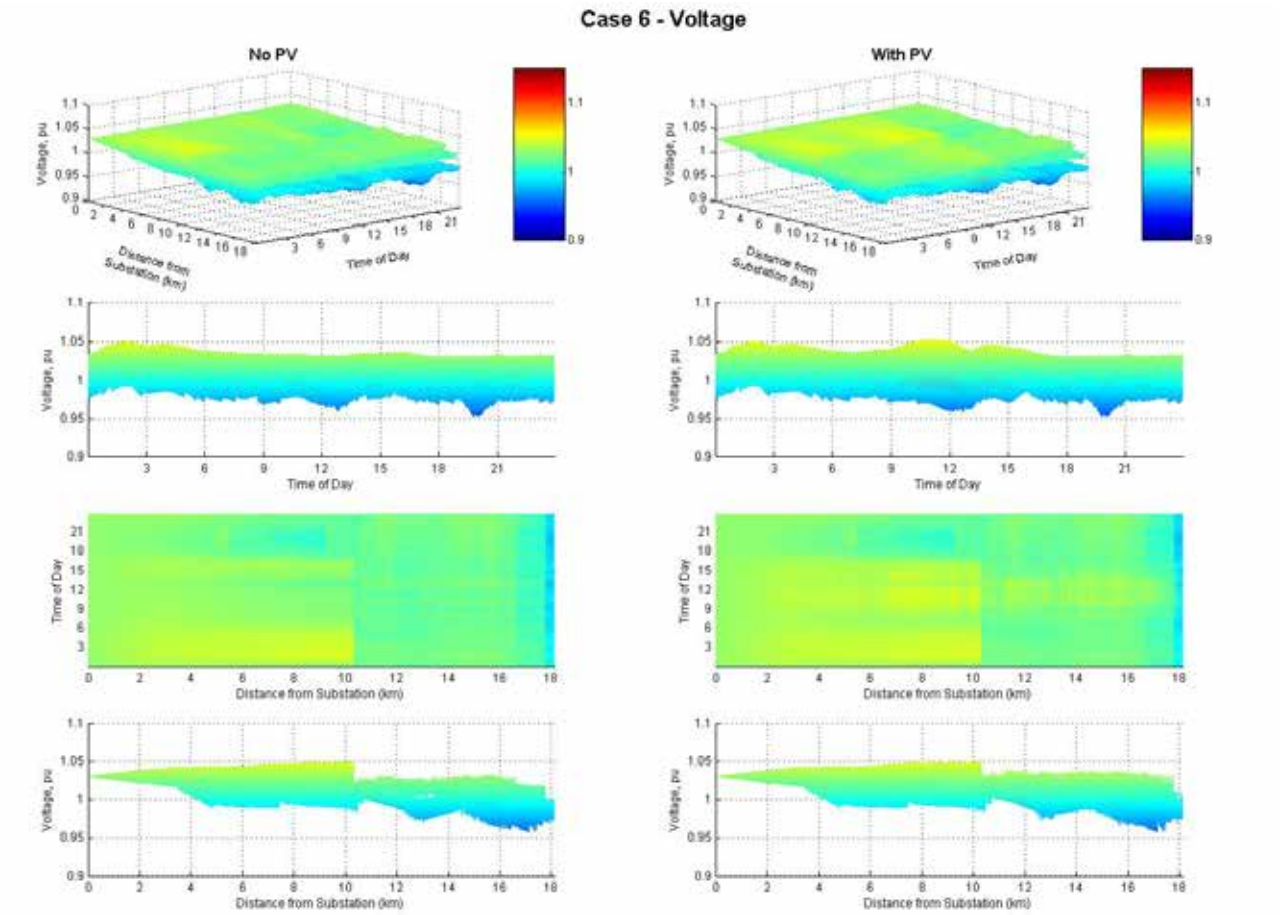

Figure D-43: Daily voltage profile for scenario 4 case 6.

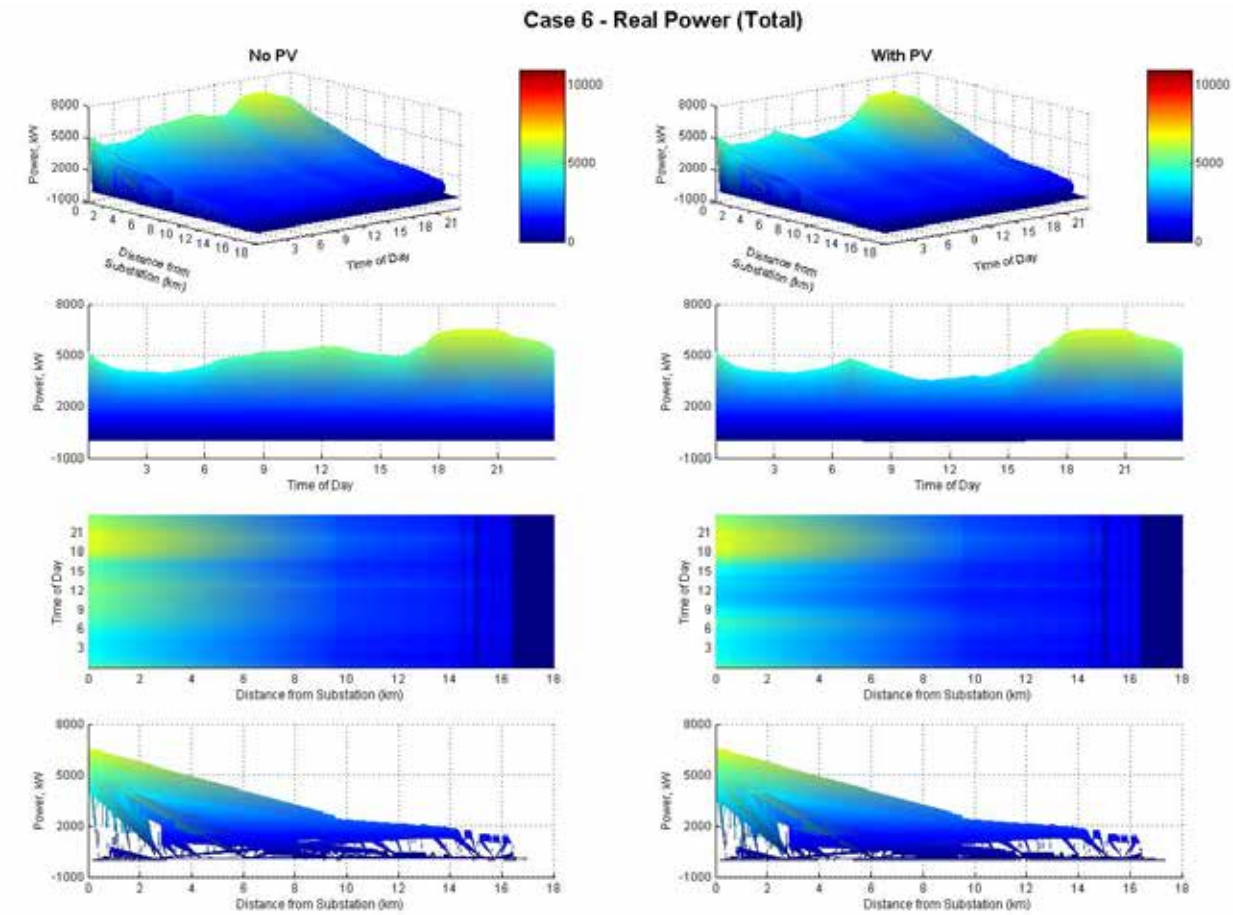

Figure D-44: Daily total real power profile for scenario 4 and case 6.

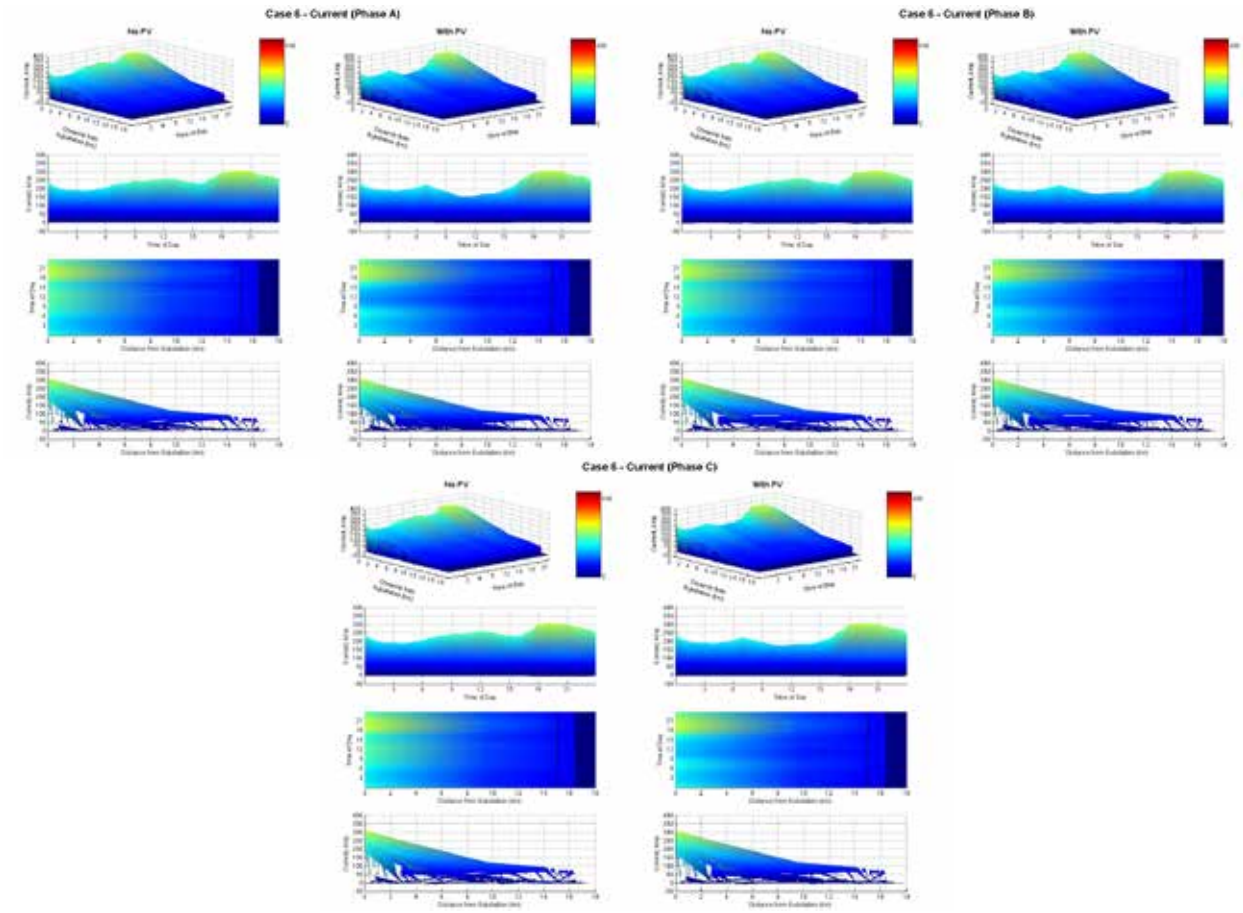

Figure D-45: Daily current profiles for scenario 4 and case 6.

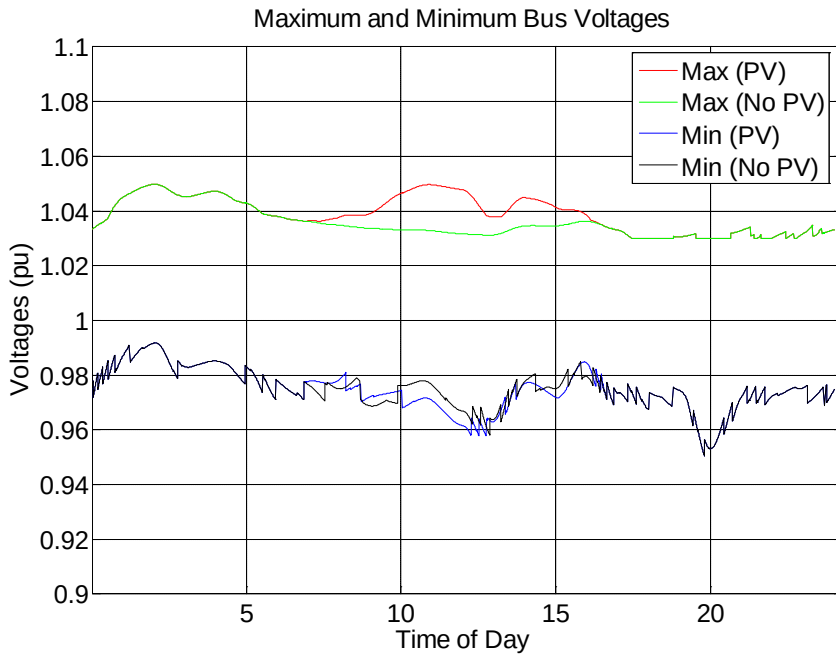

Figure D-46: Maximum and minimum voltages for scenario 4 and case 6.

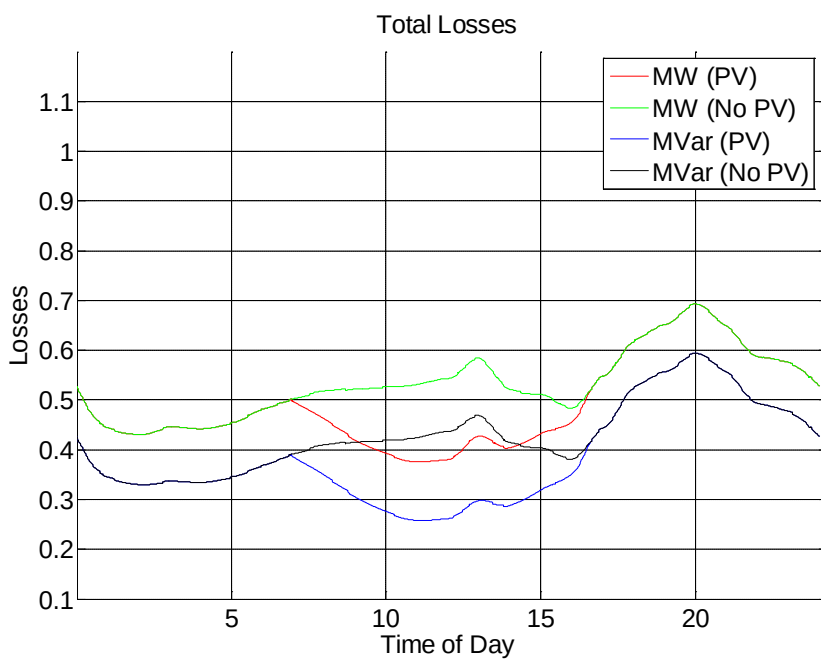

Figure D-47: MW and MVAr losses for scenario 4 and case 6.

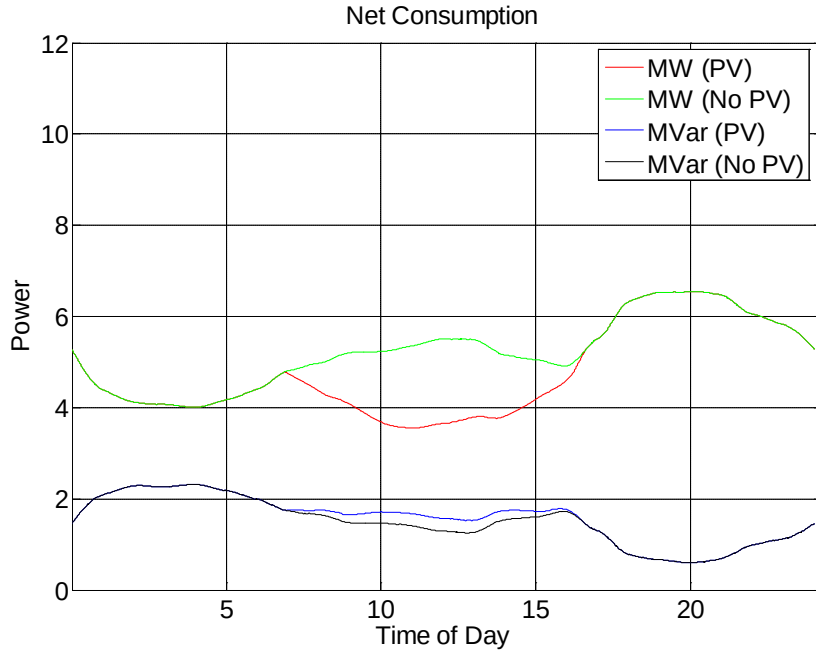

Figure D-48: MW and MVAr net consumption for scenario 4 and case 6.

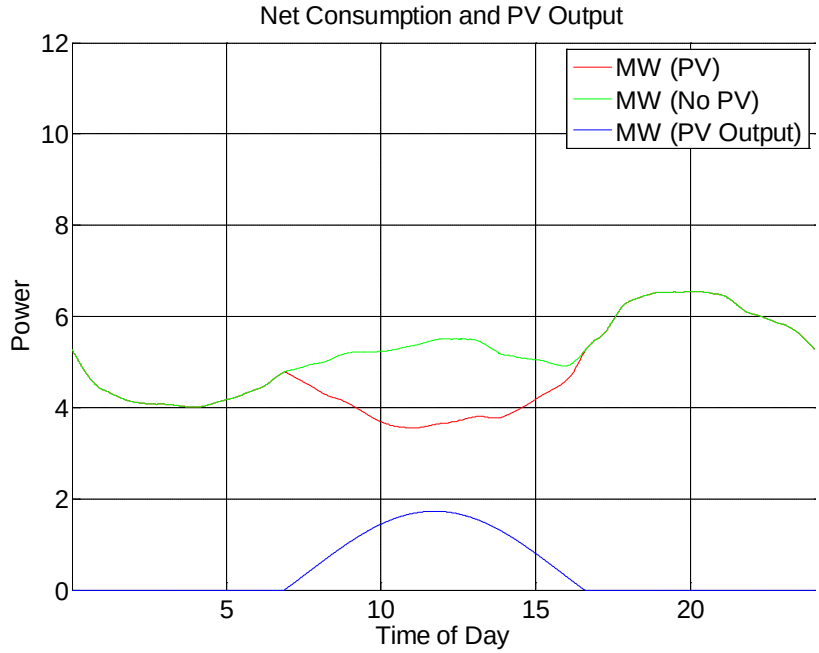

Figure D-49: MW net consumption and total PV generation for scenario 4 and case 6.